

Investigation the Role of *ATM* in Sarcomas

By

Afnan Salah Alkathiri

A thesis submitted in partial fulfilment of the requirements for the

degree of

Doctor of Philosophy



The
University
Of
Sheffield.

Supervisor: Dr. Karen Sisley

Department of Oncology and Metabolism
Faculty of Medicine, Dentistry and Health
The University of Sheffield

November 2018

ABSTRACT

Sarcomas are a rare heterogeneous group of malignant tumours arising from cells of a mesenchymal origin. They are diverse group consisting of more than 50 subgroups. Sarcomas tend to fall into two distinct genetic categories. The first group shows relatively simple karyotypes with specific genetic abnormalities. The other group however has very complex karyotypes with unspecific genetic alterations. Although their causes are still not entirely clear, the strongest links appear to be radiation exposure and inherited cancer predisposition. Previous work in our laboratory has revealed a deletion in the *ATM* gene, particularly in gastrointestinal stromal tumours and in leiomyosarcomas. The *ATM* gene is known to have a key role in the repair of DNA-DSBs, as well as in cell cycle arrest. To investigate the role that *ATM* may have in sarcoma, Western blotting was initially used in this study to look for the total *ATM* protein expression and for the phosphorylated form of the *ATM* in different sarcoma subtypes. So as to examine the potential relevance of *ATM* to the tumours in more detail, the study also measured the kinetics of γ H2ax foci formation and loss in established and primary sarcoma cells and in normal retinal cells; both endogenously and after inducing DNA-DSBs by 2Gy IR prior to, and after, the inhibition of *ATM*. The functional aspect of *ATM* in sarcoma was further explored through the clonogenic survival assay. Finally, the genetic abnormalities of the *ATM* were assessed using a combination of several techniques. Although this PhD study has confirmed *ATM* copy number deletion in sarcomas, this does not appear to affect protein expression, since expression was clearly detected by Western blotting at 370 kDa in all the cell lines tested in this study, including the control samples. This work has also demonstrated the existence of functional *ATM* in sarcoma samples while providing evidence that, even though *ATM* is inhibited in sarcomas, they are still able to undertake DNA repair, possibly via the utilisation of other pathways, or because an “abnormal” *ATM* in the sarcomas may not have been adequately inhibited due to a mutation. The importance of the *ATM* deletion/mutation to the protein expression seen in sarcoma cell lines, and the significance of *ATM* deletion/mutation to the biological behaviour of the sarcoma samples included in this work, needs further investigation in the near future.

ACKNOWLEDGMENTS

"All the praises and thanks be to Allah who is the Lord of the worlds" (Quran, 1:1). I am grateful to The Lord for making this thesis a reality.

First, I would like to express my gratitude to my supervisor, Dr. Karen Sisley, for patient guidance, valuable insights and for much-appreciated support and motivation. Further thanks are due to all the members of the Rare Tumour Research Group, particularly Dr. David Hammond for valuable advice and support, Dr. Abdulazeez Salawu, for patiently answering my questions and for the many hours he devoted for the discussions we had, Mrs. Clair Greaves for the technical help and support she offered.

I also would like to thank my country, Kingdom of Saudi Arabia, represented by The Ministry of Education, Albaha University and the Saudi Cultural Bureau in London for funding the whole journey of my postgrad studies in one of the strongest universities in the UK, Sheffield University.

To the strong shoulders, beautiful minds and kind hearts upon which I lean in my all times, my parents (Najat and Salah) and siblings (Arwa, Ahmad, Alaa and Rayan), I am forever in debt for the unconditional love, constant reassurances and support you endlessly offer.

My love, thanks and prayers reach out to the giving beautiful souls I lost lately. You will always be remembered and missed.

My greatest thanks are to my husband, Alrayan for always having my back, reassuring me during hard times with invaluable support and motivation with the meaning of everything. My blooming thanks are to my little bird, Azzam whose smile has been the source for the needed strength and positive energy to accomplish my work.

Table of Content

List of Figures	9
List of Tables	11
List of Abbreviation	12
CHAPTER ONE	17
1 INTRODUCTION	17
1.1 Sarcomas.....	18
1.2 Epidemiology and Incidence	19
1.3 Sarcoma Aetiology	21
1.3.1 Environmental Factors	21
1.3.1.1 Viral Infections	21
1.3.1.2 Ionising Radiation	22
1.3.1.3 Occupational and Chemical Exposure.....	22
1.3.1.4 Chronic Lymphoedema.....	23
1.3.2 Genetic Factors and Sarcoma	23
1.4 Major Sarcoma Subtypes.....	24
1.4.1 Leiomyosarcomas.....	24
1.4.2 Gastrointestinal Stromal Tumours.....	25
1.4.3 Ewing’s Sarcoma	26
1.4.4 Liposarcoma.....	27
1.4.5 Angiosarcoma	28
1.5 Genetics Changes in Sarcomas	28
1.5.1 <i>p53</i> and <i>Rb1</i> Tumour Suppressor Genes	31
1.5.2 Ras oncogenes	32
1.6 Diagnosis.....	33
1.7 Grading and Staging	34

1.8	Treatment of Sarcomas	37
1.8.1	Surgery.....	37
1.8.2	Radiotherapy.....	38
1.8.3	Chemotherapy.....	39
1.8.4	Molecular Targeted Therapy.....	39
1.9	DNA Damage and Repair	40
1.9.1	Ataxia Telangiectasia Mutated Gene (<i>ATM</i>).....	41
1.9.2	Role of <i>ATM</i> in the DNA Damage Response.....	42
1.9.3	Inhibition of <i>ATM</i>	45
1.9.4	Cell Cycle.....	48
1.9.4.1	Cell Cycle Regulation.....	49
1.9.4.2	<i>ATM</i> and the DNA Damage Checkpoint Activation	50
1.9.4.3	DNA-DSBs Repair Pathways.....	51
1.9.4.3.1	Homologous Recombination	51
1.9.4.3.2	Non-Homologous End Joining	53
1.10	Hypothesis and Aims of the Study	56
CHAPTER TWO		58
2	MATERIALS AND METHODS	58
2.1	Patients and Tumour Samples	59
2.1.1	Ethics Statement and Tumour Samples	59
2.1.2	Other Cell Lines	59
2.2	Materials	62
2.2.1	General Laboratory Reagents, Disposable and Basic Laboratory Equipment.....	62
2.2.2	Tissue Culture and Chromosome Preparation.....	66
2.2.3	Whole Cell Lysate Extraction and Western Blotting.....	67
2.2.4	γ H2AX Assay	72
2.2.5	Clonogenic Survival Assay.....	73

2.2.6	Fluorescence <i>In-Situ</i> Hybridisation (FISH).....	73
2.2.6.1	Reagents Preparation	73
2.2.6.2	Probes.....	74
2.2.7	DNA Extraction.....	75
2.2.8	Multiplex Ligation-Dependent Probe Amplification (MLPA)	75
2.2.9	Next Generation Sequencing (NGS).....	76
2.3	Methods.....	77
2.3.1	Routine Tissue Culture.....	77
2.3.2	Whole Cell Lysate Extraction and Protein Expression by SDS-PAGE and Western Blotting.....	77
2.3.2.1	Cell Protein Extraction	77
2.3.2.2	Protein Quantification.....	78
2.3.2.3	SDS Page Electrophoresis	79
2.3.2.4	Wet and Semi-Dry Transfer	80
2.3.2.5	Protein Detection	82
2.3.3	Immunofluorescence for γ H2AX.....	82
2.3.3.1	Sample Preparation	82
2.3.3.2	Treating Cells with Irradiation	83
2.3.3.3	Immunofluorescence Staining of γ H2AX Foci.....	83
2.3.3.4	Analysis and Quantification of γ H2AX Foci.....	84
2.3.4	Clonogenic Survival Assay.....	85
2.3.4.1	Analysis of Clonogenic Assay.....	85
2.3.5	Determination of the ATM Kinase Inhibition by Western Blotting	86
2.3.6	Fluorescence <i>In-situ</i> Hybridisation (FISH)	87
2.3.6.1	Chromosome Harvesting	87
2.3.6.2	Chromosome Spread and Slide Preparation	88
2.3.6.3	Enzyme Treatment and Cell Fixing.....	88
2.3.6.4	Hybridisation of the DNA Probes to the Target DNA	88

2.3.6.5	Post-Hybridisation Washes and Counterstaining	89
2.3.6.6	Analysis and Image Detecting	89
2.3.7	DNA Extraction.....	90
2.3.7.1	Cells Preparation and Lysis	91
2.3.7.2	DNA Adsorption to DNeasy Mini Spin Column	91
2.3.7.3	DNA Washing	91
2.3.7.4	Elution of the Genomic DNA.....	91
2.3.7.5	DNA Quantification	92
2.3.8	Multiplex Ligation-Dependent Probe Amplification (MLPA)	92
2.3.8.1	DNA Denaturation and Probes Hybridisation	93
2.3.8.2	Ligation Reaction	93
2.3.8.3	PCR Amplification.....	93
2.3.8.4	MLPA Analysis.....	94
2.3.9	Next Generation Sequencing (NGS).....	96
2.3.9.1	Library Preparation	97
2.3.9.2	Cluster Generation.....	97
2.3.9.3	Sequencing.....	98
2.3.9.4	Data Analysis.....	100

CHAPTER THREE..... 102

3 ATM FUNCTION AS PART OF THE RESPONSE OF SARCOMAS TO IONISING RADIATION (IR)..... 102

3.1 Introduction..... 103

3.2 Results..... 106

3.2.1 Determination of ATM Expression in Sarcoma and Normal Cell Lines..... 106

3.2.2 Time Course Inhibition of the ATM Kinase Activity

3.2.3 ATM Autophosphorylation and Inhibition in Different Cell Lines

3.2.4 Spontaneous γ H2AX Foci Formation is Increased in Sarcoma Cell Lines Compared to Controls..... 111

3.2.5 Sarcoma Cells are more Sensitive to IR Induced DNA-DSBs Damage Compared to Control Cells	113
3.2.6 ATM Inhibition Blocks DNA Repair in Controls However Sarcoma Cell Lines Display a Delayed Response to IR Following ATM inhibition	114
3.2.7 ATM Inhibition Prevents Kinase Activity of ATM and Blocks DNA Repair in Control Following 2 Hours of IR.....	118
3.2.8 Sensitivity of Sarcoma Cell Lines to IR, ATM Inhibition and Combination of both Treatments.....	120
3.3 Discussion.....	123
CHAPTER FOUR.....	132
4 CONFIRMATION OF LOSS OF <i>ATM</i> COPY NUMBER IN SARCOMAS USING FISH, NGS AND MLPA	132
4.1 Introduction.....	133
4.2 Results.....	135
4.2.1 Control Experiments with Chromosome 11 Probes	135
4.2.2 FISH Analysis of Chromosomal Region 11q in Normal and a Range of Sarcoma Cell lines	138
4.2.3 FISH Results Showed a Deletion of the ATM Locus in Sarcoma Cell Lines ...	138
4.2.4 ATM Copy Number Analysis using MLPA.....	141
4.2.5 The MLPA Data Showed a Similar Pattern of Findings Compared to the Previous MLPA Work Despite the Detection of Signal Sloping	147
4.2.6 MLPA Data Showed ATM Deletion in the Tumour Control	150
4.2.7 Short Tandem Repeat (STR) Analysis.....	152
4.2.8 <i>ATM</i> Copy Number Detection by Targeted NGS in Sarcoma Cell Lines	155
4.2.9 NGS Analysis Showed an Aberration of <i>ATM</i> Copy Number in Different Sarcoma Cases and Confirmed the Heterozygous Deletion of <i>ATM</i> in the Tumour Control Cell Line	156

4.3	Discussion.....	161
CHAPTER FIVE.....		168
5	FINAL DISCUSSION	168
5.1	Final Discussion	170
5.1.1	Objective of this Work	170
5.1.2	Sarcomas have frequent <i>ATM</i> CNA, but protein expression and functional response are detectable.	170
5.1.3	How are sarcomas able to respond to DNA-DSBs despite inhibition of ATM Kinase?.....	171
5.1.4	Could mutations of <i>ATM</i> or its kinase be responsible for the ability to recruit H2AX and induce a radiation damage response?.....	172
5.1.5	Is deletion of <i>ATM</i> copy number relevant or just a marker?	174
5.2	Limitations of this Study.....	175
5.3	Future Work.....	175
REFERENCES.....		176
APPENDICES.....		209

List of Figures

Figure 1.1 Sarcoma Cell Differentiation.	19
Figure 1.2 Schematic Representations of ATM Kinase Protein Structure.	42
Figure 1.3 Schematic Model of How Cells Respond to DNA-DSBs.....	47
Figure 1.4 Cell Cycle Regulation.	49
Figure 1.5 Schematic Representations of the Main Pathways of the DNA-DSBs Repair.....	55
Figure 2.1 Protein Size Markers.....	80
Figure 2.2 A Schematic Representation of a Wet Blotting Cassette (A) and Semi-Dry Transfer Unit (B).....	81
Figure 2.3 Schematic Model of γ H2AX Assay.....	84
Figure 2.4 A Schematic Outline of the Basic Principle of FISH.	90
Figure 2.5 A Schematic Representation of MLPA Principle.....	96
Figure 2.6 A Schematic Model of Illumina Sequencing Workflow.....	99
Figure 2.7 The Analytical Workflow of CNA from NGS Data using Nexus Copy Number Software.....	101
Figure 3.1 A Western Blotting Analysis of the ATM Protein in Different Sarcoma Cell Lines.	107
Figure 3.2 Western Blotting Confirming the Inhibition of ATM Phosphorylation.	109
Figure 3.3 Auto phosphorylation of ATM on ser1981 in Response to IR and inhibition.....	110
Figure 3.4 Percentage of Cells Forming Spontaneous γ H2AX Foci in Sarcoma and Control Cell Line.	112
Figure 3.5 Representative Images of γ H2AX Foci Formation in the Controls, Established and Primary Sarcoma Cell Lines.....	115
Figure 3.6 Kinetics of Formation and Elimination of IR-Induced γ H2AX Foci as a Measure of DNA Damage in Different Cell Lines with and without the Inhibition of the ATM.	117
Figure 3.7 Percentage of Cells with >10 γ H2AX Foci Following 2 Hours of 2Gy IR with and without the Inhibition of the ATM.....	119

Figure 3.8 Cell Survival for all Cell Lines Post Exposure to 2Gy IR.....	121
Figure 3.9 Cellular Survival of Controls and Sarcoma Cell lines in Response to Different Types of Treatment.....	121
Figure 3.10 Cellular Survival Following Different Types of Treatment.....	122
Figure 4.1 Representative Images from Control Experiments with Chromosome 11 Probes.	137
Figure 4.2 Detection of 11q Deletion in Sarcoma Cell Lines.	140
Figure 4.3 The MLPA Data for MFS 21/11 and LMS 11/11 Prepared as Part of a Pilot Study by Dr. Aliya UI Hassan.	144
Figure 4.4 Differences between Normal and Sloping Signal Intensity.	146
Figure 4.5 MLPA Findings for MFS 21/11 and LMS 11/11 Cases Similar to the Previous Work Done in 2012.....	149
Figure 4.6 MLPA Data for the Tumour and Non-Tumour Controls.	152
Figure 4.7 Graphical View of ATM CNA Identified in Different Sarcoma Cell Lines.	160
Figure 5.1 Summary of Approaches used and Major Findings of this PhD Study	169

List of Tables

Table 1.1 Chromosome Translocations and Fusion Genes in STS.....	31
Table 1.2 FNCLCC Soft Tissue Sarcomas Grading System	35
Table 1.3 TNM Soft Tissue Sarcomas Staging System.....	36
Table 2.1 Clinical Data for All STS Cases Used in this Study	60
Table 2.2 Details of all Commercial Cell Lines Used in This Study	61
Table 2.3 General Laboratory Reagents.....	62
Table 2.4 Disposable Laboratory Equipment.....	64
Table 2.5 Basic Laboratory Equipment.....	65
Table 2.6 Tissue Culture Medium Supplements	66
Table 2.7 Sample Preparation for Western Blotting.....	68
Table 2.8 SDS Page Resolving and Stacking Gels Components.....	69
Table 2.9 Western Blotting Antibodies Used for this Study	71
Table 2.10 H2ax Immunofluorescence Staining Antibodies	72
Table 2.11 FISH Probes	74
Table 2.12 SALSA MLPA Kit	76
Table 4.1 Cut-off Values for Chromosome 11 Probes from Interphase Nuclei of Normal Blood Samples	136
Table 4.2 Number of Chromosome 11 Signals in Normal and Sarcoma Cell Lines	139
Table 4.3 Short Tandem Repeat (STR) Profiles of STS Included in this Study.....	154

List of Abbreviation

AIDS	Acquired Immunodeficiency Syndrome
AJCC	American Joint Committee on Cancer
ATLD	Ataxia-Telangiectasia Like Disorder
APS	Ammonium persulphate
A-T	Ataxia-Telangiectasia
ATM	Ataxia-Telangiectasia Mutated
ATR	Ataxia Telangiectasia and Rad3-related
BIR	Break Induced Replication
Bp	Base Pair
BS	Bone Sarcomas
BSA	Bovine Serum Albumin
CAK	CDK-Activating Kinase
CDKs	Cyclin Dependent Kinases
CEP11	Chromosome 11 centromere probe
CNA	Copy Number Aberrations
CO₂	Carbon Dioxide
CT	Computed Tomography
DAPI	4',6-Diamidino-2-Phenylindole
dHJs	Double Holliday Junctions
dH₂O	Distilled Water
DDLPS	Dedifferentiated Liposarcoma
D-loop	Displacement Loop
DMEM	Dulbecco's Modified Eagle's Medium

DNA	Deoxyribonucleic Acid
DNA-DSBs	DNA-Double-Strand Breaks
DNA-PKcs	DNA dependent Protein Kinase Catalytic Subunit
EBV	Epstein Barr Virus
EBV-SMT	EBV-Associated Smooth Muscle Tumours
ES	Ewing's sarcoma
ESFT	Ewing's Sarcoma Family Tumours
FASST2	Fast Adaptive States Segmentation Technique 2
FAT	Focal Adhesion Targeting
FISH	<i>Fluorescence In Situ Hybridization</i>
FNCLCC	Fédération Nationale des Centres de Lutte Contre le Cancer
GIST	Gastro-intestinal Stromal Tumours
Gy	Grays
HHV-8	Human Herpesvirus 8
HIV-1	Human Immunodeficiency Virus 1
HJ	Holliday Junction
HMM	Hidden Markov Model
HR	Homologous Recombination
H-RAS	Harvey-RAS
ICC	Interstitial Cells of Cajal
IR	Ionising Radiation
KD	Kilodalton
K-RAS	Kirsten-RAS
KS	Kaposi's Sarcomas
KSHV	Kaposi's Sarcoma-Associated Herpesvirus

Lig3/Lig1	Ligase
LMS	Leiomyosarcomas
LPS	Liposarcomas
LSI	Locus Specific Identifier
Lys3016	Lysine3016
MDM2	Murine Double Minute-2
MFH	Malignant Fibrous Histiocytomas
MFS	Myxofibrosarcomas
MLPA	Multiplex Ligation-dependent Probe Amplification
MPNST	Malignant Peripheral Nerve Sheath Tumour
MRI	Magnetic resonance imaging
MRN	MRE11-RAD50-NBS1
MSR	MultiScale Reference
mTOR	Mammalian Target Of Rapamycin
NBF	Neutral-Buffered Formalin
NBS	Nijmegen Breakage Syndrome
NF1	Neurofibromatosis Type I
NGS	Next-Generation Sequencing
NHEJ	Non-Homologous End Joining
nm	Nanometre
NOS	Not Otherwise Specified
N-RAS	Neuroblastoma-RAS
OS	Osteosarcomas
PBS	Phosphate Buffered Saline
PDGFRA	Platelet-Derived Growth Factor Receptor Alpha

PE	Plating Efficiency
PET	Positron Emission Tomography
PENT	Primitive Neuroectodermal Tumour
PFA	Paraformaldehyde
PI	Protease Inhibitor
Pikks	Phosphoinositide 3-Kinase-Like Kinases
PP2A	Phosphatase 2A
PPI	Phosphates Inhibitor Cocktail
Rb	Retinoblastoma
RMS	Rhabdomyosarcomas
ROS	Reactive Oxygen Species
RPA	Replication Protein A
Rpm	Revolutions Per Minute
RPMI	Roswell Park Memorial Institute Medium
SEM	Standard Error Of Mean
Ser376	Serine 376
SD	Standard Deviation
SDSA	Synthesis Dependent Strand Annealing
ssDNA	Single Stranded DNA
SF	Surviving Fractions
SQ	Serine/Glutamine
SMG1	Suppressor Of Mutagenesis In Genitalia1
STR	Short Tandem Repeat
STS	Soft Tissue Sarcomas
Tyr15	Tyrosine 15

TKI	Tyrosine Kinase Inhibitor
TQ	Threonine/Glutamine
TRRAP	Transformation/Transcription Domain-Associated Protein
UCLH	University College London Hospital
UICC	International Union against Cancer
UPS	Undifferentiated Pleomorphic Sarcoma
US	Ultrasonography
UV	Ultraviolet
V	Volt
WHO	World Health Organisation

CHAPTER ONE

1 INTRODUCTION

1.1 Sarcomas

Sarcomas are a heterogeneous and infrequent group of malignant tumours arising from cells of mesenchymal origin; they are non-epithelial tissues derived from the embryological mesoderm and neuro-ectoderm layers and account for about 1.2% of all malignancies in the UK. They affect both bones and soft tissues including fats, muscles, peripheral nerves, blood vessels, joints and deep skin tissues. Soft tissue sarcomas (STS) comprise the vast majority of diagnosed sarcomas, while primary bone sarcomas (BS) account for approximately 13% of sarcomas (Burningham et al., 2012, Fletcher et al., 2013, Toh et al., 2017). Although they are relatively rare, they represent a higher rate of cancer morbidity and mortality in paediatric cases and adolescents compared to their proportional representation in adults; that is, they give rise to 15% of all paediatric malignancies and less than 1% of all adult neoplasms (Thway, 2009, Fletcher et al., 2013). Sarcomas such as Ewing's sarcoma (ES), osteosarcomas (OS) and rhabdomyosarcomas (RMS) are more common in children and younger patients, while other tumours such as malignant fibrous histiocytomas (MFH), leiomyosarcomas (LMS) and liposarcomas (LPS) tend to occur more in older adults over 55 years of age (Dean and Whitwell, 2009, Toh et al., 2017).

The term "sarcoma" comes from the Greek word meaning fleshy (sarcos) tumour (oma). Histologically, sarcomas are a diverse group of tumour with more than 50 subgroups categorized according to the World Health Organisation (WHO) categorisation (Fletcher et al., 2013, Toh et al., 2017). Their classification is based on the type of differentiation they exhibit, and although some sarcomas show unknown histogenesis, others exhibit features resembling those of normal cells in mesenchymal tissue such as muscle in rhabdomyosarcomas, cartilage in chondrosarcomas, synovium in synovial sarcomas (SS) and adipose tissue in LPS (Figure 1.1). The scarcity and diversity of the tumour make sarcomas very difficult to study (Mackall et al., 2002, Osuna and de Alava, 2009, Francis et al., 2013).

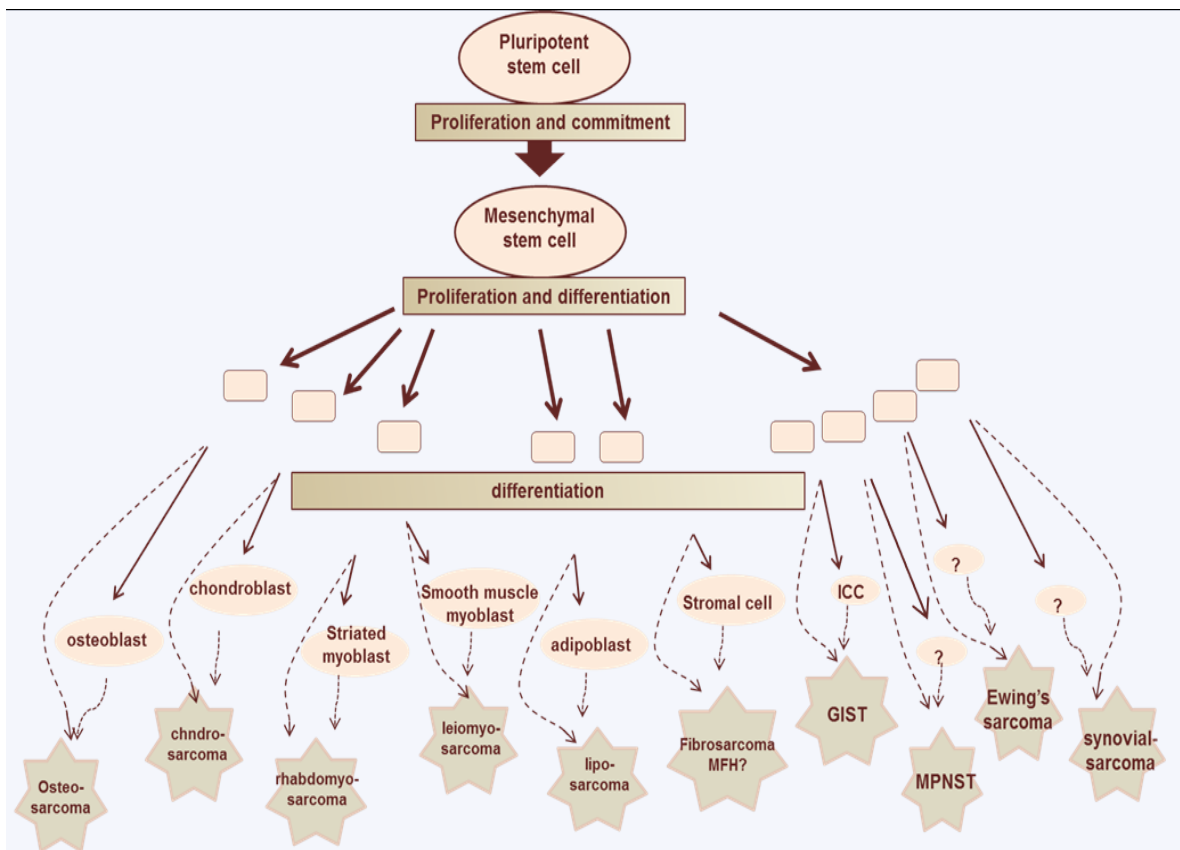


Figure 1.1 Sarcoma Cell Differentiation.

The progenitor cells for each lineage are shown in the orange boxes above. Solid lines illustrate the differentiation pattern of normal cells and dashed lines show the pathways for sarcomagenesis. The exact lineage for some sarcomas is still unknown including ES, SS and MPNST. ICC = Interstitial Cells of Cajal, GIST= Gastro-Intestinal Stromal Tumour, MPNST= Malignant Peripheral Nerve Sheath Tumour adapted from (Mackall et al., 2002).

1.2 Epidemiology and Incidence

The exact overall incidence of sarcomas is not accurately determined. However, recent estimates from WHO suggest the global incidence of STS at around 50 new diagnoses per million of the population annually without indication of any geographical differences (Ducimetiere et al., 2011, Fletcher et al., 2013). Sarcomas are infrequent entities compared to other neoplasms with only 3298 new cases of STS and 531 of BS diagnosed in the UK in 2010

(Fletcher et al., 2013, Francis et al., 2013, Toh et al., 2017). Several studies have reported that the increase in the rate of STS is assumed to be caused by the increase in the incidence of Kaposi's sarcomas (KS) among patients with acquired immunodeficiency syndrome (AIDS) or by an increase in the exposure to radiation and occupational carcinogens such as herbicides (Hoppin et al., 1999, Briggs et al., 2003, Francis et al., 2013).

STS can arise almost anywhere in the body and they are most commonly found in the large muscles of the extremities (up to 75%), the trunk (10%) and retroperitoneum (10%) (Fletcher et al., 2013, Francis et al., 2013). The frequency of STS increases with age, like most other tumours, and peaks in males aged 85 years or above. However, the impact of gender and age on the incidence rate of STS is unclear and depends on the histological subtypes of the tumours; for example, LMS frequently occur in females due to their uterine origin whereas RMS are commonly seen in young adults. Moreover, while the male-female ratio in the UK is about 1.9:1 for individuals older than 85 years of age, the incidence rate for STS in females aged between 45-59 years is somewhat greater than those in males, due to the higher number of gynaecological sarcomas in this age group (Toro et al., 2006, Ferrari et al., 2011, Fletcher et al., 2013, Francis et al., 2013, Toh et al., 2017).

Ethnicity is a well-described factor that influences disease occurrence. For example, OS are usually distributed through different racial groups unlike ES which occur predominantly in Caucasians, suggesting that there is a genetic component to ES (Dean and Whitwell, 2009, Worch et al., 2010). A recent study by Jacobs et al. (2017) found that black and Hispanic patients present with significantly advanced stage of paediatric sarcomas and have an overall worse survival than white patients, suggesting the existence of the ethnic and racial differences (Jacobs et al., 2017).

1.3 Sarcoma Aetiology

The pathogenesis of sarcomas has not been well understood however, it has been reported that a number of factors including environmental exposure, genetic susceptibility and an interaction between the two, plays an important role in the development of the disease (Dean and Whitwell, 2009, Burningham et al., 2012). Moreover, it seems that at least some types of sarcomas may initiate through a combination of defective DNA repair mechanisms, either by inherited or sporadic defects, and radiation exposure which itself induces DNA damage (So et al., 2009, Burningham et al., 2012).

1.3.1 Environmental Factors

1.3.1.1 Viral Infections

People with human immunodeficiency virus 1 (HIV-1) infection are at a higher risk of developing KS however, AIDS is not the main cause of KSs. Besides, there is strong evidence that Human Herpesvirus 8 (HHV-8), a sexually transmitted virus which is also termed Kaposi's sarcoma-associated herpesvirus (KSHV), is etiologically associated with KSs in HIV-positive patients, as these patients are frequently co-infected with HHV-8 resulting in KSs; however, the transmission of and risk factors associated with HHV-8 are not clear (Chang et al., 1994, Bagni and Whitby, 2009). Moreover, the ability of HHV-8 to lead to the development KSs in HIV-negative individuals has been documented, indicating the involvement of viral DNA in the tumour development process (Ziegler et al., 2003).

Epstein Barr virus (EBV) is similarly associated with the pathogenesis of STSs and is known to give rise to smooth muscle tumours (leiomyosarcomas) among AIDS patients and in those who are receiving therapeutic immunosuppression following transplantations (Rogatsch et al., 2000, Cheuk et al., 2002, Suwansirikul et al., 2012). Further, differences in the histological

characteristics between EBV associated smooth muscle tumours (EBV-SMT) and classic smooth muscle tumours have been reported (Deyrup et al., 2006, Suwansirikul et al., 2012).

1.3.1.2 Ionising Radiation

Ionising radiation (IR) given to treat other types of tumours can result in the development of secondary sarcomas, especially among patients under the age of 55 (Virtanen et al., 2006, De Smet et al., 2008) and in breast cancer patients who develop angiosarcomas of the breast (Lagrange et al., 2000). Sarcomas often develop in a previously irradiated field after a latency period of 3 to 20 years (Kirova et al., 2005) and there is a positive correlation between the dose and risk of sarcoma development; the higher the dose of radiation the patients were exposed to, the greater the risk of secondary sarcoma development in both adults (Rubino et al., 2005) and children (Menu-Branthomme et al., 2004). Post-radiation sarcomas predominantly occur in bone (osteosarcomas) however, STS can also occur (Fang et al., 2004, Dean and Whitwell, 2009). The risk of radiation-induced sarcomas has been highly linked to abnormalities in the tumour suppressor genes, *RB1* and *TP53* (Aerts et al., 2004, Gonin-Laurent et al., 2006).

1.3.1.3 Occupational and Chemical Exposure

Chronic exposure to certain chemicals such as vinyl chloride, which is used in making some types of plastics has been linked to the development of hepatic angiosarcoma (Makk et al., 1974). Beside the chemical exposure, several studies have revealed a significant increase in the risk of development of bone tumours among blacksmiths, machine tool operators, toolmakers and construction workers, suggesting an aetiological role of occupational factors (Hoppin et al., 1999, Merletti et al., 2006). Exposure to chlorophenol and cutting oil has also been associated with the development of STS specifically malignant fibrohistiocytic sarcomas and LMS; however, this association was not found in liposarcomas, suggesting the diversity of

occupational exposure among sarcoma subtypes (Hoppin et al., 1999). Although the association between chemical exposure and the development of sarcomas has been proven in many cases, others have found no evidence of these chemicals having an effect on the development of the disease (Huang et al., 2011).

1.3.1.4 Chronic Lymphoedema

Stewart-Treves syndrome is a rare and deadly cutaneous angiosarcoma that develops as a result of chronic and long standing lymphoedema. The syndrome was first described in 1948 in a woman who had chronic lymphoedema as a complication of the axillary lymph nodes removal following breast cancer treatment (Stewart and Treves, 1948, Mesli et al., 2017). Angiosarcoma has also been reported to develop in patients who had lymphoedema from different causes; however, this type of tumour is rarely seen in patients without lymphoedema (Sordillo et al., 1981, Mesli et al., 2017).

1.3.2 Genetic Factors and Sarcoma

Although the majority of sarcomas occur through sporadic mutations, there are some well characterised classic heritable syndromes that are associated with an increased risk of sarcoma namely neurofibromatosis, familial retinoblastoma and Li-Fraumeni syndrome (Mackall et al., 2002, Osuna and de Alava, 2009).

Neurofibromatosis Type I (NF1) also known as von Recklinghausen disease is a hereditary disorder that is caused by a mutation in the tumour suppressor gene *NF1*. It is commonly characterised by pigmentary changes in the skin, skeletal dysplasia, and benign neurofibromas. Patients with neurofibromatosis have a high risk of developing STS and particularly malignant peripheral nerve sheath tumours (MPNST) compared with normal

individuals (King et al., 2000, Korf, 2000, Brems et al., 2009). Other tumours such as gastrointestinal stromal tumours, breast cancer, somatostatinomas, and pheochromocytomas are also found in neurofibromatosis patients (Brems et al., 2009).

Familial retinoblastoma is a rare paediatric cancer of the eye caused by germline mutations in one allele of *RB1*, a tumour suppressor gene. Children diagnosed with retinoblastoma have an increased risk of developing secondary tumours and most commonly STS and BS. The tendency of sarcomas to develop has been attributed to both genetic susceptibility due to inactivation of the tumour suppressor gene *RB1* and past irradiation used to treat retinoblastoma (Dean and Whitwell, 2009, Kleinerman et al., 2012).

Another heritable syndrome, Li-Fraumeni is a rare autosomal dominant syndrome caused by germline mutations in the tumour suppressor gene, *TP53*. Individuals diagnosed with Li-Fraumeni syndrome are characterised by developing various number of malignancies with particularly high occurrence of STS, BS, brain tumours, breast cancer and adrenal cortical carcinoma at multiple primary sites; these tumours are typically diagnosed in patients before they reach 40 years of age (Ruijs et al., 2010).

1.4 Major Sarcoma Subtypes

1.4.1 Leiomyosarcomas

LMS are aggressive malignant tumours displaying different degrees of smooth muscle differentiation and represent a quarter of all STS; they can develop anywhere in the body including skin, deep soft tissues and are most frequently seen in the uterus or retroperitoneum. When uterine LMS are excluded, LMS are relatively rare, accounting for around 5-10% of all STS (Thway, 2009, Stiller et al., 2013).

While LMS are histologically similar, they have been classically subdivided into three groups based on their biological and clinical differences. LMS of the soft tissues form the most common and aggressive group, which can arise in the retroperitoneum and abdominal viscera; other sites of involvement include the peripheral and somatic soft tissue of the extremities (Weiss and Goldblum, 2001, Weiss, 2002). Retroperitoneal lesions are predominantly seen in females, possibly due to hormonal factors. They comprise the vast majority of all LMS and they frequently occur in the abdominal retroperitoneum, pelvic retroperitoneum and abdominal viscera. Retroperitoneal lesions are between 5-10cm in size when they are detected and this is because of their deep location and the different degrees of smooth muscle differentiation. Most patients with this group of disease die within the second and fifth years of the follow up period due to poor prognosis (Rajani et al., 1999, Weiss and Goldblum, 2001, Thway, 2009). Tumours deriving from peripheral or deep soft tissues of the extremities are less common and relatively smaller than retroperitoneal and affect both genders equally (Weiss and Goldblum, 2001, Farshid et al., 2002). The second group is the cutaneous LMS, which tend to occur more frequently in males between 50-70 years of age. They are quite small lesions and because of their superficial location they are associated with good prognosis (Andre et al., 2011). The last group consists of LMS of a vascular origin, which arise directly from major blood vessels, including the renal vein and inferior vena cava (Drukker et al., 2012, Shao et al., 2012).

1.4.2 Gastrointestinal Stromal Tumours

Gastrointestinal stromal tumours (GIST) are the most common sarcomas of the gastrointestinal tract, they are mainly seen in the stomach, followed by the small intestine, rectum, oesophagus, omentum and mesentery; they typically present in older patients between 55-60 years of age (Miettinen and Lasota, 2006). Previously, GIST were considered to be of smooth muscle origin

and they were therefore classified as leiomyomas, cellular leiomyomas, leiomyoblastomas, and leiomyosarcomas under the light microscope. However, electron microscopy and immunohistochemistry studies have shown no evidence of typical smooth muscle differentiation in some of these gastric neoplasms and some even show neural differentiation. For this reason, the term GIST is now used to describe mesenchymal tumours of the gastrointestinal tract (Mazur and Clark, 1983, Miettinen and Lasota, 2001, Fletcher et al., 2002a).

It has been suggested that GIST are derived from the intestinal cells of Cajal (ICC), the pacemaker cells of the gastrointestinal tract. ICC cells develop from smooth muscle cell precursors and form a complex network that coordinates slow wave activity within the gut. These cells express *c-kit* proto-oncogene, which encodes a membrane receptor tyrosine kinase (CD117) that can be detected by immunohistochemistry (Sanders et al., 1999, Graadt van Roggen et al., 2001, Ward and Sanders, 2001). The overwhelming majority of GIST patients, approximately 90% of cases harbour gain of function mutations in the *c-kit* gene. Patients without *c-kit* gene mutations have gain of function mutation in the platelet-derived growth factor receptor alpha gene (*PDGFRA*), which is another tyrosine kinase receptor (Isozaki and Hirota, 2006).

1.4.3 Ewing's Sarcoma

ES is the second most common bone and soft tissue malignancy after osteosarcomas and mainly affects children and young adults, with peak incidence at 15 years of age and males being more commonly affected than females (Riggi and Stamenkovic, 2007). It is one of the Ewing's sarcoma family tumours (ESFT); other members include peripheral primitive neuroectodermal tumour (PNET), Askin tumour and neuroepitheliomas. ES can develop

anywhere in the skeletal system primarily in the long bones, pelvis and in the bones of the chest wall but it can also develop in extra-skeletal sites, such as the deep soft tissues of the extremities, chest wall and paravertebral region. Histologically ES and ESFTs fall into a group of classical small round blue cell tumours of the bones (Arvand and Denny, 2001, Riggi and Stamenkovic, 2007, Slater and Shipley, 2007). Recent studies have shown that the knocking down of CD99, a cell surface protein highly expressed in patients with ES, results in differentiation of the neural ES cells and may reduce their ability to form tumours and bone metastases (Rocchi et al., 2010, Pasello et al., 2018).

1.4.4 Liposarcoma

Liposarcoma comprises around 20% of the sarcoma diagnosis and is the most common type of STS affecting older adults aged between 40 and 60. It may arise in fatty tissues however, its origin is believed to be an adipocyte progenitor. It can occur in almost any part of the body but most liposarcoma cases involve the extremities, particularly the thigh, followed by the abdominal cavity (Fletcher et al., 2002b). There are various subtypes of liposarcomas including well differentiated, myxoid, pleomorphic and dedifferentiated liposarcomas, each with its unique histological, biological and cytogenetic features and they range from non-metastasising neoplasms such as well differentiated liposarcoma to high grade sarcomas with high risk of metastases such as pleomorphic and dedifferentiated liposarcoma (Estourgie et al., 2002, Fletcher et al., 2002b, Gebhard et al., 2002, Hornick et al., 2004). Well differentiated is the most common form of this type of tumour accounting for 40-45% of all liposarcomas, whereas pleomorphic is a somewhat less occurring subtype and represents only 5% of all liposarcomas (Dei Tos, 2000, Fletcher et al., 2002b, Hornick et al., 2004). Myxoid liposarcoma has a highly specific pattern of metastasis especially in fat-bearing areas (Estourgie et al., 2002). Patients with this type of sarcoma often develop skeletal metastases in the spine and ribs. Non-skeletal

sites include the lungs, abdomen, and retroperitoneum (Schwab et al., 2007).

1.4.5 Angiosarcoma

Angiosarcomas are malignant tumours that occur in the inner lining of blood vessels. They are one of the rarest STS comprising of less than 1% of all sarcomas and they occur equally in men and women although rarely occur in children. The neoplasms can develop anywhere throughout the body but predominately occur in the skin and superficial soft tissue followed by the breast and rarely associated with major vessels (de Bree et al., 2002). Lymphoedema is the most widely known cause of angiosarcomas (Stewart and Treves, 1948) however, exposure to carcinogens such as vinyl chloride, arsenic and thorium dioxide (Thomas et al., 1975, Bolt, 2005) or previous radiotherapy used to treat breast cancer (de Bree et al., 2002, Torres et al., 2013) are all known risk factors.

1.5 Genetics Changes in Sarcomas

From a genetic point of view, sarcomas tend to fall into two major groups. Those with a simple or complex karyotype. Approximately 15-20% of sarcomas show relatively simple karyotypes with specific chromosomal translocations that give rise to fusion genes and act as specific markers for certain types of tumours. The group includes different sarcoma subtypes and around 30 translocations, most of which cause fusion genes (Table 1.2). In addition, small subsets in this group show specific oncogenic mutations such as the *KIT* mutations in GIST, deletions in rhabdoid tumours or amplifications in well-differentiated liposarcomas (Osuna and de Alava, 2009, Guillou and Aurias, 2010).

In translocation, certain genes are broken up, permitting the genetic material to be exchanged between two chromosomes and eventually generating gene fusions with new structures and

functions. Most of these gene fusions are believed to initiate the oncogenic events in many sarcoma types. About half of the fusion proteins that have been reported in STS are transcriptional factors up-regulating gene products that are responsible for tumour development; Ewing's sarcoma and synovial sarcomas are the best examples of chromosomal translocation (Osuna and de Alava, 2009, Guillou and Aurias, 2010). Recently, next-generation sequencing (NGS) technologies have aided in the discovery of novel chromosomal translocations and fusion genes in different tumors. The discovery of these novel fusion genes and the molecular events associated with them have led to the deduction of significant targets for novel therapeutic approaches in the treatment of sarcomas (Xiao et al., 2018).

Chromosomal translocations in Ewing's sarcoma are explained by the fusion of the *EWS* (*EWSR1*) gene that is located at 22q12 with a gene from the *ETS* family of transcription factors. The majority of ES cases (approximately 90%) are associated with the translocation t(11;22)(q24;q12) that results in the formation of *EWS-FLI1* fusion gene, in which *FLI1* is located at 11q24. A small fraction of the chromosomal translocations cases in this type of tumour (around 10%) are associated with translocation t(21;22)(q22;q12) which leads to the generation of a fusion gene called *EWS-ERG*, in which the *ERG* gene from 21q22 substitutes for *FLI* (Lessnick and Ladanyi, 2012).

Targeting the *EWS-FLI-1* breakpoint using antisense oligonucleotides and rapamycin has revealed their effectiveness in inhibiting tumour growth and inducing apoptosis (Mateo-Lozano et al., 2006). Moreover, RNA interference has been shown to downregulate the expression of the *EWS-FLI-1* protein sequence, suggesting its ability to treat ES (Takigami et al., 2011).

The second group comprises the majority of STS cases. They account for about 50% of all sarcomas and include most adult spindle cell/pleomorphic tumours. This group has very

complex unbalanced karyotypes with unspecific genetic alterations. Tumours that belong to this group include LMS, myxofibrosarcomas (MFS), pleomorphic subtypes of liposarcoma (PLPS), RMS, MPNST and undifferentiated pleomorphic sarcomas (UPS). Others are extraskeletal osteosarcomas, adult fibrosarcomas and angiosarcomas (Osuna and de Alava, 2009, Guillou and Aurias, 2010).

Many STS with complex genomic profiles such as LMS and UPS share very similar genomic aberration patterns of frequently amplified and lost sequences (Larramendy et al., 2006, Carneiro et al., 2009). MFS and PLPS are other examples displaying similarity in genomic abnormalities which are very different from those reported in LMS. Frequent copy number changes in specific regions of these four sarcoma subtypes are however very common including the amplifications in the short arm of chromosome 5 and deletion in 10q and 13q (Idbaih et al., 2005). The frequency of these changes in certain genomic regions has been attributed to the presence of oncogenes and tumour suppressor genes that are involved in tumour development (Helman and Meltzer, 2003).

Table 1.1 Chromosome Translocations and Fusion Genes in STS

Sarcoma Subtype	Translocations	Genes involved
Alveolar rhabdomyosarcoma	t(2;13)(q35;q14) t(1;13)(p36;q14)	<i>PAX3, FOXO1</i> <i>PAX7, FOXO1</i>
Alveolar soft part sarcoma	t(X;17)(p11;q25)	<i>TFE3, ASPL</i>
Angiomatoid fibrous histiocytoma	t(12;16)(q13;p11) t(12;22)(q13;q12) t(2;22)(q33;q12)	<i>ATF1, FUS</i> <i>ATF1, EWSR1</i> <i>CREB1, EWSR1</i>
Clear cell sarcoma	t(12;22)(q13;q12)	<i>ATF1, EWSR1</i>
Dermatofibrosarcoma protuberans	t(17;22)(q22;q13)	<i>COL1A1-PDGFB</i>
Desmoplastic small round cell tumour	t(11;22)(p13;q12) t(21;22)(q22;q12)	<i>WT1, EWSR1</i> <i>ERG, EWSR1</i>
Endometrial stromal sarcoma	t(7;17)(p15;q21) t(6p;7p)	<i>JAZF1, JJAZ1</i> <i>JAZF1, PHF1</i>
Ewing sarcoma/primitive neuroectodermal tumour	t(11;22)(q24;q12) t(21;22)(q22;q12) t(7;22)(p22;q12) t(2;22)(q33;q12) t(17;22)(q12;q12)	<i>FLI1, EWSR1</i> <i>ERG, EWSR1</i> <i>ETV1, EWSR1</i> <i>FEV, EWSR1</i> <i>ETV4, EWSR1</i>
Extraskeletal myxoid chondrosarcoma	t(9;22)(q21-31;q12) t(9;17)(q22;q11)	<i>NR4A3, EWSR1</i> <i>NR4A3, TAF15</i>
Infantile fibrosarcoma	t(12;15)(p13;q26)	<i>ETV6-NTRK3</i>
Inflammatory myofibroblastic tumour	2p23	<i>ALK fusions</i>
Low grade fibromyxoid sarcoma	t(7;16)(q32-34;p11) t(11;16)(p11;p11)	<i>FUS-CREB3L2</i> <i>FUS-CREB3L1</i>
Myxoid round cell liposarcoma	t(12;16)(q13;p11) t(12;22)(q13;q11-q12)	<i>DDIT3, FUS</i> <i>DDIT3, EWSR1</i>
Synovial sarcoma	t(X;18)(p11.2;q11.2)	<i>SSX1,2 or 4, SYT</i>

Table adapted from (Thway, 2009).

1.5.1 TP53 and RB1 Tumour Suppressor Genes

TP53 and *RB1* are the two main tumour suppressor genes which code for proteins that normally prevent tumourigenesis by regulating cellular proliferation. Abnormal regulation of these genes has a crucial role in the development of cancers; and alteration of both these tumour suppressor genes is commonly described in sarcomas (Sherr and McCormick, 2002,

Hanahan and Weinberg, 2011). Point mutations in the *p53* gene have been reported in OS and LMS, and the *RB1* gene has been found to be either rearranged or possess deletions in OS, ES and STS. Interestingly, the same study has reported that some of the OS cases with *RB1* alterations also had *p53* mutations (Miller et al., 1996). The murine double minute-2 (*MDM2*) in humans is an oncogene that regulates the activation of *p53* through its binding to the *p53* to form MDM2-*p53* complex that inhibits the function of *p53* and subsequently results in cancer development; *p53* and *mdm2* have been found to be frequently overexpressed in RMS (Klein and Vassilev, 2004, Takahashi et al., 2004).

1.5.2 RAS Oncogenes

Proto-oncogenes are normal genes that code for proteins responsible for cellular development. Some proto-oncogenes provide signals involved in cell division, while others control apoptosis. Mutations in proto-oncogenes lead to the alteration of normal proto-oncogenes into tumour inducing oncogenes such as the *RAS* oncogene (Hamm, 1998, Dang and Kim, 2018). The family members of the *RAS* gene include Harvey-*RAS* (*H-RAS*), Neuroblastoma-*RAS* (*N-RAS*) and Kirsten-*RAS* (*K-RAS*) genes that encode for the four highly homologous proteins, H-*RAS*, N-*RAS* and splice variants K-*RAS4B*/K-*RAS4A* (Hamm, 1998, Castellano and Santos, 2011). Mutations in the *RAS* genes are frequently found in human cancers where the activated *RAS* proteins cause the deregulation of cancer cell proliferation, cell death, metastasis and in angiogenesis (Gao et al., 2006, Langenau et al., 2007). Mutations in the *RAS* gene have also been found in STS and most commonly in RMS (Stratton et al., 1989, Liu et al., 2014). The cooperation between activated *K-RAS* and the deficiency of *TP53* has been recently associated with the development of RMS in a novel mouse model (Doyle et al., 2010). Furthermore, mutations in *K-RAS* have been detected in angiosarcomas and MFH, and *H-RAS* mutations have been found in MFH (Fernandez-Medarde and Santos, 2011). The frequency

of *H-RAS* and *K-RAS* mutations in STS is believed to range from 0-16% and 0-44% respectively however, the large range of this observation is attributed to the small size of samples and to the varied ethnic origin of patients. *N-RAS* mutations however are rarely seen in STS (Takahashi et al., 2004, Jin et al., 2010, Kodaz et al., 2017).

1.6 Diagnosis

STS frequently exist as an asymptomatic enlarged mass, with the size of which is mainly dependent on the anatomical site of the tumour. Superficial tumours and those present in the distal extremities or head and neck are commonly detected primary at a small size, whereas tumours in the proximal extremities and retroperitoneum may grow to a large size before they are detected, often as they have become symptomatic and produced pain as a result of the compression against nearby nerves, muscles or any other normal structures (Cormier and Pollock, 2004, Rastrelli et al., 2014).

Radiological imaging including computed tomography (CT), ultrasonography (US), plain radiography, magnetic resonance imaging (MRI) and positron emission tomography (PET) is the initial diagnostic tool for the soft tissue masses that may appear in any region. It is required to guide biopsy for histological diagnosis and to define the size and extent of the lesion for staging and for establishing the proper therapeutic options for the disease. Imaging in addition is critical in the follow-up stage to exclude local recurrence or metastasis and in prognostication (Cormier and Pollock, 2004, Aga et al., 2011, Rastrelli et al., 2014).

Because of the morphologic similarities between different subtypes of sarcomas as well as the heterogeneous sites of their origin, ancillary tests are also employed for obtaining a definitive diagnosis. These include immunohistochemical stains, cytogenetic and molecular genetic

techniques (Thway, 2009, Banerjee et al., 2013). The rarity of the disease combined with it being very morphologically diverse makes the accurate diagnosis for sarcomas significantly challenging for both clinicians and pathologists. Understanding the genetic features of these tumours have helped in obtaining a definitive diagnosis and clinical management as well as establishing the proper therapeutic options for the disease (Bovee and Hogendoorn, 2010, Rastrelli et al., 2014).

1.7 Grading and Staging

Usually taking a biopsy from the lesion is highly preferred to provide a definitive diagnosis and to give an indication of the histology and type of sarcoma, particularly when it is performed in conjunction with clinical and imaging studies. However, the histological diagnosis of sarcoma may not provide sufficient information to predict the prognosis in most STS. Some other factors including grade, depth and size of the tumour are also essential for providing an accurate estimation of prognosis and planning therapy (Grobmyer and Brennan, 2003, Coindre, 2006).

The most common grading system used for STS is the French Sarcoma Group or Fédération Nationale des Centres de Lutte Contre le Cancer (FNCLCC) and is based on the Trojani system (Trojani et al., 1984). The parameters that define the FNCLCC grading system are the degree of tumour differentiation, extent of tumour necrosis and the mitotic index (Table 1.2). A scoring of 1 to 3 is used for tumour differentiation (lower score means cells are very similar to the normal cells) and also for mitotic index (lower score means fewer cells are dividing) and 0 to 2 for necrosis. Grade 1 is a total of 2 or 3 (scores are added together from each parameter), grade 2 is a total of 4 or 5 and grade 3 is a total of 6 or more (Trojani et al., 1984, Coindre, 2006).

Table 1.2 FNCLCC Soft Tissue Sarcomas Grading System

Histological Parameter	Score and Description
Tumour differentiation	<p>Score 1: Sarcomas closely resembling normal adult mesenchymal tissue (e.g. well-differentiated liposarcoma)</p> <p>Score 2: Sarcomas for which histological typing is certain (e.g., myxoid Liposarcoma)</p> <p>Score 3: Embryonal and undifferentiated sarcomas, sarcomas of doubtful type, synovial sarcomas, osteosarcomas, PNET.</p>
Mitotic count	<p>Score 1: 0-9 mitoses per 10 HPF*</p> <p>Score 2: 10-19 mitoses per 10 HPF</p> <p>Score 3: ≥ 20 mitoses per 10 HPF</p>
Tumour necrosis	<p>Score 0: No necrosis</p> <p>Score 1: < 50% tumour necrosis</p> <p>Score 2: ≥ 50% tumour necrosis</p>
<i>Histological grade</i>	<p>Grade 1: Total score 2,3</p> <p>Grade 2: Total score 4,5</p> <p>Grade 3: Total score 6, 7, 8</p>

* HPF: High Powered Field. Table adapted from (Coindre, 2006).

Staging of STS mainly relies on both histological and clinical information. The most commonly accepted STS staging system is the TNM which has been produced jointly by the American Joint Committee on Cancer (AJCC) and International Union against Cancer (UICC). This system incorporates tumour size, depth, lymph nodes involvement and distant metastases with tumour grade (Table 1.3) (Fletcher et al., 2013, Dangoor et al., 2016).

Table 1.3 TNM Soft Tissue Sarcomas Staging System

Parameter	Description
Primary tumour (T)	
TX	Primary tumour cannot be assessed
T0	No evidence of primary tumour
T1	Tumour ≤ 5cm in greatest dimension
	T1a superficial tumour
	T1b deep tumour
T2	Tumour > 5cm in greatest dimension
	T2a: superficial tumour
	T2b: deep tumour
Regional lymph nodes (N)	
NX	Regional lymph nodes cannot be assessed
N0	No regional lymph node metastasis
N1	Regional lymph node metastasis
Distant metastasis (M)	
M0	No distant metastasis
M1	Distant metastasis
Grading	Grade 1 (FNCLCC) = Low grade Grade 2 and 3 (FNCLCC) = High grade
TNM Staging System	<p><u>Stage IA</u></p> <p>T1a N0, NX M0 Low grade T1b N0, NX M0 Low grade</p> <p><u>Stage IB</u></p> <p>T2a N0, NX M0 Low grade T2b N0, NX M0 Low grade</p> <p><u>Stage IIA</u></p> <p>T1a N0, NX M0 High grade T1b N0, NX M0 High grade</p> <p><u>Stage IIB</u></p> <p>T2a N0, NX M0 High grade</p> <p><u>Stage III</u></p> <p>T2b N0, NX M0 High grade</p> <p><u>Stage IV</u></p> <p>Any T N1 M0 Any grade Any T Any N M1 Any grade</p>

Table adapted from (Fletcher et al., 2013, Dangoor et al., 2016).

1.8 Treatment of Sarcomas

The treatment of sarcomas is mainly aimed to provide long-term survival, avoid local recurrence and minimise the chance of morbidity. These goals are achieved with surgery which is the standard therapeutic modality for the majority of adults with STS in the UK, along with the combination of radiation and/or chemotherapy however, the treatment for advanced STS patients is still limited (Grimer et al., 2010, Parida et al., 2012, Shingler et al., 2013).

1.8.1 Surgery

The wide surgical resection approach that implies excision of the primary tumour with a rim of 1cm or equivalent of the normal soft tissues, combined with post-operative radiotherapy is primarily used in the UK to treat STS, particularly tumours of the limbs and trunk; maintaining the optimal functions in the absence of metastasis (Grimer et al., 2010, Rastrelli et al., 2014, Dangoor et al., 2016). Sometimes, the ability of sarcomas to develop beside the muscle bundles and beyond the tumour mass boundaries elucidates the high frequency of the tumours recurrence even after wide surgical resection (Singer et al., 2000, Wunder et al., 2007).

In patients with metastatic disease, surgical excision is appropriate as a mainstay treatment; however; radiotherapy or chemotherapy may be more suitable depending on many factors such as the patient's likely prognosis, symptoms (pain or ulceration), comorbidity, the extent of metastasis, histological subtype and expected morbidity following surgery (Grimer et al., 2010, Rastrelli et al., 2014, Dangoor et al., 2016).

1.8.2 Radiotherapy

Radiotherapy has been used as a primary local control of STS and as adjuvant therapy following surgical excision. It can be either as external beam radiation pre- or post-operatively, internal radiotherapy by implanting the radioactive source in the centre of the tumour “brachytherapy” or as a combination of both. The pre-operative radiation therapy is administered at a dose of 50 Grays (Gy) and can be used in difficult surgical locations such as the head and neck, and for certain radiosensitive sarcoma subtypes such as myxoid liposarcomas to shrink the size of the tumour and to improve the possibility of achieving surgical margins (O'Sullivan et al., 2002, Wunder et al., 2007, Dangoor et al., 2016). Although the dose of post-operative radiotherapy is higher (66Gy), it is considered the standard adjuvant modality for the majority of patients with intermediate and high-grade STS as it avoids any delays in the definitive surgery that are caused by pre-operative radiotherapy (Grimer et al., 2010, Dangoor et al., 2016).

Proton beam therapy is a highly advanced method of delivering high dose radiotherapy that precisely targets the tumour whilst reducing dose and damage to the surrounding normal tissue. The treatment involves high energy proton beam rather than high energy of X-rays and is considered to be extremely effective for treating patients with cancer, particularly rare tumours including STS in both children and adults. Now two new facilities are being built in the UK at The Christie NHS Foundation Trust (Manchester) and University College London Hospital (UCLH) NHS Foundation Trust and are due to launch from 2018 at The Christie and in 2019 from UCLH (Dangoor et al., 2016, DeLaney and Haas, 2016).

1.8.3 Chemotherapy

Adjuvant chemotherapy may improve the survival rate, shrink a tumour or at least delay the local recurrence in high risk patients. However, it is not routinely recommended since its benefits have had limited success. The neoadjuvant chemotherapy in contrast, is indicated as a primary treatment for certain types of tumours such as ES and RMS. The histological subtype of STS together with age and comorbidity of the patient helps to determine whether chemotherapy would be valuable to treat the sarcomas, since certain types have been shown to be more chemo-sensitive than others (Singer et al., 2000, Grimer et al., 2010, Dangoor et al., 2016). Doxorubicin and ifosfamide are the first line treatment for most histological subtypes of advanced STS cases except GIST and have shown the ability to give an overall response in the range of 10–25%. The combination of both drugs gives a somewhat higher response than with doxorubicin alone (Milano et al., 2006, Seddon et al., 2017).

1.8.4 Molecular Targeted Therapy

Molecular targeted therapy has had a great impact on the treatment of specific STS subtypes especially GIST. Most of the GIST associated with the *c-kit* or *PDGFRA* mutations are sensitive to the imatinib tyrosine kinase inhibitor (TKI); however, the development of secondary *c-kit* or *PDGFRA* mutations show resistance to imatinib (Kitamura, 2008, Beham et al., 2012). A multi-targeted receptor TKI “sunitinib malate” has been shown to be effective in treating the imatinib-resistant GIST and to give a superior survival rate with a continuous daily dose of 50mg compared with placebos in patients with metastatic GIST (Demetri et al., 2006, George et al., 2009). Other active multi-kinase inhibitor agents have been developed including nilotinib and sorafenib and are now used to treat patients with imatinib/sunitinib-resistant GIST (Kim et al., 2011, Montemurro et al., 2013).

1.9 DNA Damage and Repair

DNA is under constant assault from endogenous and exogenous DNA damaging agents. The majority of the endogenous DNA damage arises from errors that may happen during DNA replication and from normal cellular metabolic products such as reactive oxygen species (ROS), which have the ability to attack the DNA backbone and break the phosphodiester bonds resulting in loss of nucleotide bases (Kastan and Bartek, 2004, Jackson, 2009, Perrone et al., 2016). Exogenous DNA damage on the other hand, occurs as a result of exposure to environmental factors including tobacco smoke, ultraviolet light (UV), X-rays, IR and chemotherapeutic drugs (Jackson, 2009, Chatterjee and Walker, 2017).

Cells have evolved a number of different DNA damage detection and repair systems that have the ability to repair the vast majority of DNA damage efficiently and therefore maintaining genomic stability (Jackson, 2009, Derheimer and Kastan, 2010). The DNA damage response is mediated by two parallel signal transduction pathways that involve two master kinases, ATM (ataxia telangiectasia mutated) and ATR (Ataxia Telangiectasia and Rad3-related) protein kinases that recognise different types of DNA damage. The former is activated via DNA double-strand breaks (DSBs), whereas the latter is reported to be recruited to the sites of single-strand breaks (ssDNA) (Stiff et al., 2006).

Tumourigenesis is driven by a high level of genetic instability through unrepaired or misrepaired DNA damage causing mutations. Furthermore, metastatic potential is highly associated with an overexpression of repair proteins. Therefore, the study of DNA repair systems plays a critical role in understanding the oncogenesis process and in protection from cancer development. The identification of the molecular pathways and key proteins involved during

DNA repair have been reported; however, much remains to be learnt about DNA repair mechanisms (Sarasin and Kauffmann, 2008).

1.9.1 Ataxia Telangiectasia Mutated Gene (*ATM*)

ATM was initially identified in 1995 as the gene mutated in Ataxia-Telangiectasia (A-T), a rare human autosomal recessive disorder that is characterised by progressive cerebellar degeneration, immunodeficiency, hypersensitivity to IR, chromosomal instability, cell cycle checkpoint defects and an increased risk of cancer development (Savitsky et al., 1995, Lee and Paull, 2007). *ATM* is a large gene located on chromosome 11q22-23. It has 66 exons encoding a 13kb transcript, encoding a 370-kDa protein consisting of 3056 amino acids (Rotman and Shiloh, 1998, Derheimer and Kastan, 2010).

ATM is a serine/threonine protein kinase and is a member of the phosphoinositide 3-kinase-like kinases (PIKKs), a large family that is involved in signalling following cellular stress including DNA damage. The PIKKs family also includes ATR, DNA dependent protein kinase catalytic subunit (DNA-PKcs), mammalian target of rapamycin (mTOR), suppressor of mutagenesis in genitalia1 (SMG1) and finally, the transformation-/transcription domain-associated protein (TRRAP), a transcriptional co-activator that lack ATP binding residues necessary for kinase activities. Structurally, members of the PIKKs family share common domains that distinguish them from other protein kinases (Figure 1.2). These domains are from N-terminal to C-terminal, long α -helical HEAT repeats (Huntingtin, Elongation factor 3, protein phosphatase 2A, and Yeast target of rapamycin; aa 1-1959), followed by FAT domain (FRAP-*ATM*-TRRAP; aa 1960–2566), KD (PI-3 kinase like kinase domain ;aa 2712–2962) and the FAT-C domain (FRAP, *ATM* and TRRAP C-terminal; aa 2963– 3056) (Figure 1.2) (Perry and Kleckner, 2003, Lavin, 2008, Lempiainen and Halazonetis, 2009, Sibanda et al., 2010). The

characteristic feature of this protein family is that they phosphorylate their target proteins preferentially on serine or threonine residues followed by glutamine and are recognised as SQ (serine/glutamine) or TQ (threonine/glutamine) motifs (Shiloh and Ziv, 2013). ATM protein is expressed in several tissues such as the nervous system, spleen and thymus and is shown to be essentially involved in signal transduction and cell cycle checkpoint response following DNA damage (Chen and Lee, 1996).

A recent study carried out at the University of Sheffield revealed for the first time a deletion in *ATM* with decreased and/or absent ATM protein expression in GIST and LMS, suggesting the involvement of the ATM in the biology of sarcomas (Ul-Hassan et al., 2009).

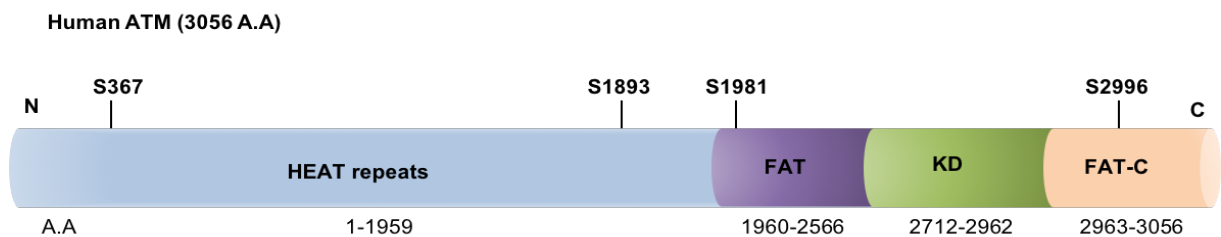


Figure 1.2 Schematic Representations of ATM Kinase Protein Structure.

The N-terminal is largely occupied by the heat repeats. The KD domain is located near to the C-terminus and is flanked by the conserved FAT (FRAP-ATM-TRRAP) and FAT carboxy-terminal (FAT-C) domains. The positions of the ATM auto-phosphorylation on serine residues (S367, S1893, S1981 and S2996) are illustrated. Figure created from (Perry and Kleckner, 2003, Lavin, 2008, Lempiainen and Halazonetis, 2009, Sibanda et al., 2010).

1.9.2 Role of ATM in the DNA Damage Response

ATM subsists normally as an inactive dimer or higher-order multimer inside the nucleoplasm until DNA damage occurs by e.g IR, upon which the DNA-DSBs is generated allowing the dissociation of the inactive ATM dimer into the active monomers through intermolecular auto-

phosphorylation on (Ser376, Ser1893, Ser1981 and Ser2996) sites (Figure 1.3) (Bakkenist and Kastan, 2003, So et al., 2009, Kozlov et al., 2011).

Although ATM auto-phosphorylation on serine residues sites is known as a marker for its activation, previous studies have demonstrated that these sites are dispensable for ATM activation by DNA damage in a mouse model expressing the mutated ATM with alanine substitute at Ser1987 (Ser1981 in human) and two other auto-phosphorylation sites; however, other studies showed the disruption in the ATM activation in human cells harbouring an ATM mutation with an alanine substitution at Ser1981 (Pellegrini et al., 2006, Daniel et al., 2008, So et al., 2009, Guo et al., 2010).

The exact process of ATM activation is still controversial. While some authors have revealed that ATM activation occurs in response to chromatin changes following DNA-DSBs rather than direct contact with DNA (Bakkenist and Kastan, 2003). Others have suggested that direct contact with DNA-DSBs end is essential for the ATM to be activated (You et al., 2007).

ATM is also reported to undergo other important post-translational modifications upon DNA damage including its acetylation at lysine 3016 (Lys 3016) by TIP60 histone acetyltransferase that is shown to be necessary for its activation (Lavin, 2008). Phosphatases such as protein phosphatase 2A (PP2A), PP5 and WIP1 have also been shown to contribute to the process of ATM activation by removing phosphate from the ATM auto-phosphorylation site (Goodarzi et al., 2004, Shreeram et al., 2006, Lavin, 2008). Moreover, the MRE11-RAD50-NBS1 (MRN) complex is essential for an optimal activation of ATM. Once the DNA-DSBs is generated, ATM is recruited toward the break site by the MRN complex through the direct interaction of the ATM with the C-terminus tail of NBS1. This complex also functions as a sensor for DNA-DSBs and

is one of the first protein complexes to be localised at the DNA-DSBs sites (Lee and Paull, 2005, Derheimer and Kastan, 2010). A reduction in ATM activation and the absence of ATM recruitment towards the DNA-DSBs sites was detected in patients with ataxia-telangiectasia like disorder (ATLD) and Nijmegen breakage syndrome (NBS) who harbour germline hypomorphic mutations in *hMre11* and *NBS1* genes respectively; both diseases have similar phenotypes to A-T, suggesting the important function of the MRN complex in ATM activation (Stewart et al., 1999, Uziel et al., 2003).

Upon recruitment, the activated ATM phosphorylates over 700 of downstream substrates such as, TP53, Chk2, BRCA1, NBS1, SMC1 and Artemis all of which are involved in cell cycle arrest, DNA repair and cell death. Most notably, ATM phosphorylates histone H2AX at Ser139. The phosphorylated H2AX termed (γ H2AX) form foci covering many megabases of chromatin directly surrounding DNA-DSBs within a short time following IR thus, γ H2AX molecules are considered as an effective marker for chromatin damage and DNA-DSBs (Burma et al., 2001, Nakamura et al., 2010).

H2AX has a significant role in the recruitment of a large number of DNA repair proteins towards DNA-DSBs such as MDC1. MDC1 protein has also shown to be necessary for the activation of ATM and it is believed to function as an adaptor that facilitates the assembly of more ATM target proteins on the damaged DNA, including those involved in the cell cycle checkpoint activation process (TP53 and Chk2) and proteins responsible for DNA repair of DSBs (Ku70/80, DNA-PKcs, XRCC4/DNA ligase IV complex) (Riballo et al., 2004, Lee and Paull, 2007, Lavin, 2008, Wang et al., 2011).

Although ATM is known to be the key protein kinase responsible for the activation of H2AX in the early response to DNA-DSBs, other members of the PIKKs family including ATR and DNA-PKcs are capable of phosphorylating H2AX and Chk2 proteins (Wang et al., 2005, Zannini et al., 2014). Previous studies have shown that mice deficient in either DNA-PKcs or ATM are viable however, mice with double deficiency are embryonic lethal phenotype. Cells show severe impairments in the DNA damage response and DNA repair mechanisms (Gurley and Kemp, 2001, Sekiguchi et al., 2001, Zha et al., 2011).

1.9.3 Inhibition of ATM

The signalling function of the ATM protein has been comprehensively reviewed above however, the possibility for ATM to have functions other than its kinase activity is still unknown. Several ATM kinase inhibitors have been developed and used in many studies (Batey et al., 2013, Golding et al., 2009, Hickson et al., 2004, Rainey et al., 2008). Caffeine (methyl xanthine) has been shown to inhibit the functions of both ATM and ATR and sensitises cancer cells to the harmful effects of genotoxic modalities, mainly ionising radiation (Weber and Ryan, 2015). Even though caffeine is an experimental tool used in *in-vitro* studies, it is not suitable to be used as a radiosensitising agent clinically because of the systemic toxicity at the doses that are needed for radiosensitisation (Weber and Ryan, 2015). Wortmannin is a potent radiosensitiser that is known to inhibit both ATM and DNA-PKcs (Rosenzweig et al., 1997). However, wortmannin is similar to caffeine in producing a very high systemic toxicity; also they both are lacking selectivity which is the reason why further improvement of this drug has been delayed in a clinical setting (Karve et al., 2012).

The first potent inhibitor specifically targeting ATM kinase was identified in 2004 and named KU55933 (2-morpholin-4-yl-6-thianthren-1-yl-pyran-4-one) (Hickson et al., 2004). KU55933

inhibitor was reported to maximally increase the cytotoxicity effect of the radio/chemotherapeutic agents in cancer cells (Hickson et al., 2004). CP466722 [2-(6, 7-dimethoxyquinazolin-4-yl)-5-(pyridin-2-yl)-2H-1,2,4-triazol-3-amine] was identified in 2008 to be a potent and reversible inhibitor of ATM kinase, that did not inhibit PI3K or any related members (Rainey et al., 2008). It has been reported that CP466722 is able to block the signalling of ATM dependent downstream substrates resulting in G2/M cell cycle arrest. CP466722 and the previously mentioned KU55933 inhibitor display similarity in rapidly and effectively inhibiting ATM for up to several hours (Rainey et al., 2008). Additionally, KU60019 (2-[(2R, 6S)-2,6-dimethylmorpholin-4-yl]-N-[5-(6-morpholin-4-yl-4-oxo-4H-pyran-2-yl)-9H-thioxanthen-2-yl]-acetamide) was identified in 2009 as a developed analogue of KU55933 and has been shown to be more efficient at blocking ATM dependent phosphorylation events and to be approximately ten times more potent than KU55933 in the radiosensitisation of human glioma cells (Golding et al., 2009, Golding et al., 2012). Recently, the role of KU-59403 has been described in the inhibition of ATM. KU-59403 has improved potency over KU-55933 and shows superior solubility and bioavailability which allows its usage in studying the effects of pharmacological ATM inhibition in animal models of human cancer. This compound also demonstrated an excellent tissue distribution after its administration in mice model and was found to significantly increase anti-tumour activity of the topoisomerase inhibitors (Batey et al., 2013).

It has been reported previously that the treatment of ATM wildtype cells by these inhibitors is effective in blocking ATM dependent phosphorylation events and increasing radio/chemosensitisation of cells to DNA damaging agents (Hickson et al., 2004, Rainey et al., 2008, Golding et al., 2009, Batey et al., 2013). However, other studies have proposed that the inhibition of the ATM kinase activity may be contributing to the initiation of further defects in

DNA repair that were not seen in ATM deficient cells, suggesting a potential structural function of ATM in DNA repair (White et al., 2010, Shiloh and Ziv, 2013).

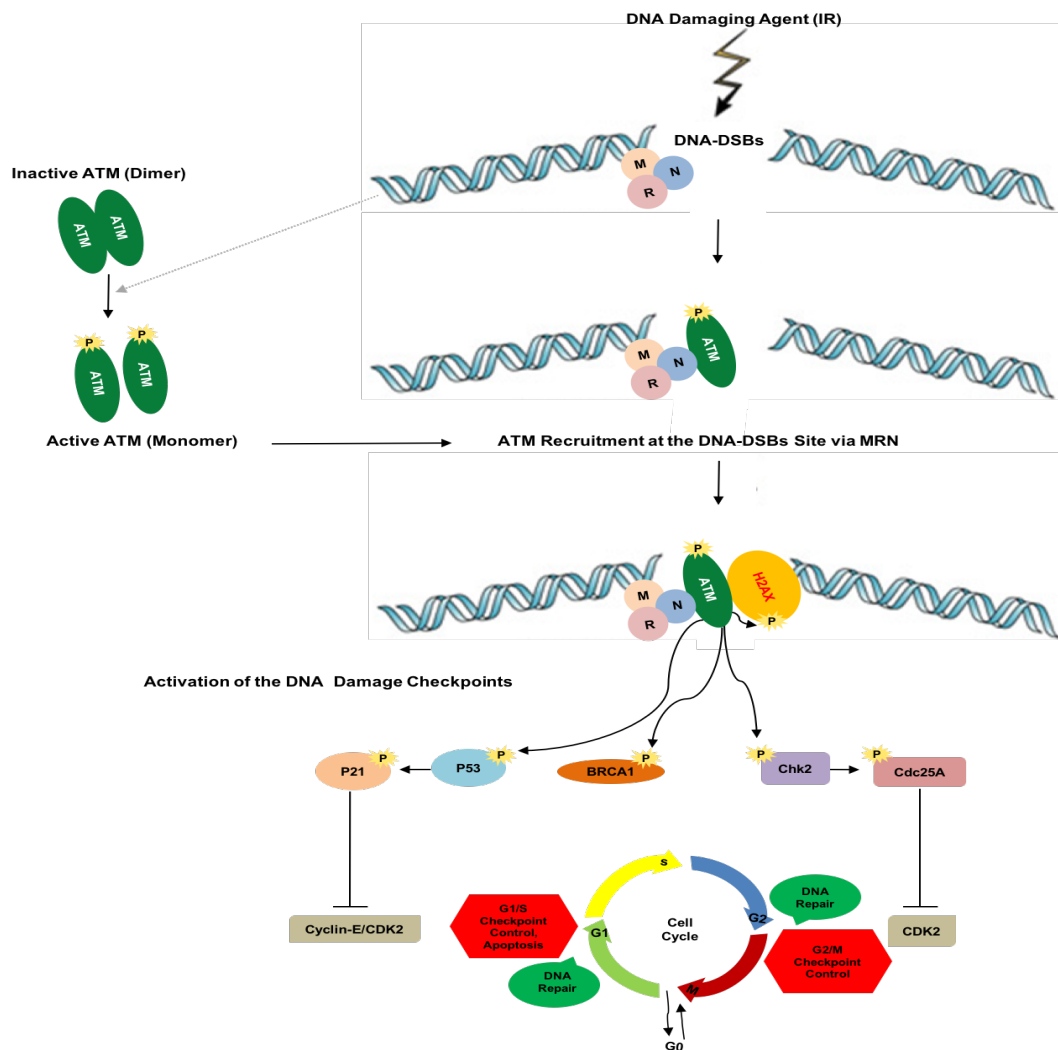


Figure 1.3 Schematic Model of How Cells Respond to DNA-DSBs.

Upon DNA-DSBs formation, ATM localises towards the break site by MRX complex, then it phosphorylates a number of key proteins including H2AX, TP53, BRCA1 and Chk2 which results in the activation of DNA damage checkpoints and subsequently leads to apoptosis or DNA repair. Figure created from (Stewart et al., 1999, Bakkenist and Kastan, 2003, Lee and Paull, 2007, Nakamura et al., 2010, Wang et al., 2011).

1.9.4 Cell Cycle

To maintain genomic stability and ensure correct transmission of undamaged and fully replicated DNA, it is essential to accurately control cellular growth and division through the cell cycle. In eukaryotes, the cell cycle consists of four distinct active phases; gap 1 phase (G1), synthesis phase (S), gap 2 phase (G2) and mitosis phase (M). In G1 phase, cells grow in preparation for DNA replication. In S phase, DNA replication takes place to create two identical copies of the cellular genome. G2 is the gap phase between DNA replication and mitosis phase, giving time for cells to be prepared for successful division. Finally, in M phase, cells stop growing and they undergo mitosis where they split their duplicated contents and divide themselves into two distinct daughter cells, each with a full copy of DNA. The cells then either re-enter the cell cycle or stop dividing and leave the cycle to enter the state of quiescence called the resting phase (G0), the fifth phase of the cell cycle (Swanton, 2004, Wang et al., 2011).

In normal cells, the development through each of the cell cycle phases and the transition from one phase to the next is precisely controlled by a complex network of regulatory proteins known as checkpoints. In response to DNA damage, the checkpoints initiate a cascade of events to accelerate DNA repair or arrest the cell cycle. Failure in the regulatory pathways of these checkpoints can lead to genomic instability and loss of cell cycle control which eventually leads to the development of serious diseases including cancer. Checkpoints exist at the G1/S, intra-S, and G2/M transitions, and are controlled by signalling pathways involving both kinases and phosphatases (Morgan, 2007, Hochegger et al., 2008, Wang et al., 2011).

1.9.4.1 Cell Cycle Regulation

Cyclin dependent kinases (CDKs) are proteins involved in the mitotic activity, proliferation and cellular growth throughout the cell cycle. CDKs are mainly regulated through activation of the phosphorylation process at their threonine 161 (Thr161) site by CDK-Activating Kinase (CAK). The inhibitory phosphorylation at Thr14 and tyrosine 15 (Tyr15) sites by Wee1 and MYT1 kinases is also necessary for the CDKs regulation. The phosphatase Cdc25A molecule removes the inhibitory phosphates from CDKs to reactivate it (Figure 1.4) (Morgan, 2007, Hochegger et al., 2008).

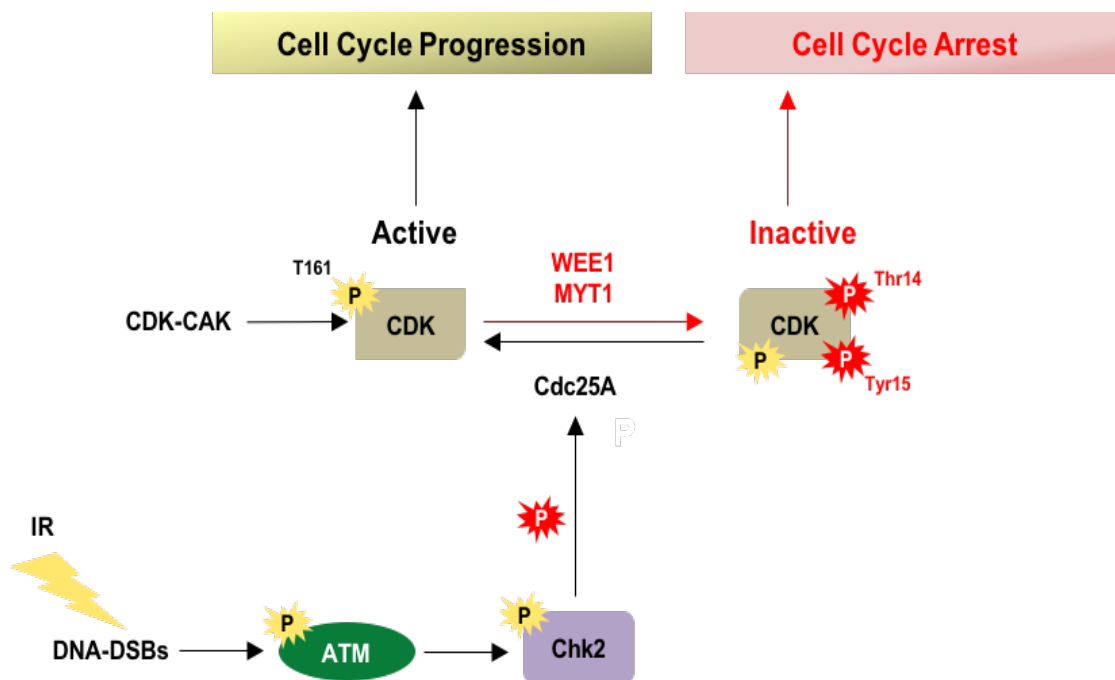


Figure 1.4 Cell Cycle Regulation.

The Phosphorylation and de-phosphorylation process mediated by multiple kinases and phosphatases control the progression of the cell cycle by regulating CDK activation. CDK-Activating Kinase (CAK) constitutively conserve the activation of CDK to stimulate cellular growth. Once the DNA-DSBs is generated, checkpoints are activated by the ATM which activates Chk2 to prevent CDK activity. The activating phosphorylation processes are shown in yellow, while red colour illustrates inhibitory phosphorylation. Figure created from (Morgan, 2007, Hochegger et al., 2008).

1.9.4.2 ATM and the DNA Damage Checkpoint Activation

The decision as to whether the cells have to proliferate or arrest is made by the first checkpoint G1. The tumour suppressor protein (TP53) has been found to be an essential protein in this checkpoint due to its role in determining the final fate of the cells following DNA-DSBs. TP53 is capable to shift between the induction of the cell cycle arrest, thus permitting DNA-DSBs repair and initiating of apoptosis which may be necessary if the DNA damage is very extensive (Bree et al., 2004, Wang et al., 2011). Normal mammalian cells express TP53 at low levels due to its interaction with MDM2 protein that targets TP53 for proteasomal degradation inside the cytoplasm. Once the DNA is damaged, ATM induces the levels of TP53 through phosphorylation on Ser15. The induction of TP53 leads to trans-activation of other important proteins including p21 that prevents the formation of cyclin-E/CDK2 complex and eventually avoids the progression from G1 into S phase via G1 checkpoint arrest. ATM also phosphorylates Chk2 protein following DNA damage, which can then phosphorylate TP53 on serine 20 promoting its dissociation from MDM2 and thus triggering its activation (Figure 1.3) (Dumaz and Meek, 1999, Bartek and Lukas, 2001, Maya et al., 2001, Wang et al., 2011).

The intra-S checkpoint acts as a monitor for cell cycle and slows the DNA replication process following DNA damage. ATM is the major player in this checkpoint. In response to DNA damage, ATM phosphorylates several proteins including NBS1 and Chk2 and enhances two pathways of the DNA damage response to activate the intra-S checkpoint. These are ATM-Chk2-Cdc25A and ATM dependent NBS1/BRCA1/SMC1 cascades. ATM has been shown to phosphorylate BRCA1 on Ser1387 site to arrest intra-S checkpoint however, the mechanism of these two cascades is not fully understood (Figure 1.3) (Falck et al., 2002, Xu et al., 2002, Wang et al., 2011).

The G2 checkpoint avoids the separation of damaged DNA into two daughter cells. The activation of this checkpoint is mainly initiated by ATM and ATR that activate their substrate Chk2 and Chk1, respectively, depending on the type of the damage induced. The activated Chk2/Chk1 proteins prevent cellular proliferation through the phosphorylation of phosphatase Cdc25A on Ser216 to inactivate it, thus preventing the activation of the CDKs molecules and leading to G2 checkpoint arrest (Figure 1.3 and 1.4) (Peng et al., 1997, Morgan, 2007, Hochegger et al., 2008, Wang et al., 2011).

1.9.4.3 DNA-DSBs Repair Pathways

DNA is vulnerable to the damage throughout the cell cycle and this damage needs to be accurately and efficiently repaired in order to maintain genomic integrity. There are two distinct DNA-DSBs repair pathways in eukaryotic cells; homologous recombination (HR) and non-homologous end joining (NHEJ). The NHEJ pathway is known to have a vital role in all phases of the cell cycle, specifically in G1 and early S phase, while the importance of HR is predominantly in late S and G2 phase (Takata et al., 1998, Shrivastav et al., 2008, Hanahan and Weinberg, 2011).

1.9.4.3.1 Homologous Recombination

HR is perceived as an error-free repair mechanism because it uses the genetic information which becomes available following replication on the undamaged sister chromatid as a template. The repair pathway is initiated through the recognition of the DNA-DSBs damage by ATM, which activates multiple downstream genes involved in HR repair, cell cycle arrest and apoptosis including BRCA1/2, p53, Chk2, H2AX and MRN complex. The MRN complex with the help of other endo/exo-nucleases including CtIP and EXO1 resect the DNA ends surrounding the break site from 5' to 3' to generate short 3' overhangs of single stranded DNA

(ssDNA) on each side of the DNA-DSBs. The generated ssDNA ends are then coated with replication protein A (RPA), which is subsequently substituted by RAD51 forming a RAD51 nucleoprotein filament (Figure 1.5) (Li and Heyer, 2008, Shrivastav et al., 2008, Heyer et al., 2010). The RPA displacement process is facilitated by a number of mediator proteins including BRCA1/2, RAD52 and RAD51 together with its related proteins RAD51B, RAD51C, RAD51D, XRCC2, and XRCC3. BRCA2 possess a number of RAD51 binding sites, suggesting its importance in the loading of RAD51 onto the ssDNA ends (Kanaar et al., 1998, Heyer et al., 2010). The Rad51 nucleoprotein filament then searches for the homologous DNA sequence, and once it has been located, the Rad51 nucleoprotein filament promotes strand exchange, where the damaged DNA strand invades the template DNA strand forming a displacement loop (D-loop) with a Holliday Junction (HJ) (Figure 1.5) (Jackson, 2002, Heyer et al., 2010). DNA synthesis is subsequently carried out by DNA polymerase that copies the sequence information from the undamaged DNA strand and extends the 3' overhangs of the damaged DNA strand forming four-way intermediate structures known as double Holliday Junctions (dHJs) (Figure 1.5). The resultant dHJs can then be resolved to produce either non-crossover or crossover products, depending primarily on the orientation of the cleavage at the two crossover sites of the dHJs (Jackson, 2002, Li and Heyer, 2008, Heyer et al., 2010).

Alternatively, HR can follow another sub-pathway to repair the damage, named synthesis dependent strand annealing (SDSA) or strand displacement. During SDSA, the invading DNA strand that has been extended is displaced from the D-loop and then re-annealed to its own complementary strand or to the complementary sequences associated with the other side of the break. The remaining gaps are then filled by DNA synthesis to complete repair. This route inherently does not result in crossovers and it lowers the possibility of genomic rearrangements (Jackson, 2002, Li and Heyer, 2008, Heyer et al., 2010). Moreover, HR may also undergo

break induced replication (BIR) to repair the damage. This occurs when the second end of the DNA break is missing (Figure 1.5) and therefore the invading strand is anticipated to establish the synthesis of the new strand until it reaches the end of the chromosome, or the D-loop may become a full-fledged replication fork capable of both lagging and leading strand synthesis (Llorente et al., 2008, Heyer et al., 2010). Defects in the HR repair proteins are greatly associated with increased sensitivity to DNA-DSBs, genomic instability and cancer development. For example, mutations in *BRCA1/2* are highly linked with increased risk for breast cancer; also, the disruptions or deletions in the *Rad51B* gene are associated with the development of different types of cancers (Thompson and Schild, 2001).

1.9.4.3.2 Non-Homologous End Joining

NHEJ is a relatively simple and fast but error-prone mechanism of repairing DNA-DSBs because it does not depend on sister chromatids for repair. It is therefore inherently associated with loss of genetic information (Jackson, 2009). The initial step in the NHEJ mechanism involves recognition and binding of a heterodimeric complex consisting of the proteins KU70/80 to the ends of DNA-DSBs site forming a ring-shaped structure that entirely encircles and protects the DNA from exonuclease digestion (Figure 1.5). The KU heterodimer complex then recruits DNA-PKcs molecules to the DNA-DSBs site. Following the binding to the KU-DNA complex, DNA-PKcs becomes auto-phosphorylated which results in the stimulation of its kinase activity and subsequently improving the NHEJ efficiency by forming a bridge between the two broken DNA ends (Kanaar et al., 1998, Ferguson and Alt, 2001, Jackson, 2002). In the final step of NHEJ, DNA-PKcs recruits XRCC4 to bind with its partner DNA ligase IV forming XRCC4-DNA ligase IV stable complex. The resultant complex then binds to the DNA ends to initiate DNA strand joining by physically bringing both ends very close to each other, although, it is not able to re-ligate the two broken ends directly before being processed (Shrivastav et al.,

2008). Processing of the DNA-DSBs is achieved by exo/endo-nucleases including MRN and DNA-PKcs-Artemis complexes that remove the excess DNA-DSBs strands at the 3' and at 5'/3' overhangs respectively during NHEJ. The remaining gaps are filled after that by DNA polymerases and ligation is performed by ligase complex (Trujillo et al., 1998, Hefferin and Tomkinson, 2005).

An alternative mechanism of NHEJ requires the presence of 5–25 base pair microhomologous sequences on either side of the DNA-DSBs to align the broken ends correctly before joining, thus it is referred to as microhomology mediated end joining (MMEJ). MMEJ constitutes a third and less well-characterised DNA-DSBs repair mechanism. It is also known as a more error-prone and mutagenic DNA-DSBs repair mechanism that has been continuously associated with insertions, deletions and contributes to chromosome translocations and rearrangements. In MMEJ, the microhomologous sequences on either strand anneal to each other once exposed following the resection of DNA ends, forming an intermediate with 3' flaps/overhangs and gaps (Figure 1.5). Upon annealing, the non-homologous 3' overhangs are removed, thus allowing DNA polymerase to fill in the gap. The final step of MMEJ is achieved by DNA ligase (Lig3/Lig1) facilitated break end ligation (McVey and Lee, 2008, Wang and Xu, 2017) (McVey *et al.*, 2008, Wang and Xu 2017).

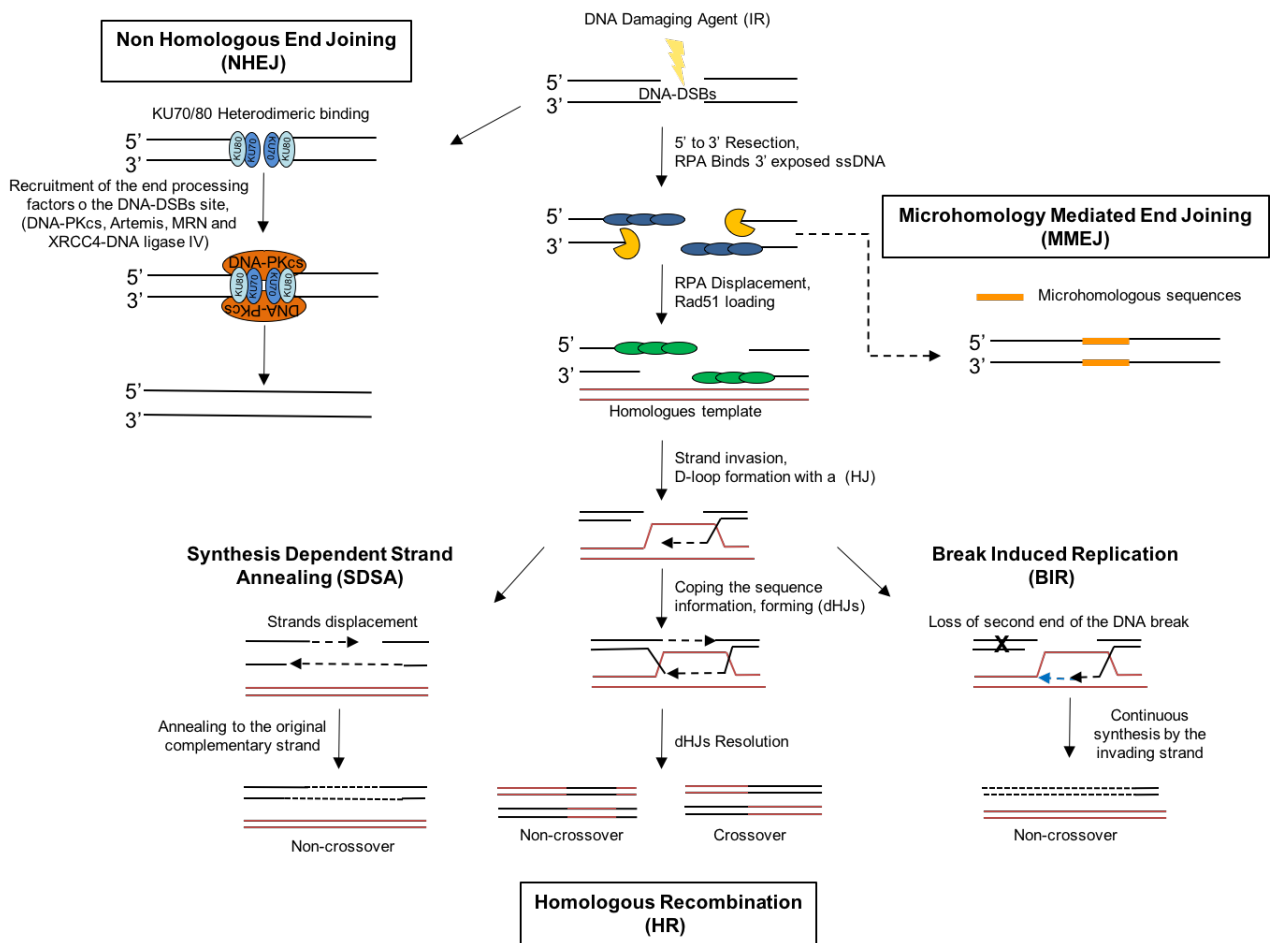


Figure 1.5 Schematic Representations of the Main Pathways of the DNA-DSBs Repair.

In mammalian cells, HR and NHEJ pathways are the two main routes taken in the repair of DNA-DSBs. MMEJ constitutes a third and an alternative mechanism of NHEJ pathway. Figure created from (Kanaar et al., 1998, Jackson, 2002, McVey and Lee, 2008, Shrivastav et al., 2008, Heyer et al., 2010).

1.10 Hypothesis and Aims of the Study

Sarcomas are genetically unstable and generally fall into two distinct genetic categories. The first group shows relatively simple karyotypes with specific genetic abnormalities, while the other group has very complex karyotypes with unspecific genetic alterations (Mackall et al., 2002, Helman and Meltzer, 2003, Osuna and de Alava, 2009). It seems that at least some types of sarcomas may initiate through a combination of defective DNA repair mechanisms, either by inherited or sporadic defects, and radiation exposure which itself induces DNA damage (So et al., 2009, Burningham et al., 2012). Previously in our lab, UI-Hassan et al. (2009) identified common abnormalities in the *ATM* gene including deletion in the gene locus with decreased/absent expression of ATM protein particularly in GIST and LMS (UI-Hassan et al., 2009). The *ATM* gene plays a central role in the DNA-DSBs repair and cell cycle arrest. Therefore, the following hypothesis was developed for this PhD project:

Sarcomas are genetically unstable and that *ATM* is a key regulator involved in sarcoma-genesis

The specific aims of this PhD project are:

1. To study the role that *ATM* may have in the development of sarcoma, initially western blotting is used to look for the total ATM protein expression and for the phosphorylated form of the ATM in different sarcoma subtypes.
2. To further examine the role of *ATM* in sarcoma development, the kinetics of γ H2ax foci formation and loss is measured, both endogenously and after inducing DNA-DSBs by 2Gy IR prior to and after the inhibition of ATM.

3. To investigate the effect of the small molecule ATM kinase inhibitor KU55933 (Calbiochem, USA) on cell viability and radiosensitivity of the normal and sarcoma cell lines, clonogenic assay is used.

4. To identify genetic alterations of *ATM* in sarcomas, a combination of fluorescence in situ hybridization (FISH), Multiplex Ligation-dependent Probe Amplification (MLPA) and Next Generation Sequencing (NGS) is used.

CHAPTER TWO

2 MATERIALS AND METHODS

2.1 Patients and Tumour Samples

2.1.1 Ethics Statement and Tumour Samples

A total of six primary sarcoma tissue samples of different subtypes were collected by an investigator in our group, Dr. Abdulazeez Salawu from patients receiving surgical treatment for STS at Royal Hallamshire Hospital, Sheffield, UK. The National Research Ethics Committee's approval was obtained for the study purpose and for the collection of fresh and archival tissue samples (reference numbers 09/H1313/52 and 09/H1313/30, respectively). All samples were collected and stored according to the principles of the Declaration of Helsinki and the use of tissue was in compliance with the Human Tissue Act, 2004. Details of all specimens used in this study are shown in table 2.1.

2.1.2 Other Cell Lines

Human bone osteosarcoma (U2OS) American Type Tissue Collection (ATCC; LGC Standards, Middlesex, UK) is an established sarcoma cell line, that was obtained from the Institute of Cancer Research Centre, G floor, University of Sheffield and was used as a tumour cell line control in this study because it has a balanced copy number of the *ATM* gene as has been advised by G floor members, human vulvar leiomyosarcoma (SK-LMS-1) is an unstable established sarcoma cell line, human uterus leiomyosarcoma (SKUT-1) and human chondrosarcoma (SW1353) are also established sarcoma cell lines, that were obtained from ATCC and were used for the sarcoma study. The normal human retinal pigmented epithelial cell line immortalised with human telomerase reverse transcriptase (hTERT RPE-1) was used as a non-tumour control cell line to compare the results between the sarcoma and the normal cell lines (Table 2.2).

Table 2.1 Clinical Data for All STS Cases Used in this Study

STS Subtype	Name	Type	Grade	Site	Gender	Age	Neoadjuvant Therapy
Undifferentiated Pleomorphic (UPS) OR Pleomorphic Sarcoma (not otherwise specified) (NOS)	STS 14/10	Cells	3	Lower Limb, left adductor compartment	Female	54	No
	STS 13/12			Lower Limb	Male	80	No
	STS 06/11			Lower Limb, Right thigh	Male	76	No
Leiomyosarcoma (LMS)	STS 02/11	Cells	3	Pelvis	Female	65	No
De-differentiated liposarcoma (DDLPS)	STS 09/10	Cells	3	Retroperitoneum	Female	72	No
	STS 20/11			Lower Limb, Left thigh	Female	70	Radiotherapy

Table 2.2 Details of all Commercial Cell Lines Used in This Study

Cell Line	Cell Type	Grade	Site	Gender	Age	Year Established in Culture	Comments
U2OS	Osteosarcoma	High	Bone-Tibia	Female	15	1953	Has a wild type of TP53 gene (Ottaviano et al., 2010).
SK-LMS-1	Leiomyosarcoma	-	Vulva	Female	43	1971	
SKUT-1	Leiomyosarcoma	3	Uterus	Female	75	1972	
SW1353	Chondrosarcoma	2	Right Humerus	Female	72	1977	
(hTERT RPE-1)	Normal human retinal pigmented epithelial cells						

2.2 Materials

2.2.1 General Laboratory Reagents, Disposable and Basic Laboratory Equipment

Table 2.3 General Laboratory Reagents

Chemicals and Regents	Suppliers
Dulbecco's phosphate buffered saline-00095M (PO4) (D PBS), without Ca ⁺² and Mg ⁺²	Lonza, BioWhittaker
Dulbecco's modified eagle's medium (DMEM), (DMEM F-12)	Lonza, BioWhittaker
Roswell park memorial institute medium (RPMI-1640)	Lonza, BioWhittaker
Fetal bovine serum	
Amphotericin B antifungal	Lonza, BioWhittaker
Penicillin/Streptomycin (10kU/ml)	Lonza, BioWhittaker
L-Glutamine (200mM in 0.85% NaCl)	Lonza, BioWhittaker
D+ glucose (45% solution)	Lonza, BioWhittaker
Trypsin-EDTA, 200 mg/L versene (EDTA), 170000 U	Sigma-Aldrich, UK
Trypsin/L	Lonza, BioWhittaker
Protease inhibitor tablets	Sigma-Aldrich, UK
Protease/phosphatase inhibitor cocktail	Sigma-Aldrich, UK
Copper sulphate CuSo4	Sigma-Aldrich, UK
BCA solution	Sigma-Aldrich, UK
Bovine Serum Albumin (BSA)	Sigma-Aldrich, UK
Sample reducing agent 10x	Fisher Scientific, UK
Sample buffer 4x	Fisher Scientific, UK
1.5M Tris-HCL pH8.8	Geneflow, UK

0.5M Tris-HCL pH6.8	Geneflow, UK
30% Acrylamide	Geneflow, UK
Ammonium persulphate (APS)	Sigma-Aldrich,UK
(N,N,N,N'-tetramethylethylenediamine) (TEMED)	Sigma-Aldrich,UK
Triton-X100	Sigma-Aldrich,UK
Normal goat serum	Vector Laboratories, USA
Colcemid	Gibco, UK
Crystal violet powder	Sigma-Aldrich,UK
RNase-A solution	Sigma-Aldrich,UK
Pepsin	Sigma-Aldrich,UK
Formaldehyde	Sigma-Aldrich,UK
Hybridisation buffers	Abbott Molecular,USA
DAPI (4',6-diamidino-2-phenylindole)	Vector Laboratories, USA
Absolute methanol and ethanol	VWR International, Prolabo
Tween20	Fischer Scientific, UK
Paraformaldehyde (PFA)	Fischer Scientific, UK
PBS tablets	Fischer Scientific, UK
Decon 90 detergent	Decon, UK
ATM kinase inhibitor KU55933	Calbiochem, USA

Table 2.4 Disposable Laboratory Equipment

Disposable Laboratory Equipment	Suppliers
Latex examination gloves	Schottlander, UK
Plastic tissue culture flasks (T25, T75 cm ²)	Corning, UK
Centrifuge tubes (15, 25 and 50ml)	Sarstedt, UK
Eppendorf Microfuge tubes (0.5, 1.5 and 2ml)	Sarstedt, UK
Pipetts tips (p10, p20, p100 and p1000µl)	Sarstedt, UK
Filter pipette tips (p10, p20, p100 and p1000µl)	Sarstedt, UK
Plastic disposable pipettes	Scientific laboratory supplies, UK
Greiner plastic pasteur pipette	Scientific laboratory supplies, UK
Glass pasteur pipette (150mm)	Fischer Scientific, UK
Sterile plastic syringes	Becton Dickinson, UK
Sterile needles (21G, 23G)	Becton Dickinson, UK
Coverslips (22x 22, 22x50mm)	VWR International Ltd., UK
Cell scraper	Fischer Scientific, UK
Blotting paper	Millipore, USA
Extra thick filter papers	Bio-Rad, UK
DNA extraction mini spin columns	Qiagen, UK
Rubber solution	Phillips Rubber, UK
Superfrost microscope slides	VWR International Ltd., UK
96-well cell culture plates	Corning, UK
6-well cell culture plates	Corning, UK
Petri dish (60mm x 15mm)	Fischer Scientific, UK
0.2ml PCR tubes	Fischer Scientific, UK

Table 2.5 Basic Laboratory Equipment

Equipment	Suppliers
Class II microbiological safety cabinet	Medical air technology Ltd., UK
Water bath	Grant
CO ₂ Incubator	Sanyo
Autovortex mixer SA2	Stuart Scientific
Rotatest Shaker R100/TW	Luckham, England
Microcnerifuge	MSE MicroCentaur/sanyo
Heating block	Techne dri-block DB.2A
Protean II electrophoresis apparatus	Bio-Rad, UK
Semi-dry transfer apparatus	Bio-Rad, UK
Fluorescence microplate reader	FLUO Star Galaxy
Cell viability analyser	Beckman Coulter, USA
Automated cell counter	Bio-Rad, UK
Colony counter	Stuart scientific, UK
Cesium 137 irradiator	CIS BioInternational, 1BL 437C
Light microscope (ULWCD 0.30)	Olympus
Fluorescent microscope	Zeiss axioscop
NanoDrop ND-1000	ThermoScientific
Thermocycler	Geneflow, UK
ABI-3730 capillary electrophoresis	ThermoScientific
Illumina HiSeq 2500	Illumina, USA

2.2.2 Tissue Culture and Chromosome Preparation

Tissue Culture Medium and Supplements: Primary STS tumour cells were maintained in Roswell Park Memorial Institute medium (RPMI-1640) (Lonza, BioWhittaker), established sarcoma cell lines were maintained in Dulbecco's modified Eagle's medium (DMEM) (Lonza, BioWhittaker) and normal hTERT RPE-1 cell line was grown in the RPMI-1640 (Lonza, BioWhittaker); the respective supplements for each cell line are given in (Table 2.6).

Table 2.6 Tissue Culture Medium Supplements

Supplement	RPMI-1640 (Primary STS Tumour Cells)	DMEM (Established Sarcoma Cells)	RPMI-1640 (Normal hTERT RPE-1 Cells)
Fetal Calf Serum (FCS) (Lonza, BioWhittaker)	20%	10%	10%
Amphotericin B (Lonza, BioWhittaker)	1%	1%	1%
Penicillin- streptomycin (Lonza, BioWhittaker)	1%	1%	1%
L-Glutamine (200mM in 0.85% NaCl) (Lonza, BioWhittaker)	1%	X	1%
D+ glucose (45% solution) (Sigma- Aldrich, UK)	0.5%	X	X

All media was then stored at 4°C and warmed to 37°C prior to use.

Trypsin-EDTA: 0.4% Trypsin-EDTA solution (Lonza, BioWhittaker) was stored in 50ml aliquots at -20°C and then defrosted in a 37°C incubator before use.

PBS (Lonza, BioWhittaker): Sterile Dulbecco's Phosphate Buffered Saline 0.0095M PO₄ without Ca²⁺ or Mg²⁺ was stored at room temperature.

Microscope Slides: Superfrost slides (VWR International Ltd., UK) were washed with Decon 90 detergent (Decon, UK) and then stored in distilled water (dH₂O) at 4°C for up to one week.

Hypotonic Solution: 0.075M potassium chloride (KCl) was prepared by dissolving 2.235mg KCl in 400ml dH₂O, the solution was then autoclaved, stored at 4°C and warmed in a 37°C incubator for 35 minutes before use.

Colcemid: 10µg/ml KaryoMAX Colcemid (Gibco), was stored at 4°C

Fixative Solution: A mixture of methanol and acetic acid at a ratio of 3:1 was freshly prepared prior to each use.

2.2.3 Whole Cell Lysate Extraction and Western Blotting

Protein Lysis Buffer: Prepared as from components outlined below in 10ml distilled water (dH₂O) using a magnetic stirrer thermostat hotplate. The pH of the solutions was adjusted to 8.0, it was aliquoted in 5ml and stored at -20°C. The buffer was divided into two parts, one had protease inhibitor tablet (PI) (Sigma-Aldrich, UK) only and the other was with protease/phosphatase inhibitor cocktail (PPI) (Sigma-Aldrich, UK), these two components are important for most cell lysis procedures as they protect proteins of interest from degradation; they also deactivate the phospholytic enzymes that are released from subcellular compartments during cells lysis, thus they preserve the phosphorylation state of the proteins.

- 50mM Tris-HCl, (pH 8.0), 78.8mg

- 150mM NaCl, 87.66mg
- 0.02% Sodium azide, 2mg
- 0.1% Sodium dodecyl sulphate (SDS), 0.01g
- 1% Igepal CA-630 (or Nonidet P-40 (NP-40)), 0.1g
- 0.5% Sodium deoxycholate, 0.05g
- Protease inhibitors Tablet, 1 Tablet
- Protease and phosphatase inhibitor cocktail tablets, 1 Tablet

Bovine Serum Albumin (BSA) (Sigma-Aldrich, UK) Protein Standards: A range of standard solutions (0µg/ml, 1µg/ml, 5µg/ml, 10µg/ml, 15µg/ml and 20µg/ml) were prepared from a 2mg/ml BSA stock to generate a standard curve.

Bicinchoninic Acid Protein Assay (BCA) Working Reagent: Freshly prepared by adding 1ml of copper sulphate CuSo4 (Sigma-Aldrich, UK) to 49ml of the BCA solution (Sigma-Aldrich, UK).

Samples Preparation for Western Blotting: Samples were prepared as outlined in (Table 2.7) and then stored on ice at room temperature until loading.

Table 2.7 Sample Preparation for Western Blotting

Solution	Volume
Sample reducing agent 10x (Fisher Scientific, UK)	4 µl
Sample buffer 4x (Fisher Scientific, UK)	10 µl
Sample (volume depending on the protein concentration)	x µl
dH ₂ O	(26-x) µl

Resolving and Stacking Gel: Resolving and stacking gels were freshly prepared as outlined in (Table 2.8) and stored at 4°C up to one day prior to use.

Table 2.8 SDS Page Resolving and Stacking Gels Components

7% Resolving Gel Components		4% Stacking Gel Components	
dH ₂ O	5.02ml	dH ₂ O	3.05ml
1.5M Tris-HCL pH8.8 (GeneFlow, UK)	2.5ml	0.5M Tris-HCL pH6.8 (GeneFlow,UK)	1.25ml
30% Acrylamide (GeneFlow, UK)	2.33ml	30% Acrylamide	0.65ml
*10% Ammonium persulphate (APS) (Sigma-Aldrich, UK)	50µl	10% APS	50µl
(N,N,N,N'- tetramethylenediamine) (TEMED) (Sigma-Aldrich, UK)	5µl	TEMED	5µl

*10% APS was made up freshly each time by adding 50mg of APS and 250µl of dH₂O in an eppendorf tube.

PreCast Gel: 4-15% precast polyacrylamide gel, 8.6 × 6.7cm (Width × Length), 10-well was purchased (Bio-Rad, UK) and stored at 4°C.

Protein Size Markers: Precision plus protein™ dual colour standards (molecular weight range: (MW) 10-250kDa) (Bio-Rad, UK) and spectra multicolour high range protein ladder (MW range: 40-300kDa) (Thermo, USA) were stored at -20°C (Figure 2.1).

Running Buffer: 100ml of running buffer (Geneflow, UK) was added to 900ml of dH₂O and stored at room temperature.

Transfer Buffer: 100ml of transfer buffer (Geneflow, UK) was added to 700ml of dH₂O, then 200ml of methanol was added to prepare transfer buffer. Buffer was stored at room temperature.

Other Western Blotting Materials: Protean II electrophoresis apparatus which comprises gel tank, running module, 1.5mm plates, 1.5mm sample comb (for 10 samples), electrodes, and power source (Bio-Rad, UK) was used. Polyvinylidene difluoride (PVDF) membrane (Millipore, USA), extra thick 7.5x10cm filter papers (Bio-Rad, UK), wet and semi-dry transfer apparatuses (Bio-Rad, UK) were also used.

5% Blocking Buffer: Was freshly prepared by dissolving 5g of semi-skimmed Marvel milk powder in 100ml of the PBST. To prepare PBST solution, 100 tablets of PBS (Fisher Scientific, UK) were dissolved in 10L of dH₂O, then 10ml of Tween®20 (Fisher Scientific, UK) was added.

Antibodies: All primary and secondary antibodies used in the study are listed in table 2.9.

Table 2.9 Western Blotting Antibodies Used for this Study

Antibodies	Species	Dilution	Storage	Source	Blocking Agent
Primary antibodies					
ATM (2C1):sc-23921	Mouse monoclonal antibody	(1:250)	Store at 4° C	(Santa Cruz, USA)	5% Milk
ATM (2C1 (1A1))	Mouse monoclonal antibody	(1:2000)	Store at -20°C	(Abcam, UK)	5% Milk
ATM (Phospho S1981) [10H11.E12]	Mouse monoclonal antibody	(1:500)	Store at -20°C	(Abcam, UK)	5% Milk
β-Actin AC-15	Mouse monoclonal antibody	(1:1000)	Store at -20°C	(Sigma-Aldrich, UK)	5% Milk
Secondary antibody					
ECL Anti-mouse IgG peroxidase linked whole antibody	Mouse	(1:2000)	Store at 4° C	(GE Healthcare Life Sciences, UK)	5% Milk

Developing Materials: Western blotting HRP detecting substrate (Millipore USA), 18x24cm amersham hyperfilm ECL (GE Healthcare Life Sciences, UK), developer and fixer solutions.

ATM Kinase Inhibitor KU55933 (ATMi): (CAS 587871-26-9), purchased from (Calbiochem, USA) and stored at -20°C. The solution was used to inhibit the kinase activity of the ATM protein.

Irradiation: 2Gy was programmed in Cesium 137 irradiator (CIS Bio-International, 1BL 437C) and used as a DNA damage-inducing agent.

2.2.4 γ H2AX Assay

4% Fixative Solution: 4g of the paraformaldehyde (PFA) (Fischer Scientific, UK) was dissolved in 100ml of sterile PBS on the magnetic stirrer thermostat hotplate at 90°C for 2 hours. The solution was then kept at 4°C and used in 1-2 days.

Triton X: 0.2ml of Triton-X100 (Sigma-Aldrich, UK) was added to 500ml of sterile PBS solution (0.4%). The solution was then stored at room temperature.

10% Normal Goat Serum (Blocking Buffer): To prepare the 10% of blocking buffer, 2ml of normal goat serum (Vector Laboratories, USA) was added to 18ml of PBS.

Antibodies: All primary and secondary antibodies used in H2AX are listed below (Table 2.10).

Table 2.10 H2ax Immunofluorescence Staining Antibodies

Antibodies	Species	Dilution	Storage	Source	Blocking Agent
Primary antibodies					
p-histone rabbit anti- γ H2AX antibody	Rabbit	(1:500)	Store at -20°C	(Cell Signaling Technology)	PBS
Secondary antibody					
Goat anti-rabbit Cy3-conjugated secondary antibody	Rabbit	(1:500)	Store at 4°C	(Invitrogen, USA)	10% Goat serum

2.2.5 Clonogenic Survival Assay

Fixative Solution: 50ml of absolute methanol was added to 50ml of acetone, the mixture was then incubated at 4°C for 10 minutes prior to use.

0.5% Crystal Violet Stain: 0.05g of crystal violet powder (Sigma-Aldrich, UK) was added to 5ml of absolute ethanol and 45ml of dH₂O (to prepare 50ml of the crystal violet stain, it was then stored at room temperature.

2.2.6 Fluorescence *In-Situ* Hybridisation (FISH)

2.2.6.1 Reagents Preparation

RNase-A Solution (Sigma-Aldrich, UK): Stored at -20°C in 25µl aliquots at 20mg/ml stock concentration then diluted in 5ml 2xSaline-Sodium Citrate (SSC) buffer.

Pepsin (proteinase): Was stored at -20°C in 25µl aliquots at stock concentration of 100mg/ml (Sigma-Aldrich, UK), it was diluted 1:2000 in 0.01N HCl to make up the working concentration, and then warmed at 37°C prior to use.

SSC Buffer: 20X SSC stock was prepared by dissolving 3M NaCl and 300mM NaHCO₃ in 1L deionised water, the pH was adjusted to 7.0 and stored at room temperature.

PBS-MgCl₂: PBS + 50mM MgCl₂ (50ml 1M MgCl₂ + 950ml PBS) was stored at room temperature.

Fixative Solution: Formaldehyde (37%) (Sigma-Aldrich, UK) was diluted to 1% in PBS-MgCl₂ (1.35ml formaldehyde + 50ml PBS-MgCl₂).

Ethanol: A series of ethanol dilutions 70%, 95%, 100% were made from absolute ethanol.

Hybridisation Buffers: Vysis LSI/WCP and CEP hybridisation buffers (Abbott Molecular, USA) were stored at -20°C.

SSCT1: 0.4xSSC/0.3% Tween 20 was prepared by adding 200ml of 2xSSC and 1.5ml of Tween 20, it was made up to 500ml with H₂O.

SSCT2: 2xSSC/0.1% Tween 20 was prepared by adding 0.5ml of Tween 20 and 500ml of 2xSSC.

Counterstain: DAPI (4',6-diamidino-2-phenylindole) (Vector Laboratories, USA), was stored in the dark at 4 °C.

2.2.6.2 Probes

FISH probes used in this study were obtained from (Abbott Molecular, USA), and stored at -20°C (Table 2.11).

Table 2.11 FISH Probes

Probe Name	Target	Locus	Spectrum	Volume for 5 slides*
Vysis, Locus Specific Identifier (LSI)	ATM	ATM 11q22.3	SpectrumOrange	3.5µl
Chromosome 11 centromere probe (CEP11)	Chromosome 11 Centromere	11p11.11-q11	SpectrumGreen	1.5µl

*Volume efficiency previously optimised by members of the Rare Tumour Research Group.

2.2.7 DNA Extraction

Purified genomic DNA was obtained from normal and tumour samples by DNeasy[®] Blood and Tissue Kit (Qiagen, UK). DNA Extraction Kit contained proteinase K, lysis buffer (Buffer AL), wash buffers (Buffers AW1 and AW2), 33ml of 100% ethanol was added to each buffer, elution buffer (Buffer AE), DNeasy mini spin columns and collection tubes.

2.2.8 Multiplex Ligation-Dependent Probe Amplification (MLPA)

SALSA MLPA kit purchased from MRC-Holland (Amsterdam, Netherlands) contains probes specifically annealing to exons within the *ATM* gene and has all the reagents required for the procedure (Table 2.12). The MLPA assay for the *ATM* gene requires two sets of probe mix due to the large number of exons (63 exons), probe mix P041-B1 *ATM* and P042-B1 *ATM*. Each set contains 45 probes, 34 of which are for the *ATM* and 11 are reference probes. The reference probes anneal to different parts of the human genome to ensure that the probes are ligating and annealing properly. When the two sets are used together, a probe for each *ATM* exon is present, including two probes for exon number 1 and 61 and three probes for exon number 62. The P041-B1 *ATM* set gives amplification products between 130 and 485 nucleotides in length and between 131 and 485 for the P042-B1 *ATM* probemix set. The position and size of both target and reference probes within *ATM* are displayed in Appendix 1.

Table 2.12 SALSA MLPA Kit

Reagent kit components	Ingredients
SALSA MLPA Buffer (yellow cap)	KCl, Tris-HCl, EDTA, PEG-6000, oligonucleotide
SALSA Ligase-65 (green cap)	Glycerol, EDTA, Beta-Mercaptoethanol, KCl, Tris-HCl, nonionic detergent, Ligase-65 enzyme (bacterial origin)
Ligase Buffer A (transparent cap)	Coenzyme NAD (bacterial origin)
Ligase Buffer B (white cap)	Tris-HCl, MgCl ₂ , non-ionic detergent
SALSA PCR Primer Mix (brown cap)	Synthetic oligonucleotides with fluorescent dye (FAM or Cy5), dNTPs, Tris-HCl, KCl, EDTA, nonionic detergent
SALSA Polymerase (orange cap)	Glycerol, non-ionic detergents, EDTA, DTT, KCl, Tris-HCl, Polymerase enzyme (bacterial origin)

2.2.9 Next Generation Sequencing (NGS)

The targeted NGS experiment was performed in this study on an Illumina HiSeq 2500 system using NGS services provided by the Children's Hospital, Sheffield, UK.

2.3 Methods

2.3.1 Routine Tissue Culture

The day-to-day culture was observed regularly to keep cells growing and to prevent any contamination. All cells were incubated at 37°C in a humidified atmosphere of 95% air and 5% CO₂. Cells were routinely passaged when they reached 80-90% confluence to maintain culture. This was done by first completely discarding the consumed medium from the tissue culture flasks and washing the cell layer twice with 4ml of PBS (Lonza, BioWhittaker). Then, 2.5ml of 1x trypsin-EDTA solution (Lonza, BioWhittaker) was added and the cells were incubated at 37°C in 95% air and 5% CO₂ incubator and observed under a light microscope to ensure dissociation. Warm fresh media (5ml) was added to the cells to inactivate the action of trypsin-EDTA (Table 2.6). The suspension was then collected in a 15ml falcon tube and centrifuged at 1000rpm for 5 minutes at room temperature. The supernatant was discarded, and the cell pellet re-suspended in 5ml of warm fresh media and seeded into new tissue culture flasks. All experiments were done between passage number 4-11 for the hTERT RPE-1 cell line, as after these passages, the cells gradually start to lose their characteristics, become bigger in size and growing slowly.

2.3.2 Whole Cell Lysate Extraction and Protein Expression by SDS-PAGE and Western Blotting

2.3.2.1 Cell Protein Extraction

The cells were lysed to release cellular proteins, remove cell debris and to extract total protein. This was done by using moderate concentrations of some detergents that possess non-ionic (uncharged), ionic (charged, either cationic or anionic) or zwitterionic (zero net charge) characteristics which compromise the integrity of cell membrane and assist in the cell lysis and protein extraction (Section 2.2.3).

When the cells became 80-85% confluent they were prepared for total protein extraction. Cells were placed first on an ice tray to prevent any endogenous protease activity. The media was then completely aspirated and the cells were washed twice with 10ml of ice cold PBS. 500µl of ice cold lysis buffer (Section 2.2.3) was added over the surface of the tissue culture flasks to lyse the cells and left for 5-10 minutes with gentle swilling. Any remaining cells were then scraped off the flasks using a cell scraper and pipetted into eppendorf tubes. The protein lysates were then passed 10 times through a 25-gauge syringe needle. After that, cells were incubated in an ice box for 30 minutes, and vortexed half way through before being centrifuged at 13000rpm for 10 minutes at 4°C. The supernatant containing the proteins was then aliquoted into new eppendorf tubes and stored at -80°C until use.

2.3.2.2 Protein Quantification

Following protein extraction, the total protein concentration of sarcoma and normal cell lines was assessed by using bicinchoninic acid protein (BCA) assay kit (Sigma-Aldrich, UK) following the manufacturer's protocol.

The BCA assay primarily relies on two reactions; firstly, the peptide bonds in protein reduce copper II (Cu^{+2}) ions to copper I (Cu^{+1}) in alkaline medium. The amount of reduction is proportional to the amount of protein present. Then, the BCA solution reacts with Cu^{+1} ions producing an intense purple-coloured product that strongly absorbs light at a wavelength between 540-570nm.

Samples were prepared in two dilutions; the first dilution was (1:4) in which 25µl of the protein sample was mixed with 75µl of dH_2O . The second dilution was 1:20 and for that, 5µl of the

protein sample was mixed with 95µl of dH₂O. Equal volume (20µl) of each dilution was loaded into a flat-bottomed 96-well plate and 200µl of BCA working reagent (Section 2.2.3) was then added for the BCA assay. In order to allow quantification of protein concentration in the samples, known concentrations of BSA (0µg/ml to 20µg/ml) were prepared and used as protein standards. In a similar way to the samples, 20µl of each standard was loaded into the wells and mixed with 200µl of BCA working reagent. Finally, the plate was incubated at 37°C for 30 minutes and the absorbance was measured at 540-570nm using a plate reading spectrometer. The concentration of protein in extracted samples was then calculated by comparing the sample absorbance to the standard curve generated.

2.3.2.3 SDS Page Electrophoresis

SDS page electrophoresis was carried out to examine the status of ATM protein in normal and sarcoma cell lines. Firstly, Protean II electrophoresis apparatus (Bio-Rad, UK) was gently washed with running tap water then wiped with 70% ethanol. The 1.5mm plates were then assembled into the running module and the gels prepared as described in section 2.2.3 (Table 2.8). The resolving gel was made at the appropriate percentage for the ATM protein size and then poured between the plates, just up to the depth of the loading comb and allowed to set. A stacking gel was then poured on top of the resolving gel and the comb was placed immediately, the gels were then left to set. The comb was gently removed afterward and the wells rinsed out with dH₂O. Samples were prepared as described in section 2.2.3 (Table 2.7), and then denatured by heating at 70°C for 10 minutes while the plates were assembled into the electrophoresis apparatus with gel running buffer (Geneflow, UK). The first well was then loaded with a protein size marker (Figure 2.1) and 15-20µg of each sample was loaded into the respective wells and analysed by SDS-PAGE separating gel. After that, electrophoresis was carried out at 100 volt (V) for approximately half an hour, the voltage was increased

afterwards to 150V until the desired separation was achieved. Once the gel run was complete, it was removed from the apparatus for blotting.

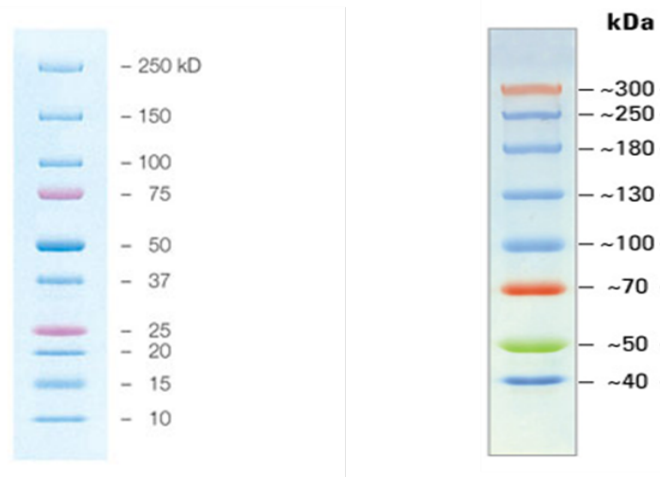


Figure 2.1 Protein Size Markers.

The precision plus protein dual colour standards ladder is presented in the left (Bio-Rad, UK) and the spectra multicolour high range protein ladder is on the right (Thermo, USA).

2.3.2.4 Wet and Semi-Dry Transfer

To transfer the protein bands to PVDF membrane, the gel was removed from the apparatus and soaked in transfer buffer (Geneflow, UK) for 5 minutes before being assembled into a wet or semi-dry blotting system. Because of the hydrophobic characteristics of the PVDF membrane, it was firstly pre-wetted with methanol prior to submersion in transfer buffer.

For wet transfer, the transfer sandwich was prepared in the following order, sponge pad, filter paper, gel, PVDF membrane, filter paper and sponge pad; all were soaked in transfer buffer for 5 minutes and pressed together within the transfer cassette (Figure 2.2 (A)). The supported

gel sandwich was then placed vertically inside the gel tank with transfer buffer along with a magnetic stirring bar and an ice pack. The gel was then electrophoresed at 30V overnight at 4°C.

In semi-dry protein transfer, the semi-dry transfer apparatus (Bio-Rad, UK) was cleaned first with 70% ethanol, then the western blot transfer sandwich was placed horizontally inside the machine in the following order; filter paper, membrane, gel and filter paper, all were sufficiently soaked in transfer buffer (Figure 2.2 (B)). The blot was run at 15V for 20 minutes.

Once the gel was semi-dry transferred or wet transferred, the membrane was removed and blocked in 5% milk-PBST for one hour at room temperature.

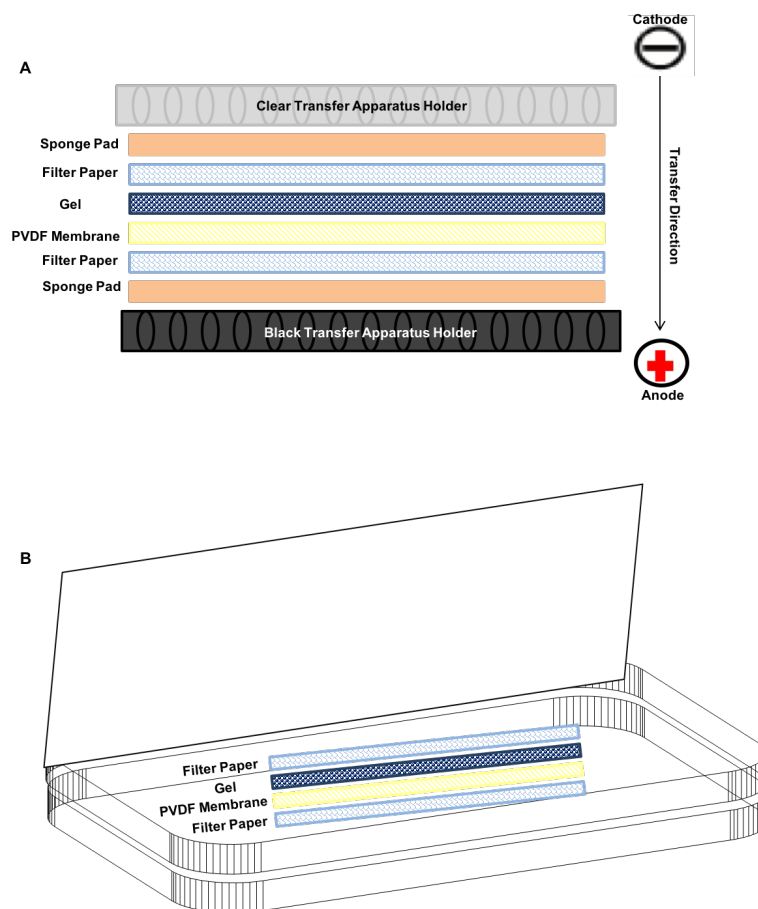


Figure 2.2 A Schematic Representation of a Wet Blotting Cassette (A) and Semi-Dry Transfer Unit (B).

2.3.2.5 Protein Detection

Blots were then incubated in primary antibody (Table 2.9) for 2 hours at room temperature with gentle shaking. The primary antibody was then washed off with PBST four times for 10 minutes each and then the membranes were incubated in secondary antibody (Table 2.9) for one hour at room temperature. Following four washes of 10 minutes each in PBST, the blots were incubated for 1 minute inside black box with 1ml of western HRP substrate (Millipore, USA), and then the blots were developed by using amersham hyperfilm ECL (GE Healthcare Life Sciences, UK) for 1, 5, 15, 30, 60 minutes and overnight incubation for ATM protein detection and for (20 seconds-1 minute) for β -actin. Films were developed by immersing them in developing solution until bands appeared; this was followed by a quick wash in water and a dip in fixer solution. Finally, the films were immersed in running tap water before being hung to dry.

2.3.3 Immunofluorescence for γ H2AX

2.3.3.1 Sample Preparation

Three separated six-well cell culture plates were prepared and labelled per cell line to measure the levels of DNA repair and the levels of spontaneous and IR-induced DNA damage with and without the inhibition of ATM using ATM inhibitor KU55933 (Calbiochem, USA) (Figure 2.3). 22 x 22mm glass coverslips were sterilised in absolute methanol for 10 minutes and then air-dried standing inside the six-well plates. The adherent 60-80% confluent cells from T75 tissue culture flask were then trypsinised and re-suspended in suitable media (Section 2.3.1 and Table 2.6). Then, 500 μ l of the re-suspension was aspirated to count the total viable cells using the cell viability analyser (Beckman Coulter, USA). For each cell line, 20,000 cells were seeded on each glass coverslip placed in six-well plates and 2ml of respective media was added in each well. The plates were then incubated overnight at 37°C in a 95% air and 5% CO₂ incubator.

2.3.3.2 Treating Cells with Irradiation

10 μ M of ATM inhibitor KU55933 (Calbiochem, USA) was added to the labelled wells 2 hours prior to 2Gy IR exposure (Figure 2.3). Cells in plates 1 and 2 were then irradiated with 2Gy by using a caesium 137 irradiator (CIS bio-International, 1BL 437C), while cells in plate 3 were treated in the same way as plate 1 and 2 but not exposed to IR and were used only to measure the spontaneous DNA damage response with and without ATM inhibition. Following the exposure to 2Gy IR, cells were incubated at 37°C to recover for different time-points of 30 minutes, 1 hour, 2 hours and 4 hours. After each time-point, media was aspirated from the wells and cells were washed twice with ice cold PBS and then fixed in 1.5ml of 4% paraformaldehyde in PBS for 10 minutes at room temperature. Cells were washed briefly in PBS before permeabilization with 0.2% Triton-X in PBS for 5 minutes at room temperature, and then rinsed twice with PBS.

2.3.3.3 Immunofluorescence Staining of γ H2AX Foci

Cells were blocked in 1.5ml of 10% normal goat serum in PBS for 1 hour at room temperature to prepare the cells for immunofluorescence staining and to suppress any non-specific antibody binding. Cells were then washed with PBS and incubated overnight at 4°C with p-histone (ser 139) rabbit anti- γ H2AX antibody at 1:500 dilution in PBS (Cell Signaling Technology) (Table 2.10). The following day cells were washed for 5 minutes three times in PBS on a shaker and then incubated for 1 hour at room temperature in the dark with goat anti-rabbit Cy3-conjugated secondary antibody at 1:500 dilution in 10% goat serum in PBS (Invitrogen, USA) (Table 2.10). Cells were then washed for 5 minutes three times in PBS with gentle shaking. Coverslips were inverted onto microscope slides and mounted with Vectashield mounting medium containing 4',6-diamidino-2-phenylindole (DAPI) (Vector Laboratories, USA). Small drops of nail varnish

were added onto the edges of the coverslips to fix them onto the microscopic slides. Finally, slides were stored at 4°C in the dark until analysis by fluorescent microscopy.

2.3.3.4 Analysis and Quantification of γ H2AX Foci

γ H2AX analysis was performed as previously prescribed (Hoh et al., 2011). γ H2AX foci were detected as red fluorescent signals inside the blue DAPI stained cells (Figure 3.6) on a UV spectrum-red fluorescent Nikon image analysis microscope at 100x magnification. The foci number per nucleus in 100 cells was visually counted and the percentage of cells having more than ten γ H2AX foci was calculated in three independent experiments for both sarcoma and normal cell lines.

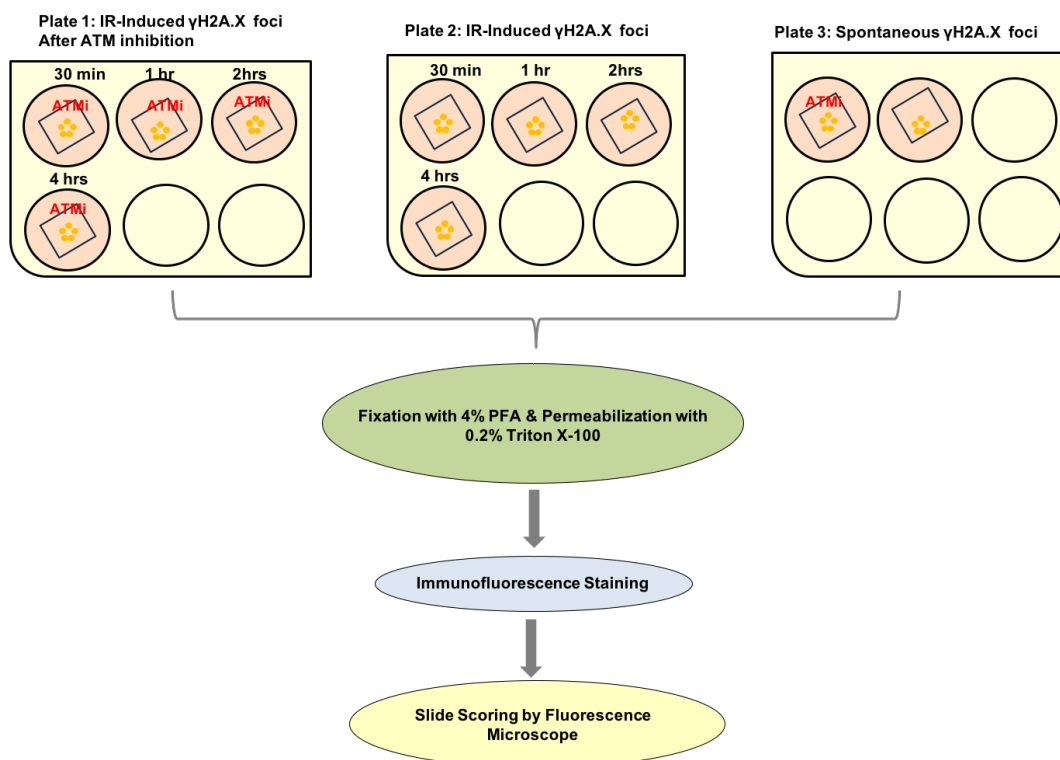


Figure 2.3 Schematic Model of γ H2AX Assay.

2.3.4 Clonogenic Survival Assay

The clonogenic survival assay was performed on normal and sarcoma cell lines following the protocol described by Hickson et al. (2004) to determine the ability of a single cell to proliferate and produce a cluster of at least 50 cells following treatment with ionising radiation, ATM inhibitor KU55933 (Calbiochem, USA) and combination of both. Cells were cultured in T75 tissue culture flasks until they were 60–80% confluent, then trypsinised and re-suspended in suitable media (Section 2.3.1 and Table 2.6). The total viable cells were counted by an automated cell counter (Bio-Rad, UK), and then two different concentrations of viable cells (1000 and 3000 cells) were seeded into 60mm x 15mm petri dish plates (four petri dish plates per concentration per cell line); these were incubated overnight at 37°C in a humidified atmosphere of 95% air and 5% CO₂. The first plate was used as an untreated control, the second plate was only exposed to 2Gy IR using a caesium 137 irradiator (CIS bio-International, 1BL 437C) and then incubated overnight, 10µM of ATM inhibitor KU55933 (Calbiochem, USA) was added to the third plate and incubated overnight before the media was replaced with fresh one, the fourth plate was treated with 10µM of ATM inhibitor KU55933 (Calbiochem, USA) 2 hours prior to 2Gy irradiation, the cells were then incubated overnight before the media was replaced with a fresh one in the absence of the inhibitor. All plates were then incubated at 37°C with 95% air and 5%CO₂ for up to 14 days, after which cells were washed gently with PBS and the colonies formed were fixed using 2ml of 1:1 (methanol/acetone solution) and then stained with 2ml 0.5% crystal violet (Sigma-Aldrich, UK) for about 30 minutes. Next, the colonies were then washed with PBS and left to dry overnight.

2.3.4.1 Analysis of Clonogenic Assay

Colonies of greater than 50 cells were only visually counted as one surviving colony under the light microscope (Olympus) and by using a colony counter (Stuart scientific, UK) (Franken et

al., 2006). The plating efficiency (PE) was calculated following colony counting by using the following formula

$$\text{PE} = \text{Number of colonies formed} / \text{Number of cells initially plated}$$

The percentage of the surviving fractions (SF) was then determined using the following formula

$$\text{SF} = \text{PE of the treated cells} / \text{PE of the controls} \times 100$$

Colonogenic assay data were obtained from three independent experiments per cell line and calculated as percentage surviving colonies with respect to control plate +/- standard error of mean (SEM).

2.3.5 Determination of the ATM Kinase Inhibition by Western Blotting

To determine the effect of the ATM kinase inhibitor KU55933 (Calbiochem, USA) on the ATM autophosphorylation on ser1981 and to validate data produced when ATM inhibitor was used in this study, four T75 tissue culture flasks of the U2OS cells were maintained in tissue culture until they reached 60-80% confluence. All flasks were then pre-incubated with 10 μ M of the ATM inhibitor for 2 hours except one flask which was used as controls. All flasks were then exposed to 2Gy IR and left in the 37C $^{\circ}$ incubator for different time-points of 2, 12 and 24 hours in the presence of the inhibitor. After each time-points, proteins were extracted and the concentrations of the proteins were then determined by the BCA protein assay (Section 2.3.2.1 and Section 2.3.2.2) to be ready for western blotting. Another western blotting gel was run at the same time for the β -actin which was used as a loading control, to confirm that there was no difference in the amount of protein loaded for different samples.

2.3.6 Fluorescence *In-situ* Hybridisation (FISH)

FISH was used in this study to visually determine the copy number aberrations. The assay uses specific labelled fluorescent DNA probes that have the ability to detect the presence or absence of the DNA sequence of interest on chromosomes (metaphase chromosome and/or interphase nuclei). FISH was performed on normal and sarcoma cell lines, probing for centromeric copies of chromosome 11 (Vysis centromeric satellite probe) and the *ATM* gene at *ATM* 11q22.3 (Vysis LSI *ATM*) (Abbott Molecular, USA) (Table 2.11). FISH was performed according to the protocol optimised by members of the Rare Tumour Research Group.

2.3.6.1 Chromosome Harvesting

Cells were cultured in T75 tissue culture flasks until they reached 60-80% confluence and media was changed one day before starting the procedure. On the day of harvesting, 6-7 drops of colcemid 0.05µg/ml was added to the actively dividing cells using a 1ml syringe and then cells were incubated in a 37°C incubator with 5% CO₂ for 4 hours to arrest the cells at metaphase. The media was then transferred to a 15ml universal tube. Cells were trypsinised after that for 2 minutes and a few millilitres of the media kept in the universal tube added to stop the action of trypsin. The cell suspension was then collected and added to the same universal tube and centrifuged at 1500rpm for 5 minutes at 37°C. The supernatant was aspirated carefully and 0.5ml of the supernatant left to re-suspend the pellet by gently flicking the tube. Then, 5ml of pre-warmed hypotonic solution (0.075M KCl) was added drop-wise while gently shaking, the cells were then incubated for 35 minutes at 37°C with 5% CO₂ to allow the cells to swell. Cells were then centrifuged at 1000rpm for 10 minutes and the supernatant discarded leaving about 0.5ml to re-suspend the pellet. 2ml of freshly prepared fixative solution (methanol and acetic acid at the ratio of 3:1) was then added in drops while gently mixing the cells. This was followed by centrifugation of the cells at 1000rpm for 10 minutes, the pellet was

then again re-suspended in 2ml of fixative solution and the harvesting tubes were then stored at -20°C until ready for slide preparation.

2.3.6.2 Chromosome Spread and Slide Preparation

Chromosome spreads were performed following the protocols described by Hsu and Pomerat (1953). Slides were cleaned overnight using Decon 90 detergent and water then washed quickly under warm and cold water sequentially. Two drops of cells that had been incubated in hypotonic solution and then fixed were added from a variable height onto the cleaned slides and 3-4 drops of fixative solution were dropped onto the cells to improve chromosome spreading. Slides were then left to dry in air and stored at -20°C until use.

2.3.6.3 Enzyme Treatment and Cell Fixing

Slides were treated with 125µl RNase loaded onto 22 × 50mm coverslips and incubated in a humid chamber at 37°C for 1 hour. They were washed after that in 2xSSC three times for 5 minutes each with gentle shaking then immersed in pre-warmed pepsin-HCl solution held at 37°C in a water bath and incubated for exactly 10 minutes. Slides were then washed twice in PBS for 5 minutes each at room temperature with gentle agitation. This was followed by a further wash in PBS-MgCl₂ for 5 minutes at room temperature on a shaker. The slides were then immersed in a freshly prepared 1% formaldehyde for 10 minutes at room temperature and washed in PBS for 5 minutes with gentle agitation. They were then dehydrated through immersion in a series of ethanol (first 70%, followed by 95% and 100%) for 3 minutes each and then air dried.

2.3.6.4 Hybridisation of the DNA Probes to the Target DNA

For 5 slide preparation, 3.5µl of the *ATM* probe was mixed with 1.5µl of CEP11, 35µl of hybridisation buffer and 10µl of dH₂O. The probe mixture was denatured for 10 minutes at 80°C

on a heated block and then pulsed down in a microcentrifuge. Then, 10µl of the probe mixture was added onto 22 x 22mm coverslips onto which the slides were placed cells-down and sealed with rubber solution. The slides were placed on a hotplate at 80°C for 2 minutes to denature target DNA then left in the dark to hybridise overnight in a humidified chamber at 37°C.

2.3.6.5 Post-Hybridisation Washes and Counterstaining

The coverslips and rubber sealing were removed using forceps and the slides were placed in pre-warmed SSCT-1 solution held at 73°C in a water bath and incubated for exactly 2 minutes. Slides were then washed in SSCT2 solution for a further 1 minute at room temperature. This was followed by dehydration through a series of ethanol dilutions (first 70% followed by 95% and 100%) for 3 minutes each and air dried in the dark. Then, 20µl of DAPI was applied in two drops onto 22 x 50mm coverslips and air-dried slides were placed on the cover slips with cells-down and sealed with nail varnish. The slides were stored at 4°C for at least 2 hours to allow the DAPI to settle prior to viewing.

2.3.6.6 Analysis and Image Detecting

The CEP11 and *ATM* probes were detected visually under a Zeiss fluorescent microscope as green and red signals respectively. Probe signals were scored from 200 non-overlapping intact nuclei or metaphase spreads in each case and images were captured using the Cytovision software.

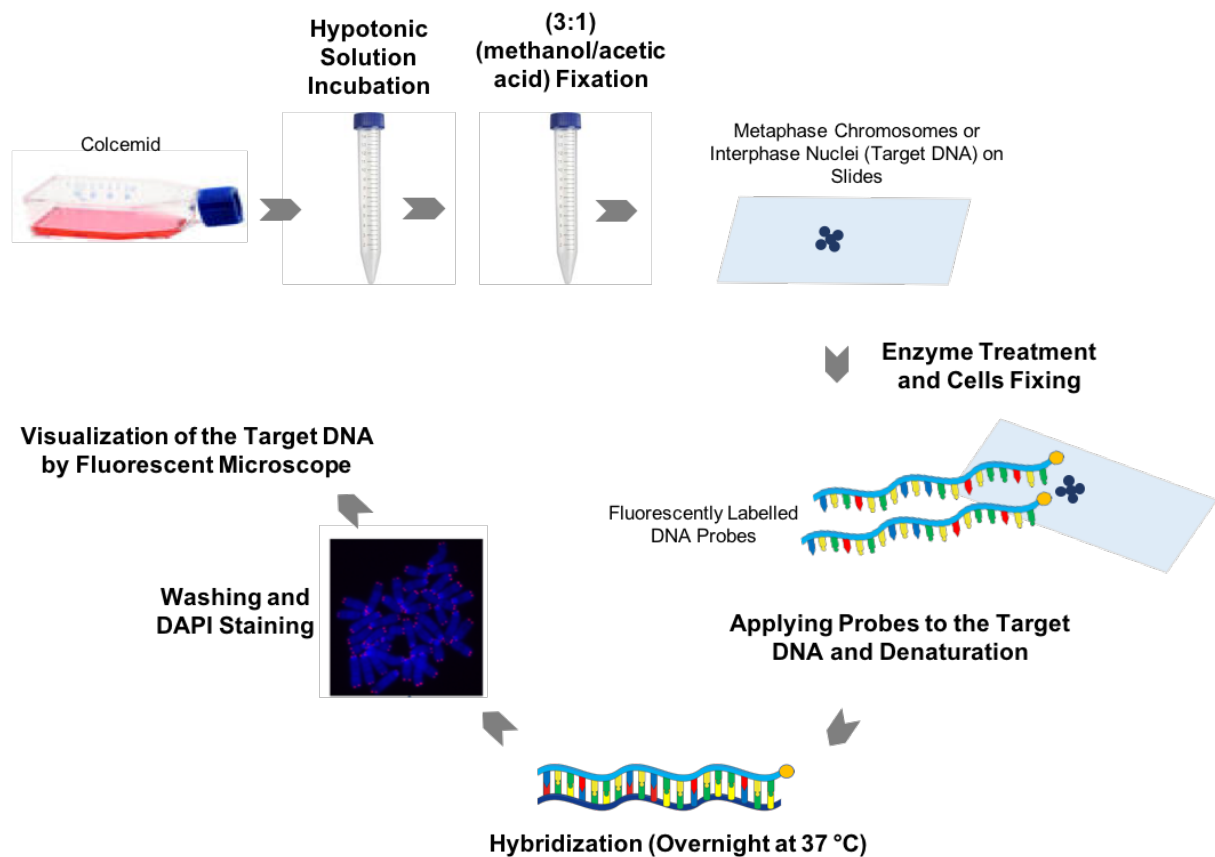


Figure 2.4 A Schematic Outline of the Basic Principle of FISH.

2.3.7 DNA Extraction

Purified genomic DNA was obtained from cultured normal and tumour cells following the Qiagen DNeasy kit methodology. Basically, the kit works on the concept of alkaline lysis, binding, washing and elution. The cells are lysed first then loaded onto a spin column coated with silica membrane that selectively adsorbs DNA in the presence of high concentrations of chaotropic salts. Centrifugation of the spin column followed by two steps of washing optimally eliminates any contaminants and the pure DNA is then eluted.

2.3.7.1 Cells Preparation and Lysis

Cells were cultured in T75 tissue culture flasks until they were 70-80% confluent. They were then trypsinised and centrifuged as explained in section 2.3.1.2. The cells were then re-suspended in 200µl PBS and transferred into a labelled 1.5ml microcentrifuge tube. 20µl of proteinase K and 200µl of lysis buffer (Buffer AL) were added to the suspension, the mixture vortexed and then incubated at 56°C on a heat block until the cells were completely lysed with periodic vortexing. 200µl of absolute ethanol was then added to the tube, vortexed and then pipetted into a mini spin column.

2.3.7.2 DNA Adsorption to DNeasy Mini Spin Column

The DNeasy mini spin column containing the lysed cells was then placed into a collection tube and centrifuged at 8000rpm for 1 minute at room temperature. The flow-through and the collection tube were discarded and the mini spin column transferred to a new collection tube.

2.3.7.3 DNA Washing

500µl of the first washing buffer (AW1) was added to the mini spin column then centrifuged at 8000rpm for 1 min at room temperature. The collection tube and contents were discarded and the mini spin column placed into a fresh collection tube. This was followed by a second washing step with 500µl of washing buffer (AW2), the tube was then centrifuged at 14,000rpm for 3 minutes at room temperature. The filtrate and the collection tube were discarded and the mini spin column moved into a labelled 1.5ml microfuge tube.

2.3.7.4 Elution of the Genomic DNA

The DNA was eluted by adding 200µl of the elution buffer (AE) to the centre of the mini spin column membrane and then incubated for 1 minute at room temperature before centrifugation

at 8000rpm for 1 minute. The spin column was then discarded and the eluted DNA stored at 4°C.

2.3.7.5 DNA Quantification

DNA measurement was assessed by UV-VIS Spectrophotometry using the NanoDrop ND-1000 instrument (ThermoScientific). Briefly, the optical surface of the Nanodrop was cleaned with lint-free tissue then 2µl of nuclease-free water was loaded into the instrument for initialisation. The optical surface was wiped again and 2µl of the elution buffer was loaded as a blank, this was followed by cleaning the surface and loading the DNA samples for measurement. Nanodrop then automatically quantified DNA concentration and assessed DNA purity. The ratio of absorbance at A260/A280nm and A260/A230nm was used to measure DNA purity. A260/A280 values from 1.8-2.0 indicated the absence of contamination with proteins, phenol or any other contaminants, whereas A260/A230 values in the range of (2.0-2.2) indicated adequate DNA purity.

2.3.8 Multiplex Ligation-Dependent Probe Amplification (MLPA)

MLPA assay was used in this study to detect copy number aberrations such as homozygous and heterozygous deletion or duplication events for exons within the *ATM* gene. Briefly, MLPA is a multiplex PCR-based method containing 45 oligonucleotide probes. Each probe synthesised as two half-probes named 5'MLPA half-probe and the 3'MLPA half-probe. Each half-probe binds specifically to the target sequences (specific exon) and is constantly amplified by a single pair of universal primers. The 5' end of one primer is labelled with a fluorescent dye called 6-carboxyfluorescein (6-FAM) to detect the amplification product of the probe via genotyping. The other half of the probe has a 'stuffer DNA sequence' with a variable length between 19 to 370 nucleotides; each stuffer sequence is unique to each probe and designed

to generate an amplification product of the probe with a unique length (Armour et al., 2002, Schouten et al., 2002, Kozlowski et al., 2008). The amplification of the probes happens only when the two halves of the probe are hybridised to the adjacent target sequence without gap and then ligated together (Figure 2.5).

2.3.8.1 DNA Denaturation and Probes Hybridisation

The total quantity of 50ng of the genomic DNA was used in a 5µl volume for each MLPA reaction. To start the procedure, 5µl of DNA samples were denatured in a thermocycler at 98°C for 5 minutes and then the samples were cooled down to 25°C. Next, 3µl of hybridisation master mix containing 1.5µl MLPA buffer and 1.5µl probemix was added to each sample and mixed well by pipetting up and down. Samples were then heated to 95°C for 1 minute and then incubated at 60°C for 16-20 hours allowing the MLPA probes to hybridise properly to the adjacent DNA target.

2.3.8.2 Ligation Reaction

On the second day, the temperature was lowered to 54°C and ligation master mix (32µl) prepared on ice by gently mixing 25µl of dH₂O, 3µl of ligase buffer A, 3µl of ligase buffer B, and 1µl of ligase and then added to each tube reaction with gentle agitation. The mixture was then incubated at 54°C for 15 minutes followed by further incubation at 98°C for 5 minutes to inactivate the ligase enzyme and then paused at 20°C.

2.3.8.3 PCR Amplification

During the incubation time for the ligation step, the polymerase master mix (10µl) was prepared on ice by gently mixing 7.5µl dH₂O, 2µl SALSA PCR primer mix and 0.5µl of pre-hand warmed SALSA polymerase and then added to each sample tube with gentle mixing using a pipette.

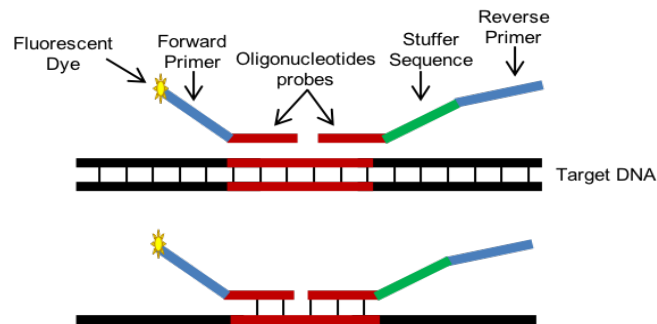
Samples were then placed into the thermocycler machine and amplified for 35 cycles with 30 seconds at 95°C (denaturation), 30 seconds at 60°C (annealing) and extension at 72°C for 1 minute, then 20 minutes at 72°C and paused at 15°C. The fluorescent label is incorporated into the amplification products (MLPA amplicons).

2.3.8.4 MLPA Analysis

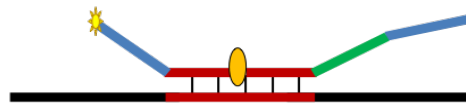
Following the amplification step, samples were sent to the core sequencing facility at Sheffield Medical School (University of Sheffield, UK) for genotyping using ABI-3730 capillary electrophoresis (ThermoScientific). The MLPA amplicons were separated by capillary electrophoresis according to their length. In term of principle of this method, up to 5 different fluorescent dyes can be used and identified in one sample by ABI, one of these dyes is used for a size standard. The size standard has fragments of known length and functions as a molecular ruler to determine the length of the MLPA amplicons. The MLPA amplicons and the size standard are labelled with different florescent dyes. Both MLPA amplicons and the size standard fragments are passed through a detector and the measured fluorescence is visualised as a peak pattern called electropherogram. The migration of the MLPA amplicons is compared to migration of the fragments of the size standard to determine the length of each MLPA amplicon. Once the length has been determined, each MLPA amplicon peak can be linked to the correct MLPA probe and by determining the fluoresce signal of each peak, each probe can be quantified during data analysis. The raw data generated by capillary electrophoresis was then analysed using Coffalyser.Net software available from MRC Holland (www.mrc-holland.com). The software normalises MLPA data to cancel out experimental variation in the data. The normalisation was done as follows: firstly, the peak height of each probe's amplification product was divided by the sum of the height of all peaks for reference probes in that sample only (intrasample-normalisation). The reference probes detect

sequences located in other genes that are assumed to remain normal (diploid) in the DNA of all used samples. Secondly, intersample-normalisation which can be done by dividing the intra-normalised probe ratio in a sample by the average intra-normalised probe ratio of all reference DNA samples. The reference samples are expected to have a normal DNA copy number for the reference probes as well as the target probes. The MLPA peak pattern of the test samples having no genomic aberrations will be identical to that of reference DNA sample and the final probe ratio determined by inter-normalisation step will be in the range from 0.70-1.3, for heterozygous deletion of an exon the range is 0.40–0.65 and the peak height should be half the height of the reference peak, while duplication is above 1.30 and the peak height should be almost twice the height of a reference peak. Homozygous deletions are represented by the absence of a peak and a ratio of 0.

Sample DNA Denaturation and Probes Hybridisation



Probes Ligation



Amplification of Ligated Probes



Fragment Analysis



Figure 2.5 A Schematic Representation of MLPA Principle.

2.3.9 Next Generation Sequencing (NGS)

Next generation DNA sequencing is a high-throughput approach that enables rapid sequencing of the base pairs in DNA samples using the concept of massively parallel sequencing of short DNA fragments. Illumina sequencing is one of the major platforms used in NGS. The genomic

DNA extracted from sarcoma samples have been sequenced on Illumina HiSeq2500 instrument using NGS services provided by the Children's Hospital, Sheffield, UK to detect the copy number of the *ATM*. Briefly, Illumina sequencing workflow consists of four basic steps; library preparation, cluster generation, sequencing and data analysis.

2.3.9.1 Library Preparation

Library construction for Illumina NGS involves random fragmentation of the genomic DNA into smaller sequence-able fragments (typically 200-500 bp insertion length) (Figure 2.6 (A)). Adaptors (short, double-stranded pieces of synthetic DNA) are then ligated to each side of the fragmented DNA forming adaptor-ligated DNA fragments. The adaptors facilitate the attachment of the DNA fragments to the surface of the glass slides, the so-called flowcells. Each flowcell has eight channels in which the amplification and/or sequencing reactions take place. The surface of the flowcell is densely coated with the adaptors and the complementary adapters.

2.3.9.2 Cluster Generation

Following DNA denaturation, single-stranded fragments are randomly bound to the surface inside the channel at one end forming a bridge structure by hybridising with its free end to the complementary adapter on the flowcell surface (Figure 2.6 (B)). The adaptors on the surface serve as primers that can synthesis the rest of the DNA. Each fragment is then amplified through a bridge PCR amplification that generates clusters of identical copies around the original DNA fragments. After several PCR cycles, about 1000 copies of each fragment are created on the flowcell surface then they are separated into single strands to be ready for sequencing.

2.3.9.3 Sequencing

The sequencing process is carried out in cycles, the primers, DNA polymerase and four different fluorescently labelled nucleotides (deoxynucleoside triphosphates) (dNTPs) are added into the flowcell surface (Figure 2.6 (C)). The appropriate nucleotide is then incorporated into the nucleic acid chains. The fluorescently labelled dNTPs act as a terminator to ensure that only one base is added to the nucleic acid chain per cycle. Excessive primers, DNA polymerase and dNTPs are then washed off the slides. Following laser excitation, the flowcell is imaged and the emission from each cluster is recoded to identify the base incorporated in each cycle (base calling). At this stage, the fluorescently labelled dNTPs are cleaved off and the flowcell is re-prepared for the next cycle. The synthesis cycle is repeated by addition of one nucleotide at a time and recording the fluorescence signal in the form of an image. Using the Illumina software, the bases are identified at each site for each image, which facilitates construction of a sequence. Following a number of cycles, such as 50-100 cycles, the DNA fragments can be optionally turned over allowing their other ends to be sequenced in a similar manner to get paired-end data. Sequencing experiment can be divided into three types. Whole genome sequencing (WGS) is used to investigate the entire human genome whereas a whole exome sequencing (WES) approach is employed when targeting the entire set of the human exons, additionally, NGS allows the sequencing of a specific set of genes. A single Illumina HiSeq 2500 instrument can produce massive data with very high yield of error-free reads. An important concept related to the Illumina system output is the number of reads or sequencing coverage that describes the number of times a single base position has been sequenced. The higher the level of sequencing coverage, the higher the degree of confidence in base calls. The current error rate for Illumina system is roughly 0.5%, and sequence coverage of at least 10× or 30× is usually recommended. Illumina HiSeq 2500 involves two run modes, rapid run and high output run mode furthermore, the system has the ability to process one flowcell alone

or two flowcells simultaneously. In the rapid run mode, fully automated sequencing for short read applications can be achieved in 7 hours and a single human genome at 30× coverage can be achieved in 27 hours. With the rapid or high run modes and single or double flowcell options, the instrument has an output of about 300 million to 4 billion reads per run, and a maximum read length of 2 × 125 bp for high output mode and 2 × 250 bp for the rapid run mode.

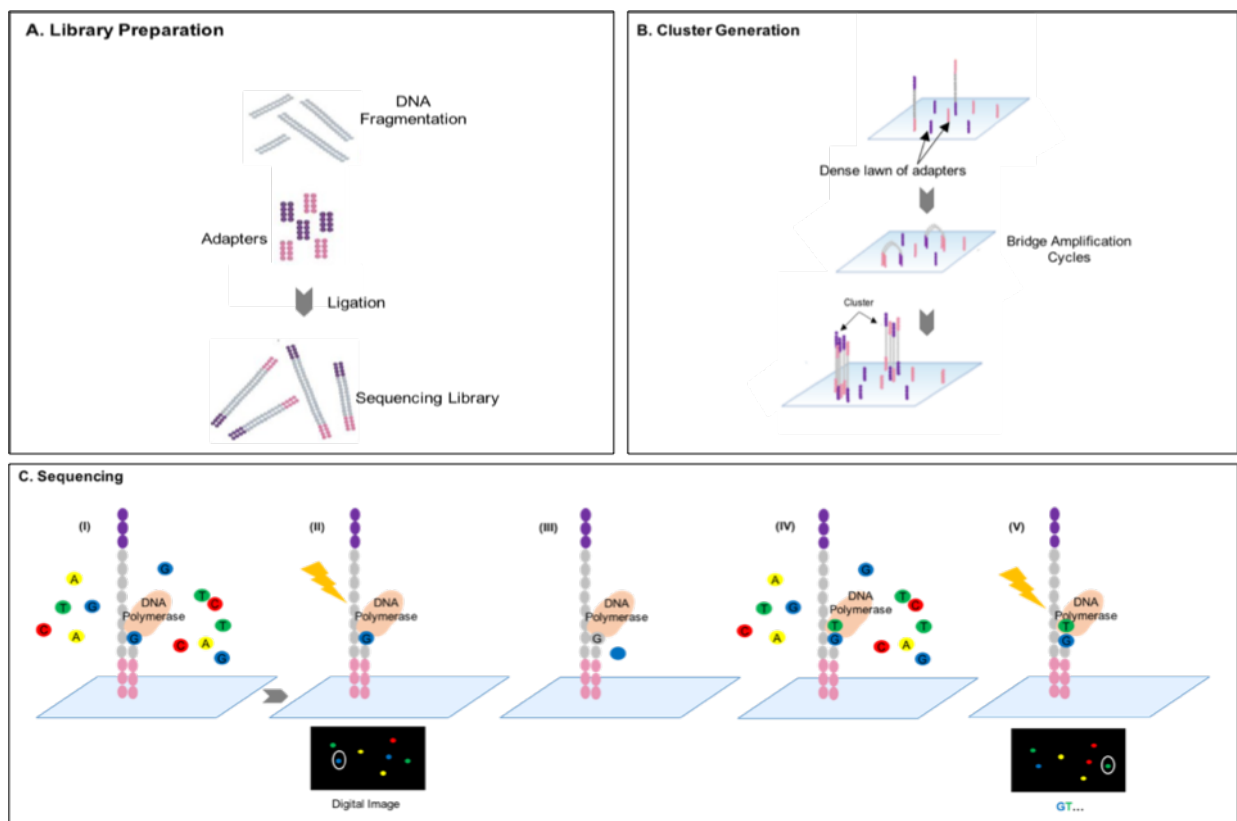


Figure 2.6 A Schematic Model of Illumina Sequencing Workflow.

A. Sequencing library is prepared by random fragmentation of the genomic DNA followed by adapters ligation. **B.** Sequence library is loaded into the flowcell and single strand fragments are hybridized to the complementary adapters on the flowcell. Cluster is then generated by PCR amplification. Final cluster has around 1000 copies of the original fragment. **C.** The flowcell surface is flooded with primers, DNA polymerase and dNTPs (I). The fluorescently labelled dNTPs acts as a terminator so only one base is added per cycle. Abundant primers, DNA polymerase and dNTPs are then washed off the slides. After laser excitation, the emitted fluorescence from each cluster on the flowcell is imaged to identify base incorporated in each cycle (II). Then, the fluorescently labelled dNTPs is cleaved off (III). And the next cycle starts (IV-V).

2.3.9.4 Data Analysis

The process of detecting the *ATM* copy number from NGS data can be split into several steps: pre-processing followed by segmentation and calling (Figure 2.7). In the pre-processing step, the biases and noises in the NGS data are eliminated, the quality control of reads is checked and the PCR duplicates are removed before importing the data into the Nexus Copy Number Software v10.0 (Biodiscovery).

During the segmentation step, BAM MultiScale Reference (MSR) algorithm in the Nexus software uses the target and off-target reads to generate a reference file which is compared to the test (sarcoma) samples. The algorithm involves an adjustable binning mechanism which employs the Hidden Markov Model (HMM) to segment the genome into target regions using the reads (depth of coverage) in targeted areas and into the backbone regions by using the off-target reads. The mechanism uses coarse binnings in the backbone regions since these deliver a baseline copy number and also large copy number events. Meanwhile, fine binnings are used to give high resolution copy number detection in targeted regions. Values in each bin are the normalised read depth defined as the number of bases within the bin divided by the product of the length of the bin and the total number of bases within all bins. The reference genome used was derived from NA12878 genome in a bottle (GIAB) DNA (vendor) that was sequenced using the same protocol as the sarcoma samples.

The whole genome is displayed in the software as a series of sections, with each section having a cluster value representing the median log-ratio value of all the reads found in that region. The cluster values together with the certain thresholds were used after that by the algorithm called Fast Adaptive States Segmentation Technique 2 (FASST2) to establish regions with copy number aberration. Log ratio threshold values of -0.2 and -1.0 were used to identify a

single and two or more copy number loss respectively, while the threshold values for gains of a single and two or more copy number are +0.2 and +0.6 respectively. The parameters in the algorithm to generate the reference and all the threshold values in this experiment were based on recommendations from the manufacturers of the analysis software. Aberrations were displayed as ideograms (graphical genomic plots) which can be viewed at whole genome, chromosome and single gene/exon levels for easy visual analysis.

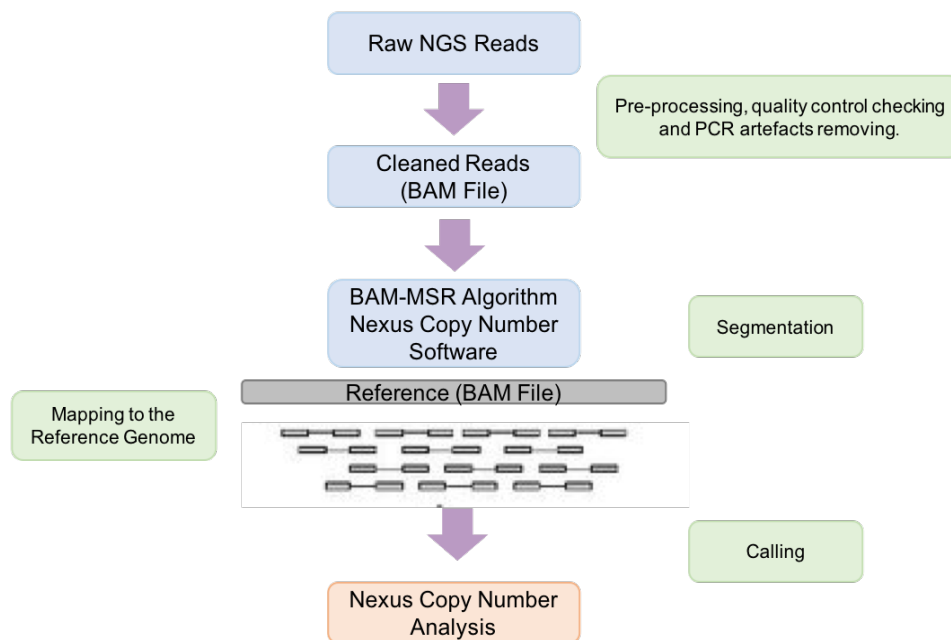


Figure 2.7 The Analytical Workflow of CNA from NGS Data using Nexus Copy Number Software.

The above figure shows a summary of the method used to estimate CNA from NGS data using Nexus Copy Number Software v10.0 (Biodiscovery). A reference file was derived from NA12878 genome in a bottle (GIAB) DNA. Individual BAM files of the test samples along with a reference BAM file were then directly loaded into the software to estimate the copy number for the ATM.

CHAPTER THREE

3 ATM FUNCTION AS PART OF THE RESPONSE OF SARCOMAS TO IONISING RADIATION (IR)

3.1 Introduction

Ionising radiation is commonly used as a stable approach for the treatment of a large percentage of cancers including sarcomas. The aim of radiotherapy is to destroy tumour cells by delivering an adequate lethal dose to the target volume of cancer while the harmful effect to normal cells should be as low as possible. Although radiotherapy could improve the survival of cancer patients and minimize morbidity, its effectiveness is limited by the toxicity to neighbouring normal tissues and the presence of radio resistant tumour cells, together with the development of secondary tumours within the treatment field (Gately et al., 1998, Yang et al., 2016).

DNA-DSBs are the most dangerous lesions that should be repaired to maintain genomic stability. This damage is induced by several factors including the exposure to IR during clinical radiotherapy and receiving anticancer chemotherapeutic drugs (Clingen et al., 2008, Bourton et al., 2011). DNA-DSBs can also arise from within the cell during DNA replication and normal cellular metabolism (Lindahl and Barnes, 2000). The irradiated cells have developed a complex and highly regulated signalling network to ensure cell survival and maintain genomic integrity. The ataxia telangiectasia mutated gene (*ATM*) product has an extensive role in response to irradiation induced genomic damage. As mentioned previously in chapter 1, ATM is auto-phosphorylated rapidly at ser376, ser1893 ser1981 and ser2996 following the exposure to IR and DNA-DSBs formation. Its phosphorylation results in the activation of over a hundred substrates that trigger cell cycle checkpoints/arrest and subsequently delay the G1/S and G2 cell cycle phases thus, allowing the repair of the DNA-DSBs by HR and by NHEJ which both play a significant role in maintaining the integrity of the genome (Bakkenist and Kastan, 2003, Nakamura et al., 2010).

A very early event in response to the DNA-DSBs following IR is the phosphorylation of H2AX molecules at ser139. Both ATM and DNA-PK are able to phosphorylate H2AX molecules to form γ H2AX in response to DNA-DSBs damage. The phosphorylated γ H2AX molecules accumulate into the chromatin regions directly surrounding the damage site as nuclear foci and signals to attract other DNA repair proteins. The formation of γ H2AX foci can thus be used as a marker of DNA damage (Rogakou et al., 1998, Burma et al., 2001, Stiff et al., 2004). Using phospho-specific antibodies, γ H2AX can be visualised under an immunofluorescence microscopy. It has been reported that elimination of the γ H2AX foci from the nucleus can serve as a marker for DNA-DSBs repair; therefore, measuring the kinetics of γ H2AX foci formation and loss has been undertaken in many studies to investigate the kinetics of DNA repair (Svetlova et al., 2010).

When normal cells undergo repair, the phosphorylation of H2AX molecules occurs rapidly following DNA damage. The majority of this damage is repaired within approximately 1-3 hours which consequently leads to the dephosphorylation and elimination of the γ H2AX foci from the nucleus (Rogakou et al., 1998). In contrast, there is prolonged persistence of γ H2AX foci in cells displaying impairment signs in the DNA repair mechanisms, which presumably is explained by the failure to repair DNA damage (Bourton et al., 2011). This has been reported in cells isolated from patients with DNA repair disorders such as ataxia telangiectasia. The *ATM* gene is mutated in this disorder and is supposed to inactivate the signalling cascades of the DNA-DSBs repair leading to the prolonged appearance of γ H2AX foci within the nucleus (Friesner et al., 2005).

Other cellular abnormalities have been also observed in cells derived from A-T patients including an extreme sensitivity to radiation. Numerous *in-vitro* studies have demonstrated that

loss of ATM kinase function caused by gene mutation, gene expression downregulation, or by small molecule inhibition remarkably increases the sensitivity of the cells to ionizing radiation, making ATM an attractive target for the development of novel therapeutics that could be used to enhance tumour cell sensitivity to radio/chemotherapy (Gately et al., 1998, Hickson et al., 2004, Rainey et al., 2008, Yang et al., 2016). Based on this observation, several inhibitors that disrupt ATM function and to radiosensitise tumour cells have been used widely in many studies. For example, Rainey *et al.*, (2008) showed that the transient inhibition of ATM is sufficient to sensitise *ATM* deficient cells to IR using clonogenic survival assays (Rainey et al., 2008).

The loss of the *ATM* copy in sarcomas has been previously correlated with the reduced expression of the protein (Ul-Hassan et al., 2009), therefore in this part of the study the expression of ATM was investigated to see if it was altered and how this may affect response to DNA damage response. In this chapter, Western blotting was primarily carried out to look for total ATM protein expression and for the phosphorylated form of ATM following the exposure of different sarcoma subtypes to ionising radiation. To further examine the role of *ATM* in sarcoma development, the induction and elimination of γ H2AX foci was measured both spontaneously and after inducing DNA-DSBs by ionising radiation prior to and following the treatment with ATM kinase inhibitor KU55933 (Calbiochem, USA). The effect of the irradiation, ATM inhibition and the combination of both treatments on cell survival was also investigated in this chapter using the *in-vitro* clonogenic survival assay. Finally, the correlation between the cellular response to IR and ATM inhibition in γ H2AX and clonogenic assays and levels of ATM protein expression was explored.

3.2 Results

3.2.1 Determination of ATM Expression in Sarcoma and Normal Cell Lines

To determine ATM expression in sarcoma, Western blot analysis was performed on six primary STS cell lines and four established sarcoma cell lines. U2OS (an established osteosarcoma that has a balanced, non-mutated copy number of *ATM*) and normal human retinal epithelial (hTERT-RPE1) cell lines were used as tumour and non-tumour cell line controls (Table 2.1 and Table 2.2). The expression of ATM in all cell lines tested was detectable at 370 kDa including control samples. Interestingly, a second band of lower molecular weight (~280 kDa) was also detected below the expression of ATM in all established sarcoma cell lines and some primary sarcoma cell lines including (STS 14/10, STS 02/11 W1 and STS 20/11), which may represent a degradation product of the higher molecular weight ATM band or likely due to the truncation of the ATM protein in sarcoma cases (Figure 3.1).

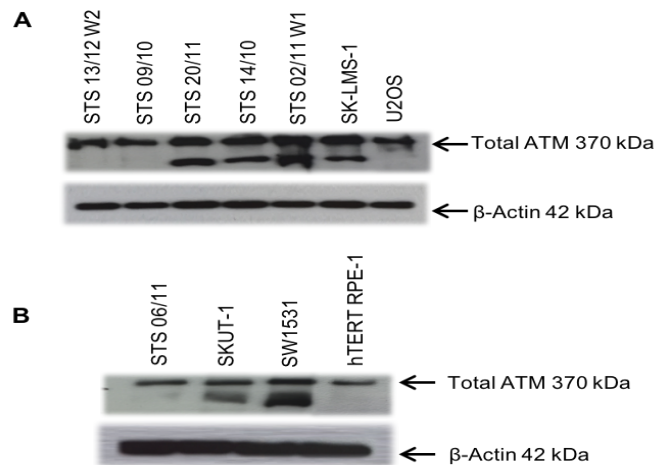


Figure 3.1 A Western Blotting Analysis of the ATM Protein in Different Sarcoma Cell Lines.

*Western blotting of ATM protein in cultured cell lines. 20µg of the whole cells lysate were separated electrophoretically on 4-7% gradient SDS-PAGE and immunoblotted with monoclonal antibody against ATM (Abcam, UK). The expression of the ATM protein was measurable at 370 kDa in the control samples (U2OS, last lane, blot **A** and hTERT RPE-1, last lane blot **B**) and in all sarcoma cell lines. The expression of the ATM was higher in the sarcoma samples that showed an additional band below the expression of the ATM protein. β-Actin was used as a loading control and was expressed at 42 kDa in all samples.*

3.2.2 Time Course Inhibition of the ATM Kinase Activity

To support the validity of the data generated in this chapter by γ H2AX and clonogenic and to prove the effective inhibition of ATM phosphorylation using ATM kinase inhibitor KU55933 (Calbiochem, USA), Western blotting was performed as explained in (Section 2.3.5). A concentration of 10 μ M ATM kinase inhibitor KU55933 was used as it has been directed by Hickson et al. (2004) to show that the ATM phosphorylation was completely inhibited in the U2OS cell line following the treatment with the ATM kinase inhibitor and the exposure of U2OS cells to 2Gy of IR. β -actin was used as a loading control to confirm that the proteins of different samples were loaded in equal amount and was essential throughout this process in order to interpret the result from Western blotting (Figure 3.2).

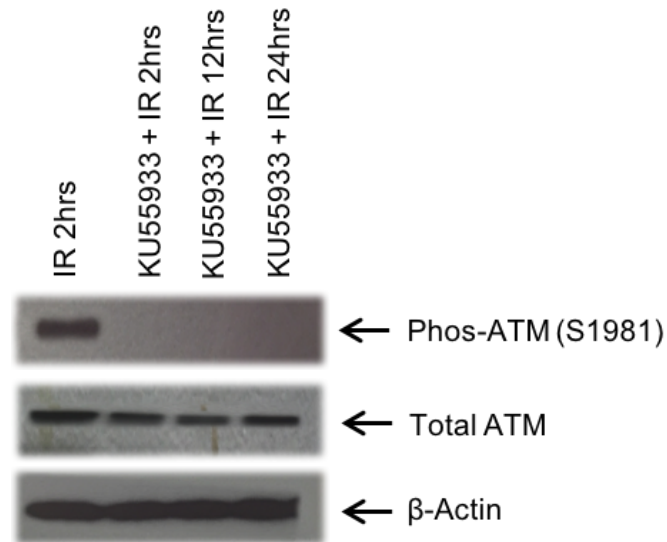


Figure 3.2 Western Blotting Confirming the Inhibition of ATM Phosphorylation.

U2OS cells were pre-incubated with or without 10 μ M ATM inhibitor for 2 hours before 2Gy IR. After time-points shown above, the cells were analyzed for the total ATM and ATM phosphoserine 1981 levels by Western blotting. 20 μ g of total cell lysate was electrophoresed on 4-15% mini precast polyacrylamide gel and immunoblotted using ATM (Phospho S1981) [10H11.E12] mouse monoclonal antibody (Abcam, UK) and monoclonal antibody against ATM (Abcam, UK).

The expression of the total ATM (middle panel) and autophosphorylated form of ATM (first lane of top panel) was detected at 370 kDa. The phosphorylation of the ATM protein was inhibited after the treatment with the ATM inhibitor (lane 2, 3 and 4, top panel). And to effectively interpret the Western blot results; β -actin was used as loading control and was expressed at 42 kDa in all loaded samples as shown in the bottom panel. This confirms that the samples had been equally loaded and ATM phosphorylation was successfully inhibited.

3.2.3 ATM Autophosphorylation and Inhibition in Different Cell Lines

Sarcoma cells were maintained in cell culture until they reached 60-80% confluency. Cells were then treated with or without 10 μ M ATM kinase inhibitor KU55933 (Calbiochem, USA) and incubated at 37°C in a 95% air and 5% CO₂ incubator for two hours prior to 2Gy of irradiation. After 2 hours, the cells were analysed for total ATM and ATM phospho-serine 1981 levels by Western blotting. Another Western blotting gel was run at the same time for β -actin which was used as a loading control (Figure 3.3).

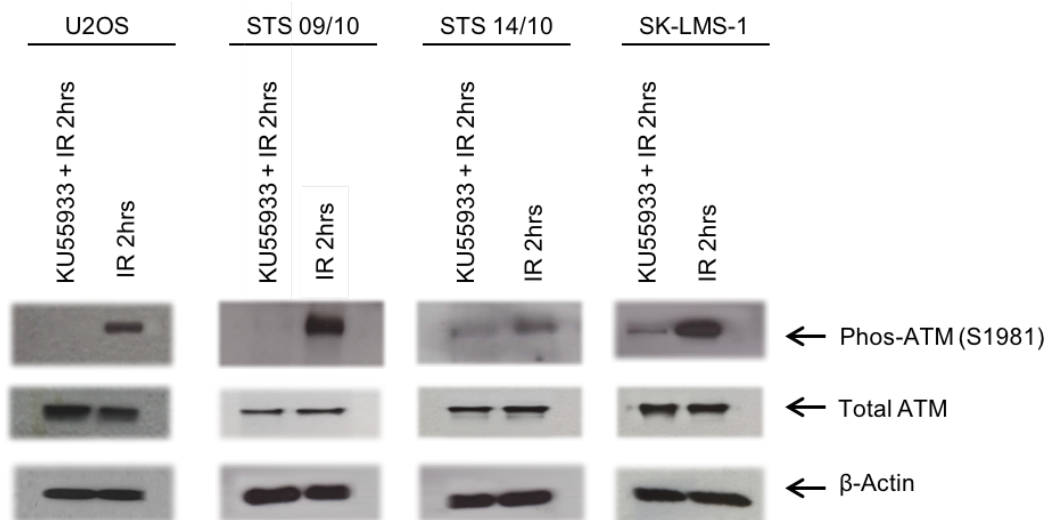


Figure 3.3 Auto phosphorylation of ATM on ser1981 in Response to IR and inhibition.

Western blot detects the total ATM and autophosphorylation form of ATM on ser1981 in response to DNA-DSBs by 2Gy IR using monoclonal antibody against ATM (Abcam, UK) and ATM (Phospho S1981) [10H11.E12] mouse monoclonal antibody (Abcam, UK) respectively. The blot also shows the effect of KU5933 on ATM serine 1981 phosphorylation and total ATM protein levels in response to IR.

The phosphorylation of the ATM was inhibited when cells were treated with ATM inhibitor prior to irradiation exposure in the control and in primary STS 09/10 whereas, it was slightly detected following the inhibition in the established sarcoma cell line SK-LMS-1 and in the primary STS14/10. Protein loading levels were monitored by probing for β -actin as shown.

3.2.4 Spontaneous γ H2AX Foci Formation is Increased in Sarcoma Cell Lines

Compared to Controls

γ H2AX analysis was performed to explore if there were any changes in the DNA damage response to IR. γ H2AX analysis was done on six primary sarcoma cell lines and four established sarcoma cell lines. The U2OS, established osteosarcoma cell line and hTERT-RPE1, normal human retinal epithelial cell line were used as tumour and non-tumour cell line controls, respectively.

The kinetics of the DNA repair was explored in all cell lines by quantifying the γ H2AX foci formation levels both endogenously and at multiple time points following the induction of DNA-DSBs by 2Gy IR. To examine the sarcomas and the function of the ATM kinase in the phosphorylation of H2AX and in the DNA-DSBs repair, the effect of inhibiting the ATM was also examined. The activity of the ATM kinase was inhibited by adding 10 μ M of ATM inhibitor KU55933 (Calbiochem, USA) 2 hours prior to the exposure to the 2Gy IR. For spontaneous response, ATM inhibitor was added on the respective well for 2 hours, the media was then changed and γ H2AX assay procedure was applied (Section 2.3.3). γ H2AX foci were identified using fluorescent microscopy at 100x magnification as red fluorescent signals subsequent to the immunostaining with anti phospho- γ H2AX (Cell Signaling Technology) and Cy3-labelled (Invitrogen, USA) antibodies. The numbers of red foci signals within the nucleus were visually quantified in 100 cells from each slide. The results were demonstrated as a percentage of cells with >10 foci per nucleus in 100 cells at different time points of 0, 30 minutes, 1 hour, 2 hours and 4 hours following 2Gy IR treatment with and without the inhibition of ATM kinase with time 0 minutes being the spontaneous result. γ H2AX data were derived from three independent experiments for both sarcoma and normal cell lines and is shown in (Figure 3.6).

The spontaneous levels of γ H2AX foci were very low in hTERT RPE-1, normal human retinal epithelial cell line with no cells forming greater than 10 γ H2AX foci. (Figure 3.4, 3.5 and 3.6 A). All the primary sarcoma cell lines however, had at least 10% of cells with a large number of γ H2AX foci as shown in figure 3.6 (F-K). The primary dedifferentiated liposarcoma (DDLPS) cell line (20/11) showed the highest number of cells having greater than 10 γ H2AX foci (~ 69% of cells showing >10 foci). Interestingly, STS 20/11 is the only cell line derived from a patient who was treated with radiotherapy prior to excision (Figure 3.4) (Salawu et al., 2016). Levels of endogenous DNA-DSBs damage were much higher in the established sarcoma cell lines (SK-LMS-1, SKUT-1 and SW1353) (Figure 3.6 C-E), suggests that the increased levels of endogenous DNA damage are occurring and not being repaired in these cell lines. Surprisingly, the tumour control, established osteosarcoma cell line (U2OS, which has a balanced copy number of *ATM*) showed relatively low level of endogenous damage (Figure 3.5 and 3.6 B)

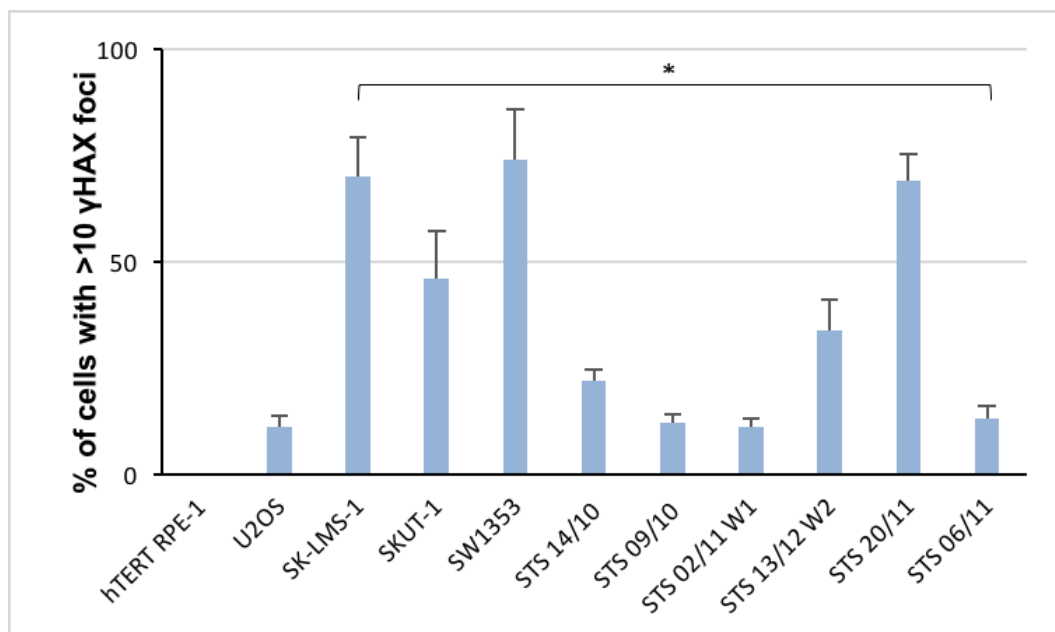


Figure 3.4 Percentage of Cells Forming Spontaneous γ H2AX Foci in Sarcoma and Control Cell Line.

*A greater proportion of sarcoma cells to form more than 10 H2AX foci in response to spontaneous damage compared with the normal control cell line (*p-value <0.05 by a t-test).*

3.2.5 Sarcoma Cells are more Sensitive to IR Induced DNA-DSBs Damage Compared to Control Cells

Rapid induction of γ H2AX foci was detected in all cell lines tested in this study at 30 minutes post IR, this is consistent with the initiation of DNA damage repair as a consequence of exposure to IR (Figure 3.5 and 3.6). U2OS and hTERT RPE-1 showed an average of 90% and 70% of cells with more than 10 γ H2AX foci respectively at 30 minutes post IR. These number was noticeably reduced within 2 hours upon repair in the control cells with an average of 30% and 3% for U2OS and hTERT RPE-1 respectively (Figure 3.6 A and B). Levels of γ H2AX formation following exposure to IR differed in sarcoma compared to the normal and U2OS. High levels of γ H2AX foci was detected in all established sarcoma cell lines at 2 hours post IR and was persistent for up to 4 hours with a mean number of 60%, 71% and 82% cells with more than 10 γ H2AX foci in SK-LMS-1, SKUT-1 and SW1353 cell lines respectively (Figure 3.6 C, D and E). Some primary sarcoma cell lines also displayed high levels of γ H2AX at 2 hours post IR and were prolonged for even 4 hours post IR these including STS 09/10, STS 20/11 and STS 06/11 with a mean number of 40%, 100% and 99% cells per each cell respectively, suggesting that sarcoma cells are significantly more sensitive to IR induced DNA damage compared to the normal control with a p-value of <0.05 calculated by a t-test (Figure 3.6 G, J and K and Figure 3.7). Although the induction of γ H2AX foci was reduced within 2 hours of IR in STS 14/10, 02/11W1 and 13/12 W2 as shown in figure 3.6 F, H and I, these cells were also significantly more sensitive to IR induced DNA-DSBs compared to the control with a p-value of <0.05 calculated by a t-test (Figure 3.7).

3.2.6 ATM Inhibition Blocks DNA Repair in Controls However Sarcoma Cell Lines

Display a Delayed Response to IR Following ATM inhibition

Although control cell lines had no induction of γ H2AX foci post IR following ATM inhibition, the sarcoma cell lines showed varying responses (Figure 3.6). All sarcomas had reduced formation levels of γ H2AX foci 30 minutes following irradiation, compared to the untreated cells, except the established sarcoma cell lines SK-LMS-1 and SW1353 (Figure 3.6 C and E). SK-LMS-1 had no significant reduction of the γ H2AX levels at all, interestingly, the formation of γ H2AX foci in this cell line slightly declined 1 hour after irradiation and in 2 to 4 hours it started again to behave as the untreated cells, whereas SW1353 showed slightly higher levels of γ H2AX foci only at 30 minutes post IR compared to untreated cells. The induction of γ H2AX foci fluctuated in this cell line and it was significantly reduced within 2 hours following IR with a p-value of 0.01 calculated by a student's t-test. Interestingly, the inhibition of ATM kinase in the SKUT-1 and in primary STS 14/10 cell lines does not induce a reduction of γ H2AX levels as observed in the control cells (Figure 3.6 D and F). These levels are detected within 4 hours after IR and surprisingly were significantly higher than the untreated cells with a p-value of 0.01 for STS 14/10 cell lines. It was however consistently observed for all the sarcomas investigated, that although ATM was inhibited in all cell lines, the greater proportion of γ H2AX foci formation was detected unlike the findings of the control cells (U2OS and normal retinal cells) (Figure 3.6).

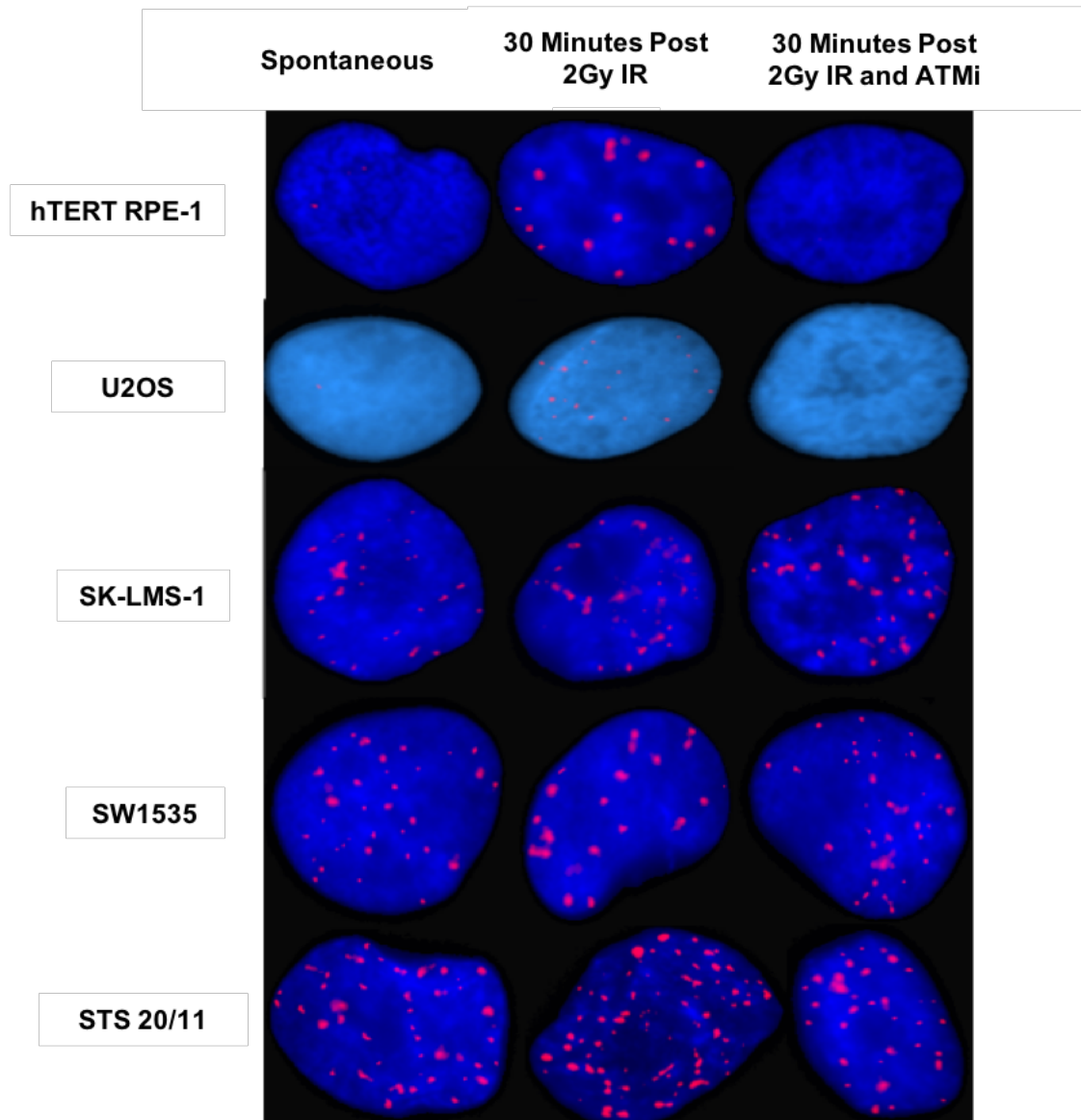
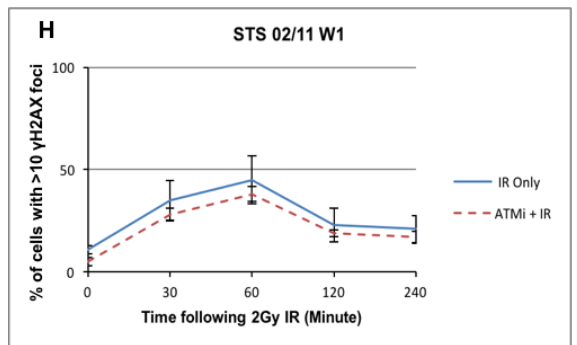
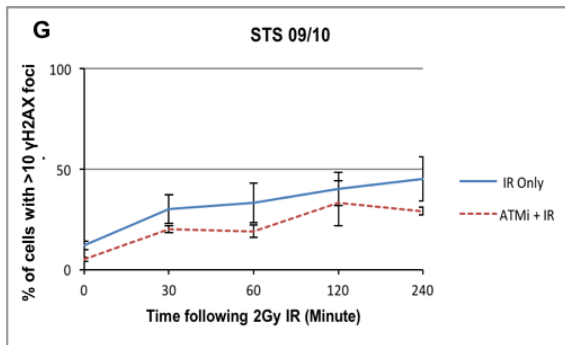
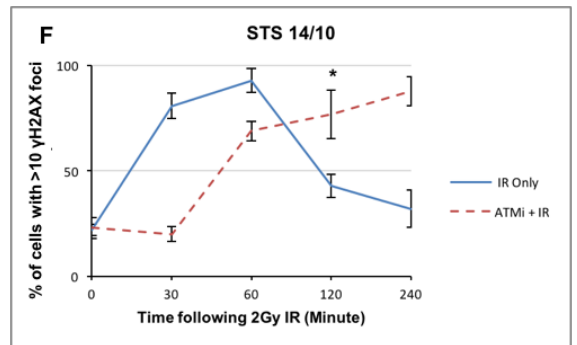
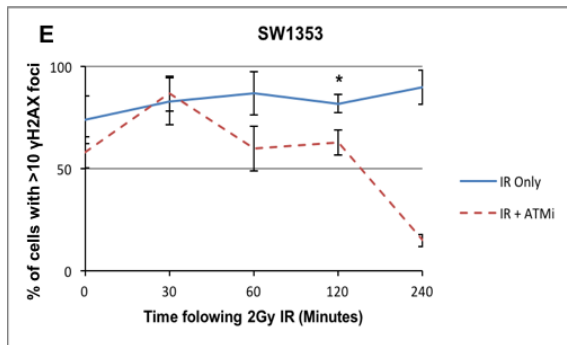
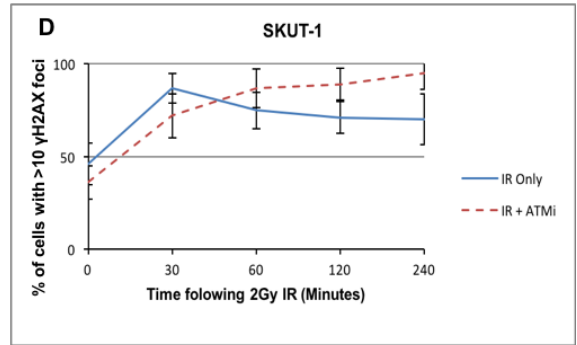
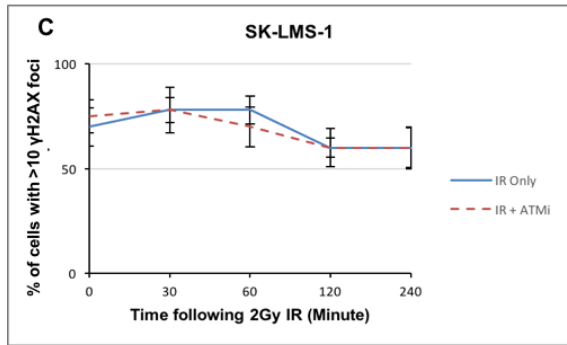
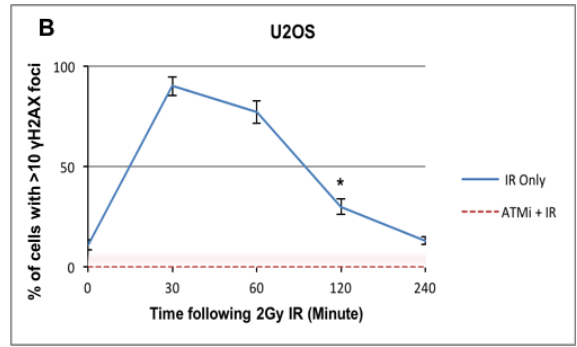
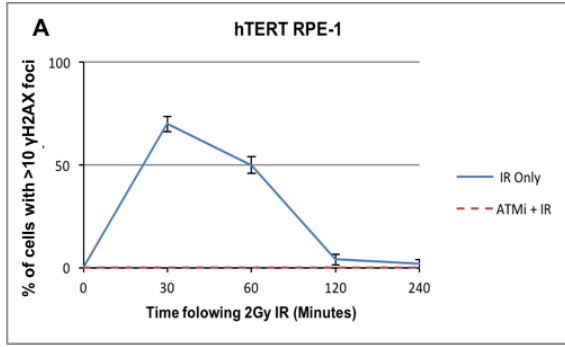


Figure 3.5 Representative Images of γ H2AX Foci Formation in the Controls, Established and Primary Sarcoma Cell Lines.

γ H2AX foci were detected as red fluorescent signals inside the blue DAPI stained cells on a fluorescence microscope with x100 magnification objective. The interphase nuclei of the control cells (U2OS and hTERT-RPE1) displaying less than ten endogenous γ H2AX foci. The established sarcoma (SK-LMS-1 and SW1353) and primary STS 20/11 cells nucleus however, showing more than ten endogenous γ H2AX foci. Levels of H2AX foci 30 minutes post IR were increased in all sarcoma cell lines. Following the treatment with the ATM inhibitor all sarcomas had a reduced level of formation of γ H2ax foci 30 minutes following radiation, compared to the untreated cells, except the SK-LMS-1 which had no reduction of the γ H2ax levels at all.



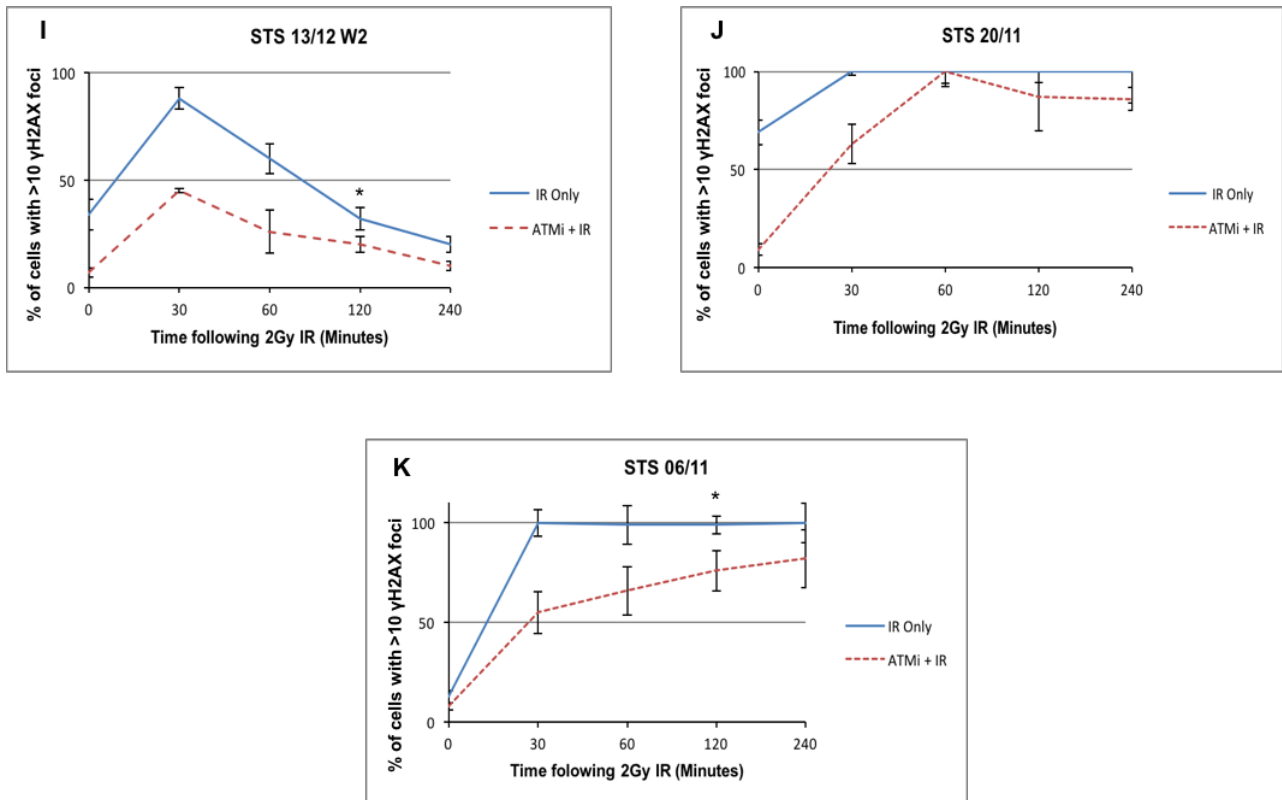


Figure 3.6 Kinetics of Formation and Elimination of IR-Induced γ H2AX Foci as a Measure of DNA Damage in Different Cell Lines with and without the Inhibition of the ATM.

Graphs show percentage of cells forming greater than ten γ H2AX foci at time point of 0, 30, 60, 120 and 240 minutes following irradiation treatment with and without the inhibition of the ATM, with time 0 minutes being the spontaneous response. γ H2AX data on the graphs represent the mean of three independent experiments with standard deviation (SD) error bars. All cell lines showed a dramatic increase of γ H2AX foci formation 30 minutes following 2Gy IR. The induction of γ H2AX foci back down to the endogenous levels within 2 hours post IR in control cells (U2OS and hTERT RPE-1). With the addition of the ATM inhibitor, there was no detectable γ H2AX response in these two cell lines. The established sarcoma cell line (SK-LMS-1), however, still showed high levels of γ H2AX formation in response to the IR, with no significant difference to γ H2AX levels when treated with the ATM inhibitor. Interestingly, SKUT-1 and STS 14/10, cell lines showed higher levels of γ H2AX formation upon ATM inhibition than untreated cells at 2 hours following IR. The induction of γ H2AX foci in STS 20/11 and STS 06/11 reached high levels at each time point of the IR. The asterisks symbol in the graphs indicate a significance difference detected in the cellular response to IR with and without ATM inhibition post 2 hours of IR.

3.2.7 ATM Inhibition Prevents Kinase Activity of ATM and Blocks DNA Repair in Control Following 2 Hours of IR

As shown in figure 3.3, the autophosphorylation of the ATM on ser1981 was detected after 2 hours of IR in different samples by Western blotting. The activity of the ATM kinase was successfully inhibited 2 hours post IR following ATM inhibition in the tumour control, U2OS. Other sarcoma cell lines however, showed low levels of ATM kinase expression upon ATM inhibition including SK-LMS-1 and STS 14/10 (Figure 3.3). Similarly, the formation of γ H2AX foci was detected in the same samples following 2 hours of IR-induced DNA damage (Figure 3.6). γ H2AX levels were significantly decreased within 2 hours post IR following ATM inhibition in the tumour control cell line compared to the untreated cells with a p-value of = 0.006 calculated by a student's t-test (Figure 3.6 B and 3.7). The established SK-LMS-1 and STS 14/10 however, were able to signal damage despite the inhibition of the ATM (Figure 3.6 C and F and Figure 3.7).

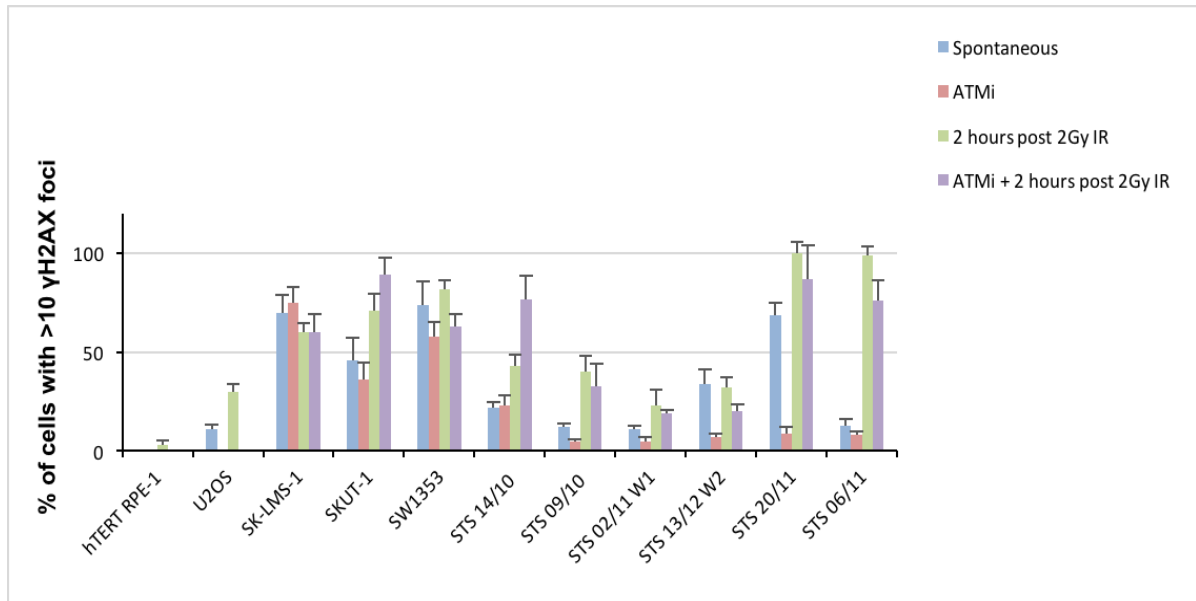


Figure 3.7 Percentage of Cells with >10 γ H2AX Foci Following 2 Hours of 2Gy IR with and without the Inhibition of the ATM.

The sarcoma cell lines displayed greater proportion to form >10 γ H2AX foci in response to spontaneous damage than normal control (p -value <0.05). Sarcoma cells were significantly more sensitive to IR induced DNA-DSBs post 2 hours of the exposure compared to normal control (p -value <0.05 by a t -test). The formation of γ H2AX foci was detected in all sarcoma at 2 hours post IR following ATM inhibition but not in the controls. Data are the mean of three independent experiments with SD error bars.

3.2.8 Sensitivity of Sarcoma Cell Lines to IR, ATM Inhibition and Combination of both Treatments

Due to the alteration in the ATM expression, STS sensitivity was investigated using clonogenic survival assay. This was performed on six primary STS cell lines, four established sarcoma cell lines and the control cell line, hTERT RPE-1. The established osteosarcoma U2OS was also used as tumour control. Cells were exposed to either no treatment, IR alone, ATM inhibitor alone or combination of both and left to form colonies for up to 14 days as explained in section 2.3.4. Results were obtained from three independent experiments per cell line and calculated as percentage surviving colonies relative to control plate +/-SEM (Figure 3.8).

The survival fraction was variable between sarcoma cases in response to 2Gy IR. Although all sarcoma cell lines including tumour control (U2OS) were significantly more sensitive to IR than normal control, p-value <0.05 calculated by t-test (Figure 3.8), they showed survival following IR exposure, suggesting the cells are able to cycle even with certain levels of induced damage. Interestingly, the primary DDLPS cell line (20/11) that derived from a patient who was irradiated before surgery showed the lowest percentage of survival following 2Gy IR (Salawu et al., 2016) (Figure 3.8). Treatment with the ATM inhibitor decreased the survival fraction in all cell lines compared to the untreated control and was significantly low in the controls, SK-LMS-1, SW1353, STS 20/11 and STS 06/11 with a p-value <0.05 calculated by t-test (Figure 3.9). The size of colony was also reduced in some sarcoma cases when the kinase activity of ATM had been inhibited (Figure 3.10). The exposure to the ATM inhibitor prior to 2Gy IR was extremely potentiate ionizing radiation induced cellular sensitivity in all sarcoma and control cell lines compared to the exposure to the ATM inhibitor alone p-value <0.05 by analysed by t-test and significantly enhanced radiosensitivity of the normal and SW1535, STS 14/10, STS 13/12 W2, STS 06/11 cell lines compared to the treatment with IR alone, p-value <0.05 calculated by t-

test, these data suggesting the existence of functional ATM in these cell lines (Figure 3.9 and 3.10).

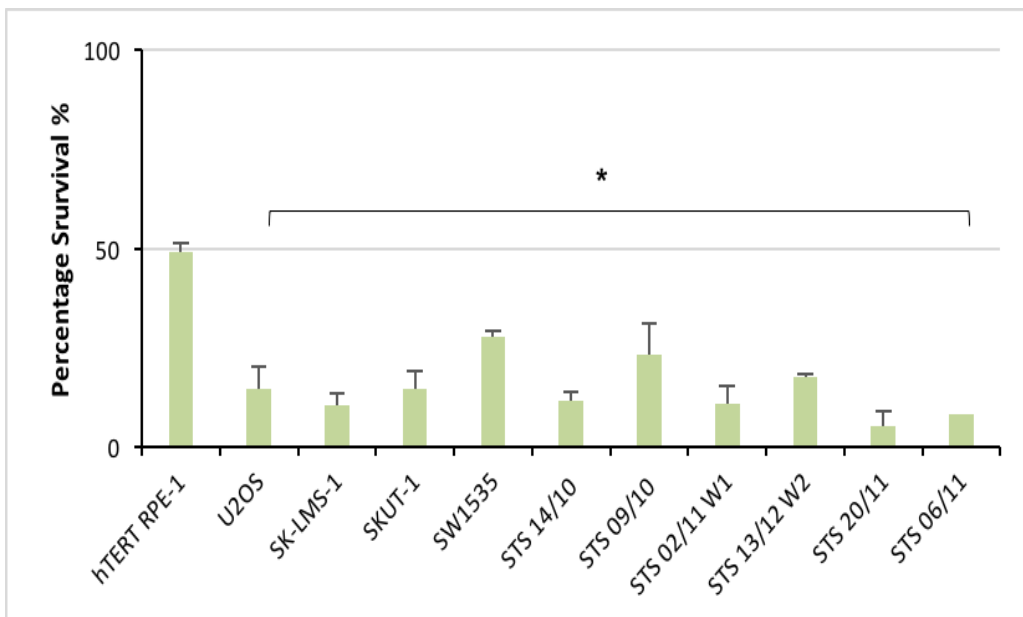


Figure 3.8 Cell Survival for all Cell Lines Post Exposure to 2Gy IR

*Sarcoma cell lines are significantly more sensitive to IR than normal hTERT RPE-1 (*p-value <0.05 by a t-test). Data represents the mean of three independent experiments +/-SE.*

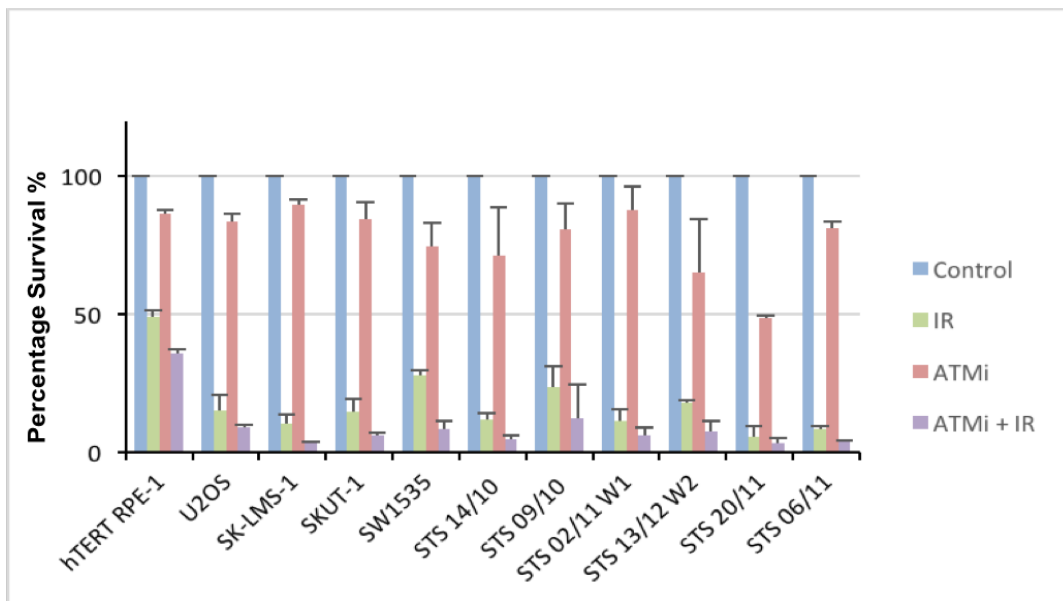


Figure 3.9 Cellular Survival of Controls and Sarcoma Cell Lines in Response to Different Types of Treatment

The survival fraction is decreased in all sarcoma cases and in control cell lines following the treatment with the ATM inhibitor. Concurrent treatment of both ATM inhibitor and IR decreases cellular survival than happened when each treatment was applied individually. Data was derived from 3 independent experiments and error bars represent standard error of the mean.

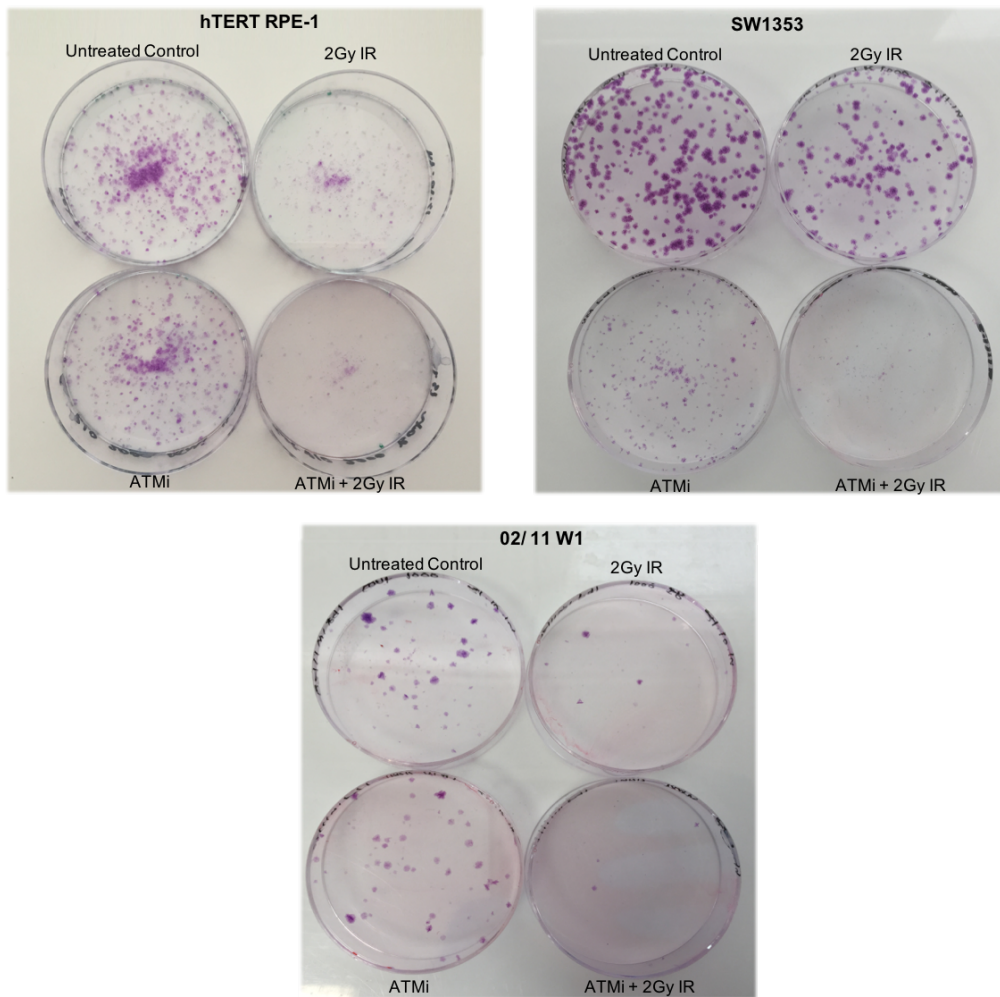


Figure 3.10 Cellular Survival Following Different Types of Treatment

Image depicting normal control hTERT RPE-1, established SW1353 and primary STS 02/11 W1 colony forming plates treated with or without 2Gy IR or 10 μ M of ATM kinase inhibitor or combination of both. Although SW1353 and STS 02/11 W1 are more sensitive to IR than normal, they still actively divide. Treatment with ATM kinase inhibitor sensitises cellular survival of all cell lines and reduces colony size in SW1353 cell line. Concurrent treatment of both ATM inhibitor and IR results in greater cellular death than happened when each treatment was applied individually.

3.3 Discussion

ATM serves as a master kinase controller that is involved in the regulation of the cell cycle checkpoint signalling pathways which are required for the cellular response to DNA-DSBs and genome stability. Previously in our laboratory, UI-Hassan et al. (2009) identified chromosomal abnormalities in the region containing the *ATM* gene, particularly in two types of sarcoma, GISTs and LMSs. Most specifically deletion of the *ATM* gene (UI-Hassan et al., 2009). Another report by Zhang *et al.*, (2003) explained an association between *ATM* deletion/mutation and the development of RMSs (Zhang et al., 2003). A recent study of 66 young patients with different sarcoma subtypes identified 13 germ line mutations in 10 cancer associated genes including missense mutations of *ATM* in alveolar RMSs and SSs (Chan et al., 2017). Ballinger et al. (2016) in addition have recently found that 638 of 1162 patients with sarcoma have deleterious variants in one or more sarcoma genes, including, but not limited to, *TP53*, *ATM*, *BRCA2*, *ATR*, and *ERCC2* (Ballinger et al., 2016). Furthermore, many studies have presented a link between the *ATM* mutation and the risk of a number of different cancers, such as leukaemia, lymphoma, breast cancer and central nervous system tumours (Stankovic et al., 1998, Zhang et al., 2015). However, the molecular mechanism associated with mutations of the *ATM* gene resulting in the development of these malignancies is not well understood (Stankovic et al., 1998, Zhang et al., 2003).

In the present study, Western blotting was performed to examine whether the ATM protein is normally translated from the mRNA of the *ATM* gene and expressed in different cell lines. ATM protein was expressed at 370 kDa in both tumour and normal control samples, consistent with previously described results (Gately et al., 1998). Although the ATM protein was expressed as a full length transcript in some primary sarcoma cell lines, there were six cases of different sarcoma subtypes, including 3 cases LMSs, one case pleomorphic sarcoma NOS, one case

DDLPS and one case chondrosarcoma that expressed an additional band which was significantly smaller than that seen in the tumour and normal control cell lines (~280 kDa) (Figure 3.1 A and B). Because *ATM* is such a large gene, consisting of numerous exons and splice sites, it is considered a sizable target for mutations that can have serious effects on the protein products (Rotman and Shiloh, 1998). Also, Broeks et al. (2000) previously detected an *ATM* splice site mutation (IVS10-6T>G) among breast cancer patients. This mutation causes improper splicing of exon 11 in addition to exon skipping which leads to a frameshift and finally results in the production of a truncated protein (Broeks et al., 2000). A recent report by Zhang et al. (2015) showed bi-allelic germline mutations in *ATM* in A-T patient with high grade glioma, these mutations include frameshift and a splice site at the splice junction of exon 52. The splice variant formed results in a novel exon junction located on 11bp downstream of the canonical exon junction of exon 52 creating a truncated ATM protein (Zhang et al., 2015). These data could explain the additional band in some sarcoma cell lines, which may possibly be the result of mutations that lead to truncated protein being produced; alternatively, it might be due to the alternative splicing of the *ATM* gene.

Even though an *ATM* gene deletion was detected and previously correlated to the pathogenesis of many different types of human malignancy including sarcomas (Stankovic et al., 1998, Zhang et al., 2003, Ul-Hassan et al., 2009), the changes in protein expression may not be altered, as shown in this study. For example, the deletion of the *ATM* gene does not appear to affect protein expression in the LMSs cases (SK-LMS-1, SKUT-1 and 02/11 W1) which highly expressed the ATM protein at 370 kDa with an additional smaller band below 370 kDa (Figure 3.1). To determine whether the presence of the additional bands found in this chapter has linked to the changes in the *ATM* status, the studies of the *ATM* alterations in these particular LMS cases and in many other subtypes of sarcoma has been confirmed by FISH,

NGS and MLPA in the following chapter.

The expression of the ATM protein in sarcoma cell lines was not identical and seemed to be higher in samples that showed an additional band below the expression of the ATM protein compared with others (Figure 3.1 A and B). The significance of *ATM* missense mutations in genetic predisposition to cancer may explain this. It has been reported that, in breast cancer patients, missense mutations in the region of the ATM protein, away from the kinase domain have a dominant interfering effect on the normal ATM kinase activation (Scott et al., 2002). The same study reported various epitope-tagged forms of ATM coimmunoprecipitating, which suggests the existence of a multimeric form of ATM in these patients (Scott et al., 2002). Therefore, if such a mutation is detected in sarcoma subtypes and if ATM exists in a multimeric form, that would explain how overexpression of the ATM protein in some sarcoma cell lines interferes with the normal function of the protein.

In order to optimise the Western blotting result, much trouble shooting was required. As *ATM* is a large gene, the size of the proteins can cause issues for blotting (Bolt and Mahoney, 1997). The exposure time of the film had to be altered and decreased each time to gain a clear picture of the protein. Moreover, the amount of protein samples had to be reduced to 50% of the total protein concentrations. Finally, the spectra multicolour high range protein ladder (MW range: 40-300 kDa) was used instead of the precision plus protein™ dual colour standards (molecular weight range: (MW) 10-250 kDa) to ensure that we effectively detected the ATM protein which is above 300 kDa. After this there still appeared to be additional bands so the mouse monoclonal primary antibody [ATM (2C1 (1A1))] (Abcam, UK) that raised against amino acids 2577-3056 of ATM of human origin was explored instead of using [ATM (2C1):sc-23921] (Santa Cruz, USA) and it gave cleaner gel pictures but also produced the same findings (Appendix 2, A). Moreover, ATM (Phospho S1981) [10H11.E12] was also used to examine the

phosphorylation of ATM in response to IR. β -actin antibody was used as a loading control to confirm that there were no differences in the amount of protein loaded for different samples. The established and primary sarcoma cell lines showed no difference in the expression of the ATM protein at 370 kDa in the whole cells lysate extracted using a lysis buffer containing protease inhibitor (PI) only or has protease and phosphates inhibitor cocktail (PPI). An additional band under the expression of the ATM appeared in some cell lines in both cell extracts, including (SK-LMS-1, SKUT-1, SW1535, STS 02/11 W1 and STS 14/10) (Appendix 2, B).

To further examine the role of ATM in the development of sarcoma, the response to endogenous and IR induced DNA-DSB damage levels was measured in established sarcoma cell lines, six primary sarcoma cells and in normal and tumour controls. Because ATM is one of the key proteins used in the phosphorylation of H2AX molecules following DNA-DSBs damage, the effect of inhibiting ATM was also explored.

The results showed distinct difference in the behaviour between sarcoma and control cell lines in term of resolving the DNA-DSBs that had been induced by the exposure of cells to a 2Gy dose of irradiation. Sarcoma cell lines displayed an abnormal response to IR induced DNA-DSBs damage, whereas the control cells showed the common response of a rapid increase in γ H2AX levels at 30 minutes post IR, which is consistent with the induction of DNA damage repair as a result of the exposure to γ -radiation (Svetlova et al., 2010), the majority of γ H2AX foci have disappeared within 2 hours following 2Gy IR in control cell lines, showing that most of the DNA damage have been repaired. Indeed, these results were expected because of the absence of the inherited genetic damage in these cell lines compared to the cancer cells. The response to IR induced DNA-DSBs was varied among each sarcoma case. The results

showed higher levels of γ H2AX foci post IR induced DNA damage in sarcoma cell lines compared to the tumour and normal control cell lines (Figure 3.6), suggesting the high sensitivity of these cell lines to IR induced DNA damage (El-Awady et al., 2003).

The primary STS 02/11 W1 showed relatively low spontaneous level of damage which was approximately like that seen in control cell lines (Figure 3.6, H). It also responded to IR induced DNA-DSBs in almost the same manner as the tumour control and normal retinal cell lines. A high induction of the γ H2AX foci 30 minutes post IR was observed in this cell line, which gradually decreased within 2 hours upon repair. These data suggest that the primary sarcoma cell line 02/11 W1 is responding to the IR induced DNA-DSBs damage and that this damage can be repaired at this level; this was represented by a decrease in the formation of the γ H2AX foci (Svetlova et al., 2010). The high spontaneous level of γ H2AX seen in other sarcoma cell lines was an interesting observation. The primary DDLPS cell line (20/11) showed the highest frequency of the spontaneous damage among all other primary cell lines evidenced by the number of γ H2AX foci (Figure 3.4). Mentioning that this primary cells was derived from a patient who had a radiotherapy before the surgery could explain the elevated level of endogenous damage seen in this sample (Salawu et al., 2016). The high level of H2AX persisted in this cell line even after 4 hours of irradiation is thought to be due to a poor ability to perform subsequent DNA repair. All established sarcoma cells included in this study exhibited high level of the endogenous damage that was particularly seen in SK-LMS-1 and SW1535 cell lines (Figure 3.4). Indeed, the genetic instability including some background levels of γ H2AX are expected in these cells, due to their adaptation to cell culture. However, γ H2AX levels were particularly higher in these cell lines compared to SKUT-1. A defective release of γ H2AX from the chromatin could be a possible reason explaining this. Subsequent to the DNA repair, two mechanisms by which γ H2AX is released from the chromatin has been suggested, one is the

direct dephosphorylation of γ H2AX by phosphatases (PP2A). The other is the replacement of γ H2AX with H2AX (Svetlova et al., 2007). The high genomic instability seen in sarcoma cell lines as the accumulation of unrepaired or incorrectly repaired DNA damage could be explained by the high spontaneous levels of γ H2AX. It is worth mentioning that sarcoma cell lines that expressed the ATM protein in higher level compared to the control cells and showed another band under the ATM expression had very high level of the intrinsic damage compared to the controls except 02/11 W1 cell line, suggesting the correlation between the high level of the ATM protein expression together with the appearance of the extra band and the elevated level of the endogenous damage seen in these samples.

It was mentioned earlier in the introduction of this chapter that both ATM and DNA-PK can phosphorylate H2AX molecules following DNA-DSBs (Rogakou et al., 1998, Burma et al., 2001, Stiff et al., 2004). The decision of which kinase is involved in the phosphorylation process may be depend on tissue specificity (Koike et al., 2008). Burma et al. (2001) detected very low levels of γ H2AX in ATM^{-/-} murine fibroblasts, this minimal level of γ H2AX was abolished by inhibiting DNA-PK, indicating that the ATM is major kinase involved in H2AX phosphorylation following IR (Burma et al., 2001).

The present study investigated the level of γ H2AX post IR in ATM inhibited controls, established and primary sarcoma cells lines. The data showed no induction of γ H2AX post IR following ATM inhibition in the tumour and normal control cell lines (Figure 3.6, A and B), confirming that under normal circumstances, ATM is crucial in initiating double stand break DNA repair. It was however consistently observed for all the sarcomas investigated in this study, that although the ATM was inhibited in all cell lines, high level of γ H2AX formation was detected unlike the findings of the control cells (Figure 3.6). These findings suggest that

sarcomas are able to signal damage despite the ATM inhibition and the formation of H2AX may not totally depend on the ATM and that sarcoma may utilise other repair pathways such as DNA-PK, which are able to phosphorylate H2AX molecules to form γ H2AX in response to DNA-DSBs (Rogakou et al., 1998, Burma et al., 2001, Stiff et al., 2004). Even though Burma *et al.*, 2001 stated that ATM is the major kinase involved in the phosphorylation of H2AX upon DNA-DSBs, another report showed slight reduction in γ H2AX post IR in ATM deficient cell lines and the formation of γ H2AX eliminated when DNA-PK was inhibited, suggesting the dominant role of DNA-PK in the phosphorylation of H2AX (Burma et al., 2001, An et al., 2010). These differences could be explained by the variations of kinase levels in different tissues. Although the expression of total and phosphorylated form of the ATM protein together with the inhibition of the ATM kinase activity was confirmed in the tumour control and STS 09/10 sarcoma cells earlier in this chapter using Western blotting (Figure 3.3), the SK-LMS-1 and STS 14/10 cell lines however, expressed low level of the ATM 2 hours post IR and following ATM inhibition, H2AX data provided same finding, the ATM was not inhibited in these cell lines and in other sarcoma cells (Figure 3.6), suggesting the possibility that in sarcomas, the inhibitor may not effectively inhibit ATM, possibly because the gene itself is mutated. The inhibition of the ATM was clearly evident in the U2OS cell line with non-mutated *ATM* following 2 hours of irradiation and was maintained for up to 24 hours (Figure 3.2), suggesting that the protein was effectively targeted by the ATM inhibitor, consistent with the previously explained data (Hickson et al., 2004).

The delayed response detected in sarcoma cells including SKUT-1 and Primary STS 14/10 following ATM inhibition could be also due to the fact that H2AX phosphorylation is also targeted by DNA-PK after IR. This delayed response however was not seen in the control cells when the ATM was inhibited. The formation of γ H2AX foci in sarcoma cells post ATM inhibition was

detected after some time, questioning about the degree of involvement of DNA-PK in the phosphorylation process. In compare to control cells sarcomas are still able to detect DNA-DS Bs following the inhibition of the ATM.

Clonogenic survival assay was performed to explore whether IR, ATM inhibition and the combination of both treatments has influenced cell survival of sarcoma cell lines. All sarcoma cell lines were significantly more sensitive to IR than the normal hTERT RPE-1 cell line, p-value >0.05 (Figure 3.8). The primary DDLPS cell line (20/11) showed an increased sensitivity to IR compared to the other sarcoma cell lines confirmed by H2AX and clonogenic assays, the pre-surgery irradiation exposure of STS 20/11 case could explain this observation (Salawu et al., 2016) however, this hypersensitivity was not exclusive for this sample alone. Although clonogenic results supported the data generated by H2AX that all sarcoma cell lines were significantly more sensitive to IR compared to the normal hTERT RPE-1 cell line with a p-value of less than 0.05 for both assays (Figure 3.7 and 3.8), these data were not correlated to the ATM protein expression. All sarcoma and controls cell lines tested this study had increased radio sensitivity following the treatment with the ATM inhibitor. Hickson et al. (2004) observed significant reduction in clonogenic survival of Hela cells post IR and following ATM inhibition, they also found no differences in radiosensitivity of cells derived from A-T patients in the presence or absence of the ATM inhibitor. As it was mentioned earlier in this chapter that *ATM* is functionally deficient in A-T cells and that one distinguishing feature of A-T cells is their increased sensitivity to IR-induced DNA damage (Hickson et al., 2004). This observation indicated that the enhancement in radiosensitivity seen in all sarcoma and controls cell lines was caused by the ATM inhibitor thus suggested the existence of functional *ATM* in these cell lines (Hickson et al., 2004). Even though the data generated by clonogenic assay indicated the presence of functional *ATM* in sarcoma cell lines, ATM kinase activity was confirmed by

western blotting and H2AX following the ATM inhibitor treatment in sarcoma cell lines (Figure 3.3 and 3.6), querying for more investigating about the *ATM* status in sarcoma cell lines.

CHAPTER FOUR

4 CONFIRMATION OF LOSS OF *ATM* COPY NUMBER IN SARCOMAS USING FISH, NGS AND MLPA

4.1 Introduction

The majority of sarcoma subtypes are characterised by complex chromosomal changes including chromosomal copy number aberrations (CNA) that are described as losses/deletions or gains/amplifications of a DNA fragment ranging from one kilobase to several mega bases in size (Freeman et al., 2006, Guillou and Aurias, 2010, Osuna and de Alava, 2009). Screening for non-random chromosomal aberrations in these sarcoma subtypes can lead to a better understanding of their pathology, classification and diagnosis, and can even help in the identification of potential therapeutic targets (Kasper et al., 2007). It is generally believed that deletions and amplifications of specific regions of chromosomes occur frequently due to the presence, respectively, of tumour suppressor genes and oncogenes in these genomic regions (Helman and Meltzer, 2003), and that chromosome abnormalities causing loss of function of tumour suppressor genes, activation of oncogenes and changes in the genes involved in DNA repair mechanisms can lead to cancer initiation (Vogelstein and Kinzler, 2004). CNAs, mostly amplifications, have been detected in most STS (Mylykangas et al., 2007). LPS represent the best example, where frequent amplified sequences are evident from the long arm of chromosome 12. This region contains the *MDM2* oncogene whose product inhibits *TP53* and thereby promotes cell survival. Another important target oncogene in this amplified region is *CDK4*, which is involved in the G1-S phase cell cycle checkpoint (Iwasaki et al., 2009).

CNAs can be detected by many cytogenetic and molecular genetic techniques. Fluorescence *in situ* hybridisation (FISH) and Multiplex ligation-dependent probe amplification (MLPA) are the methods of choice to detect CNAs in specific targeted regions (Amary et al., 2017, Asif et al., 2018). Next generation sequencing (NGS) is a more recent technology that allows for systematic screening of CNAs from the sequencing data of the whole genome, or whole exons, and from a targeted panel of genes (Liu et al., 2013).

In previous studies an association between *ATM* deletion and the development of sarcoma has been proposed (Zhang et al., 2003, Ul-Hassan et al., 2009). Investigations of STS here however has shown by Western blotting that the protein is still expressed (Section 3.2.1) and that a functional *ATM* is potentially still able to promote DNA-DSBs repair (Section 3.2.6). To explore whether there were any alterations of the *ATM* gene that may be responsible for its ability to elicit a response, despite inhibition of its kinase, and to find evidence for alternative pathways the status of the *ATM* gene was investigated in a range of different sarcomas and control cell lines using interphase FISH, targeted NGS and MLPA tests.

4.2 Results

4.2.1 Control Experiments with Chromosome 11 Probes

Initial control experiments were performed on five normal lymphocytes to determine the hybridisation efficiency of the *ATM*/CEP11 probes and to confirm the chromosomal localisation on metaphase spreads as well as the copy number in interphase nuclei. The cut-off values for red (*ATM*) and green (CEP11) probes were derived from five normal blood samples. Two hundred cells each from the five controls were evaluated for red and green signals, using non-overlapping intact nuclei or metaphase chromosomes under a Zeiss fluorescent microscope. Images were captured using the Cytovision software. The majority of interphase nuclei displayed the expected ratio of two red and green signals each (Table 4.1 and Figure 4.1) and the cut-off values were calculated as the percentages from the mean number of cells ± 3 times the SD of the signal observed in the five controls (Table 4.1). The deletion of the *ATM* locus was confirmed when abnormal signal ratios ($ATM < CEP11$) occurred with a frequency above the cut-off value of 10.95% of nuclei (Table 4.1).

Table 4.1 Cut-off Values for Chromosome 11 Probes from Interphase Nuclei of Normal Blood Samples

Samples (200 Nuclei)	Signal Ratios			Red (ATM) Signals			Green (CEP11) Signals		
	ATM<CE P	ATM=CE P	ATM>CE P	<2	2	>2	<2	2	>2
Blood 1	13	186	1	12	185	3	1	195	4
Blood 2	3	196	1	2	198	0	1	198	1
Blood 3	11	188	1	12	185	3	4	190	6
Blood 4	5	194	1	9	190	1	5	194	1
Blood 5	1	199	0	9	189	2	9	188	3
Mean	6.6	192.6	0.8	8.8	189.4	1.8	4	193	3
SD	5.17	5.45	0.44	4.0	5.3	1.3	3.3	4	2.1
Cut-off (Mean +/- 3 x SD)	10.95%	88.2%	1.06%	10.4 %	87.2 %	2.85 %	6.9 %	90.5 %	4.65 %

The table shows the number of cells having equal signals of ATM and CEP11 and cells having fewer or more ATM signals than CEP11. The table also illustrates the number of cells having (<2, 2 and >2) signals for CEP11 and ATM in normal blood samples. The cut-off value was calculated as the percentage of the mean +/- 3 times the SD. The deletion of the ATM gene locus was considered positive if the percentage of cells showing fewer ATM signals than CEP signals was ≥10.95% (highlighted in red).

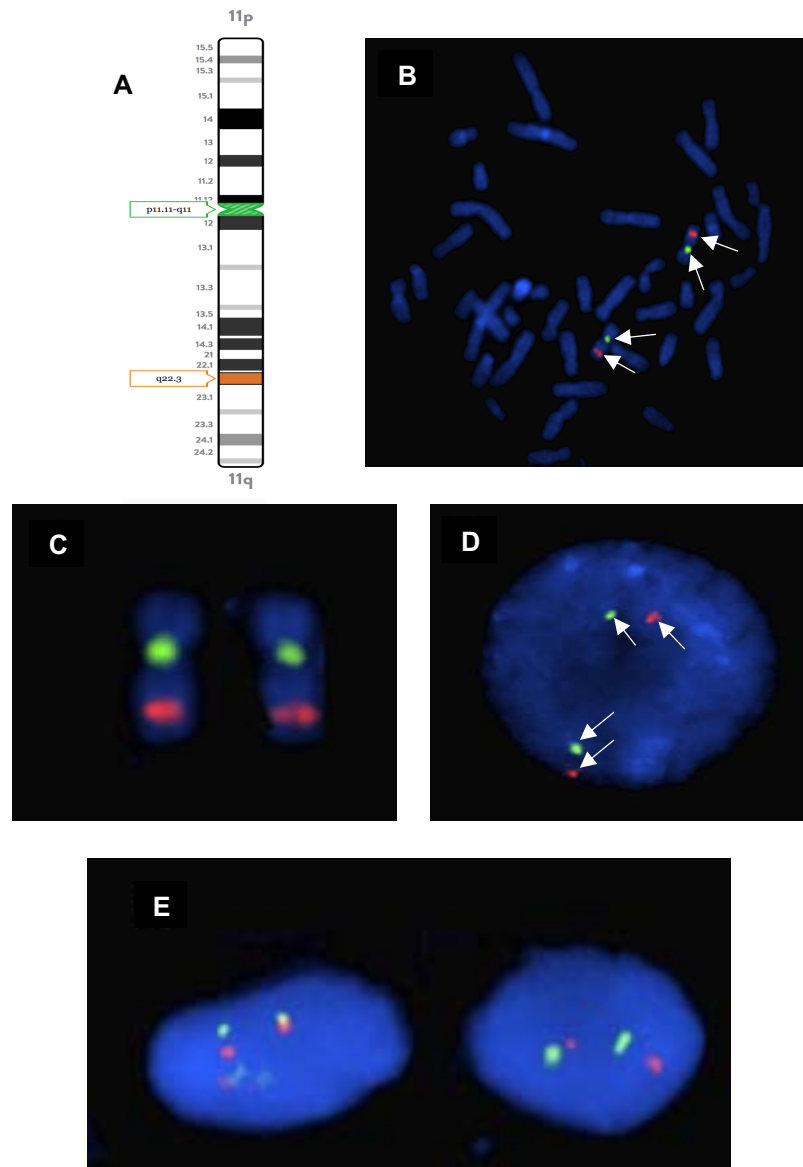


Figure 4.1 Representative Images from Control Experiments with Chromosome 11 Probes.

A. Schematic representation of the chromosome 11 banding with 11q22.3 that contains the ATM gene locus (red) and CEP11(green). **B.** Metaphase spreads from the normal control showing the hybridisation of the ATM/CEP11 probes and confirming the localisation of paired signals from each of the ATM and CEP11 probes. **C.** A close up image of hybridised probes on the chromosome 11 centromere and 11q22.3 locus. **D.** Interphase nuclei from the same experiment showing the hybridisation of probes. **E.** Confirmation of the presence of two red signals for ATM and two green signals for CEP11 inside the majority of blue DAPI stained normal control. Fluorescent signals from the ATM (red) and CEP11 (green) probes are annotated by white arrows. Thank you to Dr. Aliya Ul-Hassan for capturing the images of control experiments.

4.2.2 FISH Analysis of Chromosomal Region 11q in Normal and a Range of Sarcoma Cell Lines

FISH was performed in order to visually analyse and identify the copy number status of the *ATM* gene on a total of eleven cell lines: six primary sarcoma cell lines and four established sarcoma cell lines, including the osteosarcoma cell line (U2OS) as the tumour control, and a normal human retinal epithelial cell line (hTERT-RPE1) as the normal control. FISH probes were hybridised to the cell lines (metaphase spread or interphase nuclei prepared on glass slides) using a Vysis fluorescently labelled locus specific identifier (LSI) *ATM* probe (11q22.3) (Abbott Molecular, USA). The Vysis chromosome 11 centromeric probe (CEP11) (Abbott Molecular, USA) was used for the identification of chromosome 11 and for enumeration.

4.2.3 FISH Results Showed a Deletion of the *ATM* Locus in Sarcoma Cell Lines

All sarcoma cases analysed for 11q detected the deletion of the *ATM* region in 23-100% of the cells in the various sarcoma cell lines (Table 4.2 and Figure 4.2). The deletion of *ATM* was detected as a decrease in the *ATM* copy number in relation to the CEP11 copy number in all the sarcoma cell lines tested and, surprisingly, in the tumour control (U2OS). Most of the U2OS cells (93.5%) had extra copies of chromosome 11 with two copies of the *ATM* gene, whereas the majority of the normal control (hTERT-RPE1) cells had a balanced copy number of the *ATM* and chromosome 11 (Table 4.2 and Figure 4.2).

Table 4.2 Number of Chromosome 11 Signals in Normal and Sarcoma Cell Lines

Samples (200 Nuclei)	% of Cells with <i>ATM</i> < <i>CEP11</i>	<i>ATM</i> Signals n (%)			<i>CEP11</i> Signals n (%)		
		<2	2	>2	<2	2	>2
hTERT-RPE1	1.5	1(0.5)	171(85.5)	28(14)	1 (0.5)	169 (84.5)	30 (15)
U2OS	99.5	10 (5)	187 (93.5)	3 (1.5)	0 (0)	0 (0)	200 (100)
SK-LMS-1	94.5	61 (30.5)	74 (37)	65 (32.5)	0 (0)	1 (0.5)	199 (99.5)
SKUT-1	55	93 (46.5)	101 (50.5)	6 (3)	5 (2.5)	151 (75.5)	44 (22)
SW1535	48	77 (38.5)	108 (54)	15 (7.5)	6 (3)	150 (75)	44 (22)
STS 14/10	53	29 (14.5)	69 (34.5)	102 (51)	1 (0.5)	9 (4.5)	190 (95)
STS 09/10	44	9 (4.5)	35 (17.5)	156 (78)	0 (0)	6 (3)	194 (97)
STS 02/11 W1	100	56 (28)	64 (32)	80 (40)	0 (0)	0 (0)	200 (100)
STS 13/12 W2	23.5	3 (1.5)	49 (24.5)	148 (74)	10 (5)	11 (5.5)	179 (89.5)
STS 20/11	98	51 (25.5)	27 (13.5)	122 (61)	0 (0)	1 (0.5)	199 (99.5)
STS 06/11	91	26 (13)	142 (71)	32 (16)	0 (0)	3 (1.5)	197 (98.5)

The table summarises the number of cells having (<2, 2 and >2) signals for CEP11 and ATM probes in both normal and a range of different sarcoma cell lines. The percentage of cells with a relative deletion of ATM is also shown and reflects the ratio of CEP11 to ATM signals for individual cells, regardless of aneuploidy of chromosome 11.

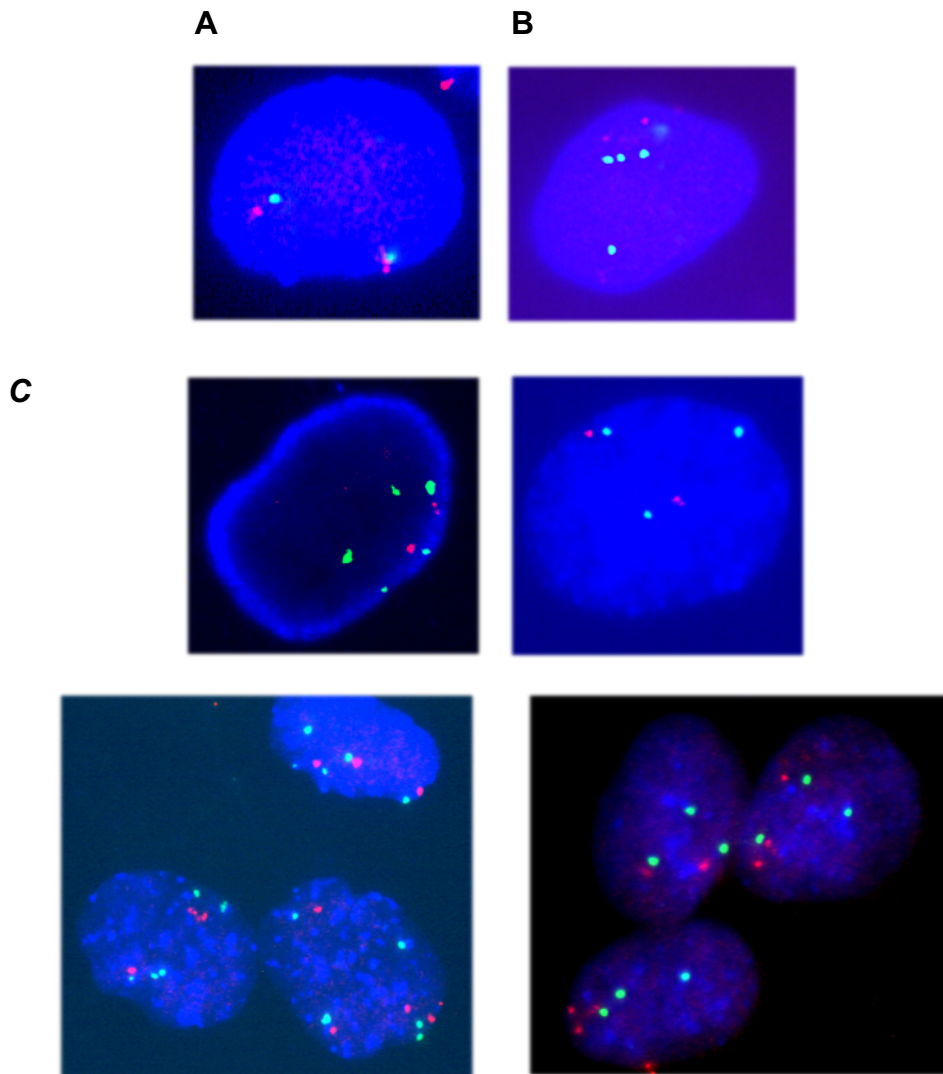


Figure 4.2 Detection of 11q Deletion in Sarcoma Cell Lines.

FISH analysis confirmed aneuploidy of chromosome 11 in all sarcoma cell lines tested. A. The normal hTERT-RPE1 cell line displayed balanced copies of ATM and CEP11. B. The majority of the U2OS cell line showed a gain of two copies of the CEP11 (green) with the presence of two ATM copies (red). C. Representative images from four primary sarcoma cell lines, including STS 02/11 W1, STS 06/11, STS 20/11 and STS 13/12 W2 (from left to right) showing a decrease in the ATM copy (red) as opposed to the copy of CEP11 (green). It is the relative decrease that is used to determine the overall percentage of cells with $ATM < CEP$ as detailed in table 4.2.

4.2.4 *ATM* Copy Number Analysis using MLPA

Having confirmed previous studies that there was a loss of *ATM* copy number in sarcoma, MLPA was performed to detect copy number changes such as homozygous and heterozygous deletion or duplication events within *ATM* exons in order to potentially identify hotspots. MLPA was performed on the primary and established sarcoma cell lines, including the osteosarcoma cell line (U2OS), and the normal human retinal epithelial cell line (hTERT-RPE1). An additional two soft tissue sarcoma samples including MFS 21/11 and LMS 11/11 were also included in order to compare and validate the MLPA results of this study with those previously generated in an initial pilot study of sarcoma tumours (not cell lines) by Dr. Aliya UI-Hassan. Six reference DNA samples (normal controls) were also included per MLPA run and were used for data normalisation and statistical analysis.

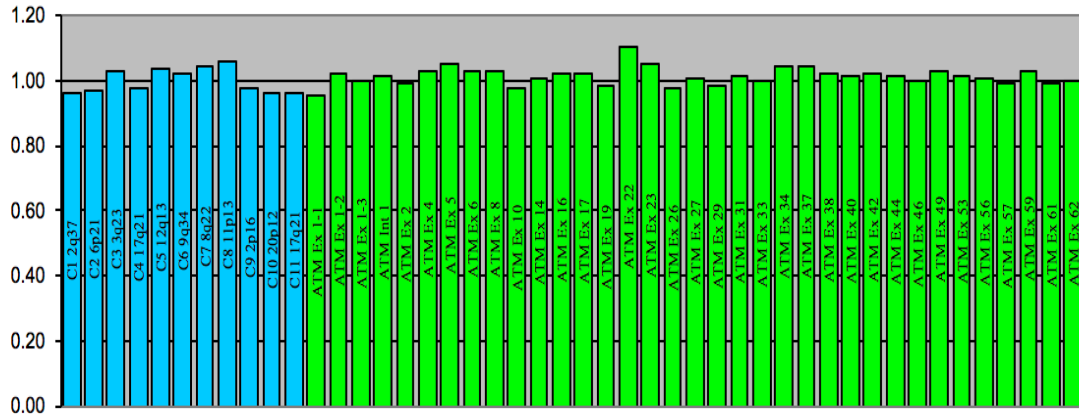
MLPA was performed with the total quantity of 50 ng of the genomic DNA extracted from normal and sarcoma samples by Qiagen DNeasy kit (Qiagen, UK). Due to the large number of exons within *ATM*, the MLPA assay required two sets of probe mix (P041-B1 *ATM* and P042-B1 *ATM*) available from MRC Holland (www.mrc-holland.com). All samples were processed as previously described in chapter 2. Following hybridization, ligation and amplification steps, samples were sent to the core sequencing facility at Sheffield Medical School (University of Sheffield, UK) for genotyping using ABI-3730 capillary electrophoresis (ThermoScientific). The resulting data were then analysed using Coffalyser.Net software available from MRC Holland (www.mrc-holland.com). This software generates peak patterns for both patient and reference DNA samples, where each peak is an amplification product of a specific probe. The test samples were compared to the reference sample to determine any differences in the relative peak height, indicating a copy number change of the DNA sequence determined by the MLPA probes. The MLPA peak pattern of the test samples, with no genomic aberrations was identical

to that of the reference DNA sample. For heterozygous deletion of an exon, the peak height should be half that of the reference peak, while in duplication, the peak should give almost twice the height of the reference peak. The absence of a peak would represent homozygous deletions. Following the visual assessment of peak heights, the final probe ratio (dosage quotient) was determined by an inter-normalisation step (Chapter 2) and displayed as a ratio chart or a histogram. A range from 0.7-1.3 was considered to be a normal exon dosage, a heterozygous deletions were between 0.40 and 0.65 and heterozygous duplications were above 1.30. A ratio of 0 would represent homozygous deletions.

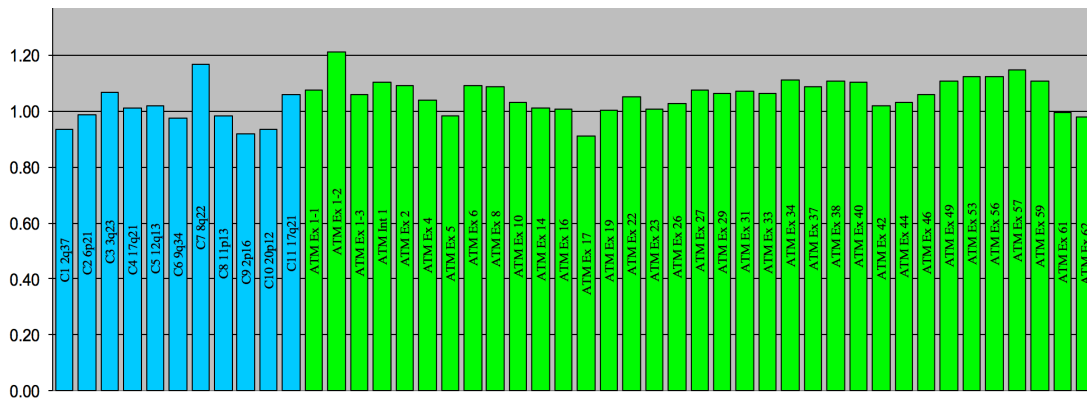
A pilot study of the MLPA analysis of sarcomas was first performed by Dr. Aliya UI-Hassan in 2012 using the old version of the MLPA probe mix (P041-A2 *ATM*) (MRC-Holland). Dr. UI-Hassan ran normal controls and DNA from STS tumour samples, including MFS 21/11 and LMS 11/11, but not cell lines examined here with data available on protein expression of *ATM*. A sample without DNA was also included to verify that no contamination was occurring during the MLPA reaction. The results were analysed using the MLPA analysis Manchester spreadsheets (Figure 4.3).

Dr. UI-Hassan's work showed that the MLPA technique was working. The probe ratio for all *ATM* exons in the reference DNA sample (normal) were close to 1 (Figure 4.3 A). The copy number ratios for MFS 21/11 showed normal results and were between 0.91-1.2 for all *ATM* exons within probe set (P041-A2) (Figure 4.3 B). The *ATM* exons for LMS 11/11 showed loss of one copy of the *ATM* (heterozygous deletion) represented by a decrease in the exon dosage that were between 0.44-0.63 (Figure 4.3 C). No *ATM* exons were detected in the sample without DNA, suggesting that there was no contamination in the MLPA reaction (Figure 4.3 D).

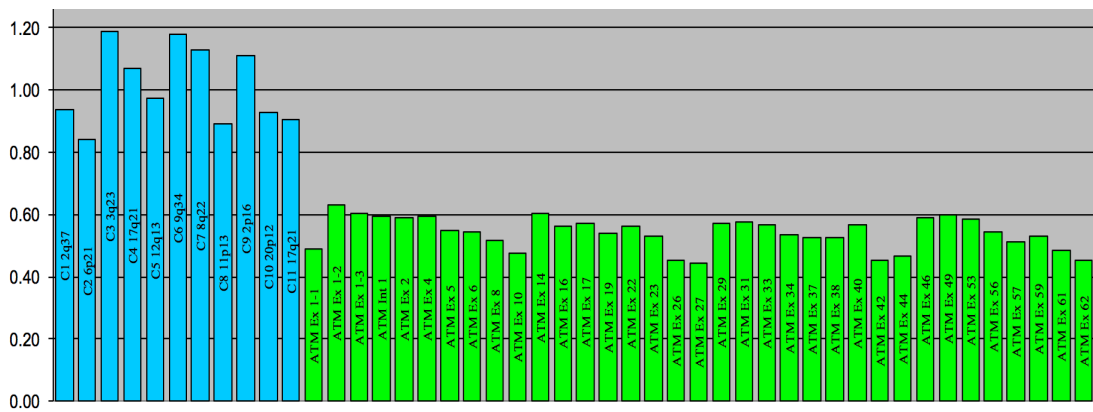
A. Normal



B. STS 21/11



C. STS 11/11



D. No DNA

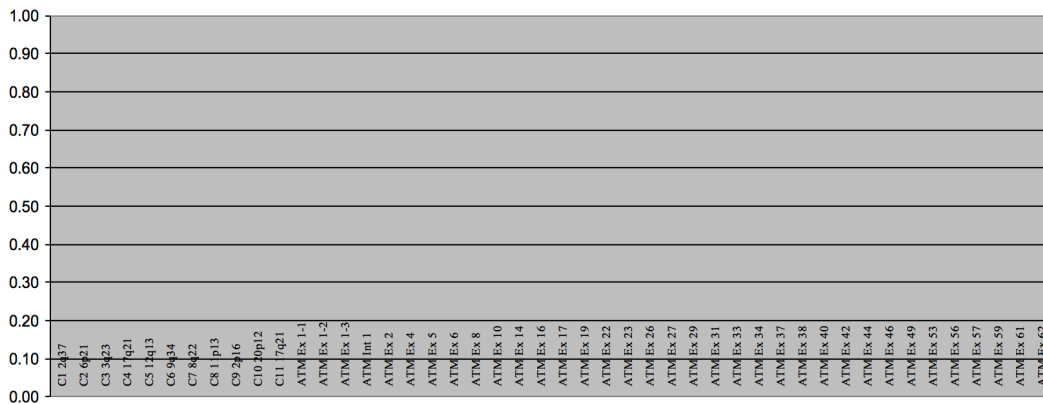


Figure 4.3 The MLPA Data for MFS 21/11 and LMS 11/11 Prepared as Part of a Pilot Study by Dr. Aliya UI Hassan.

MLPA histogram of the normal subject (A), patients with MFS 21/11 (B) and LMS 11/11 (C) and the sample without DNA (D). The numbers inside each bar indicate the relevant ATM exon probes detected in each DNA sample, while the numbers in the Y-axis represent the final probe ratios of the test samples versus the reference DNA samples calculated following the data normalisation. The normal subject (A) showed a normal probe ratio of ~ 1 for all ATM exons in the probe set (P041-A2). Compared to (A), LMS 11/11 showed a heterozygous deletion in all ATM exons with a probe ratio ranging from 0.44-0.63 (C) whereas results for MFS 21/11 displayed a normal ATM copy number in all exons (B). No contamination was detected in the MLPA reaction represented by the absence of ATM exons in the sample without DNA (D).

In the current study, three years later, MLPA was performed using the new version of the MLPA probes (P041-B1 and P042-B1 ATM) (MRC-Holland) on all the cell lines included in the present study. The MFS 21/11 and LMS 11/11 tumour samples were also included so as to be able to validate and compare with the previous MLPA work performed by Dr. Aliya UI-Hassan.

In MLPA, the signal intensity of the size standard fragments is expected to be of a similar height in order to create a standard curve for use in data comparison (Figure 4.4 A). Although some sloping of the signal in respect to the MLPA fragments is to be expected, the signal decrease

should not exceed ~ 60% (Figure 4.4 B). The MLPA for the sarcoma and reference DNA samples in this study showed too much signal sloping in both the MLPA peak pattern and size standard (Figure 4.4 C), with the signal intensities of the longer MLPA fragments being lower than those of the shorter MLPA fragments. Unfortunately, the degree of signal sloping detected by the Coffalyser.Net software in this study was higher than 70% and the signal for the longer MLPA fragments therefore became very low, meaning that these regions might appear erroneously as a deletion during the data analysis. Although the Coffalyser.Net software can correct for sloping to a certain degree during data normalisation, if sloping is very different between the test and reference samples, this correction cannot be applied correctly, leading to a biased analysis.

DNA was extracted from the cell lines and the MLPA was undertaken, but the results of the MLPA experiment were not analysed immediately, since there was a break in this study due to maternity leave. At the point of returning to the study, NGS had now become available through the Children's Hospital, Sheffield, UK. For comparison and additional confirmation, some STS samples were therefore selected and sent for NGS using a target cancer panel that included the *ATM* gene. During this timeframe, the MLPA data acquired before the break in the study was analysed and the issue with the sloping was recognised. Sloping in both the MLPA peak pattern and size standard is one of the most common problems caused during data separation, and the only solution is to repeat the experiment. Unfortunately, due to the tight timeframe for submitting the thesis the experiment could not be repeated. Despite these issues with sloping, the MLPA data included in this study could be usable, but discussion with the MRC-Holland company team suggested the findings should not be considered as totally reliable, but at least provided a comparison with data from the NGS panel.

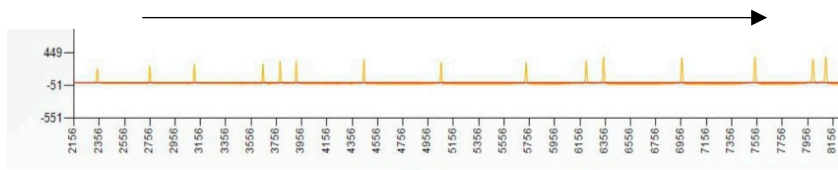
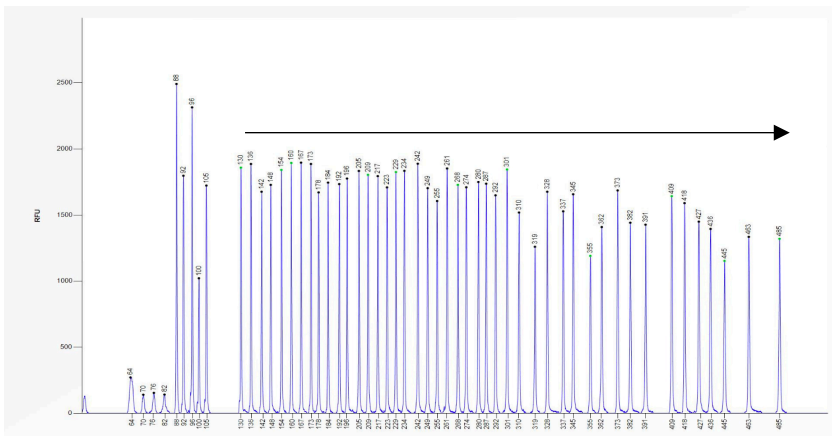
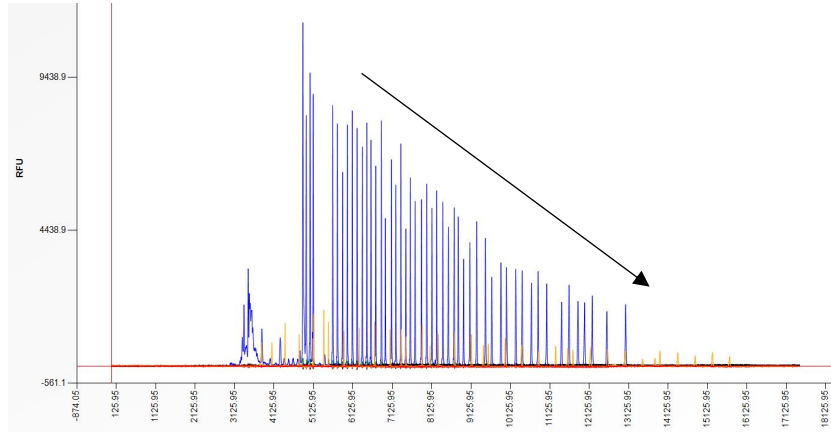
A**B****C**

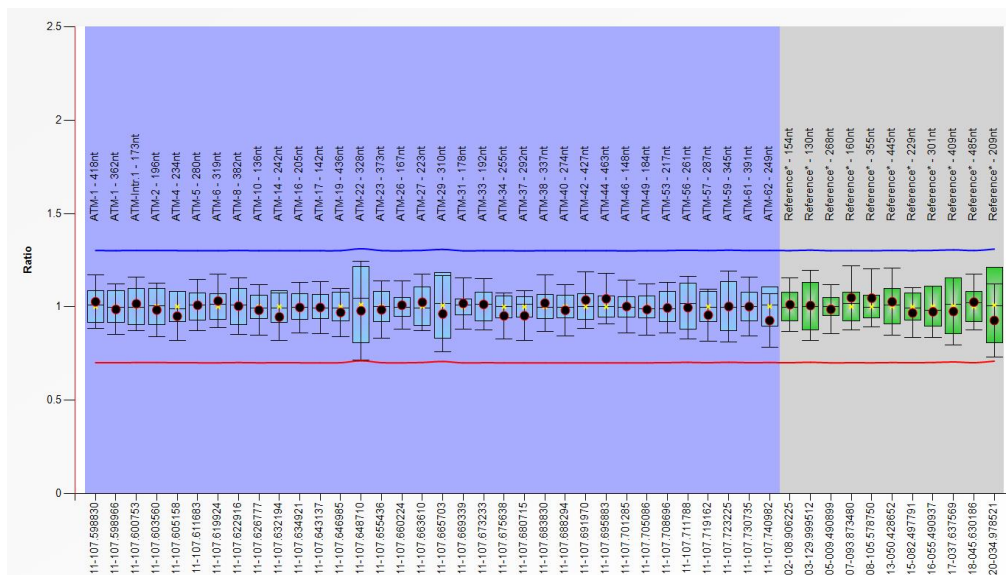
Figure 4.4 Differences between Normal and Sloping Signal Intensity.

A. A peak pattern of the size standard showing the normal signal intensity (orange). **B.** The genomic profile of the reference DNA sample showing an almost similar peak pattern across the MLPA probes (blue), peaks A and B are adopted from (www.mrc-holland.com) **C.** Both the MLPA fragments (blue) and size standard fragments (orange) showing the drop in signal size in the reference DNA sample obtained from this study, with the signal intensity of the fragments reducing with increasing fragment length.

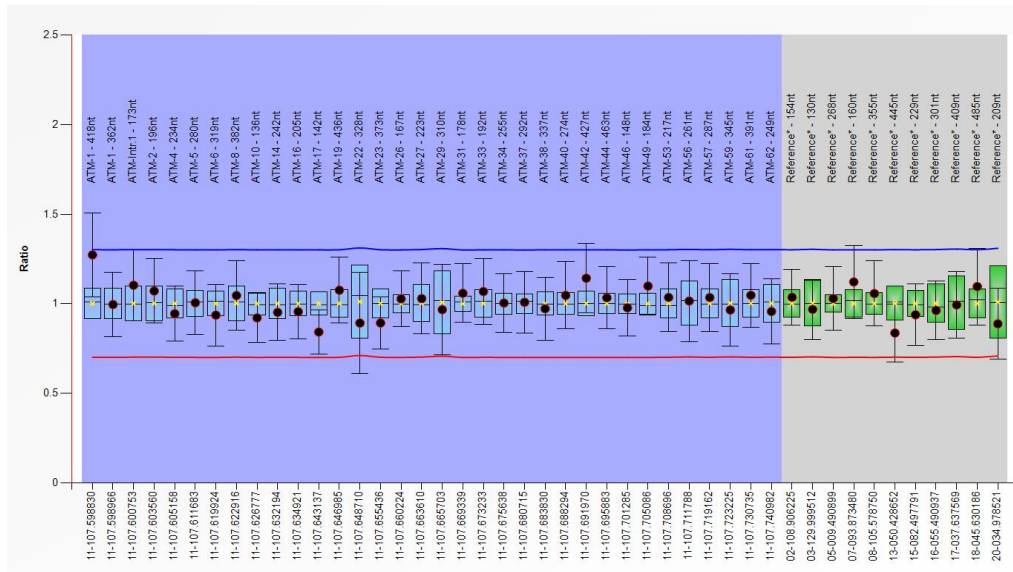
4.2.5 The MLPA Data Showed a Similar Pattern of Findings Compared to the Previous MLPA Work Despite the Detection of Signal Sloping

Notwithstanding the signal sloping issues that have been detected during the MLPA data analysis in this study, the MLPA results for the two STS samples MFS 21/11 and LMS 11/11 were similar to those produced in 2012 by Dr. Aliya UI-Hassan (Figure 4.5). The MLPA analysis Manchester spreadsheets used by Dr. UI-Hassan, however, do not give any information about quality control.

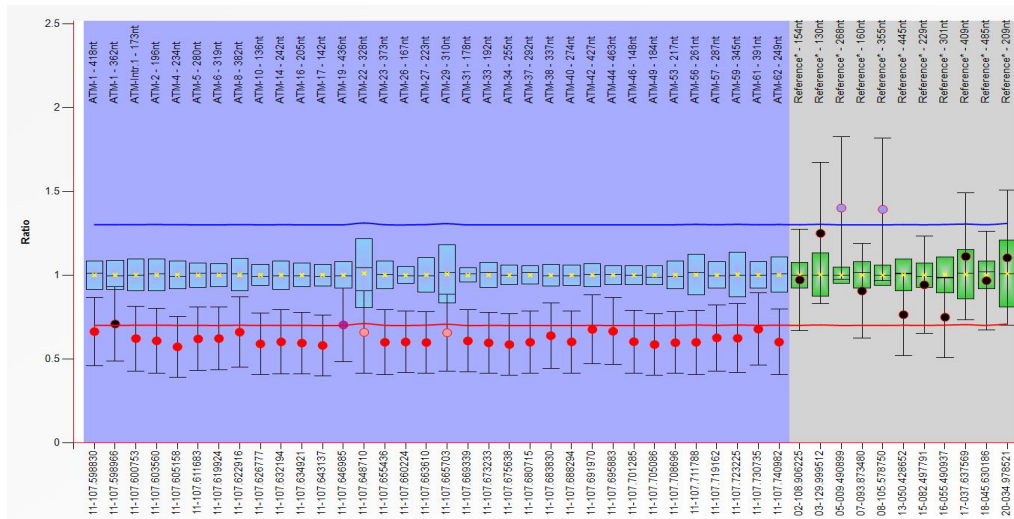
A. Normal



B. MFS 21/11



C. LMS 11/11



D. No DNA

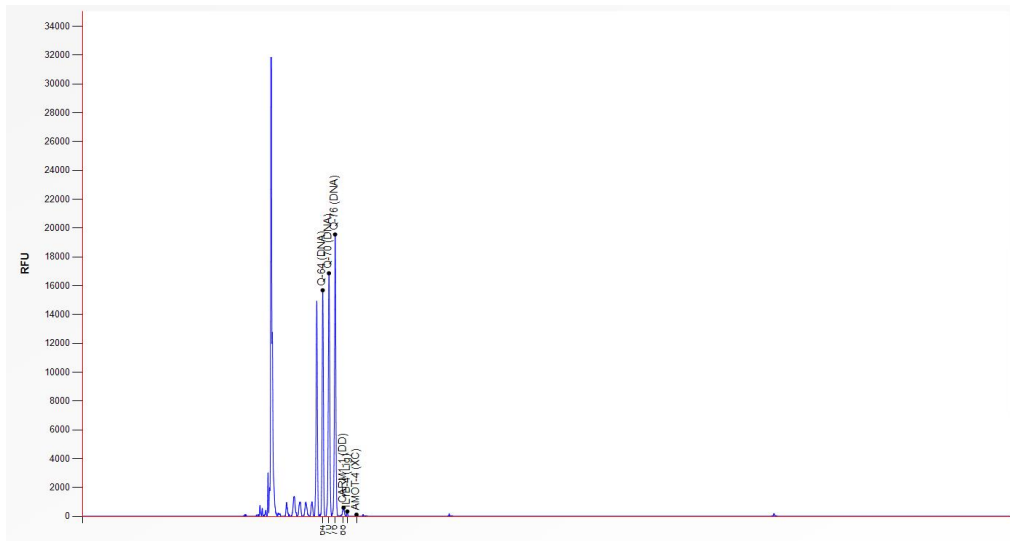


Figure 4.5 MLPA Findings for MFS 21/11 and LMS 11/11 Cases Similar to the Previous Work Done in 2012.

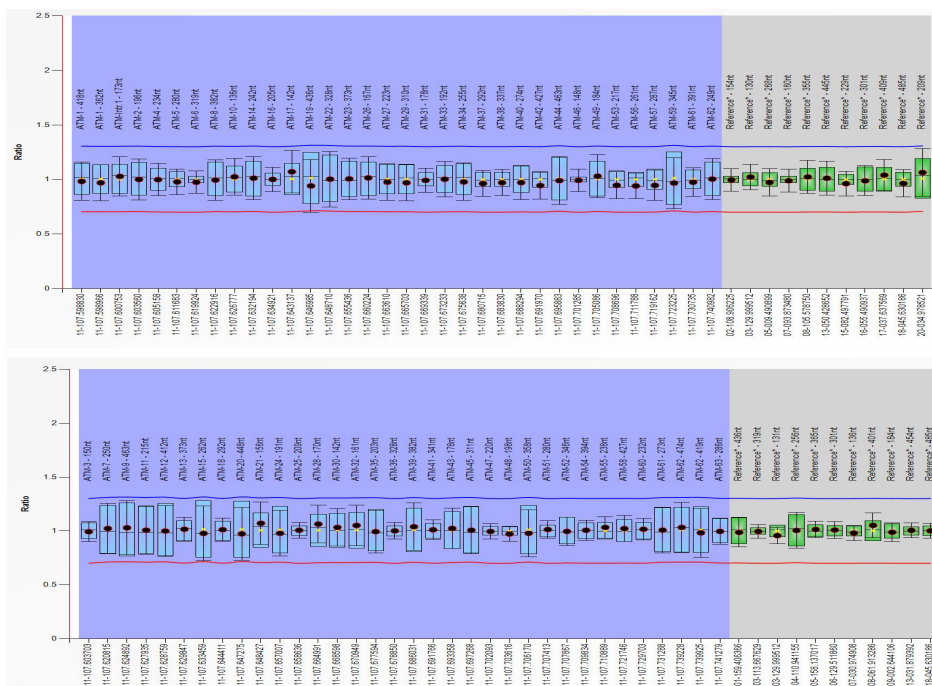
The calculated probe ratios of test samples (B and C) versus those of the reference sample (A), as displayed by Coffalyser.Net software. Probes for the ATM exons in probe set (P041-B1) are arranged by chromosomal location (X-axis). The final probe ratio of each of the exons within ATM are displayed in the Y-axis. The red and blue lines at ratio 0.7 and 1.3 in (A, B and C) show the arbitrary borders for loss and gain respectively. The green and blue boxes show the 95% confidence range of the probes over the reference samples, while the error bars show the 95% confidence range of the probes in the samples. The red dots in the LMS 11/11 figure designated the decreased signal corresponding to the deletion (C). The ATM copy number ratios in MFS 21/11 (B) were relatively similar to those in the normal (A). The genomic profile of the sample without DNA, taken from the same experiment (D), show that no peaks were detected, indicating that no DNA was contaminated in the MLPA reaction.

4.2.6 MLPA Data Showed *ATM* Deletion in the Tumour Control

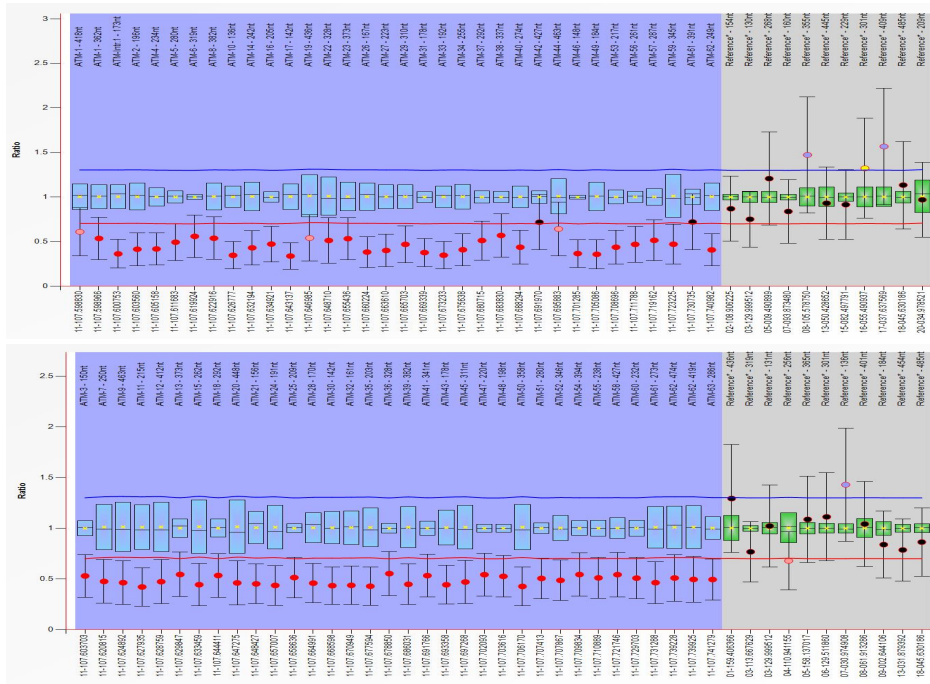
Compared to the reference DNA sample, the MLPA results showed heterozygous deletion for almost all the exons within the *ATM* gene in the tumour control (U2OS) cell line, with a probe ratio below 0.40. Exon numbers 42 and 61, however, showed a relatively normal copy number ratio ~ 0.7 (Figure 4.6 A and B). In contrast, the *ATM* copy number ratios in the non-tumour control (hTERT-RPE1) were identical to those seen in the reference DNA (Figure 4.6 C and D). Despite the sloping issues that were detected in the MLPA data, these results confirm the *ATM* copy number status for the U2OS and hTERT-RPE1 cell lines previously detected in this study by FISH (Table 4.2 and Figure 4.2 A and B).

A heterozygous deletion of *ATM* exons was also detected in other sarcoma cell lines, including STS 02/11 W1. While the SKUT-1, SW1535, STS 14/10, STS 20/11 and STS 06/11 lines showed almost normal copy number ratios for *ATM* exons, others had heterozygous duplication including SK-LMS-1 and 13/12 W2. All MLPA data details are shown in appendix 3.

A. Normal



B. U2OS



C. Normal



D. hTERT-RPE1

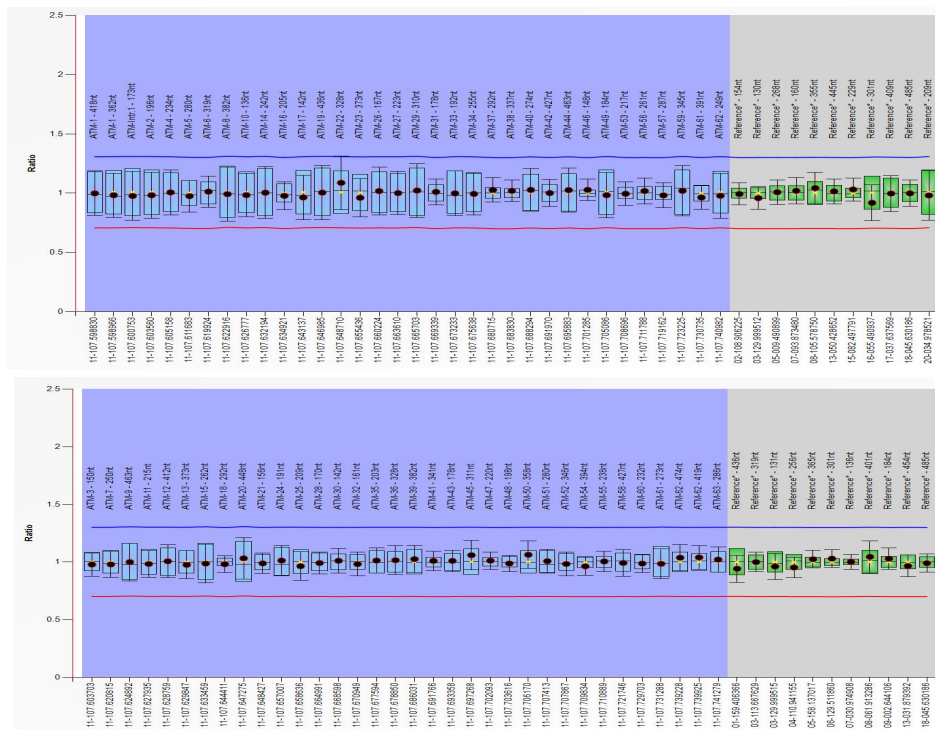


Figure 4.6 MLPA Data for the Tumour and Non-Tumour Controls.

The calculated probe ratio charts for the test samples (B and D) were compared to those of the reference samples (A and C). The ATM copy number ratios in probe sets P041-B1 (top panel) and P042-B1 (bottom panel) showed heterozygous deletions for all exons in the tumour control (red dots), except for exon numbers 42 and 61 (B), and normal ratios for the non-tumour control (D).

4.2.7 Short Tandem Repeat (STR) Analysis

At the end of this study, Short Tandem Repeat (STR) analysis was performed on all the cell lines included in this PhD thesis in order to confirm that was no kind of cross-contamination throughout the study. STR analysis was done using services provided by the University of Sheffield Core Genomic Facility service. Briefly, in STR analysis, ten STR loci of the genomic DNA extracted from the cells in culture are amplified by Multiplex PCR using fluorescent-labelled primers. The size of the PCR products is then determined using capillary electrophoresis and compared to the number of nucleotide repeats in STR (alleles) for those

of other cell lines in the laboratory. If there is a genetic match between any of the STR profiles from each cell culture with another cell line in the laboratory then contamination is indicated.

Relatedness between cell lines can be confirmed with a reliability of 99% if the proportion of alleles matching during STR analysis is between 75% and 80% and, there is 98% reliable confirmation when the proportion of alleles matching is more than 50% (American et al., 2010, Capes-Davis et al., 2013). At the University of Sheffield, however, the threshold for confirming relatedness between cell lines is when allele matches are about 70%. Other cell lines from the Children's Oncology Group Cell Culture and Xenograft Repository Database (www.COGcell.org) are also used for comparison. These include STR profiles of commercial cell lines collected by the American Cell Culture Collection (ATCC), Japanese Collection of Research Bio-resources (JCRB), Riken Research Database (RIKEN) and German Collection of Microorganisms and Cell Culture (DSMZ). Comparison of primary sarcoma cell lines was also made with previous STR results done by an investigator in our group, Dr. Abdulazeez Salawu (Salawu et al., 2016).

STR analysis for all primary tumour cultures that were profiled under the COGcell database showed less than, or up to, 75% of allele matching (Table 4 3). The cell lines that showed allele matches above 70% were not used in our laboratory, suggesting that they were an unlikely source of contamination. STR analysis for the established cell lines included in this study showed similar results to those found in the database thus confirming the identity of the cell lines.

Table 4.3 Short Tandem Repeat (STR) Profiles of STS Included in this Study

Cell Lines	THO1	D21S11	D5S818	D13S317	D7S820	D16S539	CSFIPO	AMEL	vWA	TPOX	Matching Alleles	Cell Line
hTERT-RPE1	9,9	31,32.2	11,11	11,12	10,11	11,11	12,14	X,X	17,18	8,8	100%	hTERT-RPE-1
U2OS	6,9.3	31,31	8,11	13,13	11,12	11,11	13,14	X,X	14,14	11,12	83%	U2OS
SK-LMS-1	6,7	28,30	11,13	11,12	8,9	8,11	9,10	X,X	18,20	8,9	94%	SK-LMS-1
SKUT-1	7,7	29,20,32.2	10,11	11,12,13	9,10	13,13	10,11	X,X	15,16	8,8	84%	SKUT-1
SW1535	6,9	30,32.2	10,11	12,13	9,11	11,12	12,11	X,X	16,17	8,11	94%	SW1535
STS 02/11 W1	9,9	27,30	11,11	14,14	10,11	11,11	10,10	X,X	16,16	-	<70%	-
STS 14/10	6,7	27,30	12,13	8,11	8,8	14,14	12,12	X,X	16,16	8,8	<70%	-
STS 09/10	6	29,32	12,13	8,14	9,10	9,10	10,14	X	17,18	11	74%	JURKAT
STS 13/12 W2	6,6	31.2,33.2	11,11	12,12	10,12	11,11	11,11	X,Y	18,18	8,8	72%	H1876 H1882 HDQ-P1
STS 20/11	9,9	29,29	9,9	14,14	10,12	12,12	12,12	X,X	20,20	9,11	<70%	-
STS 06/11	6,9.3	31,31	9,13	14,14	8,11	11,11	10,11	X,Y	17,18	8,8	75%	JURKAT

Table shows STR analysis of all STS included in this study in which the number of nucleotide repeats in ten STR specific loci were compared with one another as well as with STR data for other cells included in the database (www.COGcell.org). The cells that showed more than a 70% match are displayed in the last column.

4.2.8 *ATM* Copy Number Detection by Targeted NGS in Sarcoma Cell Lines

The NGS experiment was performed to detect CNA across a targeted panel of 55 distinct cancer genes, including *ATM*, which is the focus in this thesis; other cancer genes included in the experiment are shown in appendix 4. The targeted NGS experiment was performed on an Illumina HiSeq 2500 system using NGS services provided by the Children's Hospital, Sheffield, UK. The genomic DNA specimen was extracted from eight of the sarcoma cell lines included in this study following the Qiagen DNeasy kit standard protocol (Qiagen, UK). The selection of these STS cell lines was based on the earlier results found in this PhD thesis. The established osteosarcoma, U2OS, was selected because it was used as a tumour control and behaved differently to other sarcoma cell lines included in the various experiments in this study. Two LMS cases, including the established SK-LMS-1 and the primary STS 02/11 W1, were selected for NGS analysis to follow up on earlier work in our research group that suggested the presence of *ATM* abnormality with LMS (Ul-Hassan et al., 2009, Salawu et al., 2012). Other primary sarcoma cell lines STS 14/10, STS 13/12 W2, STS 06/11, STS 20/11 and STS 09/10, were included in order to detect *ATM* copy number status so that this could be compared with the FISH data shown in section 4.2.3. Another reason for including the SK-LMS-1, 02/11 W1, STS 14/10 and STS 20/11 sarcoma cell lines in this experiment is to determine if the changes in the *ATM* copy number are responsible for producing the truncated protein found in the western blotting results for these sarcoma cell lines (Figure 3.1). The normal control (hTERT-RPE1) and the established SKUT-1 and SW1535 cell lines were not included in this experiment for two reasons: firstly, as a commercial cell lines that had longer to adapt to cell culture, they would resemble the patient's tumour DNA less closely; and secondly, financial constraints limited the number of samples.

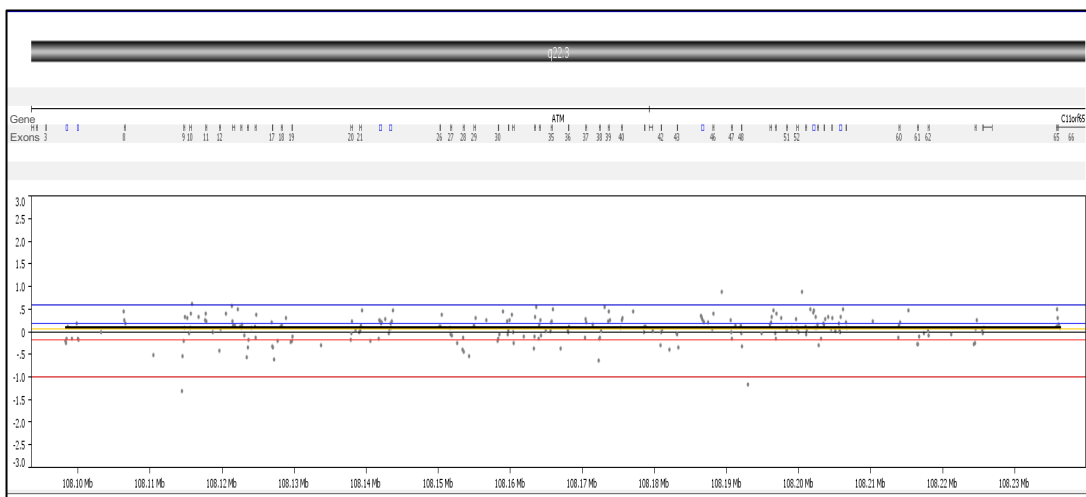
The *ATM* copy number aberrations were identified in sarcoma cell lines from genomic sequencing data using the FASST2 algorithms, Nexus Copy Number Software v10.0 (Biodiscovery). The BAM MSR algorithm employs an adjustable binning approach and utilises both target and off-target NGS reads. Genomic regions were binned across all exons of the *ATM* gene. A reference file was generated from the NA12878 genome in a bottle (GIAB) DNA (vendor) and the number of read in each bin compared to those in the sarcoma samples in order to generate pseudo-log ratios. The whole genome was denoted in the software as a series of sections with each section, having a cluster value representing the median log-ratio value of all the reads found in that region. The FASST2 calling algorithm then used the cluster values, together with the certain thresholds, to identify the regions with CNA. Log ratio threshold values of -0.2 and -1.0 were used to identify a single, and two or more, copy number losses, respectively, while the threshold values for gains of a single, and two or more, copy numbers are +0.2 and +0.6, respectively. The parameters used in the algorithm to generate the reference and all threshold values were based on the recommendations of the manufacturers of the analysis software. Aberrations were displayed as ideograms (graphical genomic plots) which can be viewed at whole genome, chromosome and single gene/exon levels for easy visual analysis. The median log-ratio values are plotted as the horizontal black lines in the ideograms (Figure 4.7).

4.2.9 NGS Analysis Showed an Aberration of *ATM* Copy Number in Different Sarcoma Cases and Confirmed the Heterozygous Deletion of *ATM* in the Tumour Control Cell Line

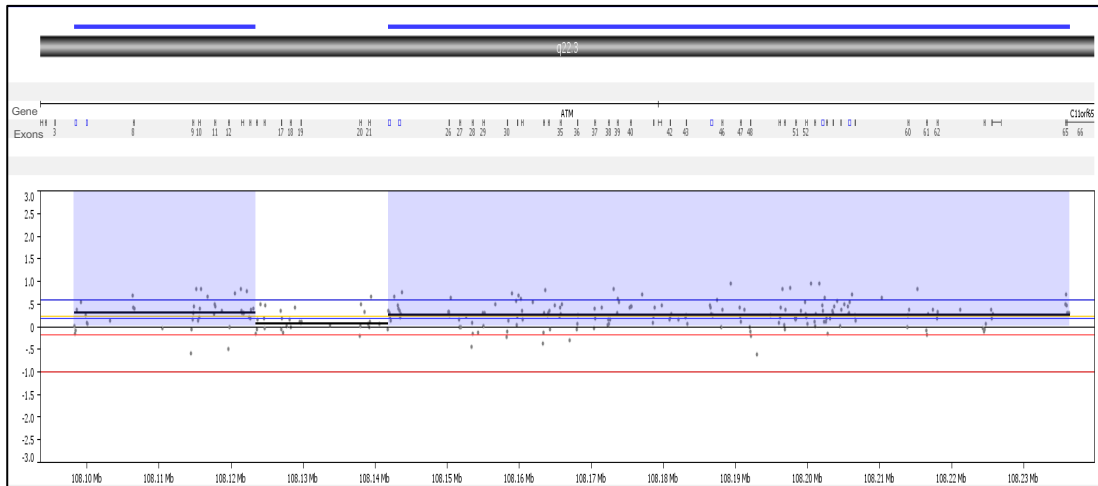
All of the sarcoma cases analysed in this experiment showed degrees of imbalance in the *ATM* copy numbers, except for UPS 14/10, which had a normal copy number for *ATM* (Figure 4.7 A). The established SK-LMS-1 cell line, the primary DDLPS 09/10 and UPS 13/12 W2 cell lines

showed an amplification of the *ATM* copy number that was detected in almost all *ATM* exons in these cases (Figure 4.7 B,C and D). In line with previous studies of *ATM* CNA in sarcoma (Ul-Hassan et al., 2009, Salawu et al., 2012), heterozygous deletion of *ATM* was detected in four sarcoma cases included in this experiment, namely the tumour control (U2OS), LMS 02/11, UPS 06/11 and DDLPS 20/11 (Figure 4.7 E-H). *ATM* heterozygous deletion affected the whole gene in U2OS and LMS 02/11, thus confirming the loss of one *ATM* copy in the tumour control found by FISH in this study. FISH also showed 100% *ATM* deletion in the LMS 02/11 W1 case in relation to the centromere (Figure 4.7 E, F and Table 4.2). The deletion of *ATM* in the other two cases, however, was only partial, affecting exons 3 to 9. The findings of the *ATM* CNA in the primary sarcoma cases included in this experiment were in concordance with a previous study done by an investigator in our group using Comparative Genomic Hybridisation CGH to detect CNA in sarcoma cell lines (Unpublished data).

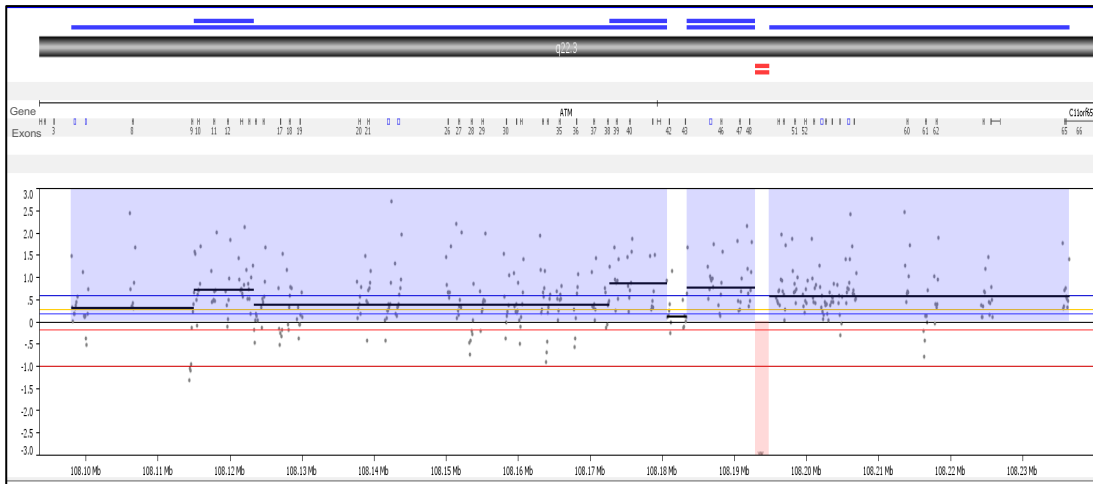
A. STS 14/10



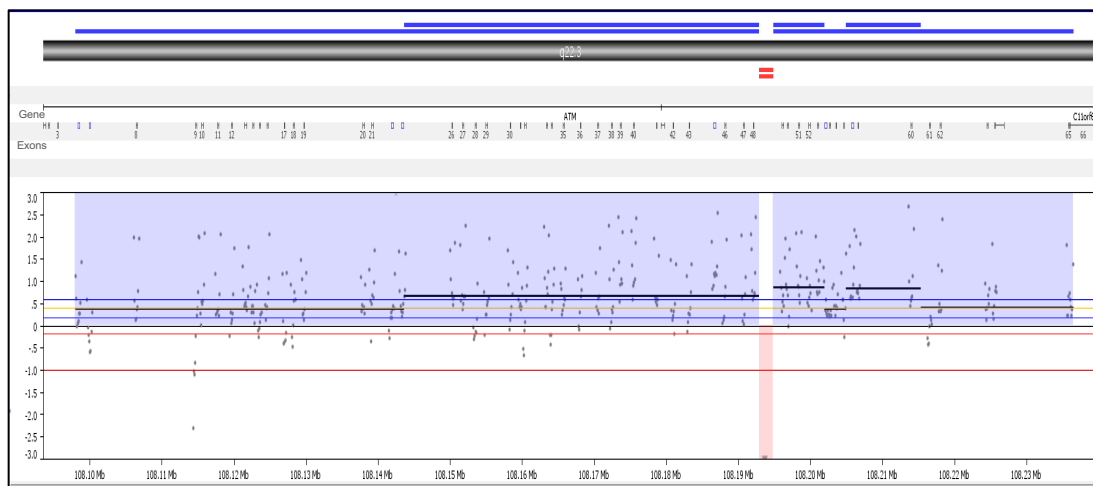
B. SK-LMS-1



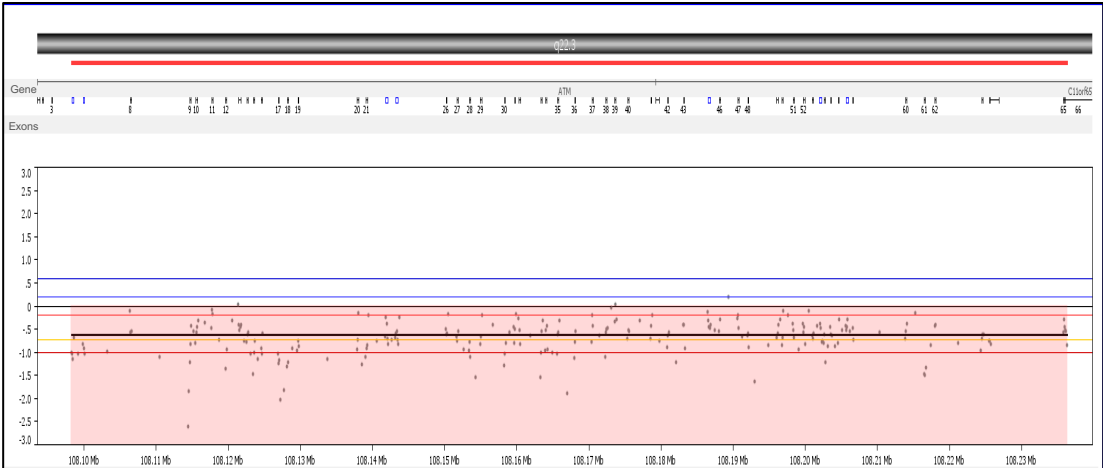
C. STS 09/10



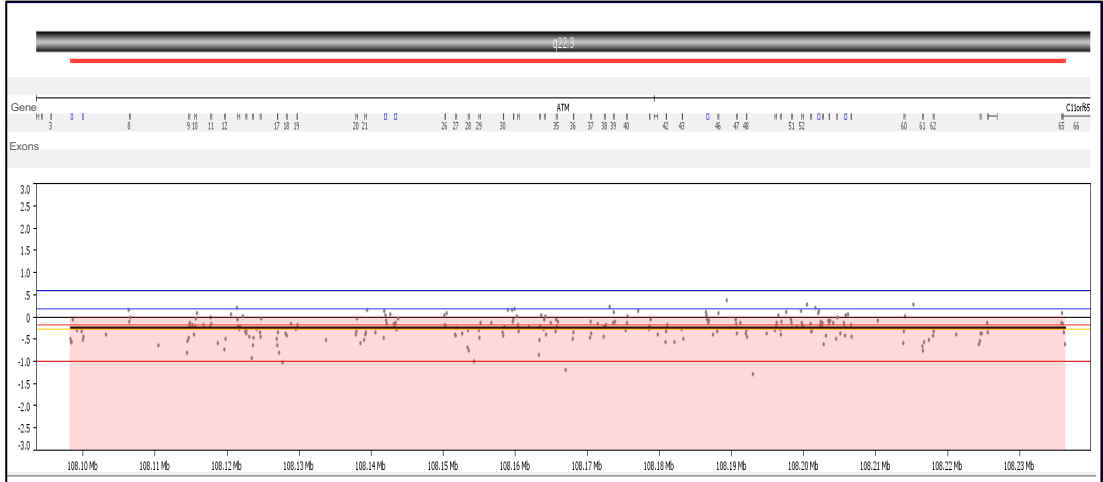
D. STS 13/12 W2



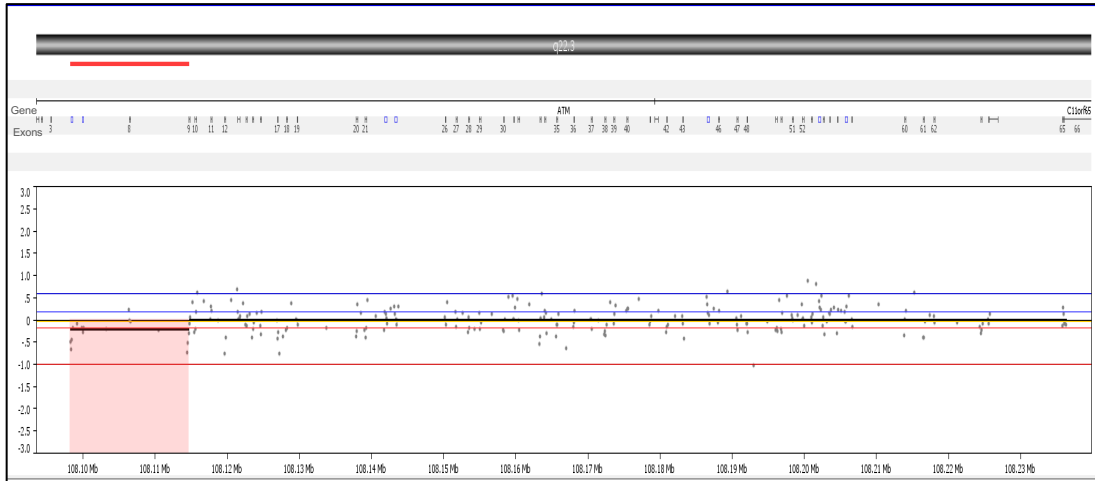
E. U2OS



F. STS 02/11 W1



G. STS 20/11



H. STS 06/11

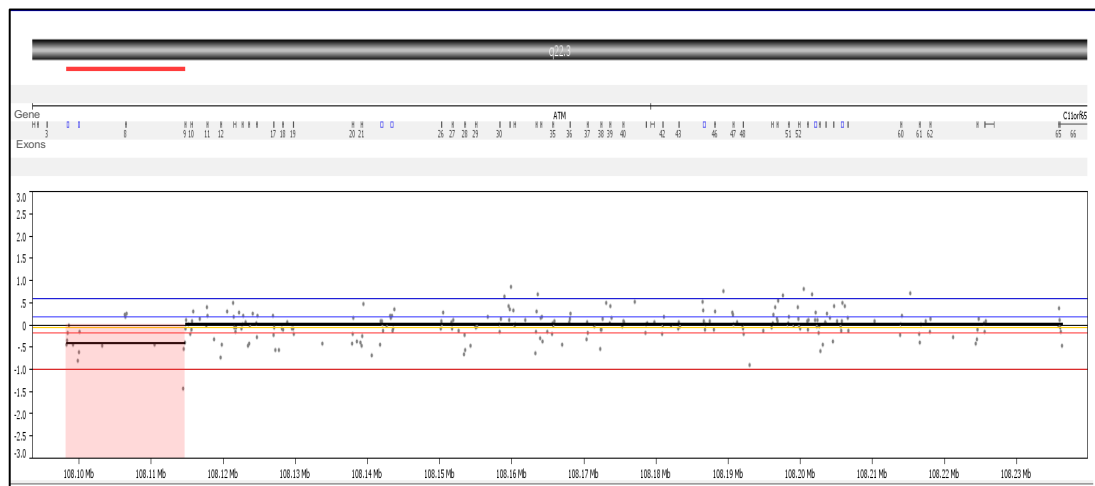


Figure 4.7 Graphical View of *ATM* CNA Identified in Different Sarcoma Cell Lines.

Graphical views of the *ATM* gene located on 11q22.3, displaying the *ATM* CNA in different sarcoma cell lines using the BAM MSR algorithm. The annotation tracks (gene and exons) at the top of each ideogram show the gene name and ordered exon numbers of the *ATM* gene. The x-axis denotes the full length of the gene, and the y-axis represents the log ratio of the tumour against the reference. The cluster/median log-ratio values are illustrated, where the thick black lines above the zero line represent the detection of *ATM* copy number amplification, with the corresponding blue shaded area above the zero line, while the thick black lines below the zero line represent the detection of the *ATM* copy number deletion, with the corresponding red shading below the zero line. The ideograms show a balanced *ATM* copy number in (A), close similarity in the gain pattern (B, C and D), loss across all *ATM* exons (E, F) and a partial loss pattern of the *ATM* (G, H) in sarcoma samples.

4.3 Discussion

Although the complexity of genomic aberrations differs significantly within similar cases of cancer, certain genomic alterations have been found to occur frequently, and to be preserved even with the progression of tumours. Accumulating evidence therefore supports the current view that genetic instability is an enabling feature that promotes the cancer phenotype, and thus that recurrent CNAs harbour clues as to the pathogenesis of the tumour (Hanahan and Weinberg, 2011, Taylor et al., 2011). CNAs have been detected in most STS (Myllykangas et al., 2007). Zhang et al. (2003) suggested an association between *ATM* deletion and the development of RMS (Zhang et al., 2003). A previous study carried out in our laboratory reported a shared common region of chromosomal 13q and 11q imbalance in two sarcoma subtypes including LMS and GIST. These abnormalities include an amplification in 13q21-q32 as well as frequent deletion in the 11q22.3 region that covers the locus of the *ATM* gene in both tumour types (Ul-Hassan et al., 2009). A recent CGH study that was also performed in our laboratory demonstrated copy number losses across the entire genome of 22 formalin-fixed and paraffin-embedded (FFPE) LMS cases, which were more common than gains. The most frequently deleted regions found in this study included the whole or near-whole arm deletion of 10p, 10q, 13q, 16q, and deletion of the telomeric end of 11q (Salawu et al., 2012).

The frequent loss in the region covering *ATM* detected in previous research were selected for comprehensive investigation and confirmation in the present study using several techniques. The detection of *ATM* copy numbers in the current study was performed by interphase FISH using an LSI-*ATM* probe that maps within the 11q22.3 region. In order to distinguish target locus-specific deletion from aneuploidy, chromosome enumeration DNA probes specifically designed for chromosome 11 (CEP11 probes) were also used (Ul-Hassan et al., 2009). These CEP11 probes hybridise to the centromeric region of chromosome 11 to permit the identification and enumeration of the chromosome 11 copy number.

All sarcoma cases were found to have a deletion at the *ATM* region in 23-100% of the cells in the various sarcoma cell lines (Table 4.2 and Figure 4.2), and compared well with previously described results generated in our laboratory (Ul-Hassan et al., 2009, Salawu et al., 2012). The pattern of deletion detected by FISH in this study was a decrease in the *ATM* copy number in relation to the chromosome 11 centromere copy number in all the sarcoma cell lines. In the blood control, the cut-off value of 10.95% represents cells that had fewer copies of *ATM* than the chromosome 11 centromere and any results from the test samples above that cut-off value were considered positive. Although, all sarcoma cell lines had greater than the cut-off from the controls (Table 4.2), it is important to mention that many of the sarcoma cell lines were polyploid, and that most of these cells had three or more chromosome 11 centromere (green signals), with relatively fewer copies of the *ATM* region 11q22.3 (red signals) (Figure 4.2 B and C). In contrast, in the blood control, no triploid cells were detected and only a small percentage were found to have one copy of the *ATM* in the presence of two copies of the chromosome 11 centromere.

The loss in the *ATM* copy number in sarcoma cell lines was further investigated in the current study by NGS and MLPA in order to ascertain a more accurate estimate of the *ATM* copy numbers. It was explained earlier in the MLPA results that Coffalyser.Net software detected a drop in signal intensity of the fragments in the peak pattern, which was not only seen in the MLPA peaks itself but also in the size standard peak pattern (Figure 4.4 C). Sloping of the size marker is one of the main issues with MLPA that is introduced during capillary electrophoresis and that commonly has a similar effect on the MLPA probe signals. This effect was clearly noted in the MLPA peak pattern, where the signal intensities of the longer MLPA fragments were lower than those of the shorter MLPA fragments (Figure 4.4 C). Unfortunately, the signal sloping in both peak patterns made data normalisation very difficult or even impossible in this study, since the degree of sloping detected was quite severe and could not be corrected by

the software, thus creating a bias in the data such that the regions with longer MLPA fragments may appear as a deletion during data analysis, even though they were just lower because of the sloping. Old gel or capillaries, too high injection or run voltages and the use of low quality of separation buffers are all factors that may play a role in signal sloping in the MLPA data produced in this chapter (<http://www.mlpa.com/>).

High injection or run voltages cause large fragments to be injected at a slower rate since there is a preferential injection of the shorter fragments, which makes the signal intensity of the smaller MLPA fragments higher than those of longer ones. Old gel or capillaries, and the poor quality of separation buffers, also have a similar effect to high injection voltages. Old gel has more resistance and therefore can result in lower peaks for longer MLPA fragments, and the quality of the buffer used influences the sensitivity of the MLPA thus a bad buffer quality can cause signal sloping. Adapting the injection settings, replacing the gel, capillaries and buffer used in the capillary electrophoresis device, and re-loading the PCR products of MLPA samples again could improve sloping issue detected in this chapter (<http://www.mlpa.com/>). Unfortunately, there were no PCR products left from the MLPA experiment to re-load them into the capillary electrophoresis device and due to the very tight timeframe window for submitting the thesis the experiment could not be repeated.

Even though the issue with sloping affected the data quality, the MLPA results included in this study showed a similar pattern of findings to the previous MLPA work generated in our laboratory in 2012 by Dr. Aliya Ul-Hassan (Figure 4.3 and 4.5). However, the Manchester spreadsheets used in the MLPA data analysis conducted by Dr. Ul-Hassan does not state if the MLPA experiment gave reliable results as they lack quality control checks. Therefore, both sets of data obtained cannot be seen as totally reliable, despite the apparently similar finding between experiments. Nonetheless, it is possible to compare and validate the MLPA data

produced for the *ATM* CNA in this study with the data generated by the FISH and NGS techniques reported in this chapter. For example, when considering control cell lines, FISH detected deletion of the *ATM* copy in the tumour control (U2OS) where the majority of the U2OS cells (93.5%) had four copies of chromosome 11 with the presence of two copies of the *ATM* gene. The majority of the normal control (hTERT-RPE1) cells had a balanced copy number in respect to *ATM* and chromosome 11, which were similar to that seen in the blood controls (Table 4.1, Table 4.2, Figure 4.2 A and B). The loss of *ATM* copy numbers in the U2OS cell line found by interphase FISH was also detected by NGS (Figure 4.2 A, B and Figure 4.7 E). Furthermore, comparable findings were also found with the MLPA results, despite the sloping issue detected (Figure 4.6 B and D).

Although the deletion of *ATM* copy number was also detected by FISH in the established SK-LMS-1 and in the primary STS 09/10 and STS 13/12 W2 sarcoma cell lines, targeted NGS data showed an amplification of the *ATM* in these cells (Table 4.2, Figure 4.7 B,C and D). As was mentioned earlier (Section 4.2.3), FISH compares *ATM* CNA in relation to the copy number of chromosome 11 centromere, and as this analysis examines individual cells it can also indicate the degree of heterogeneity within the cell line population (Stuppia et al., 2012, Liu et al., 2013). In contrast, the detection of *ATM* CNAs with either MLPA or from the targeted NGS examines the cell population in its entirety. For the targeted NGS any given region (*ATM*) will be compared with the whole reference genome. The algorithms in the Nexus Copy Number software use the depth of coverage to determine an average for the whole genome then explore if there is a certain area that looks to be lower or higher than the average in order to identify *ATM* CNAs. This means that the targeted NGS is only able to determine the DNA copy number as an average and does not provide detailed information about the aneuploidy and heterogeneity of the sample.

Although there was general agreement amongst the techniques for the control lines, for the sarcoma cell lines there was inconsistencies in relation to *ATM* copy number status. FISH indicated deletion of *ATM* in the SK-LMS-1, STS 09/10 and STS 13/12 W2 sarcoma cell lines (Table 4.2). A review of the median log ratios generated from the targeted NGS in the *ATM* region of the SK-LMS-1 cell line showed that the ratios were just around the thresholds set for the algorithm (Figure 4.7 B), and FISH analysis of this cell line suggested a significant heterogeneity which would make it less likely that NGS would be able to arrive at an accurate determination of the *ATM* copy numbers in this cell line (Liu et al., 2013). The median log ratios in STS 09/10 and STS 13/12 W2 were however more convincing and the inaccurate call by the FASST2 algorithm used to call *ATM* CNAs from NGS data in these two cell lines was probably due to the increased number of *ATM* signals, which were greater than two confirmed in FISH despite a low *ATM* to centromere ratio that was in keeping with an overall deletion of the *ATM* (Figure 4.7 C, D and Table 4.2)..

The MLPA results for the SK-LMS-1 and STS 13/12 W2 cell lines could also correlate to that generated by NGS, in spite of the difficulty in the interpretation of the MLPA data in this study (Appendix 3, Figure 4.7 B and D). The correlation between NGS and MLPA results was indeed expected. The reason is that the detection of *ATM* CNA by the MLPA test is based on the comparison with the normal DNA copy numbers of the genes located at off target parts of the genome (internal reference probes); although, with the external normal reference samples, and similar to NGS, the MLPA test is not capable of detecting the degree of heterogeneity in the sample (Stuppia et al., 2012). Although the correlation between results was expected, many factors may affect the reproducibility of the MLPA test performed on cancer cells, including a significant chance that the off target genomic loci (internal reference probes) will be abnormal in tumour samples, which would make accurate determinations difficult through MLPA alone.

The deletion of the *ATM* copy number was also detected by FISH in other sarcoma cell lines, including the primary STS 06/11 and the established SKUT-1 and SW1535 (Table 4.2). The NGS analysis and MLPA data, however, showed almost balanced copies for the *ATM* in the primary sarcoma cell line (Figure 4.7 H and Appendix 3). MLPA also showed almost normal results for the established sarcoma cell lines (Appendix 3). FISH analysis revealed that the majority of cells in STS 06/11 (71%), and about half of cells in SKUT-1 (50.5%) and SW1535 (54%) had two *ATM* signals despite signals of chromosome 11 (Table 4.2) and that could be the reason why the NGS and MLPA analysis underestimated the deletion of the *ATM* copy number detected by FISH and the population of cells with *ATM* CNA was possibly undetected.

Although results for the *ATM* CNA detected by FISH, NGS and MLPA were inconsistent in some sarcoma cases, both FISH and NGS data showed a loss of the *ATM* copy number in the tumour control (U2OS) and in the primary STS 02/11 W1 (Table 4.2 and Figure 4.7 F). Similar findings have been also generated by MLPA for these two cell lines (Appendix 3). The aneuploidy in both cell lines has been confirmed by FISH, where most of the U2OS cells had four and two copies of the chromosome 11 and *ATM*, respectively. Similarly, the vast majority of cells in STS 02/11 W1 showed an extra (8-11) copies of chromosome 11 with two or three copies of the *ATM*. Even though the NGS experiment was not focused on detecting *ATM* CNA in relation to chromosome 11, the calling algorithms were more likely to succeed in making the correct call in these two cases because of the big disparity found in the ratio between *ATM* and chromosome 11.

As it was mentioned in section 4.2.8, the targeted NGS panel examined other cancer genes than *ATM* (Appendix 4) and provided information on whether any meaningful or known mutations were detected for any of these genes in the cancer panel. There was no evidence from the initial findings of known mutations for any gene on the cancer panel. Although this at

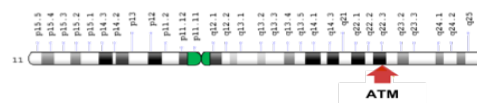
first may seem surprising sarcomas reported to be driven by CNA rather than mutational changes. Furthermore, the *ATM* gene is a large gene and reported mutations are spread throughout the genes affecting many of the 66 exons (Weber et al., 2016). It is therefore not possible from the initial NGS screening to establish if a meaningful *ATM* mutation exists in any sarcomas studied here, and further more detailed analysis of the data is required.

In summary, all sarcoma cases were found by FISH to have a relative deletion in the region containing the *ATM*, in parallel with the previously published data generated in our laboratory (Ul-Hassan et al., 2009, Salawu et al., 2012). MLPA and NGS were undertaken in order to identify if any hotspots for mutation or deletion of the *ATM* genes existed, and although there was some disagreement with the FISH data presumably resulting from the heterogeneity of the cell lines, there were some variation reported for different exons of the *ATM* gene that may provide clues for the basis of further investigation.

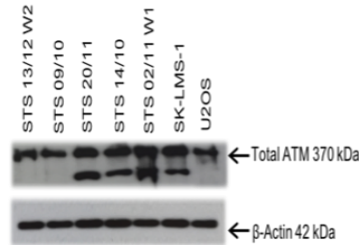
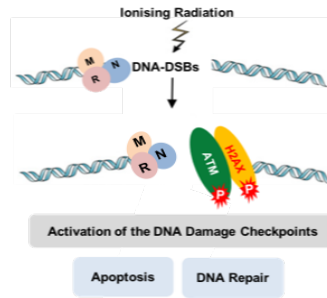
CHAPTER FIVE

5 FINAL DISCUSSION

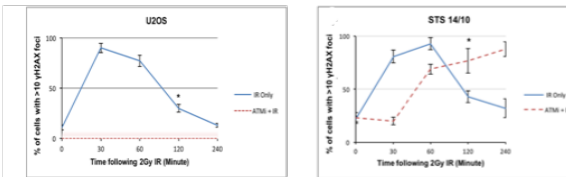
Previous study in our laboratory has revealed frequent deletion in the 11q22.3 region that covers the locus of the *ATM* gene, particularly in gastrointestinal stromal tumours and in leiomyosarcomas. *ATM* is known to have a key role in the repair of DNA-DSBs and in cell cycle arrest.



The total ATM protein levels and ATM kinase activity have been detected in all cell lines tested in this study including the controls by Western blot analysis following the exposure to 2Gy IR. However, expression of ATM was not identical and it seems to be higher in sarcoma samples showed truncated protein under the expression of ATM.



The existence of functional ATM in sarcoma samples has been further confirmed by clonogenic survival and H2AX assays, however, unlike controls, sarcoma samples in H2AX were still able to undertake DNA repair following ATM inhibitor treatment possibly via the utilisation of other pathways or because an “abnormal” ATM in the sarcomas may not have been adequately inhibited due to a mutation.



This study has also confirmed *ATM* copy number deletion in sarcomas using a combination of several techniques.

The clear expression of ATM, and the functional aspect of the kinase activity of the ATM in sarcoma samples included in this project, with FISH detected deletion in 11q22.3, could suggest genes other than *ATM* within the 11q22.3 region may also be involved, and could also raise the possibility that *ATM* may not be deleted/mutated and, therefore, is not the target. The *ATM* mutational analysis is therefore particularly required to answer all these inquiries.

Figure 5.1 Summary of Approaches used and Major Findings of this PhD Study

5.1 Final Discussion

5.1.1 Objective of this Work

As some types of sarcoma may initiate through a combination of defective DNA repair mechanisms, together with radiation exposure inducing DNA damage (So et al., 2009, Burningham et al., 2012), this investigation examined the involvement of *ATM* as a key regulator of DNA-DSBs damage (Burma et al., 2001, Nakamura et al., 2010) and previously shown as deleted in sarcoma (Ul-Hassan et al., 2009, Salawu et al., 2012).

5.1.2 Sarcomas have frequent *ATM* CNA, but protein expression and functional response are detectable.

A summary of the workflow and findings of the projects are presented in figure (5.1). Initially, to confirm if the ATM protein is expressed in the sarcoma samples, Western blotting was performed and showed clear expression of the ATM protein at 370 kDa in all cell lines tested (Figure 3.1). A loss of *ATM* copy number was confirmed for the sarcoma cell lines using a number of methodologies (Chapter 4), but did not affect expression of the ATM protein. The expression of the ATM protein was however not entirely comparable, appearing to be higher in sarcoma samples which showed a truncated protein product below the expression of the ATM (Figure 3.1). Mutations in the *ATM* gene, causing reduction/loss of protein function have also been reported and linked to the development of other tumours (Scott et al., 2002), suggesting that mechanisms other than deletion may be important to the expression of ATM in the sarcoma cell lines tested in this study. Non-identical expression of the ATM found in this study, together with the appearance of truncated protein product have also been detected previously in rhabdomyosarcoma study, and attributed to the possibility of *ATM* mutations in sarcoma samples (Zhang et al., 2003). On the other hand, alternative mechanisms for causing

ATM inactivation in sarcoma are possible, such as DNA methylation, as has been described in breast cancer (Vo et al., 2004).

To establish if mutations of *ATM* were present in sarcomas a two-stage approach was taken. Initially because of the large size of the *ATM* gene, MLPA was used, rather than sequencing, to potentially identify hotspots of CNA worthy of further exploration. Latterly, NGS was performed on a subsection of sarcomas using a cancer gene panel, but although there was some indication of selective exon targeting for CNA with both methodologies, no known mutations were reported for the *ATM* gene or indeed any other genes in the cancer panel.

Inhibition of the *ATM* kinase was undertaken to explore the ability of the sarcomas to repair DNA-DSBs following radiation, and to see how mutations / deletion of *ATM* may affect the response. A significant increase in radio-sensitivity in all cell lines tested, was found following inhibition (Figure 3.9), indicating that *ATM* was functional, as this response was not seen in A-T patients who had functionally deficient *ATM* (Hickson et al., 2004). There is however some conflict on the impact of this inhibition, as control samples in the H2AX assay could not respond following inhibition *ATM* kinase activity whilst sarcomas (not U2OS) could all initiate a response (Figure 3.3 and 3.6).

5.1.3 How are sarcomas able to respond to DNA-DSBs despite inhibition of *ATM* Kinase?

It is important to note that the kinetics of the H2AX response for the sarcomas was varied after inhibition, while the H2AX data showed complete inhibition of *ATM* kinase activity in the control samples following *ATM* inhibitor treatment, a higher proportion of γ H2AX foci formation was detected in sarcoma samples. This would be explained by the utilisation of sarcoma to other repair pathways, such as DNA-PK, however, this was not seen in the control when *ATM* kinase

was inhibited. A very high degree of heterogeneity in *ATM* copy signals was detected by FISH in the sarcoma samples, in contrast to the results for both the normal hTERT-RPE1, and the tumour control, U2OS, which showed only two cell populations, with the majority having two *ATM* signals. This also could be another explanation for why the kinetics of H2AX response for the sarcomas was varied after ATM inhibition. The observations for both sarcoma and control samples could also raise the possibility that an “abnormal” ATM in the sarcomas may not have been adequately inhibited due to a mutation; this is especially because ATM kinase activity was blocked in the control samples when the ATM was inhibited.

5.1.4 Could mutations of *ATM* or its kinase be responsible for the ability to recruit H2AX and induce a radiation damage response?

Despite loss of a single *ATM* copy, for the tumour control, U2OS, the H2AX data for this cell line demonstrated proficient phosphorylation of H2AX post 2Gy IR, which was equivalent to the response in the normal control, hTERT-RPE1 (Table 4.2, Figure 4.7 E, Figure 3.6 A and B) and both cell lines were equally inhibited following treatment with the ATM inhibitor. In a previous study, U2OS was used as it was considered to be wild type for *ATM* (Takagi et al., 2004) and thus able to respond to damage, so it could be assumed that there is wild type *ATM*, inhibition of its kinase affects its ability to respond.

The possibility that *ATM* mutations can be detected in sarcoma is interesting, and potentially raises the important question of how that interferes with the pattern of functional response seen in this project for sarcoma samples. Since ATM exists as a dimer in the cell, the possibility that mutation in the *ATM* can exert a dominant interfering effect on the normal ATM kinase activity in sarcoma samples should be considered, alongside the dominant interfering effect previously described among breast cancer patients who had certain *ATM* mutations (Scott et al., 2002).

As stated earlier in this thesis, the dominant interfering effect appears with missense mutations that result in the production of a full-length protein, similar to that seen in the Western blotting data in this project (Figure 3.1), although, this protein contains amino acid changes that may affect/compromise the protein function. Moreover, it is important to note that even though *ATM* was found to be deleted in this study, this deletion was in relation to the chromosome copy number, and many of the sarcomas had at least one or more copies of *ATM*. If one were to assume that the sarcoma samples had one mutant *ATM* allele but retained a second wild type second allele, this would then explain the dominant interfering effect of this mutation on the sarcoma samples and clarify the differences in behaviour between the sarcoma and control samples. *ATM* mutations including truncating, frame-shift or splice sites have been reported to affect protein function and expression in cancer, however, around 70% of the *ATM* mutations described in cancer to date are missense mutations. Recently, Weber et al. (2016), showed no or only limited impact of the *ATM* missense mutations on its normal function in non-small cell lung cancer following IR response (Weber et al., 2016). In order to investigate this possibility, however, it would be necessary to conduct *ATM* mutational analysis of the sarcoma samples.

Previous studies have demonstrated that mutation either in S1987 (the *ATM* autophosphorylation site in mice which corresponds to the *ATM* autophosphorylation site, S1981, that acts as an *ATM* activation marker in humans) or in the three conserved *ATM* autophosphorylation sites, S367, S1899 and S1987 in mice (which correspond, respectively, to S367, S1893 and S1981 in humans) showed no effect on the signalling of *ATM* dependent downstream substrates. These findings suggest the involvement of other mechanisms of DNA damage induced activation of *ATM* rather than the prominent *ATM* autophosphorylation sites (Pellegrini et al., 2006, Daniel et al., 2008). If this were the case with the sarcoma samples included in this study, however, this observation would not be in a line with the finding that

controls displayed complete inhibition of the ATM kinase activity following the treatment with the ATM inhibitor.

5.1.5 Is deletion of *ATM* copy number relevant or just a marker?

Although, FISH analysis of the sarcoma samples included in this study revealed *ATM* deletion, it is worth mentioning that *ATM* may not be the exclusive target because the size of the FISH probe used for *ATM* in this study was approximately 732 kb, thus spanning the entire 150 kb of *ATM* gene in addition to a number of other genes, including *RAB39*, *CUL5* and *EXPH5*. *EXPH5* is a *RAS* related protein *RAB27B* effector protein and the deregulation of *RAB27b* has been associated with the pathogenesis of bladder cancer (Ho et al., 2012). The downregulation of *CUL5*, *PPP2R1B* and *NPAT* genes involved in cell cycle regulation and apoptosis has been implicated previously with the pathogenesis of B-cell leukaemia (Kalla et al., 2007). Also, *CUL5* has been found to be downregulated in breast cancer (Fay et al., 2003). Recently, *RAB39*, a member of a *RAS* oncogene family that had never previously been studied in cancer biology, has been found to promote tumorigenesis (Chano and Avnet, 2018). The clear expression of *ATM*, and the functional aspect of the kinase activity of the *ATM* in sarcoma samples included in this project, with FISH detected deletion in 11q22.3, could suggest genes other than *ATM* within the 11q22.3 region may also be involved, and could also raise the possibility that *ATM* may not be deleted/mutated and, therefore, is not the target. The *ATM* mutational analysis is therefore particularly required to answer all these inquiries. Unfortunately, the three genes other than *ATM* are not in the cancer panel and therefore it is difficult to verify their status. The NGS data did not indicate any mutations of *ATM* or any other genes on the cancer panel. This data however because of the analysis pipeline only reflects well characterised mutations, and therefore does not mean that variants/mutations exist both for the *ATM* gene and other genes

on the cancer panel. Unfortunately, because of time constraints, a more in depth analysis of the NGS data, to explore this possibility for “silent” mutations, was not permissible.

5.2 Limitations of this Study

The main limitation of this study was the inability to repeat the MLPA test due to the lack of time at the end of this PhD. Since *ATM* is a very large gene and contains about 66 exons, its mutational screening would be expensive and time consuming and therefore, the plan of the study was to look at the gene as its entirety by performing the MLPA to give an overall answer across such a big gene and to determine if there are any specific hotspots. Any regions containing mutations identified by MLPA were then subjected to DNA sequencing in order to determine the specific mutation(s) present.

5.3 Future Work

The results from the current study confirmed the previous suggestion of *ATM* deletion in sarcoma, however, this does not affect protein expression in sarcoma samples included in this study. *ATM* mutations have been reported previously in cancer. For both these reasons, *ATM* mutational analysis is the immediate future work in this study, since this will provide further information about many issues raised in this study, including the truncated protein found in the Western blotting results for the sarcoma cell lines and the differences in the mechanisms of *ATM* functioning between the sarcoma and control cell lines.

REFERENCES

- AERTS, I., PACQUEMENT, H., DOZ, F., MOSSERI, V., DESJARDINS, L., SASTRE, X., MICHON, J., RODRIGUEZ, J., SCHLIENGER, P., ZUCKER, J. M. & QUINTANA, E. 2004. Outcome of second malignancies after retinoblastoma: a retrospective analysis of 25 patients treated at the Institut Curie. *Eur J Cancer*, 40, 1522-9.
- AGA, P., SINGH, R., PARIHAR, A. & PARASHARI, U. 2011. Imaging spectrum in soft tissue sarcomas. *Indian J Surg Oncol*, 2, 271-9.
- AMARY, F., PILLAY, N. & FLANAGAN, A. M. 2017. Molecular testing of sarcomas. *Diagnostic Histopathology*.
- AMERICAN, TYPE, CULTURE, COLLECTION, STANDARDS, DEVELOPMENT, ORGANIZATION & WORKGROUP 2010. Cell line misidentification: the beginning of the end. *Nat Rev Cancer*, 10, 441-8.
- AN, J., HUANG, Y. C., XU, Q. Z., ZHOU, L. J., SHANG, Z. F., HUANG, B., WANG, Y., LIU, X. D., WU, D. C. & ZHOU, P. K. 2010. DNA-PKcs plays a dominant role in the regulation of H2AX phosphorylation in response to DNA damage and cell cycle progression. *BMC Mol Biol*, 11, 18.
- ANDRE, M. C., ANTUNES, J. V., REIS, M. D., FILIPE, P. L. & ALMEIDA, L. M. 2011. Cutaneous leiomyosarcoma on the trunk. *An Bras Dermatol*, 86, 999-1002.
- ARMOUR, J. A., BARTON, D. E., COCKBURN, D. J. & TAYLOR, G. R. 2002. The detection of large deletions or duplications in genomic DNA. *Hum Mutat*, 20, 325-37.
- ARVAND, A. & DENNY, C. T. 2001. Biology of EWS/ETS fusions in Ewing's family tumors. *Oncogene*, 20, 5747-54.

- ASIF, A., MUSHTAQ, S., HASSAN, U., AKHTAR, N., HUSSAIN, M., AZAM, M. & QAZI, R. 2018. Fluorescence in Situ Hybridization (FISH) for Differential Diagnosis of Soft Tissue Sarcomas. *Asian Pac J Cancer Prev*, 19, 655-660.
- BAGNI, R. & WHITBY, D. 2009. Kaposi's sarcoma-associated herpesvirus transmission and primary infection. *Curr Opin HIV AIDS*, 4, 22-6.
- BAKKENIST, C. J. & KASTAN, M. B. 2003. DNA damage activates ATM through intermolecular autophosphorylation and dimer dissociation. *Nature*, 421, 499-506.
- BALLINGER, M. L., GOODE, D. L., RAY-COQUARD, I., JAMES, P. A., MITCHELL, G., NIEDERMAYR, E., PURI, A., SCHIFFMAN, J. D., DITE, G. S., CIPPONI, A., MAKI, R. G., BROHL, A. S., MYKLEBOST, O., STRATFORD, E. W., LORENZ, S., AHN, S. M., AHN, J. H., KIM, J. E., SHANLEY, S., BESHAY, V., RANDALL, R. L., JUDSON, I., SEDDON, B., CAMPBELL, I. G., YOUNG, M. A., SARIN, R., BLAY, J. Y., O'DONOGHUE, S. I. & THOMAS, D. M. 2016. Monogenic and polygenic determinants of sarcoma risk: an international genetic study. *Lancet Oncol*, 17, 1261-71.
- BANERJEE, R., BANDOPADHYAY, D. & ABILASH, V. 2013. Epidemiology, pathology, types and diagnosis of soft tissue sarcoma: A research review. *Asian J Pharm Clin Res*, 6, 18-25.
- BARTEK, J. & LUKAS, J. 2001. Mammalian G1- and S-phase checkpoints in response to DNA damage. *Curr Opin Cell Biol*, 13, 738-47.
- BATEY, M. A., ZHAO, Y., KYLE, S., RICHARDSON, C., SLADE, A., MARTIN, N. M., LAU, A., NEWELL, D. R. & CURTIN, N. J. 2013. Preclinical evaluation of a novel ATM inhibitor, KU59403, in vitro and in vivo in p53 functional and dysfunctional models of human cancer. *Mol Cancer Ther*, 12, 959-67.

- BEHAM, A. W., SCHAEFER, I. M., SCHULER, P., CAMERON, S. & GHADIMI, B. M. 2012. Gastrointestinal stromal tumors. *Int J Colorectal Dis*, 27, 689-700.
- BOLT, H. M. 2005. Vinyl chloride-a classical industrial toxicant of new interest. *Crit Rev Toxicol*, 35, 307-23.
- BOLT, M. W. & MAHONEY, P. A. 1997. High-efficiency blotting of proteins of diverse sizes following sodium dodecyl sulfate-polyacrylamide gel electrophoresis. *Anal Biochem*, 247, 185-92.
- BOURTON, E. C., PLOWMAN, P. N., SMITH, D., ARLETT, C. F. & PARRIS, C. N. 2011. Prolonged expression of the gamma-H2AX DNA repair biomarker correlates with excess acute and chronic toxicity from radiotherapy treatment. *Int J Cancer*, 129, 2928-34.
- BOVEE, J. V. & HOGENDOORN, P. C. 2010. Molecular pathology of sarcomas: concepts and clinical implications. *Virchows Arch*, 456, 193-9.
- BREE, R. T., NEARY, C., SAMALI, A. & LOWNDES, N. F. 2004. The switch from survival responses to apoptosis after chromosomal breaks. *DNA Repair (Amst)*, 3, 989-95.
- BREMS, H., BEERT, E., DE RAVEL, T. & LEGIUS, E. 2009. Mechanisms in the pathogenesis of malignant tumours in neurofibromatosis type 1. *Lancet Oncol*, 10, 508-15.
- BRIGGS, N. C., LEVINE, R. S., HALL, H. I., COSBY, O., BRANN, E. A. & HENNEKENS, C. H. 2003. Occupational risk factors for selected cancers among African American and White men in the United States. *Am J Public Health*, 93, 1748-52.
- BROEKS, A., URBANUS, J. H., FLOORE, A. N., DAHLER, E. C., KLIJN, J. G., RUTGERS, E. J., DEVILEE, P., RUSSELL, N. S., VAN LEEUWEN, F. E. &

- VAN 'T VEER, L. J. 2000. ATM-heterozygous germline mutations contribute to breast cancer-susceptibility. *Am J Hum Genet*, 66, 494-500.
- BURMA, S., CHEN, B. P., MURPHY, M., KURIMASA, A. & CHEN, D. J. 2001. ATM phosphorylates histone H2AX in response to DNA double-strand breaks. *J Biol Chem*, 276, 42462-7.
- BURNINGHAM, Z., HASHIBE, M., SPECTOR, L. & SCHIFFMAN, J. D. 2012. The epidemiology of sarcoma. *Clin Sarcoma Res*, 2, 14.
- CAPE-DAVIS, A., REID, Y. A., KLINE, M. C., STORTS, D. R., STRAUSS, E., DIRKS, W. G., DREXLER, H. G., MACLEOD, R. A., SYKES, G., KOHARA, A., NAKAMURA, Y., ELMORE, E., NIMS, R. W., ALSTON-ROBERTS, C., BARALLON, R., LOS, G. V., NARDONE, R. M., PRICE, P. J., STEUER, A., THOMSON, J., MASTERS, J. R. & KERRIGAN, L. 2013. Match criteria for human cell line authentication: where do we draw the line? *Int J Cancer*, 132, 2510-9.
- CARNEIRO, A., FRANCIS, P., BENDAHL, P. O., FERNEBRO, J., AKERMAN, M., FLETCHER, C., RYDHOLM, A., BORG, A. & NILBERT, M. 2009. Indistinguishable genomic profiles and shared prognostic markers in undifferentiated pleomorphic sarcoma and leiomyosarcoma: different sides of a single coin? *Lab Invest*, 89, 668-75.
- CASTELLANO, E. & SANTOS, E. 2011. Functional specificity of ras isoforms: so similar but so different. *Genes Cancer*, 2, 216-31.
- CHAN, S. H., LIM, W. K., ISHAK, N. D. B., LI, S. T., GOH, W. L., TAN, G. S., LIM, K. H., TEO, M., YOUNG, C. N. C., MALIK, S., TAN, M. H., TEH, J. Y. H., CHIN, F. K. C., KESAVAN, S., SELVARAJAN, S., TAN, P., TEH, B. T., SOO, K. C.,

- FARID, M., QUEK, R. & NGEOW, J. 2017. Germline Mutations in Cancer Predisposition Genes are Frequent in Sporadic Sarcomas. *Sci Rep*, 7, 10660.
- CHANG, Y., CESARMAN, E., PESSIN, M. S., LEE, F., CULPEPPER, J., KNOWLES, D. M. & MOORE, P. S. 1994. Identification of herpesvirus-like DNA sequences in AIDS-associated Kaposi's sarcoma. *Science*, 266, 1865-9.
- CHANO, T. & AVNET, S. 2018. RAB39A: a Rab small GTPase with a prominent role in cancer stemness. *J Biochem*, 164, 9-14.
- CHATTERJEE, N. & WALKER, G. C. 2017. Mechanisms of DNA damage, repair, and mutagenesis. *Environ Mol Mutagen*, 58, 235-263.
- CHEN, G. & LEE, E. 1996. The product of the ATM gene is a 370-kDa nuclear phosphoprotein. *J Biol Chem*, 271, 33693-7.
- CHEUK, W., LI, P. C. & CHAN, J. K. 2002. Epstein-Barr virus-associated smooth muscle tumour: a distinctive mesenchymal tumour of immunocompromised individuals. *Pathology*, 34, 245-9.
- CLINGEN, P. H., WU, J. Y., MILLER, J., MISTRY, N., CHIN, F., WYNNE, P., PRISE, K. M. & HARTLEY, J. A. 2008. Histone H2AX phosphorylation as a molecular pharmacological marker for DNA interstrand crosslink cancer chemotherapy. *Biochem Pharmacol*, 76, 19-27.
- COINDRE, J. M. 2006. Grading of soft tissue sarcomas: review and update. *Arch Pathol Lab Med*, 130, 1448-53.
- CORMIER, J. N. & POLLOCK, R. E. 2004. Soft tissue sarcomas. *CA Cancer J Clin*, 54, 94-109.
- DANG, C. V. & KIM, J. W. 2018. Convergence of Cancer Metabolism and Immunity: an Overview. *Biomol Ther (Seoul)*, 26, 4-9.

- DANGOOR, A., SEDDON, B., GERRAND, C., GRIMER, R., WHELAN, J. & JUDSON, I. 2016. UK guidelines for the management of soft tissue sarcomas. *Clin Sarcoma Res*, 6, 20.
- DANIEL, J. A., PELLEGRINI, M., LEE, J. H., PAULL, T. T., FEIGENBAUM, L. & NUSSENZWEIG, A. 2008. Multiple autophosphorylation sites are dispensable for murine ATM activation in vivo. *J Cell Biol*, 183, 777-83.
- DE BREE, E., VAN COEVORDEN, F., PETERSE, J. L., RUSSELL, N. S. & RUTGERS, E. J. 2002. Bilateral angiosarcoma of the breast after conservative treatment of bilateral invasive carcinoma: genetic predisposition? *Eur J Surg Oncol*, 28, 392-5.
- DE SMET, S., VANDERMEEREN, L., CHRISTIAENS, M. R., SAMSON, I., STAS, M., VAN LIMBERGEN, E. & DE WEVER, I. 2008. Radiation-induced sarcoma: analysis of 46 cases. *Acta Chir Belg*, 108, 574-9.
- DEAN, B. J. F. & WHITWELL, D. 2009. (i) Epidemiology of bone and soft-tissue sarcomas. *Orthopaedics and Trauma*, 23, 223-230.
- DEI TOS, A. P. 2000. Liposarcoma: new entities and evolving concepts. *Ann Diagn Pathol*, 4, 252-66.
- DELANEY, T. F. & HAAS, R. L. 2016. Innovative radiotherapy of sarcoma: Proton beam radiation. *Eur J Cancer*, 62, 112-23.
- DEMETRI, G. D., VAN OOSTEROM, A. T., GARRETT, C. R., BLACKSTEIN, M. E., SHAH, M. H., VERWEIJ, J., MCARTHUR, G., JUDSON, I. R., HEINRICH, M. C., MORGAN, J. A., DESAI, J., FLETCHER, C. D., GEORGE, S., BELLO, C. L., HUANG, X., BAUM, C. M. & CASALI, P. G. 2006. Efficacy and safety of sunitinib in patients with advanced gastrointestinal stromal tumour after failure of imatinib: a randomised controlled trial. *Lancet*, 368, 1329-38.

- DERHEIMER, F. A. & KASTAN, M. B. 2010. Multiple roles of ATM in monitoring and maintaining DNA integrity. *FEBS Lett*, 584, 3675-81.
- DEYRUP, A. T., LEE, V. K., HILL, C. E., CHEUK, W., TOH, H. C., KESAVAN, S., CHAN, E. W. & WEISS, S. W. 2006. Epstein-Barr virus-associated smooth muscle tumors are distinctive mesenchymal tumors reflecting multiple infection events: a clinicopathologic and molecular analysis of 29 tumors from 19 patients. *Am J Surg Pathol*, 30, 75-82.
- DOYLE, B., MORTON, J. P., DELANEY, D. W., RIDGWAY, R. A., WILKINS, J. A. & SANSOM, O. J. 2010. p53 mutation and loss have different effects on tumorigenesis in a novel mouse model of pleomorphic rhabdomyosarcoma. *J Pathol*, 222, 129-37.
- DRUKKER, L., ALBERTON, J. & REISSMAN, P. 2012. Leiomyosarcoma of the inferior vena cava: radical surgery without vascular reconstruction. *Vasc Endovascular Surg*, 46, 688-90.
- DUCIMETIERE, F., LURKIN, A., RANCHERE-VINCE, D., DECOUVELAERE, A. V., PEOC'H, M., ISTIER, L., CHALABREYSSE, P., MULLER, C., ALBERTI, L., BRINGUIER, P. P., SCOAZEC, J. Y., SCHOTT, A. M., BERGERON, C., CELLIER, D., BLAY, J. Y. & RAY-COQUARD, I. 2011. Incidence of sarcoma histotypes and molecular subtypes in a prospective epidemiological study with central pathology review and molecular testing. *PLoS One*, 6, e20294.
- DUMAZ, N. & MEEK, D. W. 1999. Serine15 phosphorylation stimulates p53 transactivation but does not directly influence interaction with HDM2. *Embo j*, 18, 7002-10.

- EL-AWADY, R. A., DIKOMEY, E. & DAHM-DAPHI, J. 2003. Radiosensitivity of human tumour cells is correlated with the induction but not with the repair of DNA double-strand breaks. *Br J Cancer*, 89, 593-601.
- ESTOURGIE, S. H., NIELSEN, G. P. & OTT, M. J. 2002. Metastatic patterns of extremity myxoid liposarcoma and their outcome. *J Surg Oncol*, 80, 89-93.
- FALCK, J., PETRINI, J. H., WILLIAMS, B. R., LUKAS, J. & BARTEK, J. 2002. The DNA damage-dependent intra-S phase checkpoint is regulated by parallel pathways. *Nat Genet*, 30, 290-4.
- FANG, Z., MATSUMOTO, S., AE, K., KAWAGUCHI, N., YOSHIKAWA, H., UEDA, T., ISHII, T., ARAKI, N. & KITO, M. 2004. Postradiation soft tissue sarcoma: a multiinstitutional analysis of 14 cases in Japan. *J Orthop Sci*, 9, 242-6.
- FARSHID, G., PRADHAN, M., GOLDBLUM, J. & WEISS, S. W. 2002. Leiomyosarcoma of somatic soft tissues: a tumor of vascular origin with multivariate analysis of outcome in 42 cases. *Am J Surg Pathol*, 26, 14-24.
- FAY, M. J., LONGO, K. A., KARATHANASIS, G. A., SHOPE, D. M., MANDERNACH, C. J., LEONG, J. R., HICKS, A., PHERSON, K. & HUSAIN, A. 2003. Analysis of CUL-5 expression in breast epithelial cells, breast cancer cell lines, normal tissues and tumor tissues. *Mol Cancer*, 2, 40.
- FERGUSON, D. O. & ALT, F. W. 2001. DNA double strand break repair and chromosomal translocation: lessons from animal models. *Oncogene*, 20, 5572-9.
- FERNANDEZ-MEDARDE, A. & SANTOS, E. 2011. Ras in cancer and developmental diseases. *Genes Cancer*, 2, 344-58.
- FERRARI, A., SULTAN, I., HUANG, T. T., RODRIGUEZ-GALINDO, C., SHEHADEH, A., MEAZZA, C., NESS, K. K., CASANOVA, M. & SPUNT, S. L.

2011. Soft tissue sarcoma across the age spectrum: a population-based study from the Surveillance Epidemiology and End Results database. *Pediatr Blood Cancer*, 57, 943-9.
- FLETCHER, C., BRIDGE, J., HOGENDOORN, P. & MERTENS, F. 2013. World Health Organization Classification of tumours of soft tissue and bone 4 edition IARC Press. Lyon.
- FLETCHER, C. D., BERMAN, J. J., CORLESS, C., GORSTEIN, F., LASOTA, J., LONGLEY, B. J., MIETTINEN, M., O'LEARY, T. J., REMOTTI, H., RUBIN, B. P., SHMOOKLER, B., SOBIN, L. H. & WEISS, S. W. 2002a. Diagnosis of gastrointestinal stromal tumors: A consensus approach. *Hum Pathol*, 33, 459-65.
- FLETCHER, C. D., UNNI, K. K. & MERTENS, F. 2002b. *Pathology and genetics of tumours of soft tissue and bone*, IARC.
- FRANCIS, M., DENNIS, N., CHARMAN, J., LAWRENCE, G. & GRIMER, R. 2013. Bone and Soft Tissue Sarcomas UK Incidence and Survival: 1996 to 2010 Version 2.0. *National Cancer Intelligence Network*.
- FRANKEN, N. A., RODERMOND, H. M., STAP, J., HAVEMAN, J. & VAN BREE, C. 2006. Clonogenic assay of cells in vitro. *Nat Protoc*, 1, 2315-9.
- FREEMAN, J. L., PERRY, G. H., FEUK, L., REDON, R., MCCARROLL, S. A., ALTSHULER, D. M., ABURATANI, H., JONES, K. W., TYLER-SMITH, C., HURLES, M. E., CARTER, N. P., SCHERER, S. W. & LEE, C. 2006. Copy number variation: new insights in genome diversity. *Genome Res*, 16, 949-61.
- FRIESNER, J. D., LIU, B., CULLIGAN, K. & BRITT, A. B. 2005. Ionizing radiation-dependent gamma-H2AX focus formation requires ataxia telangiectasia

- mutated and ataxia telangiectasia mutated and Rad3-related. *Mol Biol Cell*, 16, 2566-76.
- GAO, L., FENG, Y., BOWERS, R., BECKER-HAPAK, M., GARDNER, J., COUNCIL, L., LINETTE, G., ZHAO, H. & CORNELIUS, L. A. 2006. Ras-associated protein-1 regulates extracellular signal-regulated kinase activation and migration in melanoma cells: two processes important to melanoma tumorigenesis and metastasis. *Cancer Res*, 66, 7880-8.
- GATELY, D. P., HITTLE, J. C., CHAN, G. K. & YEN, T. J. 1998. Characterization of ATM expression, localization, and associated DNA-dependent protein kinase activity. *Mol Biol Cell*, 9, 2361-74.
- GEBHARD, S., COINDRE, J. M., MICHELS, J. J., TERRIER, P., BERTRAND, G., TRASSARD, M., TAYLOR, S., CHATEAU, M. C., MARQUES, B., PICOT, V. & GUILLOU, L. 2002. Pleomorphic liposarcoma: clinicopathologic, immunohistochemical, and follow-up analysis of 63 cases: a study from the French Federation of Cancer Centers Sarcoma Group. *Am J Surg Pathol*, 26, 601-16.
- GEORGE, S., BLAY, J. Y., CASALI, P. G., LE CESNE, A., STEPHENSON, P., DEPRIMO, S. E., HARMON, C. S., LAW, C. N., MORGAN, J. A., RAY-COQUARD, I., TASSELL, V., COHEN, D. P. & DEMETRI, G. D. 2009. Clinical evaluation of continuous daily dosing of sunitinib malate in patients with advanced gastrointestinal stromal tumour after imatinib failure. *Eur J Cancer*, 45, 1959-68.
- GOLDING, S. E., ROSENBERG, E., ADAMS, B. R., WIGNARAJAH, S., BECKTA, J. M., O'CONNOR, M. J. & VALERIE, K. 2012. Dynamic inhibition of ATM

- kinase provides a strategy for glioblastoma multiforme radiosensitization and growth control. *Cell Cycle*, 11, 1167-73.
- GOLDING, S. E., ROSENBERG, E., VALERIE, N., HUSSAINI, I., FRIGERIO, M., COCKCROFT, X. F., CHONG, W. Y., HUMMERSONE, M., RIGOREAU, L., MENEAR, K. A., O'CONNOR, M. J., POVIRK, L. F., VAN METER, T. & VALERIE, K. 2009. Improved ATM kinase inhibitor KU-60019 radiosensitizes glioma cells, compromises insulin, AKT and ERK prosurvival signaling, and inhibits migration and invasion. *Mol Cancer Ther*, 8, 2894-902.
- GONIN-LAURENT, N., GIBAUD, A., HUYGUE, M., LEFEVRE, S. H., LE BRAS, M., CHAUVEINC, L., SASTRE-GARAU, X., DOZ, F., LUMBROSO, L., CHEVILLARD, S. & MALFOY, B. 2006. Specific TP53 mutation pattern in radiation-induced sarcomas. *Carcinogenesis*, 27, 1266-72.
- GOODARZI, A. A., JONNALAGADDA, J. C., DOUGLAS, P., YOUNG, D., YE, R., MOORHEAD, G. B., LEES-MILLER, S. P. & KHANNA, K. K. 2004. Autophosphorylation of ataxia-telangiectasia mutated is regulated by protein phosphatase 2A. *Embo j*, 23, 4451-61.
- GRAADT VAN ROGGEN, J. F., VAN VELTHUYSEN, M. L. & HOGENDOORN, P. C. 2001. The histopathological differential diagnosis of gastrointestinal stromal tumours. *J Clin Pathol*, 54, 96-102.
- GRIMER, R., JUDSON, I., PEAKE, D. & SEDDON, B. 2010. Guidelines for the management of soft tissue sarcomas. *Sarcoma*, 2010, 506182.
- GROBMYER, S. R. & BRENNAN, M. F. 2003. Predictive variables detailing the recurrence rate of soft tissue sarcomas. *Curr Opin Oncol*, 15, 319-26.
- GUILLOU, L. & AURIAS, A. 2010. Soft tissue sarcomas with complex genomic profiles. *Virchows Arch*, 456, 201-17.

- GUO, Z., KOZLOV, S., LAVIN, M. F., PERSON, M. D. & PAULL, T. T. 2010. ATM activation by oxidative stress. *Science*, 330, 517-21.
- GURLEY, K. E. & KEMP, C. J. 2001. Synthetic lethality between mutation in Atm and DNA-PK(cs) during murine embryogenesis. *Curr Biol*, 11, 191-4.
- HAMM, H. E. 1998. The many faces of G protein signaling. *J Biol Chem*, 273, 669-72.
- HANAHAHAN, D. & WEINBERG, R. A. 2011. Hallmarks of cancer: the next generation. *Cell*, 144, 646-74.
- HEFFERIN, M. L. & TOMKINSON, A. E. 2005. Mechanism of DNA double-strand break repair by non-homologous end joining. *DNA Repair (Amst)*, 4, 639-48.
- HELMAN, L. J. & MELTZER, P. 2003. Mechanisms of sarcoma development. *Nat Rev Cancer*, 3, 685-94.
- HEYER, W. D., EHMTSEN, K. T. & LIU, J. 2010. Regulation of homologous recombination in eukaryotes. *Annu Rev Genet*, 44, 113-39.
- HICKSON, I., ZHAO, Y., RICHARDSON, C. J., GREEN, S. J., MARTIN, N. M., ORR, A. I., REAPER, P. M., JACKSON, S. P., CURTIN, N. J. & SMITH, G. C. 2004. Identification and characterization of a novel and specific inhibitor of the ataxia-telangiectasia mutated kinase ATM. *Cancer Res*, 64, 9152-9.
- HO, J. R., CHAPEAUBLANC, E., KIRKWOOD, L., NICOLLE, R., BENHAMOU, S., LEBRET, T., ALLORY, Y., SOUTHGATE, J., RADVANYI, F. & GOUD, B. 2012. Deregulation of Rab and Rab effector genes in bladder cancer. *PLoS One*, 7, e39469.
- HOCHEGGER, H., TAKEDA, S. & HUNT, T. 2008. Cyclin-dependent kinases and cell-cycle transitions: does one fit all? *Nat Rev Mol Cell Biol*, 9, 910-6.

- HOH, L., GRAVELLS, P., CANOVAS, D., UL-HASSAN, A., RENNIE, I. G., BRYANT, H. & SISLEY, K. 2011. Atypically low spontaneous sister chromatid exchange formation in uveal melanoma. *Genes Chromosomes Cancer*, 50, 34-42.
- HOPPIN, J. A., TOLBERT, P. E., FLANDERS, W. D., ZHANG, R. H., DANIELS, D. S., RAGSDALE, B. D. & BRANN, E. A. 1999. Occupational risk factors for sarcoma subtypes. *Epidemiology*, 10, 300-6.
- HORNICK, J. L., BOSENBERG, M. W., MENTZEL, T., MCMENAMIN, M. E., OLIVEIRA, A. M. & FLETCHER, C. D. 2004. Pleomorphic liposarcoma: clinicopathologic analysis of 57 cases. *Am J Surg Pathol*, 28, 1257-67.
- HSU, T. C. & POMERAT, C. M. 1953. MAMMALIAN CHROMOSOMES IN VITRO II. A Method for Spreading the Chromosomes of Cells in Tissue Culture. *Journal of Heredity*, 44, 23-30.
- HUANG, N. C., WANN, S. R., CHANG, H. T., LIN, S. L., WANG, J. S. & GUO, H. R. 2011. Arsenic, vinyl chloride, viral hepatitis, and hepatic angiosarcoma: a hospital-based study and review of literature in Taiwan. *BMC Gastroenterol*, 11, 142.
- IDBAIH, A., COINDRE, J. M., DERRE, J., MARIANI, O., TERRIER, P., RANCHERE, D., MAIRAL, A. & AURIAS, A. 2005. Myxoid malignant fibrous histiocytoma and pleomorphic liposarcoma share very similar genomic imbalances. *Lab Invest*, 85, 176-81.
- ISOZAKI, K. & HIROTA, S. 2006. Gain-of-Function Mutations of Receptor Tyrosine Kinases in Gastrointestinal Stromal Tumors. *Curr Genomics*, 7, 469-75.
- IWASAKI, H., NABESHIMA, K., NISHIO, J., JIMI, S., AOKI, M., KOGA, K., HAMASAKI, M., HAYASHI, H. & MOGI, A. 2009. Pathology of soft-tissue

- tumors: daily diagnosis, molecular cytogenetics and experimental approach. *Pathol Int*, 59, 501-21.
- JACKSON, S. P. 2002. Sensing and repairing DNA double-strand breaks. *Carcinogenesis*, 23, 687-96.
- JACKSON, S. P. 2009. The DNA-damage response: new molecular insights and new approaches to cancer therapy. *Biochem Soc Trans*, 37, 483-94.
- JACOBS, A. J., LINDHOLM, E. B., LEVY, C. F., FISH, J. D. & GLICK, R. D. 2017. Racial and ethnic disparities in treatment and survival of pediatric sarcoma. *J Surg Res*, 219, 43-49.
- JIN, Y., SHIMA, Y., FURU, M., AOYAMA, T., NAKAMATA, T., NAKAYAMA, T., NAKAMURA, T. & TOGUCHIDA, J. 2010. Absence of oncogenic mutations of RAS family genes in soft tissue sarcomas of 100 Japanese patients. *Anticancer Res*, 30, 245-51.
- KALLA, C., SCHEUERMANN, M. O., KUBE, I., SCHLOTTER, M., MERTENS, D., DOHNER, H., STILGENBAUER, S. & LICHTER, P. 2007. Analysis of 11q22-q23 deletion target genes in B-cell chronic lymphocytic leukaemia: evidence for a pathogenic role of NPAT, CUL5, and PPP2R1B. *Eur J Cancer*, 43, 1328-35.
- KANAAR, R., HOEIJMAKERS, J. H. & VAN GENT, D. C. 1998. Molecular mechanisms of DNA double strand break repair. *Trends Cell Biol*, 8, 483-9.
- KARVE, S., WERNER, M. E., SUKUMAR, R., CUMMINGS, N. D., COPP, J. A., WANG, E. C., LI, C., SETHI, M., CHEN, R. C., PACOLD, M. E. & WANG, A. Z. 2012. Revival of the abandoned therapeutic wortmannin by nanoparticle drug delivery. *Proc Natl Acad Sci U S A*, 109, 8230-5.

- KASPER, B., GIL, T., D'HONDT, V., GEBHART, M. & AWADA, A. 2007. Novel treatment strategies for soft tissue sarcoma. *Crit Rev Oncol Hematol*, 62, 9-15.
- KASTAN, M. B. & BARTEK, J. 2004. Cell-cycle checkpoints and cancer. *Nature*, 432, 316-23.
- KIM, K. P., RYU, M. H., YOO, C., RYOO, B. Y., CHOI, D. R., CHANG, H. M., LEE, J. L., BECK, M. Y., KIM, T. W. & KANG, Y. K. 2011. Nilotinib in patients with GIST who failed imatinib and sunitinib: importance of prior surgery on drug bioavailability. *Cancer Chemother Pharmacol*, 68, 285-91.
- KING, A. A., DEBAUN, M. R., RICCARDI, V. M. & GUTMANN, D. H. 2000. Malignant peripheral nerve sheath tumors in neurofibromatosis 1. *Am J Med Genet*, 93, 388-92.
- KIROVA, Y. M., VILCOQ, J. R., ASSELAIN, B., SASTRE-GARAU, X. & FOURQUET, A. 2005. Radiation-induced sarcomas after radiotherapy for breast carcinoma: a large-scale single-institution review. *Cancer*, 104, 856-63.
- KITAMURA, Y. 2008. Gastrointestinal stromal tumors: past, present, and future. *J Gastroenterol*, 43, 499-508.
- KLEIN, C. & VASSILEV, L. T. 2004. Targeting the p53-MDM2 interaction to treat cancer. *Br J Cancer*, 91, 1415-9.
- KLEINERMAN, R. A., SCHONFELD, S. J. & TUCKER, M. A. 2012. Sarcomas in hereditary retinoblastoma. *Clin Sarcoma Res*, 2, 15.
- KODAZ, H., KOSTEK, O., HACIOGLU, M. B., ERDOGAN, B., ELPEN KODAZ, C., HACIBEKIROGLU, I., TURKMEN, E., UZUNOGLU, S. & CICIN, I. 2017. Frequency of Ras Mutations (Kras, Nras, Hras) in Human Solid Cancer. *EURASIAN JOURNAL OF MEDICINE AND ONCOLOGY*, 1, 1-7.

- KOIKE, M., MASHINO, M., SUGASAWA, J. & KOIKE, A. 2008. Histone H2AX phosphorylation independent of ATM after X-irradiation in mouse liver and kidney in situ. *J Radiat Res*, 49, 445-9.
- KORF, B. R. 2000. Malignancy in neurofibromatosis type 1. *Oncologist*, 5, 477-85.
- KOZLOV, S. V., GRAHAM, M. E., JAKOB, B., TOBIAS, F., KIJAS, A. W., TANUJI, M., CHEN, P., ROBINSON, P. J., TAUCHER-SCHOLZ, G., SUZUKI, K., SO, S., CHEN, D. & LAVIN, M. F. 2011. Autophosphorylation and ATM activation: additional sites add to the complexity. *J Biol Chem*, 286, 9107-19.
- KOZLOWSKI, P., JASINSKA, A. J. & KWIATKOWSKI, D. J. 2008. New applications and developments in the use of multiplex ligation-dependent probe amplification. *Electrophoresis*, 29, 4627-36.
- LAGRANGE, J. L., RAMAIOLI, A., CHATEAU, M. C., MARCHAL, C., RESBEUT, M., RICHAUD, P., LAGARDE, P., RAMBERT, P., TORTECHAUX, J., SENG, S. H., DE LA FONTAN, B., REME-SAUMON, M., BOF, J., GHNASSIA, J. P. & COINDRE, J. M. 2000. Sarcoma after radiation therapy: retrospective multiinstitutional study of 80 histologically confirmed cases. Radiation Therapist and Pathologist Groups of the Federation Nationale des Centres de Lutte Contre le Cancer. *Radiology*, 216, 197-205.
- LANGENAU, D. M., KEEFE, M. D., STORER, N. Y., GUYON, J. R., KUTOK, J. L., LE, X., GOESSLING, W., NEUBERG, D. S., KUNKEL, L. M. & ZON, L. I. 2007. Effects of RAS on the genesis of embryonal rhabdomyosarcoma. *Genes Dev*, 21, 1382-95.
- LARRAMENDY, M. L., KAUR, S., SVARVAR, C., BOHLING, T. & KNUUTILA, S. 2006. Gene copy number profiling of soft-tissue leiomyosarcomas by array-comparative genomic hybridization. *Cancer Genet Cytogenet*, 169, 94-101.

- LAVIN, M. F. 2008. Ataxia-telangiectasia: from a rare disorder to a paradigm for cell signalling and cancer. *Nat Rev Mol Cell Biol*, 9, 759-69.
- LEE, J. H. & PAULL, T. T. 2005. ATM activation by DNA double-strand breaks through the Mre11-Rad50-Nbs1 complex. *Science*, 308, 551-4.
- LEE, J. H. & PAULL, T. T. 2007. Activation and regulation of ATM kinase activity in response to DNA double-strand breaks. *Oncogene*, 26, 7741-8.
- LEMPIAINEN, H. & HALAZONETIS, T. D. 2009. Emerging common themes in regulation of PIKKs and PI3Ks. *Embo j*, 28, 3067-73.
- LESSNICK, S. L. & LADANYI, M. 2012. Molecular pathogenesis of Ewing sarcoma: new therapeutic and transcriptional targets. *Annu Rev Pathol*, 7, 145-59.
- LI, X. & HEYER, W. D. 2008. Homologous recombination in DNA repair and DNA damage tolerance. *Cell Res*, 18, 99-113.
- LINDAHL, T. & BARNES, D. E. 2000. Repair of endogenous DNA damage. *Cold Spring Harb Symp Quant Biol*, 65, 127-33.
- LIU, B., MORRISON, C. D., JOHNSON, C. S., TRUMP, D. L., QIN, M., CONROY, J. C., WANG, J. & LIU, S. 2013. Computational methods for detecting copy number variations in cancer genome using next generation sequencing: principles and challenges. *Oncotarget*, 4, 1868-81.
- LIU, C. X., LI, X. Y., LI, C. F., CHEN, Y. Z., CUI, X. B., HU, J. M. & LI, F. 2014. Compound HRAS/PIK3CA mutations in Chinese patients with alveolar rhabdomyosarcomas. *Asian Pac J Cancer Prev*, 15, 1771-4.
- LLORENTE, B., SMITH, C. E. & SYMINGTON, L. S. 2008. Break-induced replication: what is it and what is it for? *Cell Cycle*, 7, 859-64.
- MACKALL, C. L., MELTZER, P. S. & HELMAN, L. J. 2002. Focus on sarcomas. *Cancer Cell*, 2, 175-8.

- MAKK, L., CREECH, J. L., WHELAN, J. G., JR. & JOHNSON, M. N. 1974. Liver damage and angiosarcoma in vinyl chloride workers. A systematic detection program. *Jama*, 230, 64-8.
- MATEO-LOZANO, S., GOKHALE, P. C., SOLDATENKOV, V. A., DRITSCHILO, A., TIRADO, O. M. & NOTARIO, V. 2006. Combined transcriptional and translational targeting of EWS/FLI-1 in Ewing's sarcoma. *Clin Cancer Res*, 12, 6781-90.
- MAYA, R., BALASS, M., KIM, S. T., SHKEDY, D., LEAL, J. F., SHIFMAN, O., MOAS, M., BUSCHMANN, T., RONAI, Z., SHILOH, Y., KASTAN, M. B., KATZIR, E. & OREN, M. 2001. ATM-dependent phosphorylation of Mdm2 on serine 395: role in p53 activation by DNA damage. *Genes Dev*, 15, 1067-77.
- MAZUR, M. T. & CLARK, H. B. 1983. Gastric stromal tumors. Reappraisal of histogenesis. *Am J Surg Pathol*, 7, 507-19.
- MCVEY, M. & LEE, S. E. 2008. MMEJ repair of double-strand breaks (director's cut): deleted sequences and alternative endings. *Trends Genet*, 24, 529-38.
- MENU-BRANTHOMME, A., RUBINO, C., SHAMSALDIN, A., HAWKINS, M. M., GRIMAUD, E., DONDON, M. G., HARDIMAN, C., VASSAL, G., CAMPBELL, S., PANIS, X., DALY-SCHVEITZER, N., LAGRANGE, J. L., ZUCKER, J. M., CHAVAUDRA, J., HARTMAN, O. & DE VATHAIRE, F. 2004. Radiation dose, chemotherapy and risk of soft tissue sarcoma after solid tumours during childhood. *Int J Cancer*, 110, 87-93.
- MERLETTI, F., RICHIARDI, L., BERTONI, F., AHRENS, W., BUEMI, A., COSTA-SANTOS, C., ERIKSSON, M., GUENEL, P., KAERLEV, L., JOCKEL, K. H., LLOPIS-GONZALEZ, A., MERLER, E., MIRANDA, A., MORALES-SUAREZ-VARELA, M. M., OLSSON, H., FLETCHER, T. & OLSEN, J. 2006.

- Occupational factors and risk of adult bone sarcomas: a multicentric case-control study in Europe. *Int J Cancer*, 118, 721-7.
- MESLI, S. N., GHOUALI, A. K., BENAMARA, F., TALEB, F. A., TAHRAOUI, H. & ABI-AYAD, C. 2017. Stewart-Treves Syndrome Involving Chronic Lymphedema after Mastectomy of Breast Cancer. *Case Rep Surg*, 2017, 4056459.
- MIETTINEN, M. & LASOTA, J. 2001. Gastrointestinal stromal tumors--definition, clinical, histological, immunohistochemical, and molecular genetic features and differential diagnosis. *Virchows Arch*, 438, 1-12.
- MIETTINEN, M. & LASOTA, J. 2006. Gastrointestinal stromal tumors: review on morphology, molecular pathology, prognosis, and differential diagnosis. *Arch Pathol Lab Med*, 130, 1466-78.
- MILANO, A., APICE, G., FERRARI, E., FAZIOLI, F., DE ROSA, V., DE LUNA, A. S., IAFFAIOLI, R. V. & CAPONIGRO, F. 2006. New emerging drugs in soft tissue sarcoma. *Crit Rev Oncol Hematol*, 59, 74-84.
- MILLER, C. W., ASLO, A., WON, A., TAN, M., LAMPKIN, B. & KOEFFLER, H. P. 1996. Alterations of the p53, Rb and MDM2 genes in osteosarcoma. *J Cancer Res Clin Oncol*, 122, 559-65.
- MONTEMURRO, M., GELDERBLOM, H., BITZ, U., SCHUTTE, J., BLAY, J. Y., JOENSUU, H., TRENT, J., BAUER, S., RUTKOWSKI, P., DUFFAUD, F. & PINK, D. 2013. Sorafenib as third- or fourth-line treatment of advanced gastrointestinal stromal tumour and pretreatment including both imatinib and sunitinib, and nilotinib: A retrospective analysis. *Eur J Cancer*, 49, 1027-31.
- MORGAN, D. O. 2007. *The cell cycle: principles of control*, New Science Press.

- MYLLYKANGAS, S., BOHLING, T. & KNUUTILA, S. 2007. Specificity, selection and significance of gene amplifications in cancer. *Semin Cancer Biol*, 17, 42-55.
- NAKAMURA, A. J., RAO, V. A., POMMIER, Y. & BONNER, W. M. 2010. The complexity of phosphorylated H2AX foci formation and DNA repair assembly at DNA double-strand breaks. *Cell Cycle*, 9, 389-97.
- O'SULLIVAN, B., DAVIS, A. M., TURCOTTE, R., BELL, R., CATTON, C., CHABOT, P., WUNDER, J., KANDEL, R., GODDARD, K., SADURA, A., PATER, J. & ZEE, B. 2002. Preoperative versus postoperative radiotherapy in soft-tissue sarcoma of the limbs: a randomised trial. *Lancet*, 359, 2235-41.
- OSUNA, D. & DE ALAVA, E. 2009. Molecular pathology of sarcomas. *Rev Recent Clin Trials*, 4, 12-26.
- OTTAVIANO, L., SCHAEFER, K. L., GAJEWSKI, M., HUCKENBECK, W., BALDUS, S., ROGEL, U., MACKINTOSH, C., DE ALAVA, E., MYKLEBOST, O., KRESSE, S. H., MEZA-ZEPEDA, L. A., SERRA, M., CLETON-JANSEN, A. M., HOGENDOORN, P. C., BUERGER, H., AIGNER, T., GABBERT, H. E. & POREMBA, C. 2010. Molecular characterization of commonly used cell lines for bone tumor research: a trans-European EuroBoNet effort. *Genes Chromosomes Cancer*, 49, 40-51.
- PARIDA, L., FERNANDEZ-PINEDA, I., UFFMAN, J., NAVID, F., DAVIDOFF, A. M., NEEL, M., KRASIN, M. J. & RAO, B. N. 2012. Clinical management of Ewing sarcoma of the bones of the hands and feet: a retrospective single-institution review. *J Pediatr Surg*, 47, 1806-10.
- PASELLO, M., MANARA, M. C. & SCOTLANDI, K. 2018. CD99 at the crossroads of physiology and pathology. *J Cell Commun Signal*, 12, 55-68.

- PELLEGRINI, M., CELESTE, A., DIFILIPPANTONIO, S., GUO, R., WANG, W., FEIGENBAUM, L. & NUSSENZWEIG, A. 2006. Autophosphorylation at serine 1987 is dispensable for murine Atm activation in vivo. *Nature*, 443, 222-5.
- PENG, C. Y., GRAVES, P. R., THOMA, R. S., WU, Z., SHAW, A. S. & PIWNICAWORMS, H. 1997. Mitotic and G2 checkpoint control: regulation of 14-3-3 protein binding by phosphorylation of Cdc25C on serine-216. *Science*, 277, 1501-5.
- PERRONE, S., LOTTI, F., GERONZI, U., GUIDONI, E., LONGINI, M. & BUONOCORE, G. 2016. Oxidative Stress in Cancer-Prone Genetic Diseases in Pediatric Age: The Role of Mitochondrial Dysfunction. *Oxid Med Cell Longev*, 2016, 4782426.
- PERRY, J. & KLECKNER, N. 2003. The ATRs, ATMs, and TORs are giant HEAT repeat proteins. *Cell*, 112, 151-5.
- RAINEY, M. D., CHARLTON, M. E., STANTON, R. V. & KASTAN, M. B. 2008. Transient inhibition of ATM kinase is sufficient to enhance cellular sensitivity to ionizing radiation. *Cancer Res*, 68, 7466-74.
- RAJANI, B., SMITH, T. A., REITH, J. D. & GOLDBLUM, J. R. 1999. Retroperitoneal leiomyosarcomas unassociated with the gastrointestinal tract: a clinicopathologic analysis of 17 cases. *Mod Pathol*, 12, 21-8.
- RASTRELLI, M., TROPEA, S., BASSO, U., ROMA, A., MARUZZO, M. & ROSSI, C. R. 2014. Soft tissue limb and trunk sarcomas: diagnosis, treatment and follow-up. *Anticancer Res*, 34, 5251-62.
- RIBALLO, E., KUHNE, M., RIEF, N., DOHERTY, A., SMITH, G. C., RECIO, M. J., REIS, C., DAHM, K., FRICKE, A., KREMPLER, A., PARKER, A. R., JACKSON, S. P., GENNERY, A., JEGGO, P. A. & LOBRICH, M. 2004. A

- pathway of double-strand break rejoining dependent upon ATM, Artemis, and proteins locating to gamma-H2AX foci. *Mol Cell*, 16, 715-24.
- RIGGI, N. & STAMENKOVIC, I. 2007. The Biology of Ewing sarcoma. *Cancer Lett*, 254, 1-10.
- ROCCHI, A., MANARA, M. C., SCIANDRA, M., ZAMBELLI, D., NARDI, F., NICOLETTI, G., GAROFALO, C., MESCHINI, S., ASTOLFI, A., COLOMBO, M. P., LESSNICK, S. L., PICCI, P. & SCOTLANDI, K. 2010. CD99 inhibits neural differentiation of human Ewing sarcoma cells and thereby contributes to oncogenesis. *J Clin Invest*, 120, 668-80.
- ROGAKOU, E., NIEVES-NIERA, W., BOON, C., POMMIER, Y. & BONNER, W. Histone H2AX serine-139 phosphorylation is induced by the introduction of the initial breaks into DNA as a result of the apoptotic endonuclease. *Molecular Biology of the Cell*, 1998. AMER SOC CELL BIOLOGY PUBL OFFICE, 9650 ROCKVILLE PIKE, BETHESDA, MD 20814 USA, 109A-109A.
- ROGATSCH, H., BONATTI, H., MENET, A., LARCHER, C., FEICHTINGER, H. & DIRNHOFER, S. 2000. Epstein-Barr virus-associated multicentric leiomyosarcoma in an adult patient after heart transplantation: case report and review of the literature. *Am J Surg Pathol*, 24, 614-21.
- ROSENZWEIG, K. E., YOUMELL, M. B., PALAYOOR, S. T. & PRICE, B. D. 1997. Radiosensitization of human tumor cells by the phosphatidylinositol3-kinase inhibitors wortmannin and LY294002 correlates with inhibition of DNA-dependent protein kinase and prolonged G2-M delay. *Clin Cancer Res*, 3, 1149-56.
- ROTMAN, G. & SHILOH, Y. 1998. ATM: from gene to function. *Hum Mol Genet*, 7, 1555-63.

- RUBINO, C., SHAMSALDIN, A., LE, M. G., LABBE, M., GUINEBRETIERE, J. M., CHAVAUDRA, J. & DE VATHAIRE, F. 2005. Radiation dose and risk of soft tissue and bone sarcoma after breast cancer treatment. *Breast Cancer Res Treat*, 89, 277-88.
- RUIJS, M. W., VERHOEF, S., ROOKUS, M. A., PRUNTEL, R., VAN DER HOUT, A. H., HOGERVORST, F. B., KLUIJT, I., SIJMONS, R. H., AALFS, C. M., WAGNER, A., AUSEMS, M. G., HOOGERBRUGGE, N., VAN ASPEREN, C. J., GOMEZ GARCIA, E. B., MEIJERS-HEIJBOER, H., TEN KATE, L. P., MENKO, F. H. & VAN 'T VEER, L. J. 2010. TP53 germline mutation testing in 180 families suspected of Li-Fraumeni syndrome: mutation detection rate and relative frequency of cancers in different familial phenotypes. *J Med Genet*, 47, 421-8.
- SALAWU, A., FERNANDO, M., HUGHES, D., REED, M. W., WOLL, P., GREAVES, C., DAY, C., ALHAJIMOHAMMED, M. & SISLEY, K. 2016. Establishment and molecular characterisation of seven novel soft-tissue sarcoma cell lines. *Br J Cancer*, 115, 1058-1068.
- SALAWU, A., UL-HASSAN, A., HAMMOND, D., FERNANDO, M., REED, M. & SISLEY, K. 2012. High quality genomic copy number data from archival formalin-fixed paraffin-embedded leiomyosarcoma: optimisation of universal linkage system labelling. *PLoS One*, 7, e50415.
- SANDERS, K. M., ORDOG, T., KOH, S. D., TORIHASHI, S. & WARD, S. M. 1999. Development and plasticity of interstitial cells of Cajal. *Neurogastroenterol Motil*, 11, 311-38.
- SARASIN, A. & KAUFFMANN, A. 2008. Overexpression of DNA repair genes is associated with metastasis: a new hypothesis. *Mutat Res*, 659, 49-55.

- SAVITSKY, K., BAR-SHIRA, A., GILAD, S., ROTMAN, G., ZIV, Y., VANAGAITE, L., TAGLE, D. A., SMITH, S., UZIEL, T., SFEZ, S., ASHKENAZI, M., PECKER, I., FRYDMAN, M., HARNIK, R., PATANJALI, S. R., SIMMONS, A., CLINES, G. A., SARTIEL, A., GATTI, R. A., CHESSA, L., SANAL, O., LAVIN, M. F., JASPERS, N. G., TAYLOR, A. M., ARLETT, C. F., MIKI, T., WEISSMAN, S. M., LOVETT, M., COLLINS, F. S. & SHILOH, Y. 1995. A single ataxia telangiectasia gene with a product similar to PI-3 kinase. *Science*, 268, 1749-53.
- SCHOUTEN, J. P., MCELGUNN, C. J., WAAIJER, R., ZWIJNENBURG, D., DIEPVENS, F. & PALS, G. 2002. Relative quantification of 40 nucleic acid sequences by multiplex ligation-dependent probe amplification. *Nucleic Acids Res*, 30, e57.
- SCHWAB, J. H., BOLAND, P., GUO, T., BRENNAN, M. F., SINGER, S., HEALEY, J. H. & ANTONESCU, C. R. 2007. Skeletal metastases in myxoid liposarcoma: an unusual pattern of distant spread. *Ann Surg Oncol*, 14, 1507-14.
- SCOTT, S. P., BENDIX, R., CHEN, P., CLARK, R., DORK, T. & LAVIN, M. F. 2002. Missense mutations but not allelic variants alter the function of ATM by dominant interference in patients with breast cancer. *Proc Natl Acad Sci U S A*, 99, 925-30.
- SEDDON, B., STRAUSS, S. J., WHELAN, J., LEAHY, M., WOLL, P. J., COWIE, F., ROTHERMUNDT, C., WOOD, Z., BENSON, C., ALI, N., MARPLES, M., VEAL, G. J., JAMIESON, D., KUVER, K., TIRABOSCO, R., FORSYTH, S., NASH, S., DEHBI, H. M. & BEARE, S. 2017. Gemcitabine and docetaxel versus doxorubicin as first-line treatment in previously untreated advanced

- unresectable or metastatic soft-tissue sarcomas (GeDDiS): a randomised controlled phase 3 trial. *Lancet Oncol*, 18, 1397-1410.
- SEKIGUCHI, J., FERGUSON, D. O., CHEN, H. T., YANG, E. M., EARLE, J., FRANK, K., WHITLOW, S., GU, Y., XU, Y., NUSSENZWEIG, A. & ALT, F. W. 2001. Genetic interactions between ATM and the nonhomologous end-joining factors in genomic stability and development. *Proc Natl Acad Sci U S A*, 98, 3243-8.
- SHAO, I. H., LEE, W. C., CHEN, T. D. & CHIANG, Y. J. 2012. Leiomyosarcoma of the adrenal vein. *Chang Gung Med J*, 35, 428-31.
- SHERR, C. J. & MCCORMICK, F. 2002. The RB and p53 pathways in cancer. *Cancer Cell*, 2, 103-12.
- SHILOH, Y. & ZIV, Y. 2013. The ATM protein kinase: regulating the cellular response to genotoxic stress, and more. *Nat Rev Mol Cell Biol*, 14, 197-210.
- SHINGLER, S. L., SWINBURN, P., LLOYD, A., DIAZ, J., ISBELL, R., MANSON, S. & BENSON, C. 2013. Elicitation of health state utilities in soft tissue sarcoma. *Qual Life Res*, 22, 1697-706.
- SHREERAM, S., DEMIDOV, O. N., HEE, W. K., YAMAGUCHI, H., ONISHI, N., KEK, C., TIMOFEEV, O. N., DUDGEON, C., FORNACE, A. J., ANDERSON, C. W., MINAMI, Y., APPELLA, E. & BULAVIN, D. V. 2006. Wip1 phosphatase modulates ATM-dependent signaling pathways. *Mol Cell*, 23, 757-64.
- SHRIVASTAV, M., DE HARO, L. P. & NICKOLOFF, J. A. 2008. Regulation of DNA double-strand break repair pathway choice. *Cell Res*, 18, 134-47.
- SIBANDA, B. L., CHIRGADZE, D. Y. & BLUNDELL, T. L. 2010. Crystal structure of DNA-PKcs reveals a large open-ring cradle comprised of HEAT repeats. *Nature*, 463, 118-21.

- SINGER, S., DEMETRI, G. D., BALDINI, E. H. & FLETCHER, C. D. 2000. Management of soft-tissue sarcomas: an overview and update. *Lancet Oncol*, 1, 75-85.
- SLATER, O. & SHIPLEY, J. 2007. Clinical relevance of molecular genetics to paediatric sarcomas. *J Clin Pathol*, 60, 1187-94.
- SO, S., DAVIS, A. J. & CHEN, D. J. 2009. Autophosphorylation at serine 1981 stabilizes ATM at DNA damage sites. *J Cell Biol*, 187, 977-90.
- SORDILLO, P. P., CHAPMAN, R., HAJDU, S. I., MAGILL, G. B. & GOLBEY, R. B. 1981. Lymphangiosarcoma. *Cancer*, 48, 1674-9.
- STANKOVIC, T., KIDD, A. M., SUTCLIFFE, A., MCGUIRE, G. M., ROBINSON, P., WEBER, P., BEDENHAM, T., BRADWELL, A. R., EASTON, D. F., LENNOX, G. G., HAITES, N., BYRD, P. J. & TAYLOR, A. M. 1998. ATM mutations and phenotypes in ataxia-telangiectasia families in the British Isles: expression of mutant ATM and the risk of leukemia, lymphoma, and breast cancer. *Am J Hum Genet*, 62, 334-45.
- STEWART, F. W. & TREVES, N. 1948. Lymphangiosarcoma in postmastectomy lymphedema; a report of six cases in elephantiasis chirurgica. *Cancer*, 1, 64-81.
- STEWART, G. S., MASER, R. S., STANKOVIC, T., BRESSAN, D. A., KAPLAN, M. I., JASPERS, N. G., RAAMS, A., BYRD, P. J., PETRINI, J. H. & TAYLOR, A. M. 1999. The DNA double-strand break repair gene hMRE11 is mutated in individuals with an ataxia-telangiectasia-like disorder. *Cell*, 99, 577-87.
- STIFF, T., O'DRISCOLL, M., RIEF, N., IWABUCHI, K., LOBRICH, M. & JEGGO, P. A. 2004. ATM and DNA-PK function redundantly to phosphorylate H2AX after exposure to ionizing radiation. *Cancer Res*, 64, 2390-6.

- STIFF, T., WALKER, S. A., CEROSALETTI, K., GOODARZI, A. A., PETERMANN, E., CONCANNON, P., O'DRISCOLL, M. & JEGGO, P. A. 2006. ATR-dependent phosphorylation and activation of ATM in response to UV treatment or replication fork stalling. *Embo j*, 25, 5775-82.
- STILLER, C. A., TRAMA, A., SERRAINO, D., ROSSI, S., NAVARRO, C., CHIRLAQUE, M. D. & CASALI, P. G. 2013. Descriptive epidemiology of sarcomas in Europe: report from the RARECARE project. *Eur J Cancer*, 49, 684-95.
- STRATTON, M. R., FISHER, C., GUSTERSON, B. A. & COOPER, C. S. 1989. Detection of point mutations in N-ras and K-ras genes of human embryonal rhabdomyosarcomas using oligonucleotide probes and the polymerase chain reaction. *Cancer Res*, 49, 6324-7.
- STUPPIA, L., ANTONUCCI, I., PALKA, G. & GATTA, V. 2012. Use of the MLPA assay in the molecular diagnosis of gene copy number alterations in human genetic diseases. *Int J Mol Sci*, 13, 3245-76.
- SUWANSIRIKUL, S., SUKPAN, K., SITTITRAI, P., SUWIWAT, S. & KHUNAMORNPOONG, S. 2012. Epstein-Barr virus-associated smooth muscle tumor of the tonsil. *Auris Nasus Larynx*, 39, 329-32.
- SVETLOVA, M., SOLOVJEVA, L., NISHI, K., NAZAROV, I., SIINO, J. & TOMILIN, N. 2007. Elimination of radiation-induced gamma-H2AX foci in mammalian nucleus can occur by histone exchange. *Biochem Biophys Res Commun*, 358, 650-4.
- SVETLOVA, M. P., SOLOVJEVA, L. V. & TOMILIN, N. V. 2010. Mechanism of elimination of phosphorylated histone H2AX from chromatin after repair of DNA double-strand breaks. *Mutat Res*, 685, 54-60.

- SWANTON, C. 2004. Cell-cycle targeted therapies. *Lancet Oncol*, 5, 27-36.
- TAKAGI, M., TSUCHIDA, R., OGUCHI, K., SHIGETA, T., NAKADA, S., SHIMIZU, K., OHKI, M., DELIA, D., CHESSA, L., TAYA, Y., NAKANISHI, M., TSUNEMATSU, Y., BESSHO, F., ISOYAMA, K., HAYASHI, Y., KUDO, K., OKAMURA, J. & MIZUTANI, S. 2004. Identification and characterization of polymorphic variations of the ataxia telangiectasia mutated (ATM) gene in childhood Hodgkin disease. *Blood*, 103, 283-90.
- TAKAHASHI, Y., ODA, Y., KAWAGUCHI, K., TAMIYA, S., YAMAMOTO, H., SUITA, S. & TSUNEYOSHI, M. 2004. Altered expression and molecular abnormalities of cell-cycle-regulatory proteins in rhabdomyosarcoma. *Mod Pathol*, 17, 660-9.
- TAKATA, M., SASAKI, M. S., SONODA, E., MORRISON, C., HASHIMOTO, M., UTSUMI, H., YAMAGUCHI-IWAI, Y., SHINOHARA, A. & TAKEDA, S. 1998. Homologous recombination and non-homologous end-joining pathways of DNA double-strand break repair have overlapping roles in the maintenance of chromosomal integrity in vertebrate cells. *Embo j*, 17, 5497-508.
- TAKIGAMI, I., OHNO, T., KITADE, Y., HARA, A., NAGANO, A., KAWAI, G., SAITOU, M., MATSUHASHI, A., YAMADA, K. & SHIMIZU, K. 2011. Synthetic siRNA targeting the breakpoint of EWS/Fli-1 inhibits growth of Ewing sarcoma xenografts in a mouse model. *Int J Cancer*, 128, 216-26.
- TAYLOR, B. S., BARRETINA, J., MAKI, R. G., ANTONESCU, C. R., SINGER, S. & LADANYI, M. 2011. Advances in sarcoma genomics and new therapeutic targets. *Nat Rev Cancer*, 11, 541-57.

- THOMAS, L. B., POPPER, H., BERK, P. D., SELIKOFF, I. & FALK, H. 1975. Vinyl-chloride-induced liver disease. From idiopathic portal hypertension (Banti's syndrome) to Angiosarcomas. *N Engl J Med*, 292, 17-22.
- THOMPSON, L. H. & SCHILD, D. 2001. Homologous recombinational repair of DNA ensures mammalian chromosome stability. *Mutat Res*, 477, 131-53.
- THWAY, K. 2009. Pathology of soft tissue sarcomas. *Clin Oncol (R Coll Radiol)*, 21, 695-705.
- TOH, V. V., HASSAN, S. & RAURELL, A. 2017. Sarcomas: Bone and soft tissue tumours. *InnovAiT*, 10, 514-520.
- TORO, J. R., TRAVIS, L. B., WU, H. J., ZHU, K., FLETCHER, C. D. & DEVESA, S. S. 2006. Incidence patterns of soft tissue sarcomas, regardless of primary site, in the surveillance, epidemiology and end results program, 1978-2001: An analysis of 26,758 cases. *Int J Cancer*, 119, 2922-30.
- TORRES, K. E., RAVI, V., KIN, K., YI, M., GUADAGNOLO, B. A., MAY, C. D., ARUN, B. K., HUNT, K. K., LAM, R., LAHAT, G., HOFFMAN, A., CORMIER, J. N., FEIG, B. W., LAZAR, A. J., LEV, D. & POLLOCK, R. E. 2013. Long-term outcomes in patients with radiation-associated angiosarcomas of the breast following surgery and radiotherapy for breast cancer. *Ann Surg Oncol*, 20, 1267-74.
- TROJANI, M., CONTESSO, G., COINDRE, J. M., ROUESSE, J., BUI, N. B., DE MASCAREL, A., GOUSSOT, J. F., DAVID, M., BONICHON, F. & LAGARDE, C. 1984. Soft-tissue sarcomas of adults; study of pathological prognostic variables and definition of a histopathological grading system. *Int J Cancer*, 33, 37-42.

- TRUJILLO, K. M., YUAN, S. S., LEE, E. Y. & SUNG, P. 1998. Nuclease activities in a complex of human recombination and DNA repair factors Rad50, Mre11, and p95. *J Biol Chem*, 273, 21447-50.
- UL-HASSAN, A., SISLEY, K., HUGHES, D., HAMMOND, D. W., ROBINSON, M. H. & REED, M. W. 2009. Common genetic changes in leiomyosarcoma and gastrointestinal stromal tumour: implication for ataxia telangiectasia mutated involvement. *Int J Exp Pathol*, 90, 549-57.
- UZIEL, T., LERENTHAL, Y., MOYAL, L., ANDEGEKO, Y., MITTELMAN, L. & SHILOH, Y. 2003. Requirement of the MRN complex for ATM activation by DNA damage. *Embo j*, 22, 5612-21.
- VIRTANEN, A., PUKKALA, E. & AUVINEN, A. 2006. Incidence of bone and soft tissue sarcoma after radiotherapy: a cohort study of 295,712 Finnish cancer patients. *Int J Cancer*, 118, 1017-21.
- VO, Q. N., KIM, W. J., CVITANOVIC, L., BOUDREAU, D. A., GINZINGER, D. G. & BROWN, K. D. 2004. The ATM gene is a target for epigenetic silencing in locally advanced breast cancer. *Oncogene*, 23, 9432-7.
- VOGELSTEIN, B. & KINZLER, K. W. 2004. Cancer genes and the pathways they control. *Nat Med*, 10, 789-99.
- WANG, H., SHEN, P. & ZHU, W.-G. 2011. Damage and Replication Stress Responses. *DNA Replication-Current Advances*. InTech.
- WANG, H., WANG, M., WANG, H., BOCKER, W. & ILIAKIS, G. 2005. Complex H2AX phosphorylation patterns by multiple kinases including ATM and DNA-PK in human cells exposed to ionizing radiation and treated with kinase inhibitors. *J Cell Physiol*, 202, 492-502.

- WANG, H. & XU, X. 2017. Microhomology-mediated end joining: new players join the team. *Cell Biosci*, 7, 6.
- WARD, S. M. & SANDERS, K. M. 2001. Physiology and pathophysiology of the interstitial cell of Cajal: from bench to bedside. I. Functional development and plasticity of interstitial cells of Cajal networks. *Am J Physiol Gastrointest Liver Physiol*, 281, G602-11.
- WEBER, A. M., DROBNITZKY, N., DEVERY, A. M., BOKOBZA, S. M., ADAMS, R. A., MAUGHAN, T. S. & RYAN, A. J. 2016. Phenotypic consequences of somatic mutations in the ataxia-telangiectasia mutated gene in non-small cell lung cancer. *Oncotarget*, 7, 60807-60822.
- WEBER, A. M. & RYAN, A. J. 2015. ATM and ATR as therapeutic targets in cancer. *Pharmacol Ther*, 149, 124-38.
- WEISS, S. W. 2002. Smooth muscle tumors of soft tissue. *Adv Anat Pathol*, 9, 351-9.
- WEISS, S. W. & GOLDBLUM, J. 2001. Enzinger and Weiss's soft tissue tumors. Mosby, St. Louis, MO, 1622.
- WHITE, J. S., CHOI, S. & BAKKENIST, C. J. 2010. Transient ATM kinase inhibition disrupts DNA damage-induced sister chromatid exchange. *Sci Signal*, 3, ra44.
- WORCH, J., MATTHAY, K. K., NEUHAUS, J., GOLDSBY, R. & DUBOIS, S. G. 2010. Ethnic and racial differences in patients with Ewing sarcoma. *Cancer*, 116, 983-8.
- WUNDER, J. S., NIELSEN, T. O., MAKI, R. G., O'SULLIVAN, B. & ALMAN, B. A. 2007. Opportunities for improving the therapeutic ratio for patients with sarcoma. *Lancet Oncol*, 8, 513-24.

- XIAO, X., GARBUTT, C. C., HORNICEK, F., GUO, Z. & DUAN, Z. 2018. Advances in chromosomal translocations and fusion genes in sarcomas and potential therapeutic applications. *Cancer Treat Rev*, 63, 61-70.
- XU, B., O'DONNELL, A. H., KIM, S. T. & KASTAN, M. B. 2002. Phosphorylation of serine 1387 in Brca1 is specifically required for the Atm-mediated S-phase checkpoint after ionizing irradiation. *Cancer Res*, 62, 4588-91.
- YANG, G., YU, D., LI, W., ZHAO, Y., WEN, X., LIANG, X., ZHANG, X., ZHOU, L., HU, J., NIU, C., TIAN, H., HAN, F., CHEN, X., DONG, L., CAI, L. & CUI, J. 2016. Distinct biological effects of low-dose radiation on normal and cancerous human lung cells are mediated by ATM signaling. *Oncotarget*, 7, 71856-71872.
- YOU, Z., BAILIS, J. M., JOHNSON, S. A., DILWORTH, S. M. & HUNTER, T. 2007. Rapid activation of ATM on DNA flanking double-strand breaks. *Nat Cell Biol*, 9, 1311-8.
- ZANNINI, L., DELIA, D. & BUSCEMI, G. 2014. CHK2 kinase in the DNA damage response and beyond. *J Mol Cell Biol*, 6, 442-57.
- ZHA, S., JIANG, W., FUJIWARA, Y., PATEL, H., GOFF, P. H., BRUSH, J. W., DUBOIS, R. L. & ALT, F. W. 2011. Ataxia telangiectasia-mutated protein and DNA-dependent protein kinase have complementary V(D)J recombination functions. *Proc Natl Acad Sci U S A*, 108, 2028-33.
- ZHANG, J., WALSH, M. F., WU, G., EDMONSON, M. N., GRUBER, T. A., EASTON, J., HEDGES, D., MA, X., ZHOU, X., YERGEAU, D. A., WILKINSON, M. R., VADODARIA, B., CHEN, X., MCGEE, R. B., HINES-DOWELL, S., NUCCIO, R., QUINN, E., SHURTLEFF, S. A., RUSCH, M., PATEL, A., BECKSFORT, J. B., WANG, S., WEAVER, M. S., DING, L., MARDIS, E. R., WILSON, R. K.,

- GAJJAR, A., ELLISON, D. W., PAPPO, A. S., PUI, C. H., NICHOLS, K. E. & DOWNING, J. R. 2015. Germline Mutations in Predisposition Genes in Pediatric Cancer. *N Engl J Med*, 373, 2336-2346.
- ZHANG, P., BHAKTA, K. S., PURI, P. L., NEWBURY, R. O., FERAMISCO, J. R. & WANG, J. Y. 2003. Association of ataxia telangiectasia mutated (ATM) gene mutation/deletion with rhabdomyosarcoma. *Cancer Biol Ther*, 2, 87-91.
- ZIEGLER, J., NEWTON, R., BOURBOULIA, D., CASABONNE, D., BERAL, V., MBIDDE, E., CARPENTER, L., REEVES, G., PARKIN, D. M., WABINGA, H., MBULAITEYE, S., JAFFE, H., WEISS, R. & BOSHOFF, C. 2003. Risk factors for Kaposi's sarcoma: a case-control study of HIV-seronegative people in Uganda. *Int J Cancer*, 103, 233-40.

APPENDICES

Appendix 1

Table A: Probe Position and Size for SALSA MLPA Probe Set (P041-B1 ATM)

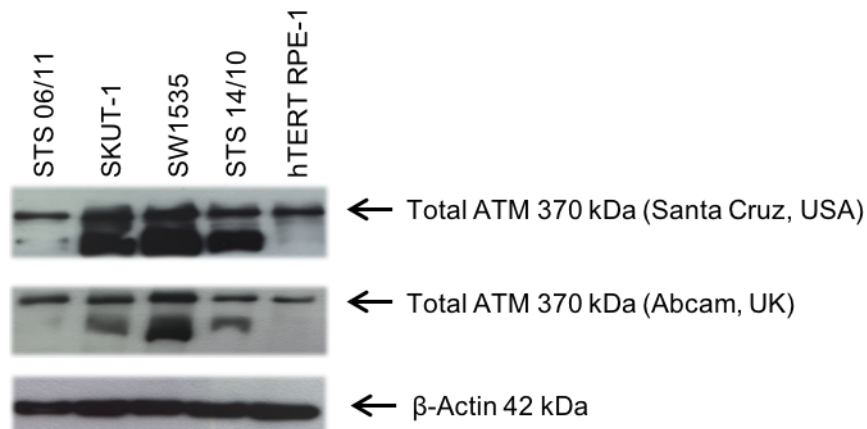
Length of the Nucleotide (nt)	Probe Position
130	3q21
136	Exon 10
142	Exon 17
148	Exon 46
154	2q12
160	7q21
167	Exon 26
173	Intron 1
178	Exon 31
184	Exon 49
192	Exon 33
196	Exon 2
205	Exon 16
209	20q11
217	Exon 53
223	Exon 27
229	15q25
234	Exon 4
242	Exon 14
249	Exon 62
255	Exon 34
261	Exon 56
268	5p15
274	Exon 40
280	Exon 5
287	Exon 57
292	Exon 37
301	16q13
310	Exon 29
319	Exon 6
328	Exon 22
337	Exon 38
345	Exon 59
355	8q22
362	Exon 1
373	Exon 23
382	Exon 8
391	Exon 61
409	17q21
418	Exon 1
427	Exon 42
436	Exon 19
445	13q14
463	Exon 44
485	18q21

Table B: Probe Position and Size for SALSA MLPA Probe Set (P042-B1 ATM)

Length of the Nucleotide (nt)	Probe Position
131	3q21
136	7p14
142	Exon 30
150	Exon 3
156	Exon 21
161	Exon 32
170	Exon 28
178	Exon 43
184	9p24
191	Exon 24
198	Exon 48
203	Exon 35
209	Exon 25
215	Exon 11
220	Exon 47
232	Exon 60
238	Exon 55
250	Exon 7
256	4q25
262	Exon 15
273	Exon 61
280	Exon 51
286	Exon 63
292	Exon 18
301	6q22
311	Exon 45
319	3q13
328	Exon 36
341	Exon 41
346	Exon 52
358	Exon 50
365	5q33
373	Exon 13
382	Exon 39
394	Exon 54
401	8q12
412	Exon 12
419	Exon 62
427	Exon 58
436	1q23
448	Exon 20
454	13q13
463	Exon 9
474	Exon 62
485	18q21

Appendix 2

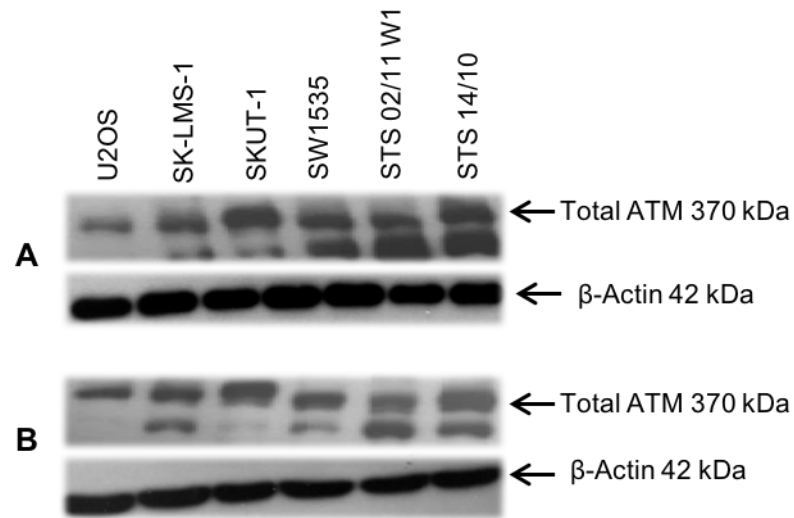
A.



Western Blot Analysis of the Total ATM using Two Antibodies Provided from (Santa Cruz, USA) and (Abcam, UK).

Western blotting of ATM protein in different sarcoma cell lines. 20 μ g of the whole cells lysate were separated on 4-7% gradient SDS-PAGE gels and immunoblotted with two monoclonal antibodies raised against ATM (Santa Cruz, USA) (top panel) and (Abcam, UK) (middle panel). The expression of the ATM protein was detected at 370 kDa in all sarcoma cells by both antibodies however, bands obtained by using (Abcam, UK) (middle panel) were clearer. β -Actin was used as a loading control and was expressed at 42 kDa in all samples.

B.



Western Blotting Analysis of the ATM Protein Extracted from Established and Primary Sarcoma Cell Lines Using (PI) and (PPI).

Western blot displays the expression of ATM at 370 kDa using mouse monoclonal primary antibody [ATM (2C1 (1A1))] (Abcam, UK). The whole cells lysates were obtained by using lysis buffer with (PI) (A) and with (PPI) (B). The extracts from the established and primary cell lines showed a 350 kDa band corresponding to the ATM protein of normal size in both lysate extracted with (PI) and (PPI). The expression of the extra band under the ATM was detected in both cellular extracts (A) and (B). β -Actin was used as a loading control and was expressed at 42 kDa in all samples.

Appendix 3

MLPA PDF Reports Generated by Coffalyser.Net Software for Normal and Sarcoma Cell Lines Included in this Study

Reference DNA Sample



Sample report: 15

Sample type: Reference | Project: ATM analysis | Experiment: ATM1
 Machine: ABI-3730 | Report date: 15/08/2018 | Run date: 09/11/2015 | Software Version: v.140721.1958 | Normal range: 0.7 - 1.3

[Dye: 6-FAM | Performed by: Admin

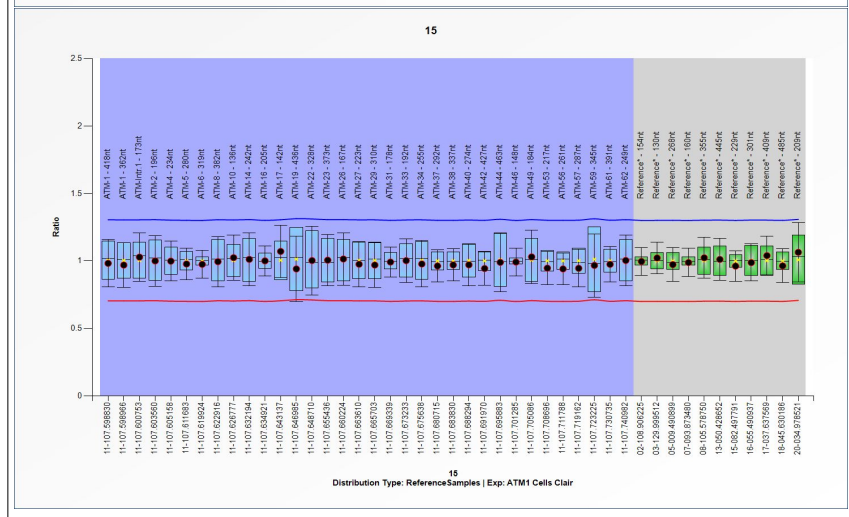
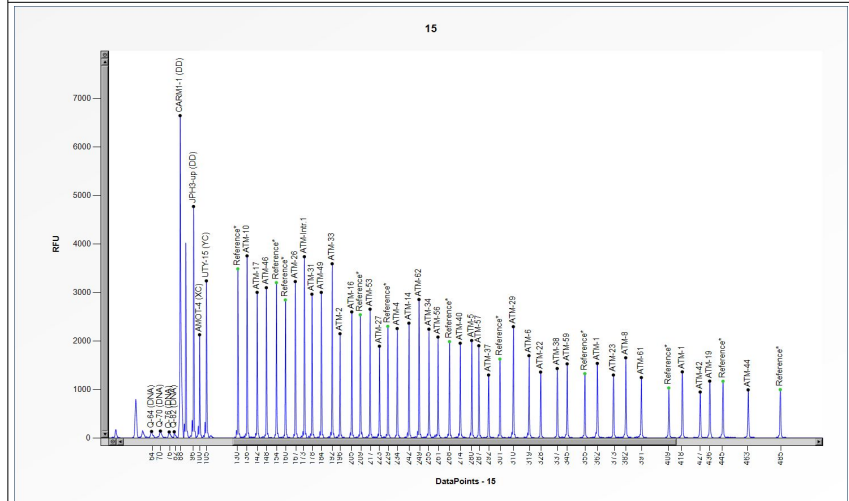
Authorization	
Date	

MLPA probe mix: P041-ATM-1
 Lot number: B1-0314
 Sheet date: 09/11/2015 17:01:48
 Control fragments: CF-003-[brown] QDX2 (A2-0)
 Analysis method: Block SSC: On
 Used metric: Peak height

Nr of test probes: 45/45
 Nr of ref probes: 11/11
 DNA concentration: NA
 DNA denaturation: NA
 Expected gender: Female
 Residual primer %: OK 13%

FRSS: Warning 70%
 FRMS: OK 95%
 PSPL: OK 0%
 RSQ: OK
 RPQ: OK
 CAS: OK 100%

Reference Samples: 7 | 6 | 3 | 1 | 5 | 1 | 4 | 1 | 2



D [nt]	Gene-Exon	Chr.band	hg18 loc.	Height	Area	Ratio ^h	Stdev	[REF]	[Sam]	Width	d[nt]
418	ATM-1	11q22.3	11-107.598830	1363	10643	0.98	0.09	=	=	46	-0.1
362	ATM-1	11q22.3	11-107.598966	1538	11502	0.97	0.08	=	=	45	0.0
173	ATM-Intr.1	11q22.3	11-107.600753	3740	21170	1.03	0.09	=	=	47	-0.1
196	ATM-2	11q22.3	11-107.603560	2150	12377	1	0.09	=	=	43	0.0
234	ATM-4	11q22.3	11-107.605158	2257	13205	1	0.07	=	=	41	0.0
280	ATM-5	11q22.3	11-107.611683	2010	12680	0.98	0.06	=	=	42	0.0
319	ATM-6	11q22.3	11-107.619924	1697	11586	0.98	0.05	=	=	42	0.0
382	ATM-8	11q22.3	11-107.622916	1654	12268	1	0.09	=	=	48	0.0
136	ATM-10	11q22.3	11-107.626777	3757	20988	1.02	0.08	=	=	33	0.0
242	ATM-14	11q22.3	11-107.632194	2368	14096	1.01	0.1	=	=	39	0.0
205	ATM-16	11q22.3	11-107.634921	2601	14733	1	0.06	=	=	37	0.0
142	ATM-17	11q22.3	11-107.643137	3004	17124	1.07	0.1	=	=	35	0.0
436	ATM-19	11q22.3	11-107.646985	1172	9818	0.94	0.12	=	=	49	-0.1
328	ATM-22	11q22.3	11-107.648710	1359	8919	1	0.13	=	=	39	0.0
373	ATM-23	11q22.3	11-107.655436	1298	9303	1.01	0.09	=	=	44	0.0
167	ATM-26	11q22.3	11-107.660224	3227	17791	1.01	0.1	=	=	41	0.0
223	ATM-27	11q22.3	11-107.663610	1893	11129	0.98	0.08	=	=	32	0.0
310	ATM-29	11q22.3	11-107.665703	2296	14900	0.97	0.08	=	=	35	0.0
178	ATM-31	11q22.3	11-107.669339	2966	16788	0.99	0.05	=	=	39	0.0
192	ATM-33	11q22.3	11-107.673233	3594	20181	1	0.08	=	=	34	0.0
255	ATM-34	11q22.3	11-107.675638	2244	13520	0.98	0.09	=	=	39	0.0
292	ATM-37	11q22.3	11-107.680715	1298	8165	0.96	0.06	=	=	34	0.0
337	ATM-38	11q22.3	11-107.683830	1432	9529	0.97	0.06	=	=	40	0.0
274	ATM-40	11q22.3	11-107.688294	1954	12501	0.97	0.08	=	=	38	0.0
427	ATM-42	11q22.3	11-107.691970	947	7590	0.94	0.06	=	=	36	-0.1
463	ATM-44	11q22.3	11-107.695883	992	8376	0.99	0.11	=	=	49	0.0
148	ATM-46	11q22.3	11-107.701285	3100	17331	0.99	0.05	=	=	39	0.0
184	ATM-49	11q22.3	11-107.705086	3003	16854	1.03	0.1	=	=	37	0.0
217	ATM-53	11q22.3	11-107.708696	2657	15430	0.95	0.06	=	=	39	-0.1
261	ATM-56	11q22.3	11-107.711788	2081	12406	0.94	0.06	=	=	39	0.0
287	ATM-57	11q22.3	11-107.719162	1903	11844	0.95	0.07	=	=	40	0.0
345	ATM-59	11q22.3	11-107.723225	1528	10767	0.97	0.12	=	=	39	-0.1
391	ATM-61	11q22.3	11-107.730735	1245	9391	0.98	0.07	=	=	37	-0.1
249	ATM-62	11q22.3	11-107.740982	2857	17144	1	0.09	=	=	46	0.0
154	Reference*	02q12.3	02-108.906225	3204	18036	1	0.05	=	=	39	0.0
130	Reference*	03q21.3	03-129.999512	3489	19857	1.02	0.06	=	=	42	0.0
268	Reference*	05p15.31	05-009.490899	1988	12244	0.97	0.06	=	=	34	0.0
160	Reference*	07q21.3	07-093.873480	2847	16120	0.99	0.05	=	=	36	0.0
355	Reference*	08q22.3	08-105.578750	1327	9301	1.02	0.08	=	=	40	-0.1
445	Reference*	13q14.3	13-050.428652	1169	9794	1.01	0.08	=	=	52	-0.1
229	Reference*	15q25.2	15-082.497791	2303	13325	0.96	0.06	=	=	35	0.0
301	Reference*	16q13	16-055.490937	1628	10475	0.99	0.07	=	=	38	0.0
409	Reference*	17q21.2	17-037.637569	1031	7857	1.04	0.07	=	=	44	0.0
485	Reference*	18q21.1	18-045.630186	998	8642	0.96	0.06	=	=	46	0.0
209	Reference*	20q11.23	20-034.978521	2542	14695	1.06	0.11	=	=	41	0.0
Median value all probe values:				2010	12406	0.99	0.08			39	-0.01

215



Sample report: 15

Sample type: Reference | Project: ATM analysis | Experiment: ATM2 | Dye: 6-FAM | Performed by: Admin
Machine: ABI-3730 | Report date: 15/08/2018 | Run date: 07/10/2015 | Software Version: v.140721.1958 | Normal range: 0.7 - 1.3

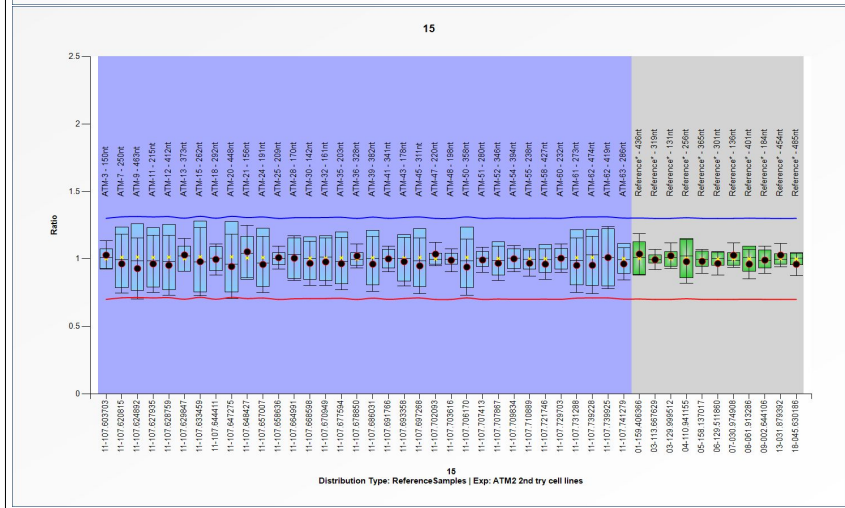
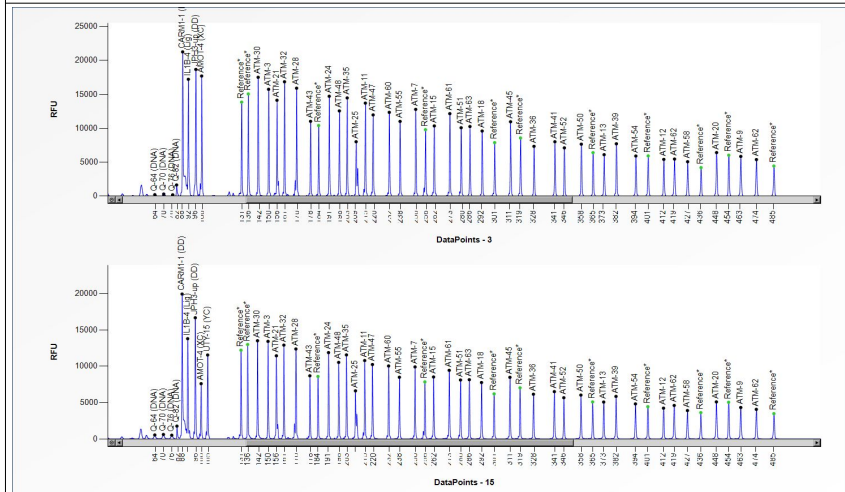
Table with 2 columns: Authorization, Date

MLPA probe mix: P042-ATM-2
Lot number: B1-0314
Sheet date: 28/08/2015 11:01:16
Control fragments: CF-003-[brown] QDX2 (A2-0)
Analysis method: Block SSC: On
Used metric: Peak height

Nr of test probes: 45/45
Nr of ref probes: 11/11
DNA concentration: OK
DNA denaturation: OK
Expected gender: Male
Residual primer %: OK 11%

FRSS: Warning 70%
FRMS: OK? 75%
PSLP: OK -2%
RSQ: OK
RPQ: OK
CAS: OK 90%

Reference Samples: 7 | 6 | 1 | 3 | 1 | 5 | 1 | 1 | 4 | 1 | 2



Main data table with columns: D [nt], Gene-Exon, Chr.band, hg18 loc., Height, Area, Ratio, Stdev, [REF], [Sam], Width, d[nt]. Includes rows for ATM-3 to ATM-63 and Reference* samples.

Median value all probe values:

7853 86203 0.98 0.06 71 -0.01

Normal range: 0.7 - 1.3 Essential information on the use of this product is present in the product description which is available on http://www.mlpa.com. For questions, mailto:info@mlpa.com.
MRC-Holland does not and cannot warrant the performance or results you may obtain by using the software. In no event will MRC-Holland be liable for any damages, claims or costs whatsoever or any consequential, indirect, incidental, damages, or any lost profits or lost savings, even if an MRC-Holland representative has been advised of the possibility of such loss, damages, claims or costs.

U2OS



Sample report: 1

Sample type: Sample | Project: ATM analysis | Experiment: ATM1 | Machine: ABI-3730 | Report date: 15/08/2018 | Run date: 09/11/2015 | Software Version: v.140721.1958 | Normal range: 0.7 - 1.3

| Dye: 6-FAM | Performed by: Admin

Authorization
Date

MLPA probe mix: P041-ATM-1
Lot number: B1-0314
Sheet date: 09/11/2015 17:01:48
Control fragments: CF-003-[brown] QDX2 (A2-0)
Analysis method: Block SSC: On
Used metric: Peak height

Nr of test probes: 45/45
Nr of ref probes: 11/11
DNA concentration: NA
DNA denaturation: NA
Expected gender: Female
Residual primer %: OK 11%

FRSS: Warning 70%
FRMS: OK 95%
PSLP: Bad 75%
RSQ: OK
RPQ: Bad
CAS: Warning 65%

Reference Samples: 7 | 6 | 1 | 3 | 1 | 5 | 1 | 4 | 1 | 2

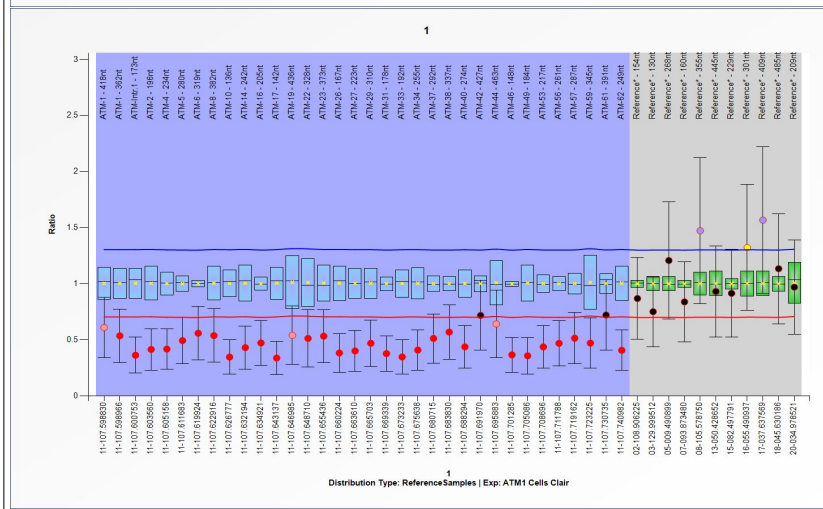
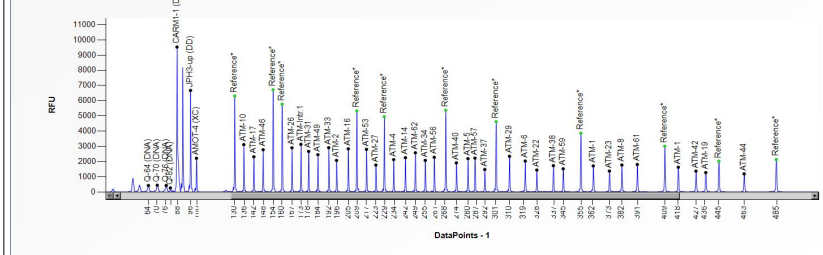
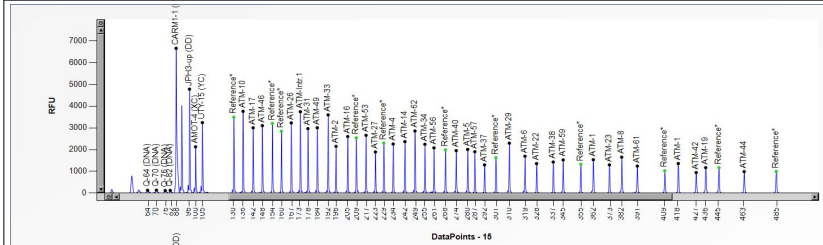


Table with columns: D [nt], Gene-Exon, Chr.band, hg18 loc., Height, Area, Ratio, Stdev, [REF], [Sam], Width, d[nt]. Contains data for various ATM probes and reference samples.

Median value all probe values:

2252 14189 0.51* 0.11* 44 0.02

Normal range: 0.7 - 1.3 Essential information on the use of this product is present in the product description which is available on http://www.mlpa.com. For questions, mailto:info@mlpa.com.



Sample report: 1

Sample type: Sample | Project: ATM analysis | Experiment: ATM2 | Dye: 6-FAM | Performed by: Admin
Machine: ABI-3730 | Report date: 15/08/2018 | Run date: 07/10/2015 | Software Version: v.140721.1958 | Normal range: 0.7 - 1.3

Authorization
Date

MLPA probe mix: P042-ATM-2
Lot number: B1-0314
Sheet date: 28/08/2015 11:01:16
Control fragments: CF-003-[brown] QDX2 (A2-0)
Analysis method: Block SSC: On
Used metric: Peak height
Nr of test probes: 45/45
Nr of ref probes: 11/11
DNA concentration: OK
DNA denaturation: OK
Expected gender: Female
Residual primer %: OK 9%
FRSS: Warning 70%
FRMS: OK? 80%
PSLP: Bad 81%
RSQ: OK
RPQ: Bad
CAS: Warning 65%

Reference Samples: 7 | 6 | 1 | 3 | 15 | 14 | 1 | 2

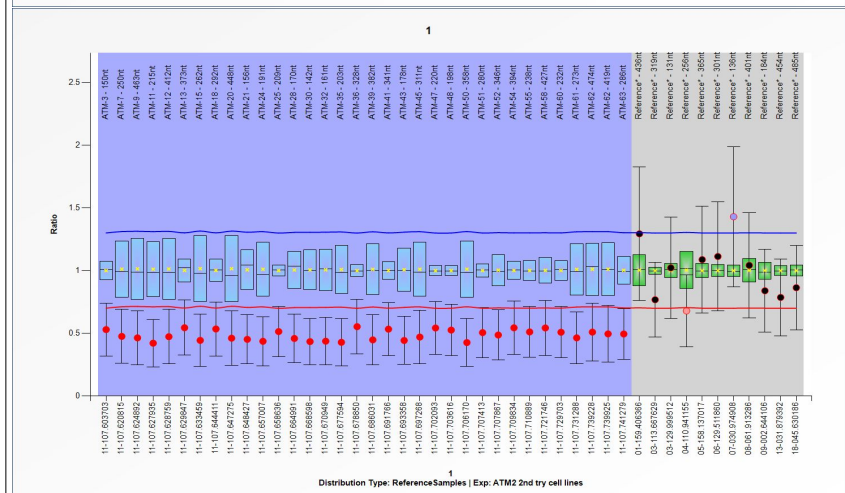
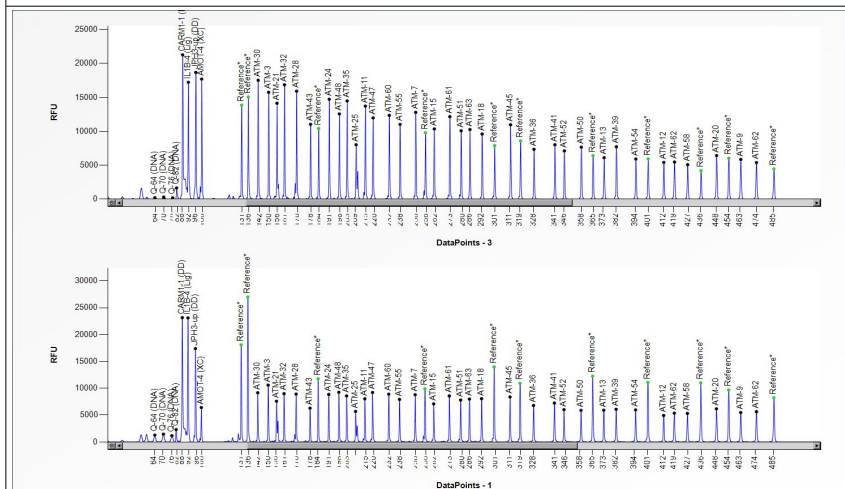


Table with columns: D [nt], Gene-Exon, Chr.band, hg18 loc., Height, Area, Ratio, Stdev, [REF], [Sam], Width, d[nt]. Contains data for probes ATM-3 through ATM-63 and Reference* probes.

Median value all probe values: 8239 90809 0.51* 0.11* 64 0.02

SK-LMS-1



Sample report: 2

Sample type: Sample | Project: ATM analysis | Experiment: ATM1 | Dye: 6-FAM | Performed by: Admin
Machine: ABI-3730 | Report date: 15/08/2018 | Run date: 09/11/2015 | Software Version: v.140721.1958 | Normal range: 0.7 - 1.3

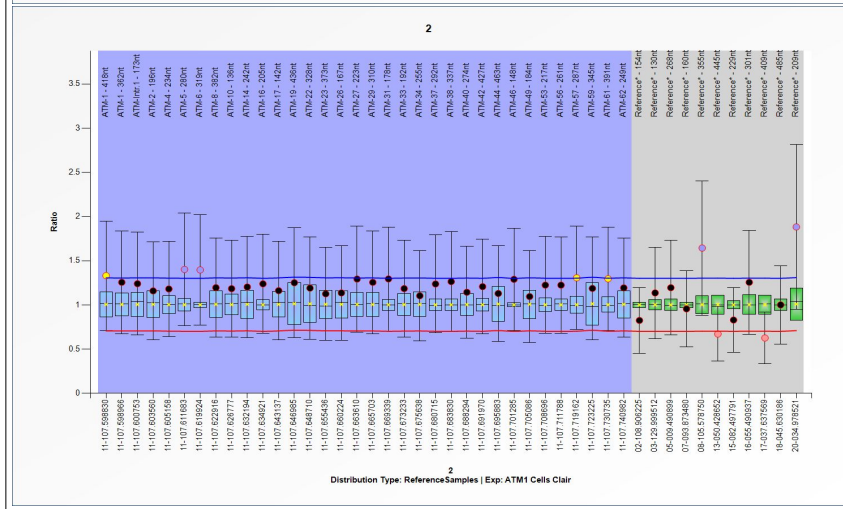
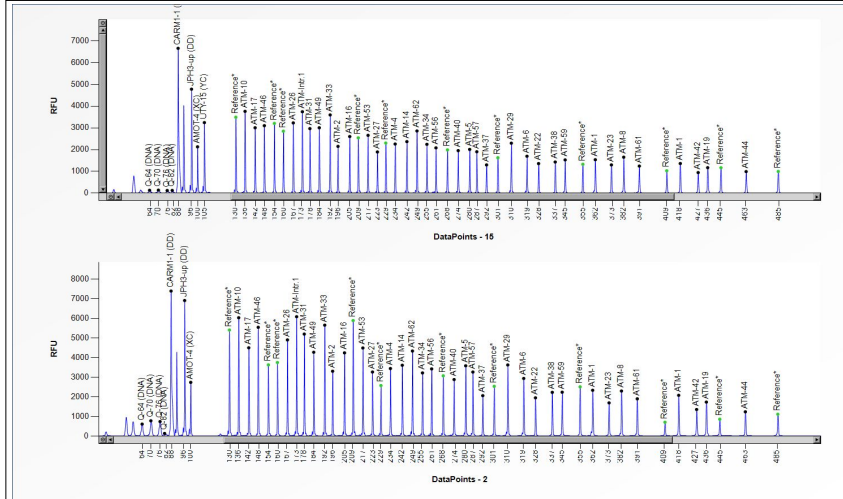
Authorization	
Date	

MLPA probe mix: P041-ATM-1
Lot number: B1-0314
Sheet date: 09/11/2015 17:01:48
Control fragments: CF-003-[brown] QDX2 (A2-0
Analysis method: Block SSC: On
Used metric: Peak height

Nr of test probes: 45/45
Nr of ref probes: 11/11
DNA concentration: NA
DNA denaturation: NA
Expected gender: Female
Residual primer %: OK 12%

FRSS: Warning 70%
FRMS: Warning 70%
PSLP: OK -8%
RSQ: Warning
RPQ: Bad
CAS: Bad 35%

Reference Samples: 7 | 6 | 1 | 3 | 15 | 14 | 1 | 2



D [nt]	Gene-Exon	Chr.band	hg18 loc.	Height	Area	Ratio	Stdev	[REF]	[Sam]	Width	d[nt]
418	ATM-1	11q22.3	11-107.598830	2069	15432	1.33	0.31	?	?	38	0.0
362	ATM-1	11q22.3	11-107.598966	2327	17377	1.26	0.29	=	=	41	0.0
173	ATM-Intr.1	11q22.3	11-107.600753	6077	34247	1.24	0.29	=	=	34	-0.1
196	ATM-2	11q22.3	11-107.603560	3297	18337	1.16	0.28	=	=	34	0.0
234	ATM-4	11q22.3	11-107.605158	3435	20132	1.18	0.27	=	=	38	0.0
280	ATM-5	11q22.3	11-107.611683	3574	22606	1.4	0.32	>*	?	50	0.0
319	ATM-6	11q22.3	11-107.619924	2930	19738	1.4	0.31	>*	?	46	0.0
382	ATM-8	11q22.3	11-107.622916	2289	16741	1.19	0.28	=	=	52	0.0
136	ATM-10	11q22.3	11-107.626777	6025	34625	1.18	0.27	=	=	50	0.0
242	ATM-14	11q22.3	11-107.632194	3602	21579	1.2	0.29	=	=	52	0.0
205	ATM-16	11q22.3	11-107.634921	4234	24253	1.24	0.28	=	=	42	0.0
142	ATM-17	11q22.3	11-107.643137	4493	26423	1.16	0.28	=	=	47	0.1
436	ATM-19	11q22.3	11-107.646985	1724	14383	1.25	0.31	=	=	40	0.0
328	ATM-22	11q22.3	11-107.648710	1942	12234	1.19	0.29	=	=	35	0.0
373	ATM-23	11q22.3	11-107.655436	1684	12188	1.13	0.26	=	=	42	0.0
167	ATM-26	11q22.3	11-107.660224	4893	27419	1.14	0.27	=	=	42	0.0
223	ATM-27	11q22.3	11-107.663610	3258	18597	1.29	0.3	=	=	45	0.0
310	ATM-29	11q22.3	11-107.665703	3618	23446	1.26	0.29	=	=	46	0.0
178	ATM-31	11q22.3	11-107.669339	5190	30098	1.29	0.29	=	=	50	0.0
192	ATM-33	11q22.3	11-107.673233	5645	31695	1.18	0.27	=	=	36	0.0
255	ATM-34	11q22.3	11-107.675638	3211	19262	1.1	0.26	=	=	51	0.0
292	ATM-37	11q22.3	11-107.680715	2053	12824	1.24	0.28	=	=	44	0.0
337	ATM-38	11q22.3	11-107.683830	2221	14878	1.26	0.28	=	=	41	0.0
274	ATM-40	11q22.3	11-107.688294	2872	17988	1.14	0.26	=	=	50	0.0
427	ATM-42	11q22.3	11-107.691970	1346	11174	1.21	0.27	=	=	61	0.0
463	ATM-44	11q22.3	11-107.695883	1229	9983	1.13	0.27	=	=	38	0.0
148	ATM-46	11q22.3	11-107.701285	5536	30821	1.29	0.29	=	=	39	0.0
184	ATM-49	11q22.3	11-107.705086	4265	24468	1.09	0.26	=	=	36	0.0
217	ATM-53	11q22.3	11-107.708696	4483	26498	1.22	0.27	=	=	35	0.0
261	ATM-56	11q22.3	11-107.711788	3416	20078	1.22	0.27	=	=	38	0.0
287	ATM-57	11q22.3	11-107.719162	3256	20080	1.31	0.29	?	>*	38	0.0
345	ATM-59	11q22.3	11-107.723225	2227	14824	1.19	0.29	=	=	35	0.0
391	ATM-61	11q22.3	11-107.730735	1891	14011	1.3	0.29	?	?	41	-0.1
249	ATM-62	11q22.3	11-107.740982	4328	25905	1.19	0.28	=	=	44	0.0
154	Reference*	02q12.3	02-108.906225	3621	20843	0.82	0.19	=	=	44	0.0
130	Reference*	03q21.3	03-129.999512	5397	31255	1.14	0.26	=	=	43	0.0
268	Reference*	05p15.31	05-009.490899	3063	18592	1.19	0.27	=	=	53	0.0
160	Reference*	07q21.3	07-093.873480	3741	21072	0.95	0.21	=	=	42	0.0
355	Reference*	08q22.3	08-105.578750	2503	17143	1.64	0.38	>*	?	41	0.0
445	Reference*	13q14.3	13-050.428652	852	7058	0.67	0.15	<*	?	42	0.0
229	Reference*	15q25.2	15-082.497791	2567	15065	0.83	0.18	=	=	40	0.0
301	Reference*	16p13.3	16-055.490937	2529	16062	1.26	0.29	=	=	52	0.0
409	Reference*	17q21.2	17-037.637569	698	5663	0.63	0.15	<*	<*	53	0.0
485	Reference*	18q21.1	18-045.630186	1106	9737	1	0.22	=	=	51	0.0
209	Reference*	20q11.23	20-034.978521	5881	34458	1.88	0.47	>*	?	49	0.0
Median value all probe values:				3256	19262	1.19	0.28*			42	-0.01

Normal range: 0.7 - 1.3 Essential information on the use of this product is present in the product description which is available on <http://www.mlpa.com>. For questions, <mailto:info@mlpa.com>. MRC-Holland does not and cannot warrant the performance or results you may obtain by using the software. In no event will MRC-Holland be liable for any damages, claims or costs whatsoever or any consequential, indirect, incidental, damages, or any lost profits or lost savings, even if an MRC-Holland representative has been advised of the possibility of such loss, damages, claims or costs.



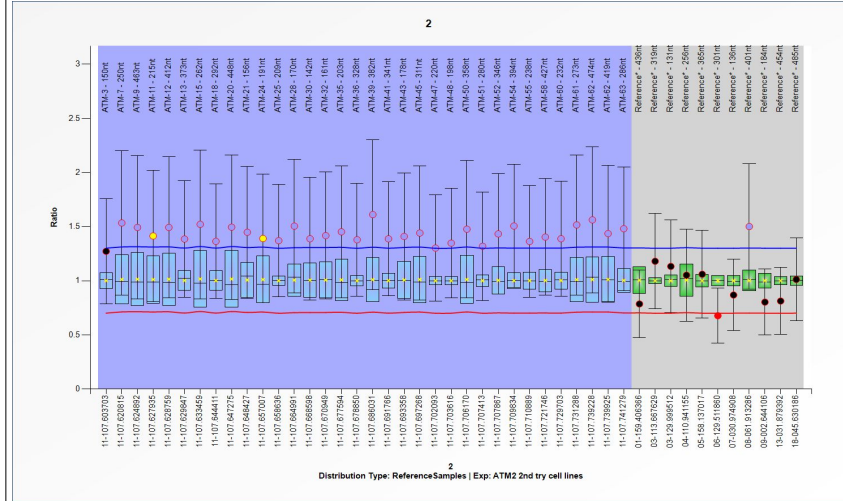
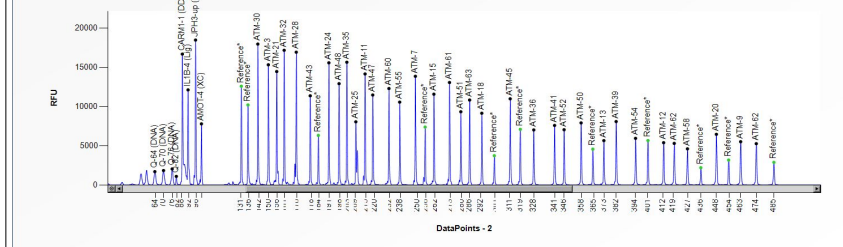
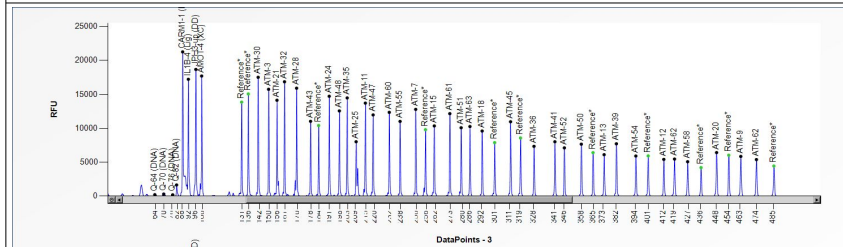
Sample report: 2

Sample type: Sample | Project: ATM analysis | Experiment: ATM2 | Dye: 6-FAM | Performed by: Admin
Machine: ABI-3730 | Report date: 15/08/2018 | Run date: 07/10/2015 | Software Version: v.140721.1958 | Normal range: 0.7 - 1.3

Authorization Date table

MLPA probe mix: P042-ATM-2 Nr of test probes: 45/45 FRSS: Warning 70%
Lot number: B1-0314 Nr of ref probes: 11/11 FRMS: OK? 75%
Sheet date: 28/08/2015 11:01:16 DNA concentration: OK PSLP: OK -3%
Control fragments: CF-003-[brown] QDX2 (A2-0 DNA denaturation: OK RSQ: Warning
Analysis method: Block SSC: On Expected gender: Female RPQ: Bad
Used metric: Peak height Residual primer % OK 10% CAS: Warning 50%

Reference Samples: 7 | 6 | 1 | 3 | 1 | 5 | 1 | 14 | 1 | 12



Main data table with columns: D [nt], Gene-Exon, Chr.band, hg18 loc., Height, Area, Ratio, Stdev, [REF], [Sam], Width, d[nt]. Includes median values at the bottom.

Normal range: 0.7 - 1.3 Essential information on the use of this product is present in the product description which is available on http://www.mlpa.com. For questions, mailto:info@mlpa.com.
MRC-Holland does not and cannot warrant the performance or results you may obtain by using the software. In no event will MRC-Holland be liable for any damages, claims or costs whatsoever or any consequential, indirect, incidental, damages, or any lost profits or lost savings, even if an MRC-Holland representative has been advised of the possibility of such loss, damages, claims or costs.

SKUT-1



Sample report: 4

Sample type: Sample | Project: ATM analysis | Experiment: Machine: ABI-3730 | Report date: 15/08/2018 | Run date: 09/11/2015 | Software Version: v.140721.1958 | Normal range: 0.7 - 1.3

[Dye: 6-FAM | Performed by: Admin

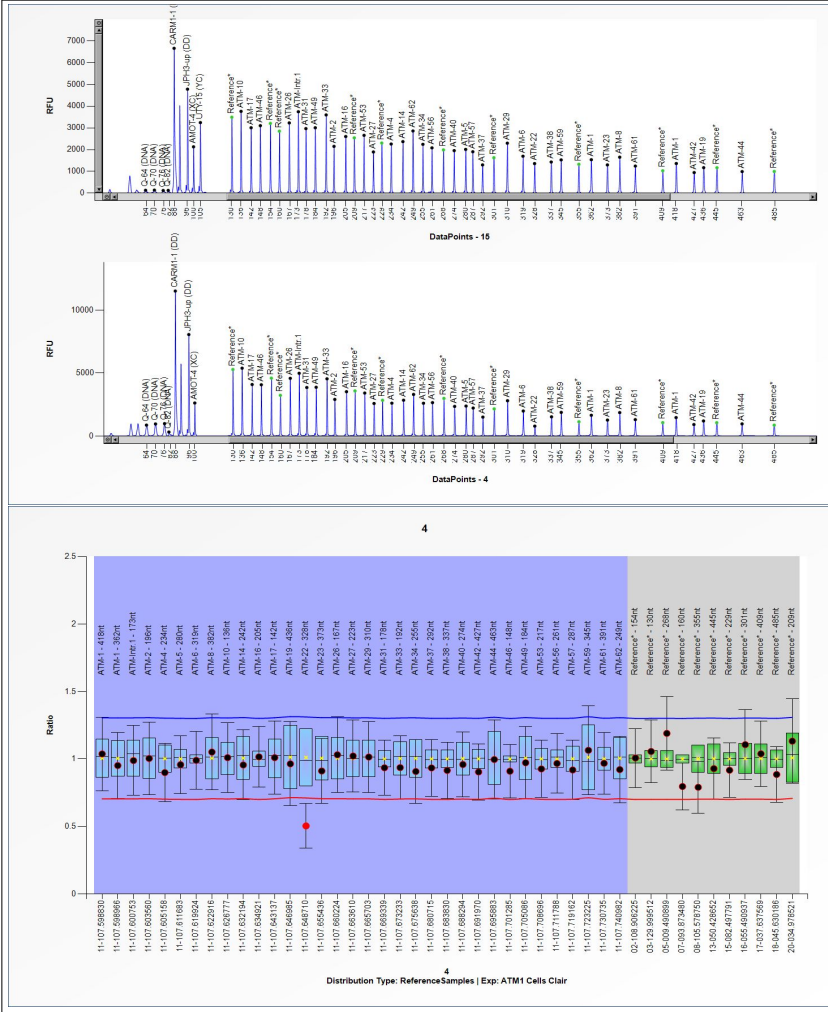
Authorization	
Date	

MLPA probe mix: P041-ATM-1
Lot number: B1-0314
Sheet date: 09/11/2015 17:01:48
Control fragments: CF-003-[brown] QDX2 (A2-0)
Analysis method: Block SSC: On
Used metric: Peak height

Nr of test probes: 45/45
Nr of ref probes: 11/11
DNA concentration: NA
DNA denaturation: NA
Expected gender: Female
Residual primer %: OK 13%

FRSS: Warning 70%
FRMS: Warning 70%
PSLP: Bad -36%
RSQ: OK
RPG: Warning
CAS: Warning 60%

Reference Samples: 7 | 6 | 1 | 3 | 1 | 5 | 1 | 1 | 4 | 1 | 2



D [nt]	Gene-Exon	Chr.band	hg18 loc.	Height	Area	Ratio ⁿ	Stdev	[REF]	[Sam]	Width	d[nt]
418	ATM-1	11q22.3	11-107.598830	1459	11504	1.04	0.14	=	=	46	0.1
362	ATM-1	11q22.3	11-107.598966	1641	12200	0.95	0.12	=	=	41	0.1
173	ATM-Intr.1	11q22.3	11-107.600753	4984	28373	0.99	0.13	=	=	35	0.0
196	ATM-2	11q22.3	11-107.603560	2902	16534	1	0.13	=	=	38	0.0
234	ATM-4	11q22.3	11-107.605158	2606	15407	0.9	0.11	=	=	39	0.0
280	ATM-5	11q22.3	11-107.611683	2375	14880	0.96	0.11	=	=	43	0.1
319	ATM-6	11q22.3	11-107.619924	1982	13101	0.99	0.11	=	=	37	0.1
382	ATM-8	11q22.3	11-107.622916	1856	13387	1.05	0.14	=	=	47	0.0
136	ATM-10	11q22.3	11-107.626777	5390	30640	1.01	0.13	=	=	48	0.0
242	ATM-14	11q22.3	11-107.632194	2840	16871	0.96	0.13	=	=	36	0.0
205	ATM-16	11q22.3	11-107.634921	3517	20137	1.02	0.11	=	=	40	0.0
142	ATM-17	11q22.3	11-107.643137	4089	23106	1.01	0.13	=	=	34	0.0
436	ATM-19	11q22.3	11-107.646985	1190	9949	0.96	0.16	=	=	47	0.1
328	ATM-22	11q22.3	11-107.648710	778	5131	0.5	0.08	<<*	>*	32	0.1
373	ATM-23	11q22.3	11-107.655436	1261	9200	0.91	0.12	=	=	44	0.0
167	ATM-26	11q22.3	11-107.660224	4580	26052	1.03	0.14	=	=	42	0.0
223	ATM-27	11q22.3	11-107.663610	2580	15314	1.02	0.13	=	=	37	0.1
310	ATM-29	11q22.3	11-107.665703	2799	18129	1.01	0.13	=	=	42	0.1
178	ATM-31	11q22.3	11-107.669339	3851	21933	0.94	0.1	=	=	33	0.0
192	ATM-33	11q22.3	11-107.673233	4543	25507	0.94	0.12	=	=	35	0.0
255	ATM-34	11q22.3	11-107.675638	2600	15627	0.91	0.12	=	=	48	0.0
292	ATM-37	11q22.3	11-107.680715	1497	9394	0.93	0.1	=	=	38	0.1
337	ATM-38	11q22.3	11-107.683830	1517	10314	0.92	0.1	=	=	46	0.0
274	ATM-40	11q22.3	11-107.688294	2347	14982	0.96	0.12	=	=	43	0.0
427	ATM-42	11q22.3	11-107.691970	906	7208	0.9	0.1	=	=	35	0.1
463	ATM-44	11q22.3	11-107.695883	957	8064	1	0.15	=	=	48	0.0
148	ATM-46	11q22.3	11-107.701285	4070	23027	0.91	0.1	=	=	42	0.0
184	ATM-49	11q22.3	11-107.705086	3871	22818	0.97	0.13	=	=	55	0.0
217	ATM-53	11q22.3	11-107.708696	3410	19630	0.93	0.11	=	=	41	0.0
261	ATM-56	11q22.3	11-107.711788	2649	15531	0.97	0.11	=	=	38	0.0
287	ATM-57	11q22.3	11-107.719162	2216	13742	0.92	0.11	=	=	38	0.1
345	ATM-59	11q22.3	11-107.723225	1874	12926	1.06	0.16	=	=	55	0.0
391	ATM-61	11q22.3	11-107.730735	1296	9760	0.97	0.11	=	=	38	0.0
249	ATM-62	11q22.3	11-107.740982	3302	19997	0.92	0.12	=	=	44	0.0
154	Reference*	02q12.3	02-108.906225	4597	25699	1.01	0.11	=	=	38	0.0
130	Reference*	03q21.3	03-129.999512	5286	30205	1.06	0.12	=	=	36	0.0
268	Reference*	05p15.31	05-009.490899	2983	18108	1.19	0.14	=	=	38	0.0
160	Reference*	07q21.3	07-093.873480	3229	18490	0.8	0.09	=	=	48	0.0
355	Reference*	08q22.3	08-105.578750	1126	7951	0.79	0.1	=	=	48	0.0
445	Reference*	13q14.3	13-050.428652	1052	8792	0.93	0.11	=	=	53	0.1
229	Reference*	15q25.2	15-082.497791	2836	16651	0.92	0.1	=	=	38	0.0
301	Reference*	16q13	16-055.490937	2149	13954	1.11	0.13	=	=	35	0.1
409	Reference*	17q21.2	17-037.637569	1056	8130	1.04	0.12	=	=	41	0.0
485	Reference*	18q21.1	18-045.630186	855	7493	0.89	0.1	=	=	38	0.0
209	Reference*	20q11.23	20-034.978521	3580	20739	1.13	0.16	=	=	39	0.1
Median value all probe values:				2600	15407	0.96	0.12*	=	=	40	0.02



Sample report: 4

Sample type: Sample | Project: ATM analysis | Experiment: ATM2
Machine: ABI-3730 | Report date: 15/08/2018 | Run date: 07/10/2015 | Software Version: v.140721.1958 | Normal range: 0.7 - 1.3

| Dye: 6-FAM | Performed by: Admin

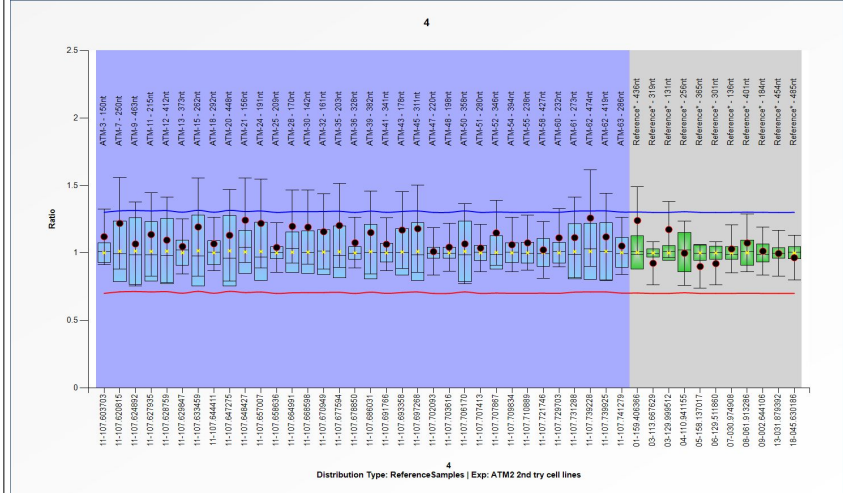
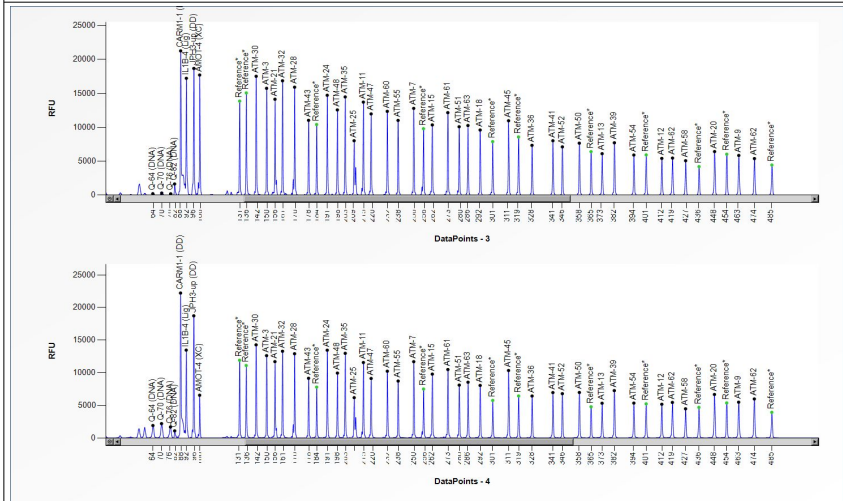
Authorization	
Date	

MLPA probe mix: P042-ATM-2
 Lot number: B1-0314
 Sheet date: 28/08/2015 11:01:16
 Control fragments: CF-003-[brown] QDX2 (A2-0)
 Analysis method: Block SSC: On
 Used metric: Peak height

Nr of test probes: 45/45
 Nr of ref probes: 11/11
 DNA concentration: OK
 DNA denaturation: OK
 Expected gender: Female
 Residual primer %: OK 11%

FRSS: Warning 70%
 FRMS: OK 90%
 PSLP: Warning 17%
 RSQ: OK
 RPQ: OK
 CAS: OK 100%

Reference Samples: 7 | 6 | 1 | 3 | 15 | 14 | 12



D [nt]	Gene-Exon	Chr.band	hg18 loc.	Height	Area	Ratio	Stdev	[REF]	[Sam]	Width	d[nt]
150	ATM-3	11q22.3	11-107.603703	12622	129056	1.12	0.1	=	=	65	0.0
250	ATM-7	11q22.3	11-107.620815	11698	130632	1.22	0.17	=	=	61	0.0
463	ATM-9	11q22.3	11-107.624892	5482	86800	1.07	0.16	=	=	79	0.0
215	ATM-11	11q22.3	11-107.627935	11568	118610	1.14	0.16	=	=	33	0.0
412	ATM-12	11q22.3	11-107.628759	5162	73609	1.1	0.16	=	=	75	0.0
373	ATM-13	11q22.3	11-107.629847	5320	72343	1.05	0.1	=	=	80	0.0
262	ATM-15	11q22.3	11-107.633459	9786	114070	1.19	0.18	=	=	76	0.1
292	ATM-18	11q22.3	11-107.644411	8048	93969	1.07	0.1	=	=	61	0.1
448	ATM-20	11q22.3	11-107.647275	6661	100904	1.13	0.17	=	=	85	0.0
156	ATM-21	11q22.3	11-107.648427	11699	131268	1.24	0.16	=	=	50	0.0
191	ATM-24	11q22.3	11-107.657007	13459	137817	1.22	0.16	=	=	59	0.0
209	ATM-25	11q22.3	11-107.658636	6175	63703	1.04	0.09	=	=	20	1.0
170	ATM-28	11q22.3	11-107.664991	12912	129804	1.2	0.14	=	=	34	0.0
142	ATM-30	11q22.3	11-107.668598	14277	144689	1.19	0.14	=	=	59	0.0
161	ATM-32	11q22.3	11-107.670949	13294	138484	1.16	0.14	=	=	72	0.0
203	ATM-35	11q22.3	11-107.677594	12979	132218	1.2	0.16	=	=	34	-0.1
328	ATM-36	11q22.3	11-107.678850	6427	79178	1.08	0.09	=	=	65	0.0
382	ATM-39	11q22.3	11-107.686031	7258	98482	1.15	0.15	=	=	81	0.0
341	ATM-41	11q22.3	11-107.691766	6953	89207	1.06	0.1	=	=	91	0.0
178	ATM-43	11q22.3	11-107.693358	9151	91029	1.17	0.14	=	=	33	0.0
311	ATM-45	11q22.3	11-107.697268	10341	125702	1.18	0.16	=	=	63	0.1
220	ATM-47	11q22.3	11-107.702093	9120	97451	1.01	0.09	=	=	62	0.0
198	ATM-48	11q22.3	11-107.703616	9944	105463	1.04	0.09	=	=	56	0.0
358	ATM-50	11q22.3	11-107.706170	6972	92521	1.07	0.15	=	=	83	0.0
280	ATM-51	11q22.3	11-107.707413	8101	89512	1.04	0.09	=	=	35	0.0
346	ATM-52	11q22.3	11-107.707867	6789	82518	1.15	0.12	=	=	69	0.0
394	ATM-54	11q22.3	11-107.709834	5343	73862	1.06	0.1	=	=	74	0.0
238	ATM-55	11q22.3	11-107.710889	8723	96924	1.08	0.1	=	=	62	0.0
427	ATM-58	11q22.3	11-107.721746	4468	65347	1.02	0.11	=	=	87	0.0
232	ATM-60	11q22.3	11-107.729703	10234	108002	1.11	0.11	=	=	35	0.0
273	ATM-61	11q22.3	11-107.731288	10491	122724	1.11	0.15	=	=	57	0.1
474	ATM-62	11q22.3	11-107.739228	5976	95241	1.26	0.18	=	=	90	0.0
419	ATM-62	11q22.3	11-107.739925	5444	80301	1.12	0.16	=	=	82	0.1
286	ATM-63	11q22.3	11-107.741279	8547	100183	1.05	0.11	=	=	75	0.0
436	Reference*	01q23.3	01-159.406366	4686	68474	1.24	0.13	=	=	64	0.0
319	Reference*	03q13.2	03-113.667629	6440	78423	0.92	0.08	=	=	62	0.0
131	Reference*	03q21.3	03-129.999512	11910	126031	1.17	0.1	=	=	75	0.0
256	Reference*	04q25	04-110.941155	7498	79888	1	0.12	=	=	46	0.1
365	Reference*	05q33.3	05-158.137017	4777	63893	0.9	0.08	=	=	93	0.0
301	Reference*	06q22.33	06-129.511860	5754	70332	0.92	0.08	=	=	68	0.1
136	Reference*	07p14.3	07-030.974908	11112	116434	1.03	0.09	=	=	75	0.1
401	Reference*	08q12.2	08-061.913286	5225	73031	1.07	0.11	=	=	80	0.0
184	Reference*	09p24.2	09-002.644106	7793	80917	1.01	0.09	=	=	69	0.0
454	Reference*	13q13.1	13-031.879392	5366	80394	1	0.08	=	=	69	0.0
485	Reference*	18q21.1	18-045.630186	3929	63579	0.97	0.08	=	=	70	0.0
				7793	93969	1.08	0.11*	=	=	68	0.03

Median value all probe values:

Normal range: 0.7 - 1.3 Essential information on the use of this product is present in the product description which is available on <http://www.mlpa.com>. For questions, <mailto:info@mlpa.com>. MRC-Holland does not and cannot warrant the performance or results you may obtain by using the software. In no event will MRC-Holland be liable for any damages, claims or costs whatsoever or any consequential, indirect, incidental, damages, or any lost profits or lost savings, even if an MRC-Holland representative has been advised of the possibility of such loss, damages, claims or costs.



Sample report: 5

Sample type: Sample | Project: ATM analysis | Experiment: ATM1 | Machine: ABI-3730 | Report date: 15/08/2018 | Run date: 09/11/2015 | Software Version: v.140721.1958 | Normal range: 0.7 - 1.3

Authorization
Date

MLPA probe mix: P041-ATM-1
Lot number: B1-0314
Sheet date: 09/11/2015 17:01:48
Control fragments: CF-003-[brown] QDX2 (A2-0)
Analysis method: Block SSC: On
Used metric: Peak height

Nr of test probes: 45/45
Nr of ref probes: 11/11
DNA concentration: NA
DNA denaturation: NA
Expected gender: Female
Residual primer %: OK 15%

FRSS: Warning 70%
FRMS: Warning 70%
PSL: Bad -42%
RSQ: OK
RPQ: OK
CAS: OK? 75%

Reference Samples: 7 | 6 | 1 | 3 | 1 | 5 | 1 | 4 | 1 | 2

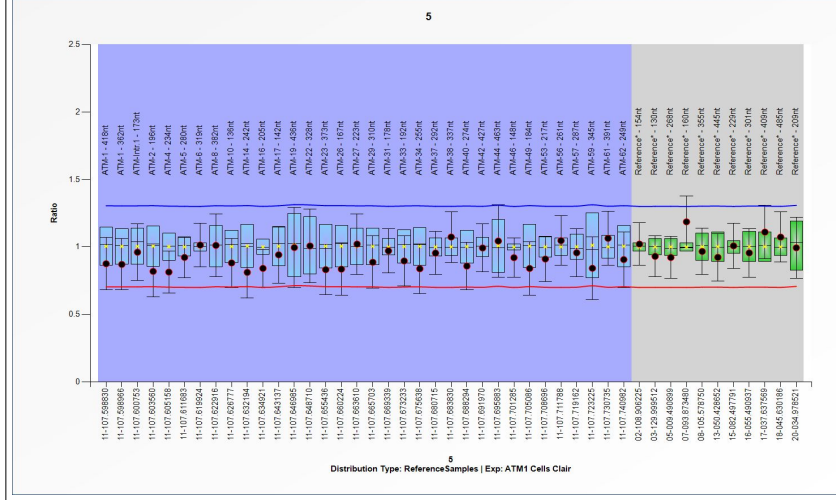
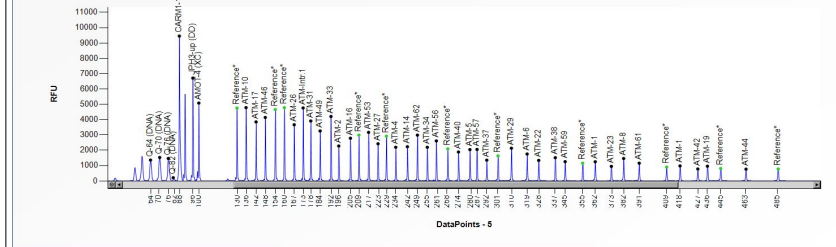
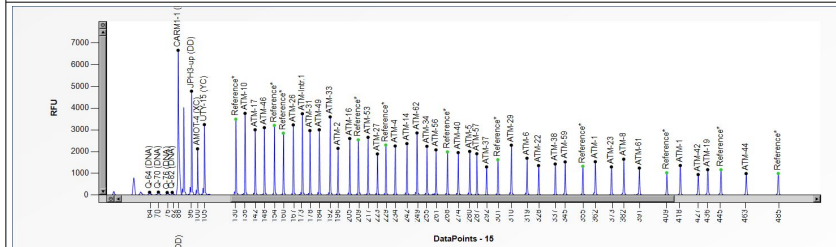


Table with columns: D [nt], Gene-Exon, Chr.band, hg18 loc., Height, Area, Ratio, Stdev, [REF], [Sam], Width, d[nt]. Contains data for 49 ATM probes and 209 reference samples.

Median value all probe values:

2134 13098 0.94 0.09 42 0.04



Sample report: 5

Sample type: Sample | Project: ATM analysis | Experiment: ATM2 | Dye: 6-FAM | Performed by: Admin
Machine: ABI-3730 | Report date: 15/08/2015 | Run date: 07/10/2015 | Software Version: v.140721.1958 | Normal range: 0.7 - 1.3

Table with 2 columns: Authorization, Date

MLPA probe mix: P042-ATM-2
Lot number: B1-0314
Sheet date: 28/08/2015 11:01:16
Control fragments: CF-003-[brown] QDX2 (A2-0)
Analysis method: Block SSC: On
Used metric: Peak height
Nr of test probes: 45/45
Nr of ref probes: 11/11
DNA concentration: OK
DNA denaturation: OK
Expected gender: Female
Residual primer %: OK 12%
FRSS: Warning 70%
FRMS: OK? 85%
PSLP: OK -5%
RSQ: OK
RPQ: OK
CAS: OK 90%

Reference Samples: 7 | 6 | 1 | 3 | 15 | 14 | 1 | 2

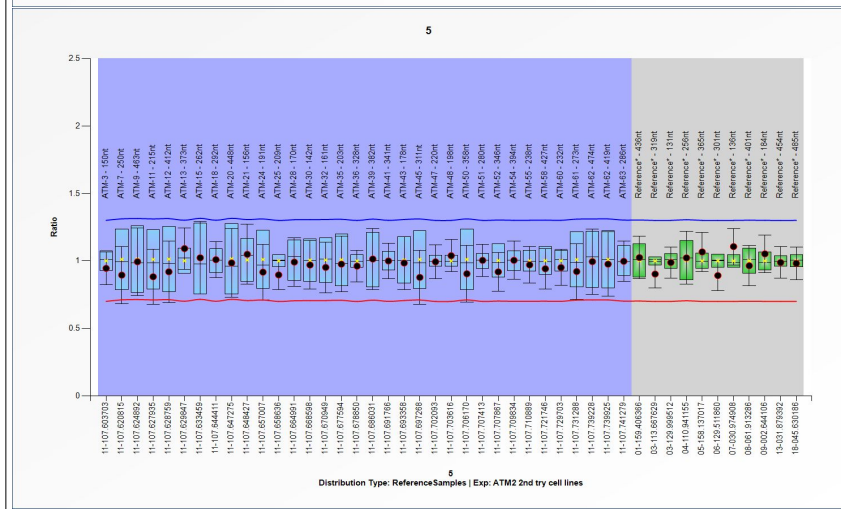
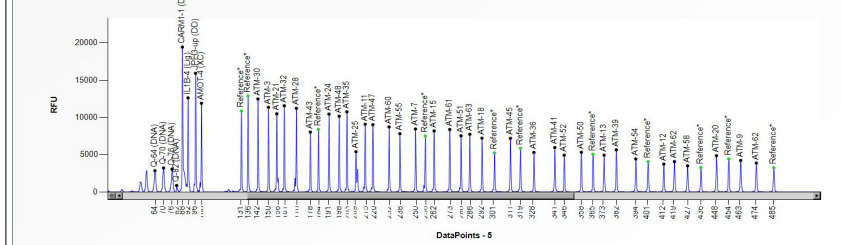
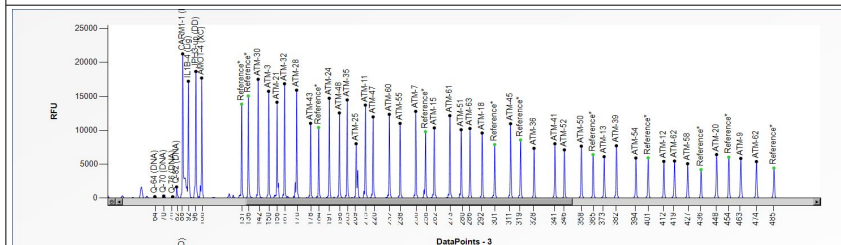


Table with columns: D [nt], Gene-Exon, Chr.band, hg18 loc., Height, Area, Ratio, Stdev, [REF], [Sam], Width, d[nt]. Contains data for probes 150-485 and reference probes.

Median value all probe values:

Normal range: 0.7 - 1.3 Essential information on the use of this product is present in the product description which is available on http://www.mlpa.com. For questions, mailto:info@mlpa.com.
MRC-Holland does not and cannot warrant the performance or results you may obtain by using the software. In no event will MRC-Holland be liable for any damages, claims or costs whatsoever or any consequential, indirect, incidental, damages, or any lost profits or lost savings, even if an MRC-Holland representative has been advised of the possibility of such loss, damages, claims or costs.



Sample report: 10

Sample type: Sample | Project: ATM analysis | Experiment: ATM1 |
 Machine: ABI-3730 | Report date: 09/11/2015 | Run date: 09/11/2015 | Software Version: v.140721.1958 | Normal range: 0.7 - 1.3 |
 | Dye: 6-FAM | Performed by: Admin

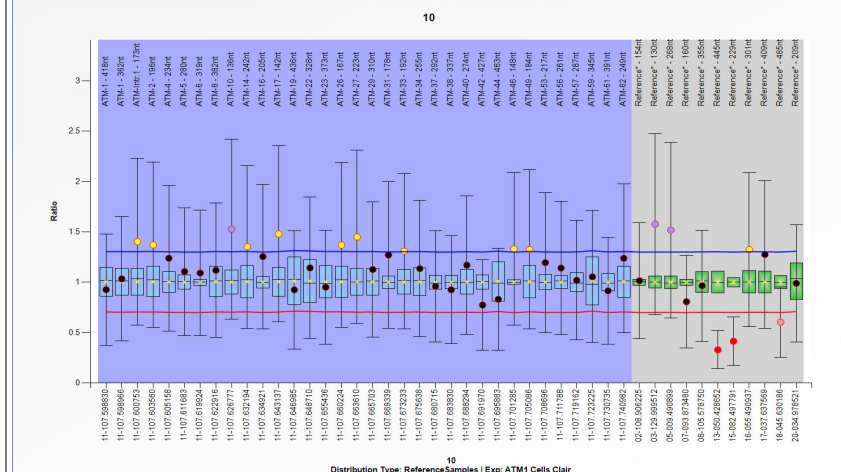
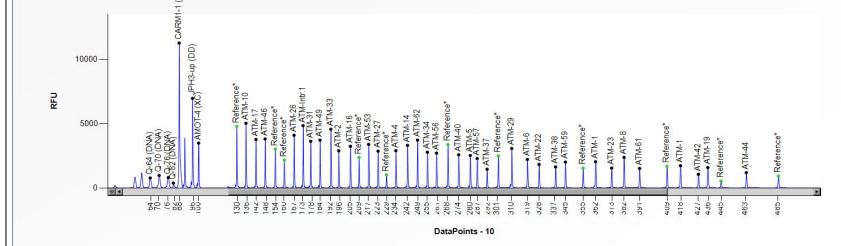
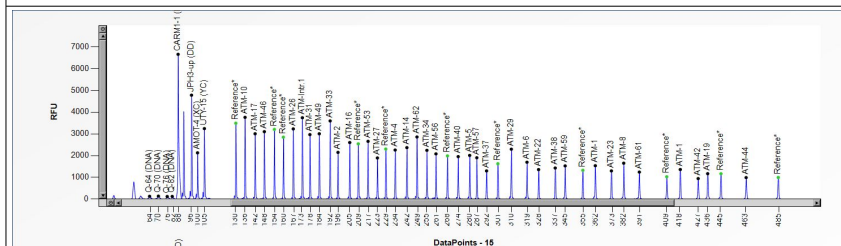
Authorization
Date

MLPA probe mix: P041-ATM-1
 Lot number: B1-0314
 Sheet date: 09/11/2015 17:01:48
 Control fragments: CF-003-[brown] QDX2 (A2-0)
 Analysis method: Block SSC: On
 Used metric: Peak height

Nr of test probes: 45/45
 Nr of ref probes: 11/11
 DNA concentration: NA
 DNA denaturation: NA
 Expected gender: Female
 Residual primer %: OK 12%

FRSS: Warning 70%
 FRMS: OK 100%
 PSLP: Warning 25%
 RSQ: OK
 RPO: Bad
 CAS: OK? 75%

Reference Samples: 7 | 6 | 1 | 3 | 1 | 5 | 1 | 4 | 1 | 1 | 2



D [nt]	Gene-Exon	Chr.band	hg18 loc.	Height	Area	Ratio ⁴¹	Stdev	[REF]	[Sam]	Width	d[nt]
418	ATM-1	11q22.3	11-107.598830	1730	12946	0.93	0.28	=	=	43	-0.1
362	ATM-1	11q22.3	11-107.598966	2041	14728	1.03	0.31	=	=	38	-0.1
173	ATM-Intr.1	11q22.3	11-107.600753	4850	27503	1.4	0.41	?	?	42	0.0
196	ATM-2	11q22.3	11-107.603560	2894	16308	1.37	0.41	?	?	54	0.0
234	ATM-4	11q22.3	11-107.605158	2901	16590	1.24	0.36	=	=	54	0.0
280	ATM-5	11q22.3	11-107.611683	2527	15820	1.11	0.32	=	=	49	-0.1
319	ATM-6	11q22.3	11-107.619924	2223	14512	1.09	0.31	=	=	35	0.0
382	ATM-8	11q22.3	11-107.622916	2376	16827	1.12	0.33	=	=	35	-0.1
136	ATM-10	11q22.3	11-107.626777	5040	28536	1.53	0.45	>*	?	45	0.0
242	ATM-14	11q22.3	11-107.632194	3317	19780	1.35	0.4	?	?	50	0.0
205	ATM-16	11q22.3	11-107.634921	3243	18420	1.26	0.36	=	=	43	0.0
142	ATM-17	11q22.3	11-107.643137	3773	21048	1.48	0.44	?	?	31	0.0
436	ATM-19	11q22.3	11-107.646985	1590	12706	0.93	0.29	=	=	41	0.0
328	ATM-22	11q22.3	11-107.648710	1833	11631	1.14	0.35	=	=	39	-0.1
373	ATM-23	11q22.3	11-107.655436	1551	10842	0.95	0.28	=	=	36	0.0
167	ATM-26	11q22.3	11-107.660224	4102	22603	1.37	0.41	?	?	45	0.0
223	ATM-27	11q22.3	11-107.663610	2865	16681	1.45	0.43	?	?	43	0.0
310	ATM-29	11q22.3	11-107.665703	3073	20585	1.13	0.34	=	=	51	0.0
178	ATM-31	11q22.3	11-107.669339	3637	20744	1.27	0.36	=	=	47	0.0
192	ATM-33	11q22.3	11-107.673233	4574	25121	1.31	0.38	?	?	42	0.0
255	ATM-34	11q22.3	11-107.675638	2781	16317	1.14	0.34	=	=	47	0.0
292	ATM-37	11q22.3	11-107.680715	1460	8766	0.96	0.28	=	=	27	-0.1
337	ATM-38	11q22.3	11-107.683830	1639	10948	0.93	0.27	=	=	52	0.0
274	ATM-40	11q22.3	11-107.688294	2584	16113	1.17	0.34	=	=	50	-0.1
427	ATM-42	11q22.3	11-107.691970	1063	8061	0.77	0.22	=	=	41	-0.1
463	ATM-44	11q22.3	11-107.695883	1193	9332	0.83	0.25	=	=	49	0.0
148	ATM-46	11q22.3	11-107.701285	3813	21033	1.33	0.38	?	?	46	0.0
184	ATM-49	11q22.3	11-107.705086	3727	21346	1.32	0.4	?	?	38	0.1
217	ATM-53	11q22.3	11-107.708696	3391	19550	1.2	0.35	=	=	42	0.0
261	ATM-56	11q22.3	11-107.711788	2715	15116	1.14	0.33	=	=	27	-0.1
287	ATM-57	11q22.3	11-107.719162	2292	13989	1.02	0.3	=	=	36	0.0
345	ATM-59	11q22.3	11-107.723225	2016	13273	1.05	0.33	=	=	41	-0.1
391	ATM-61	11q22.3	11-107.730735	1515	11169	0.92	0.27	=	=	38	0.0
249	ATM-62	11q22.3	11-107.740982	3726	21776	1.24	0.37	=	=	41	0.0
154	Reference*	02q12.3	02-108.906225	3023	17186	1.02	0.29	=	=	49	0.0
130	Reference*	03q21.3	03-129.999512	4802	28393	1.58	0.45	>*	?	54	0.0
268	Reference*	05p15.31	05-009.490899	3372	20784	1.52	0.44	>*	?	55	-0.1
160	Reference*	07q21.3	07-093.873480	2168	12382	0.81	0.23	=	=	32	-0.1
355	Reference*	08q22.3	08-105.578750	1545	10534	0.97	0.28	=	=	36	0.0
445	Reference*	13q14.3	13-050.428652	533	4270	0.33	0.1	<<*	?	34	0.0
229	Reference*	15q25.2	15-082.497791	1021	6250	0.42	0.12	<<*	?	38	0.0
301	Reference*	16q13	16-055.490937	2485	15901	1.32	0.38	?	?	60	-0.1
409	Reference*	17q21.2	17-037.637569	1684	12383	1.28	0.37	=	=	37	0.0
485	Reference*	18q21.1	18-045.630186	924	7720	0.6	0.17	<*	?	41	-0.1
209	Reference*	20q11.23	20-034.978521	2370	13734	0.99	0.29	=	=	39	-0.1
Median value all probe values:				2527	15901	1.14	0.34*			42	-0.01

225



Sample report: 10

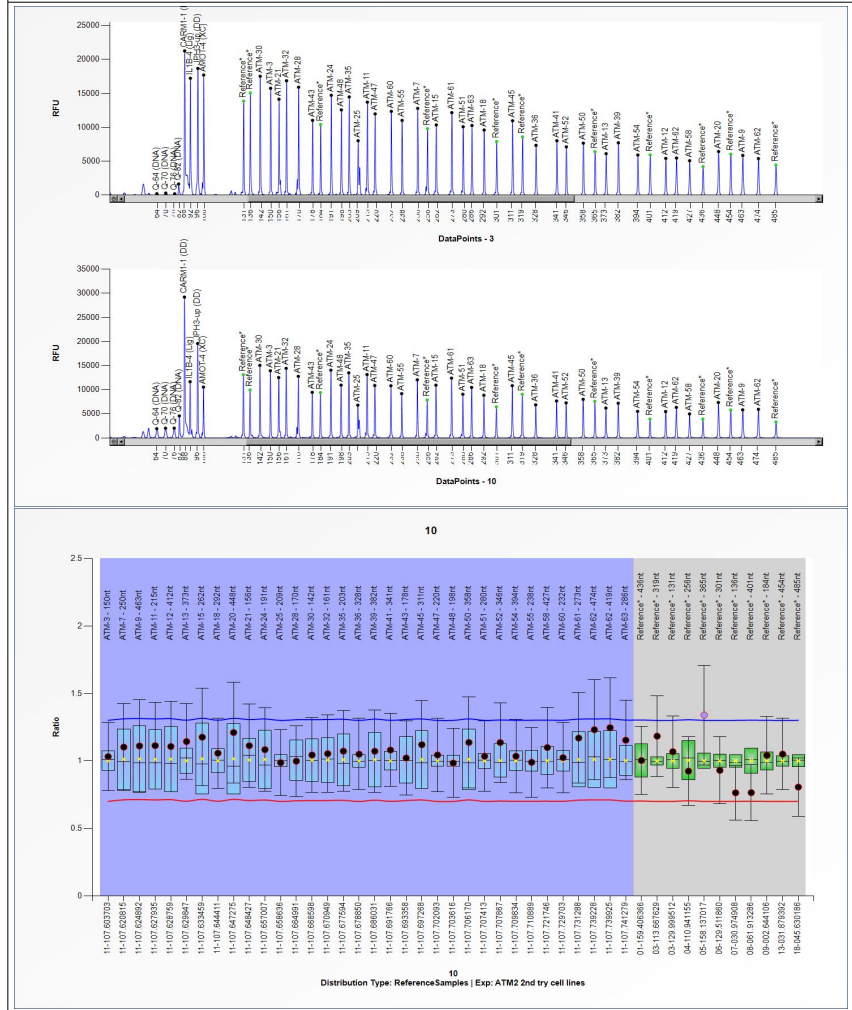
Sample type: Sample | Project: ATM analysis | Experiment: ATM2
Machine: ABI-3730 | Report date: 15/08/2018 | Run date: 07/10/2015 | Software Version: v.140721.1958 | Normal range: 0.7 - 1.3

| Dye: 6-FAM | Performed by: Admin

Authorization
Date

MLPA probe mix:	P042-ATM-2	Nr of test probes:	45/45	FRSS:	Warning 70%
Lot number:	B1-0314	Nr of ref probes:	11/11	FRMS:	Warning 60%
Sheet date:	28/08/2015 11:01:16	DNA concentration:	OK	PSLP:	OK 10%
Control fragments:	CF-003-[brown] QDX2 (A2-0	DNA denaturation:	Warning	RSQ:	OK
Analysis method:	Block SSC: On	Expected gender:	Female	RPG:	Warning
Used metric:	Peak height	Residual primer %:	OK 10%	CAS:	Warning 60%

Reference Samples: 7 | 6 | 1 | 3 | 15 | 14 | 1 | 2



D [nt]	Gene-Exon	Chr.band	hg18 loc.	Height	Area	Ratio	Stdev	[REF]	[Sam]	Width	d[nt]
150	ATM-3	11q22.3	11-107.603703	13932	139916	1.03	0.13	=	=	73	0.0
250	ATM-7	11q22.3	11-107.620815	12058	122259	1.1	0.16	=	=	33	0.0
463	ATM-9	11q22.3	11-107.624892	5833	88819	1.11	0.17	=	=	100	0.0
215	ATM-11	11q22.3	11-107.627935	13146	132584	1.11	0.16	=	=	34	0.0
412	ATM-12	11q22.3	11-107.628759	5470	72208	1.11	0.17	=	=	80	0.0
373	ATM-13	11q22.3	11-107.629847	6199	79356	1.14	0.14	=	=	79	0.0
262	ATM-15	11q22.3	11-107.633459	10940	114092	1.18	0.18	=	=	37	0.0
292	ATM-18	11q22.3	11-107.644411	8859	98277	1.06	0.13	=	=	56	-0.1
448	ATM-20	11q22.3	11-107.647275	7348	103606	1.21	0.19	=	=	91	0.0
156	ATM-21	11q22.3	11-107.648427	12527	138524	1.11	0.15	=	=	70	0.0
191	ATM-24	11q22.3	11-107.657007	14052	145856	1.08	0.15	=	=	78	-0.1
209	ATM-25	11q22.3	11-107.658636	6796	67615	0.99	0.12	=	=	18	0.9
170	ATM-28	11q22.3	11-107.664991	12783	125162	1	0.13	=	=	34	-0.1
142	ATM-30	11q22.3	11-107.668598	15059	158405	1.04	0.14	=	=	80	0.0
161	ATM-32	11q22.3	11-107.670949	14433	144836	1.05	0.14	=	=	64	0.0
203	ATM-35	11q22.3	11-107.677594	13500	134297	1.07	0.15	=	=	36	0.0
328	ATM-36	11q22.3	11-107.678850	6854	81107	1.05	0.13	=	=	66	0.0
382	ATM-39	11q22.3	11-107.686031	7195	90483	1.07	0.15	=	=	77	-0.1
341	ATM-41	11q22.3	11-107.691766	7659	92713	1.08	0.13	=	=	75	0.0
178	ATM-43	11q22.3	11-107.693358	9448	95796	1.02	0.14	=	=	60	0.0
311	ATM-45	11q22.3	11-107.697268	10833	123819	1.12	0.16	=	=	98	0.0
220	ATM-47	11q22.3	11-107.702093	10871	112019	1.04	0.14	=	=	61	0.0
198	ATM-48	11q22.3	11-107.703616	10952	113349	0.99	0.13	=	=	68	-0.1
358	ATM-50	11q22.3	11-107.706170	8002	98555	1.14	0.17	=	=	89	0.0
280	ATM-51	11q22.3	11-107.707413	9053	92760	1.04	0.13	=	=	38	-0.1
346	ATM-52	11q22.3	11-107.707867	7267	84162	1.14	0.15	=	=	73	0.0
394	ATM-54	11q22.3	11-107.709834	5501	72004	1.04	0.14	=	=	80	0.0
238	ATM-55	11q22.3	11-107.710889	9184	91773	0.99	0.13	=	=	33	0.0
427	ATM-58	11q22.3	11-107.721746	4979	66875	1.1	0.15	=	=	76	0.0
232	ATM-60	11q22.3	11-107.729703	10821	110204	1.02	0.13	=	=	36	0.0
273	ATM-61	11q22.3	11-107.731288	12404	128481	1.17	0.17	=	=	34	0.0
474	ATM-62	11q22.3	11-107.739228	5940	88862	1.23	0.19	=	=	102	-0.1
419	ATM-62	11q22.3	11-107.739925	6336	86343	1.25	0.18	=	=	83	0.0
286	ATM-63	11q22.3	11-107.741279	10474	113530	1.15	0.15	=	=	66	-0.1
436	Reference*	01q23.3	01-159.406366	3920	54081	1	0.13	=	=	82	0.0
319	Reference*	03q13.2	03-113.667629	9049	106007	1.18	0.15	=	=	65	0.0
131	Reference*	03q21.3	03-129.999512	13110	127297	1.07	0.13	=	=	34	0.0
256	Reference*	04q25	04-110.941155	7879	78778	0.92	0.13	=	=	45	-0.1
365	Reference*	05q33.3	05-158.137017	7604	96029	1.34	0.18	>*	?	71	0.0
301	Reference*	06q22.33	06-129.511860	6422	70129	0.93	0.12	=	=	34	0.0
136	Reference*	07p14.3	07-030.974908	9938	99024	0.76	0.1	=	=	46	0.0
401	Reference*	08q12.2	08-061.913286	3912	51184	0.77	0.1	=	=	73	-0.1
184	Reference*	09p24.2	09-002.644106	9395	96892	1.04	0.14	=	=	70	-0.1
454	Reference*	13q13.1	13-031.879392	5790	80499	1.05	0.13	=	=	86	-0.1
485	Reference*	18q21.1	18-045.630186	3306	49384	0.81	0.11	=	=	71	-0.1
Median value all probe values:				9049	96892	1.07	0.14*			70	-0.04

226

Normal range: 0.7 - 1.3 Essential information on the use of this product is present in the product description which is available on <http://www.mlpa.com>. For questions, mailto:info@mlpa.com.
MRC-Holland does not and cannot warrant the performance or results you may obtain by using the software. In no event will MRC-Holland be liable for any damages, claims or costs whatsoever or any consequential, indirect, incidental, damages, or any lost profits or lost savings, even if an MRC-Holland representative has been advised of the possibility of such loss, damages, claims or costs.

STS 02/11 W1



Sample report: 8

Sample type: Sample | Project: ATM analysis | Experiment: ATM1
Machine: ABI-3730 | Report date: 15/08/2018 | Run date: 09/11/2015 | Software Version: v.140721.1958 | Normal range: 0.7 - 1.3

| Dye: 6-FAM | Performed by: Admin

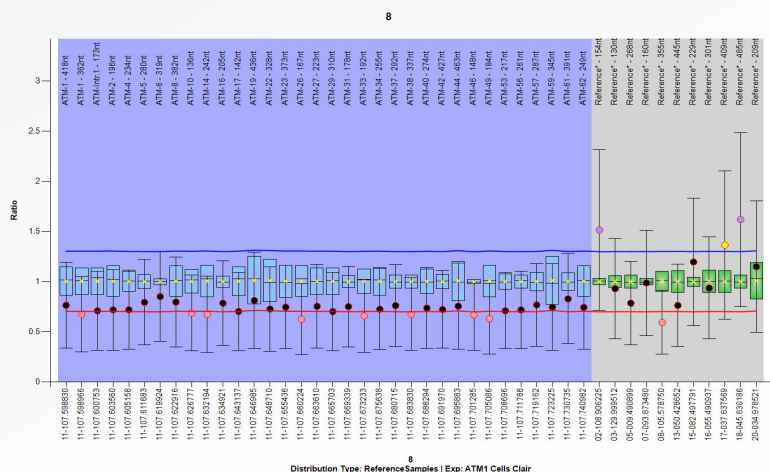
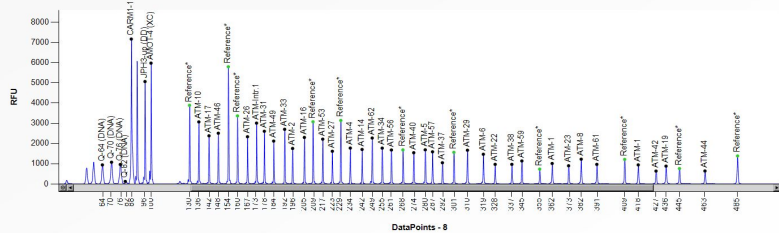
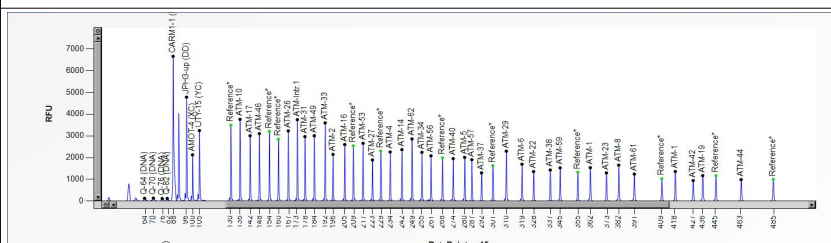
Authorization	
Date	

MLPA probe mix: P041-ATM-1
 Lot number: B1-0314
 Sheet date: 09/11/2015 17:01:48
 Control fragments: CF-003-[brown] QDX2 (A2-0)
 Analysis method: Block SSC: On
 Used metric: Peak height

Nr of test probes: 45/45
 Nr of ref probes: 11/11
 DNA concentration: NA
 DNA denaturation: NA
 Expected gender: Female
 Residual primer %: OK 14%

FRSS: Warning 70%
 FRMS: OK? 85%
 PSPL: Bad -40%
 RSQ: OK
 RPK: Bad
 CAS: Warning 55%

Reference Samples: 7 | 6 | 1 | 3 | 15 | 14 | 12



D [nt]	Gene-Exon	Chr.band	hg18 loc.	Height	Area	Ratio	Stdev	[REF]	[Sam]	Width	d[nt]
418	ATM-1	11q22.3	11-107.598830	942	8150	0.77	0.21	=	=	40	0.2
362	ATM-1	11q22.3	11-107.598966	1012	8550	0.68	0.19	<*	?	55	0.3
173	ATM-Intr.1	11q22.3	11-107.600753	3011	17930	0.71	0.2	=	=	46	0.0
196	ATM-2	11q22.3	11-107.603560	1756	10622	0.72	0.2	=	=	47	0.0
234	ATM-4	11q22.3	11-107.605158	1774	11041	0.72	0.2	=	=	44	0.1
280	ATM-5	11q22.3	11-107.611683	1688	11653	0.79	0.21	=	=	50	0.2
319	ATM-6	11q22.3	11-107.619924	1469	10950	0.85	0.23	=	=	47	0.1
382	ATM-8	11q22.3	11-107.622916	1225	10174	0.8	0.22	=	=	49	0.1
136	ATM-10	11q22.3	11-107.626777	3070	18246	0.69	0.19	<*	?	46	0.0
242	ATM-14	11q22.3	11-107.632194	1706	10739	0.68	0.19	<*	?	41	0.1
205	ATM-16	11q22.3	11-107.634921	2302	13695	0.79	0.21	=	=	41	0.1
142	ATM-17	11q22.3	11-107.643137	2382	13944	0.7	0.2	=	=	35	0.0
436	ATM-19	11q22.3	11-107.646985	881	8462	0.81	0.24	=	=	56	0.1
328	ATM-22	11q22.3	11-107.648710	968	7103	0.73	0.21	=	=	57	0.1
373	ATM-23	11q22.3	11-107.655436	899	7311	0.75	0.21	=	=	49	0.1
167	ATM-26	11q22.3	11-107.660224	2337	13663	0.63	0.18	<*	?	51	0.0
223	ATM-27	11q22.3	11-107.663610	1617	10201	0.76	0.21	=	=	37	0.1
310	ATM-29	11q22.3	11-107.665703	1668	11998	0.7	0.2	=	=	37	0.1
178	ATM-31	11q22.3	11-107.669339	2607	15354	0.75	0.2	=	=	42	0.0
192	ATM-33	11q22.3	11-107.673233	2704	15795	0.66	0.18	<*	?	35	0.0
255	ATM-34	11q22.3	11-107.675638	1773	11697	0.73	0.2	=	=	54	0.1
292	ATM-37	11q22.3	11-107.680715	1048	7305	0.76	0.2	=	=	41	0.2
337	ATM-38	11q22.3	11-107.683830	969	7241	0.68	0.18	<*	?	43	0.1
274	ATM-40	11q22.3	11-107.688294	1545	10867	0.74	0.2	=	=	51	0.1
427	ATM-42	11q22.3	11-107.691970	636	5903	0.72	0.19	=	=	46	0.3
463	ATM-44	11q22.3	11-107.695883	641	5921	0.76	0.22	=	=	48	0.2
148	ATM-46	11q22.3	11-107.701285	2510	14737	0.67	0.18	<*	?	42	0.0
184	ATM-49	11q22.3	11-107.705086	2121	12736	0.63	0.18	<*	?	38	0.0
217	ATM-53	11q22.3	11-107.708696	2217	13762	0.71	0.19	=	=	58	0.1
261	ATM-56	11q22.3	11-107.711788	1681	11424	0.72	0.19	=	=	47	0.1
287	ATM-57	11q22.3	11-107.719162	1590	10559	0.77	0.21	=	=	35	0.1
345	ATM-59	11q22.3	11-107.723225	1137	8714	0.75	0.22	=	=	47	0.1
391	ATM-61	11q22.3	11-107.730735	968	8191	0.83	0.22	=	=	46	0.1
249	ATM-62	11q22.3	11-107.740982	2272	14716	0.74	0.21	=	=	41	0.1
154	Reference*	02q12.3	02-108.906225	5803	35102	1.52	0.4	>*	?	58	0.1
130	Reference*	03q21.3	03-129.999512	3892	23619	0.93	0.25	=	=	39	0.1
268	Reference*	05p15.31	05-009.490899	1686	11481	0.79	0.21	=	=	51	0.1
160	Reference*	07q21.3	07-093.873480	3367	19702	0.99	0.26	=	=	39	0.0
355	Reference*	08q22.3	08-105.578750	734	5605	0.59	0.16	<*	?	34	0.2
445	Reference*	13q14.3	13-050.428652	761	7117	0.76	0.21	=	=	52	0.1
229	Reference*	15q25.2	15-082.497791	3143	19682	1.2	0.32	=	=	57	0.1
301	Reference*	16q13	16-055.490937	1564	10889	0.94	0.25	=	=	48	0.1
409	Reference*	17q21.2	17-037.637569	1214	10224	1.37	0.37	?	?	41	0.1
485	Reference*	18q21.1	18-045.630186	1385	13222	1.62	0.43	>*	?	55	0.2
209	Reference*	20q11.23	20-034.978521	3076	18775	1.15	0.33	=	=	45	0.1
Median value all probe values:				1681	11041	0.75	0.21*			46	0.09

227



Sample report: 8

Sample type: Sample | Project: ATM analysis | Experiment: ATM2
 Machine: ABI-3730 | Report date: 15/08/2018 | Run date: 07/10/2015 | Software Version: v.140721.1958 | Normal range: 0.7 - 1.3

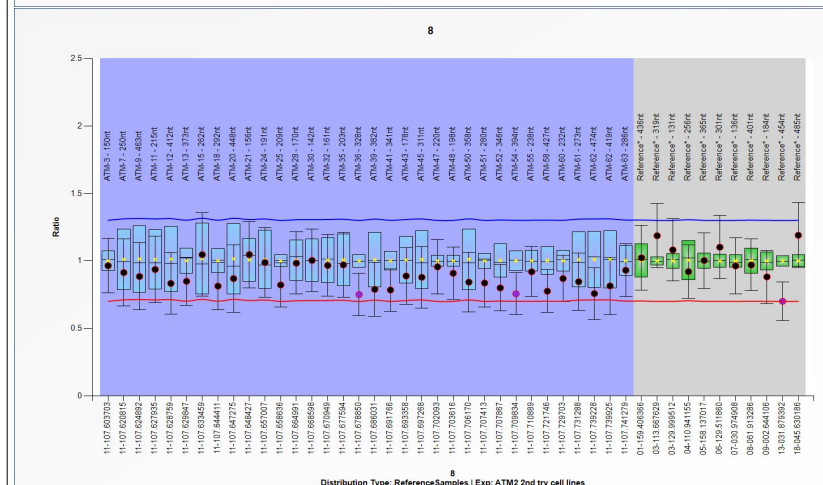
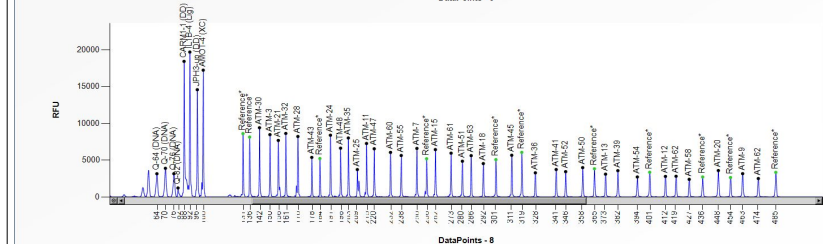
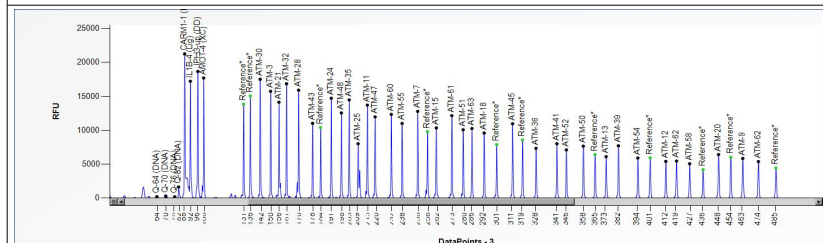
Authorization	
Date	

MLPA probe mix: P042-ATM-2
Lot number: B1-0314
Sheet date: 28/08/2015 11:01:16
Control fragments: CF-003-[brown] QDX2 (A2-0)
Analysis method: Block SSC: On
Used metric: Peak height

Nr of test probes: 45/45
Nr of ref probes: 11/11
DNA concentration: OK
DNA denaturation: OK
Expected gender: Female
Residual primer %: OK 14%

FRSS: Warning 70%
FRSL: OK 90%
PSL: OK 13%
RSQ: OK
RPQ: Warning
CAS: OK? 85%

Reference Samples: 7 | 6 | 13 | 15 | 14 | 12



D [nt]	Gene-Exon	Chr.band	hg18 loc.	Height	Area	Ratio ^H	Stdev	[REF]	[Sam]	Width	d[nt]
150	ATM-3	11q22.3	11-107.603703	8476	88425	0.96	0.1	=	=	52	0.1
250	ATM-7	11q22.3	11-107.620815	6603	72906	0.91	0.12	=	=	34	0.0
463	ATM-9	11q22.3	11-107.624892	3167	53991	0.89	0.12	=	=	69	0.1
215	ATM-11	11q22.3	11-107.627935	7273	76578	0.94	0.12	=	=	39	0.1
412	ATM-12	11q22.3	11-107.628759	2788	42304	0.83	0.11	=	=	91	0.1
373	ATM-13	11q22.3	11-107.629847	3098	44455	0.85	0.09	=	=	88	0.1
262	ATM-15	11q22.3	11-107.633459	6440	71899	1.05	0.15	=	=	35	0.1
292	ATM-18	11q22.3	11-107.644411	4537	54586	0.81	0.09	=	=	67	0.1
448	ATM-20	11q22.3	11-107.647275	3588	58807	0.87	0.13	=	=	87	0.1
156	ATM-21	11q22.3	11-107.648427	7685	89321	1.05	0.12	=	=	42	0.1
191	ATM-24	11q22.3	11-107.657007	8395	87393	0.99	0.13	=	=	38	0.0
209	ATM-25	11q22.3	11-107.658636	3721	39975	0.82	0.08	=	=	42	1.0
170	ATM-28	11q22.3	11-107.664991	8223	83463	0.98	0.11	=	=	33	0.0
142	ATM-30	11q22.3	11-107.668598	9419	100545	1	0.12	=	=	82	0.0
161	ATM-32	11q22.3	11-107.670949	8638	91992	0.97	0.11	=	=	84	0.0
203	ATM-35	11q22.3	11-107.677594	8022	83573	0.97	0.12	=	=	36	0.0
328	ATM-36	11q22.3	11-107.678850	3279	42662	0.75	0.08	<<	=	84	0.0
382	ATM-39	11q22.3	11-107.686031	3571	50627	0.79	0.1	=	=	79	0.1
341	ATM-41	11q22.3	11-107.691766	3728	49739	0.79	0.08	=	=	81	0.1
178	ATM-43	11q22.3	11-107.693358	5374	56914	0.89	0.11	=	=	63	0.0
311	ATM-45	11q22.3	11-107.697268	5670	72650	0.88	0.11	=	=	92	0.1
220	ATM-47	11q22.3	11-107.702093	6553	74579	0.96	0.1	=	=	91	0.1
198	ATM-48	11q22.3	11-107.703616	6636	69383	0.91	0.1	=	=	42	0.0
358	ATM-50	11q22.3	11-107.706170	3988	54330	0.84	0.11	=	=	81	0.1
280	ATM-51	11q22.3	11-107.707413	4859	59969	0.84	0.09	=	=	89	0.0
346	ATM-52	11q22.3	11-107.707867	3434	44340	0.8	0.09	=	=	78	0.1
394	ATM-54	11q22.3	11-107.709834	2717	40298	0.76	0.08	<<	=	71	0.1
238	ATM-55	11q22.3	11-107.710899	5638	62932	0.92	0.09	=	=	66	0.0
427	ATM-58	11q22.3	11-107.721746	2390	36218	0.78	0.08	=	=	65	0.2
232	ATM-60	11q22.3	11-107.729703	6058	65475	0.87	0.09	=	=	36	0.0
273	ATM-61	11q22.3	11-107.731288	5953	70551	0.85	0.11	=	=	66	0.0
474	ATM-62	11q22.3	11-107.739228	2501	42528	0.76	0.1	=	=	94	0.1
419	ATM-62	11q22.3	11-107.739925	2809	43047	0.82	0.11	=	=	89	0.1
286	ATM-63	11q22.3	11-107.741279	5619	66885	0.93	0.1	=	=	73	0.0
436	Reference*	01q23.3	01-159.406366	2714	42389	1.02	0.12	=	=	95	0.1
319	Reference*	03q13.2	03-113.667629	6063	77957	1.19	0.12	=	=	76	0.1
131	Reference*	03q21.3	03-129.999512	8620	88188	1.08	0.12	=	=	33	0.0
256	Reference*	04q25	04-110.941155	5199	58153	0.92	0.1	=	=	35	0.1
365	Reference*	05q33.3	05-158.137017	3836	52965	1	0.1	=	=	65	0.1
301	Reference*	06q22.33	06-129.511860	5072	63927	1.1	0.12	=	=	90	0.1
136	Reference*	07p14.3	07-030.974908	8146	87350	0.96	0.1	=	=	74	0.0
401	Reference*	08q12.2	08-061.913286	3358	50773	0.97	0.1	=	=	98	0.1
184	Reference*	09p24.2	09-002.644106	5219	53148	0.88	0.1	=	=	35	0.0
454	Reference*	13q13.1	13-031.879392	2634	42143	0.7	0.07	<<	=	74	0.1
485	Reference*	18q21.1	18-045.630186	3341	57695	1.19	0.12	=	=	91	0.1
				5199	58807	0.91	0.1*			73	0.06

Median value all probe values:



Sample report: 11

Sample type: Sample | Project: ATM analysis | Experiment: ATM1 | Dye: 6-FAM | Performed by: Admin
Machine: ABI-3730 | Report date: 15/08/2018 | Run date: 09/11/2018 | Software Version: v.140721.1958 | Normal range: 0.7 - 1.3

Authorization table with Date field

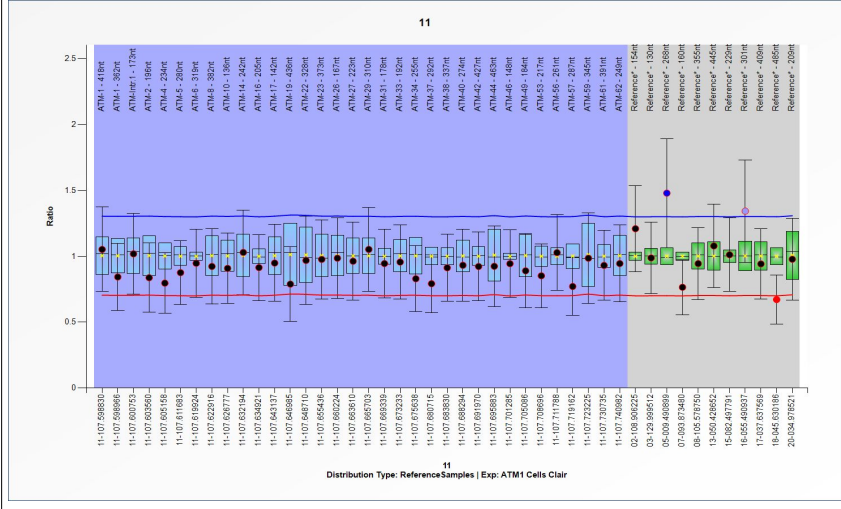
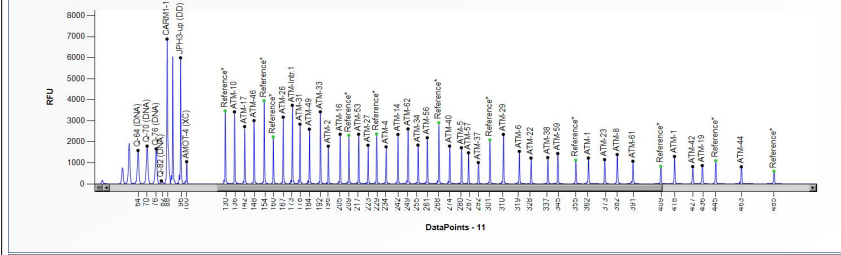
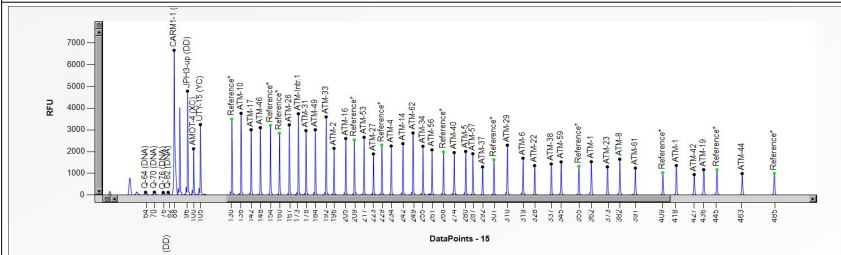
MLPA probe mix: P041-ATM-1, Lot number: B1-0314, Sheet date: 09/11/2015 17:01:48, Control fragments: CF-003-[brown] QDX2 (A2-0), Analysis method: Block SSC: On, Used metric: Peak height

Nr of test probes: 45/45, Nr of ref probes: 11/11, DNA concentration: NA, DNA denaturation: NA, Expected gender: Female, Residual primer %: OK 15%

FRSS: Warning 70%, FRMS: OK 95%, PSLP: OK -9%, RSQ: OK, RPQ: Warning, CAS: OK? 85%

Reference Samples: 7 | 1 | 6 | 1 | 3 | 1 | 5 | 1 | 4 | 1 | 1 | 2

Main data table with columns: D [nt], Gene-Exon, Chr.band, hg18 loc., Height, Area, Ratio, Stdev, [REF], [Sam], Width, d[nt]. Includes median values at the bottom: 1839, 11349, 0.95, 0.14*, 42, -0.05



229

Normal range: 0.7 - 1.3 Essential information on the use of this product is present in the product description which is available on http://www.mipa.com. For questions, mailto:info@mipa.com.



Sample report: 11

Sample type: Sample | Project: ATM analysis | Experiment: ATM2 | Dye: 6-FAM | Performed by: Admin | Machine: ABI-3730 | Report date: 15/08/2018 | Run date: 07/10/2015 | Software Version: v.140721.1958 | Normal range: 0.7 - 1.3

Authorization | Date

MLPA probe mix: P042-ATM-2 | Nr of test probes: 45/45 | FRSS: Warning 70% | Lot number: B1-0314 | Nr of ref probes: 11/11 | FRMS: Warning 55% | Sheet date: 28/08/2015 11:01:16 | DNA concentration: OK | PSLP: Bad -37% | Control fragments: CF-003-[brown] QDX2 (A2-0 | DNA denaturation: OK | RSQ: OK | Analysis method: Block SSC: On | Expected gender: Female | RPQ: Bad | Used metric: Peak height | Residual primer %: OK 11% | CAS: Bad 40%

Reference Samples: 7 | 6 | 1 | 3 | 15 | 11 | 4 | 1 | 2

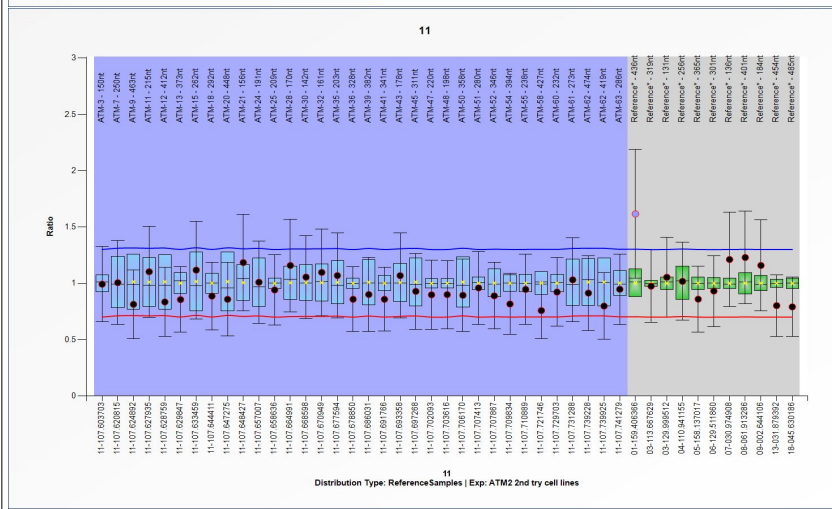
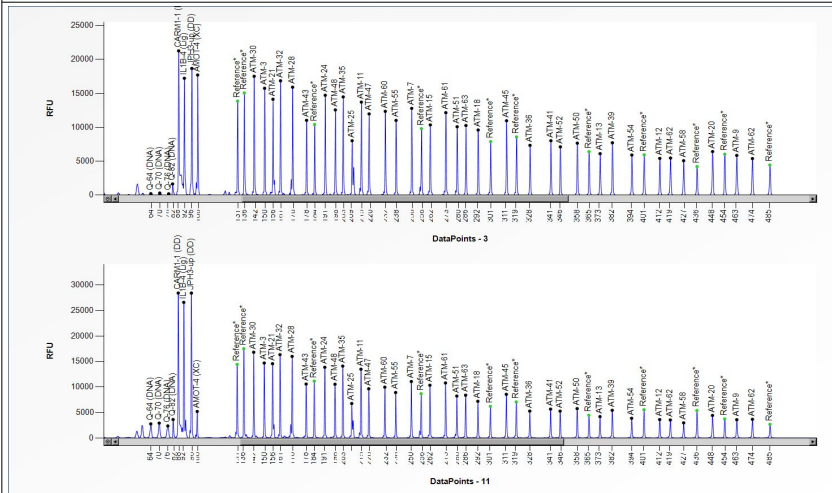


Table with 13 columns: D [nt], Gene-Exon, Chr.band, hg18 loc., Height, Area, Ratio, Stdev, [REF], [Sam], Width, d[nt]. Contains data for probes 150-485 and Reference* probes.



Sample report: 13

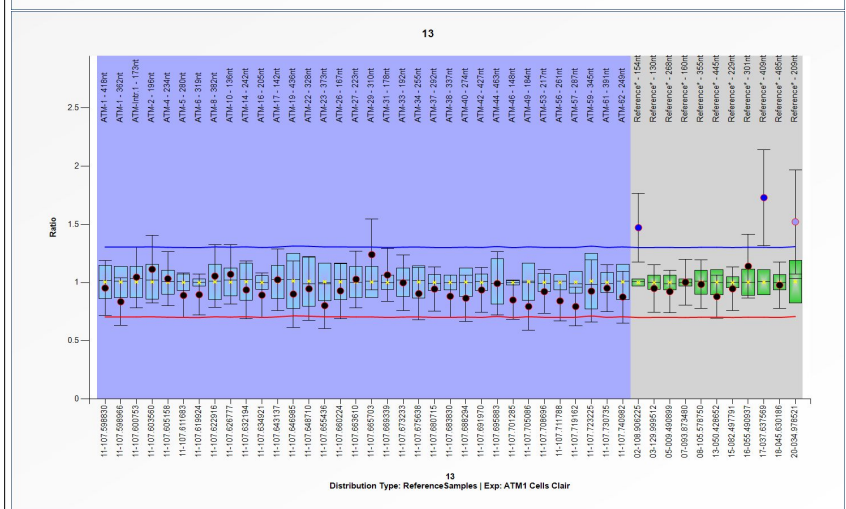
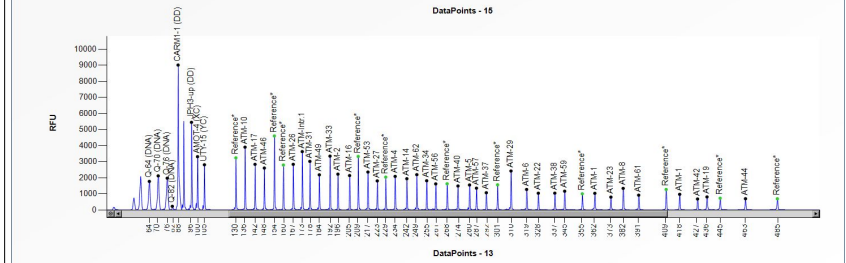
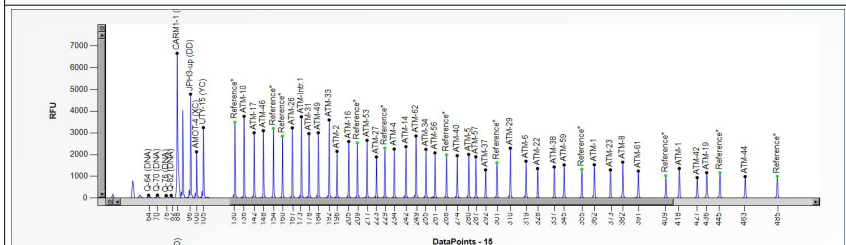
Sample type: Sample | Project: ATM analysis | Experiment: ATM1 | Dye: 6-FAM | Performed by: Admin
Machine: ABI-3730 | Report date: 15/08/2018 | Run date: 09/11/2015 | Software Version: v.140721.1958 | Normal range: 0.7 - 1.3

Authorization	
Date	

MLPA probe mix: P041-ATM-1 Nr of test probes: 45/45 FRSS: Warning 70%
 Lot number: B1-Q314 Nr of ref probes: 11/11 FRMS: OK? 85%
 Sheet date: 09/11/2015 17:01:48 DNA concentration: NA PS�: Warning -18%
 Control fragments: CF-003-[brown] QDX2 (A2-0 DNA denaturation: NA RSQ: Warning
 Analysis method: Block SSC: On Expected gender: Female RPQ: Warning
 Used metric: Peak height Residual primer %: OK 16% CAS: Warning 60%

Reference Samples: 7 16 1 3 1 15 1 14 1 12

D [nt]	Gene-Exon	Chr.band	hg18 loc.	Height	Area	Ratio [#]	Stdev	[REF]	[Sam]	Width	d[nt]
418	ATM-1	11q22.3	11-107.598830	970	7334	0.95	0.12	=	=	41	-0.1
362	ATM-1	11q22.3	11-107.598966	1031	7839	0.84	0.1	=	=	46	-0.1
173	ATM-Intr.1	11q22.3	11-107.600753	3629	20492	1.05	0.13	=	=	37	0.0
196	ATM-2	11q22.3	11-107.603560	2226	12335	1.11	0.15	=	=	46	0.0
234	ATM-4	11q22.3	11-107.605158	2085	12356	1.03	0.11	=	=	34	-0.1
280	ATM-5	11q22.3	11-107.611683	1551	10025	0.89	0.1	=	=	40	-0.1
319	ATM-6	11q22.3	11-107.619924	1272	8432	0.9	0.09	=	=	33	0.0
382	ATM-8	11q22.3	11-107.622916	1339	9846	1.06	0.13	=	=	59	0.0
136	ATM-10	11q22.3	11-107.626777	3903	21417	1.07	0.13	=	=	45	0.0
242	ATM-14	11q22.3	11-107.632194	1942	11889	0.94	0.12	=	=	55	-0.1
205	ATM-16	11q22.3	11-107.634921	2138	12056	0.89	0.09	=	=	42	0.0
142	ATM-17	11q22.3	11-107.643137	2834	15787	1.02	0.13	=	=	36	0.0
436	ATM-19	11q22.3	11-107.646985	808	6933	0.9	0.14	=	=	45	-0.1
328	ATM-22	11q22.3	11-107.648710	1039	6750	0.95	0.14	=	=	51	-0.1
373	ATM-23	11q22.3	11-107.655436	797	5871	0.8	0.1	=	=	42	-0.1
167	ATM-26	11q22.3	11-107.660224	2836	15788	0.93	0.12	=	=	42	0.0
223	ATM-27	11q22.3	11-107.663610	1805	10552	1.03	0.12	=	=	36	0.0
310	ATM-29	11q22.3	11-107.665703	2421	15500	1.24	0.15	=	=	36	0.0
178	ATM-31	11q22.3	11-107.669339	3021	16925	1.07	0.11	=	=	37	0.0
192	ATM-33	11q22.3	11-107.673233	3346	18657	1	0.12	=	=	34	0.0
255	ATM-34	11q22.3	11-107.675638	1815	10705	0.91	0.11	=	=	47	-0.1
292	ATM-37	11q22.3	11-107.680715	1068	6545	0.94	0.1	=	=	26	-0.1
337	ATM-38	11q22.3	11-107.683830	1042	7044	0.88	0.09	=	=	39	0.0
274	ATM-40	11q22.3	11-107.688294	1489	9552	0.87	0.1	=	=	41	-0.1
427	ATM-42	11q22.3	11-107.691970	681	5546	0.94	0.1	=	=	48	-0.2
463	ATM-44	11q22.3	11-107.695883	697	5766	0.99	0.14	=	=	33	-0.1
148	ATM-46	11q22.3	11-107.701285	2604	14915	0.85	0.08	=	=	39	0.0
184	ATM-49	11q22.3	11-107.705086	2183	13047	0.79	0.1	=	=	38	0.0
217	ATM-53	11q22.3	11-107.708696	2357	13828	0.92	0.09	=	=	41	-0.1
261	ATM-56	11q22.3	11-107.711788	1618	9296	0.84	0.09	=	=	22	0.0
287	ATM-57	11q22.3	11-107.719162	1351	8339	0.79	0.08	=	=	39	0.0
345	ATM-59	11q22.3	11-107.723225	1164	7847	0.93	0.13	=	=	35	-0.1
391	ATM-61	11q22.3	11-107.730735	918	7021	0.95	0.1	=	=	43	0.0
249	ATM-62	11q22.3	11-107.740982	2194	13338	0.88	0.11	=	=	45	-0.1
154	Reference*	02q12.3	02-108.906225	4602	25098	1.47	0.15	>>*	>*	33	0.0
130	Reference*	03q21.3	03-129.999512	3238	18693	0.95	0.1	=	=	58	-0.1
268	Reference*	05p15.31	05-009.490899	1625	10009	0.92	0.09	=	=	39	0.0
160	Reference*	07q21.3	07-093.873480	2792	15232	1	0.1	=	=	35	0.0
355	Reference*	08q22.3	08-105.578750	1003	7183	0.98	0.1	=	=	52	0.0
445	Reference*	13q14.3	13-050.428652	726	6286	0.88	0.09	=	=	50	-0.1
229	Reference*	15q25.2	15-082.497791	2038	11626	0.95	0.09	=	=	42	0.0
301	Reference*	16q13	16-055.490937	1562	9755	1.14	0.14	=	=	49	-0.1
409	Reference*	17q21.2	17-037.637569	1269	9449	1.73	0.21	>>*	>*	48	0.0
485	Reference*	18q21.1	18-045.630186	694	6250	0.98	0.1	=	=	45	0.0
209	Reference*	20q11.23	20-034.978521	3325	18549	1.52	0.22	>*	?	47	-0.1
Median value all probe values:	1625	10025	0.95	0.11*	41	-0.04					



231



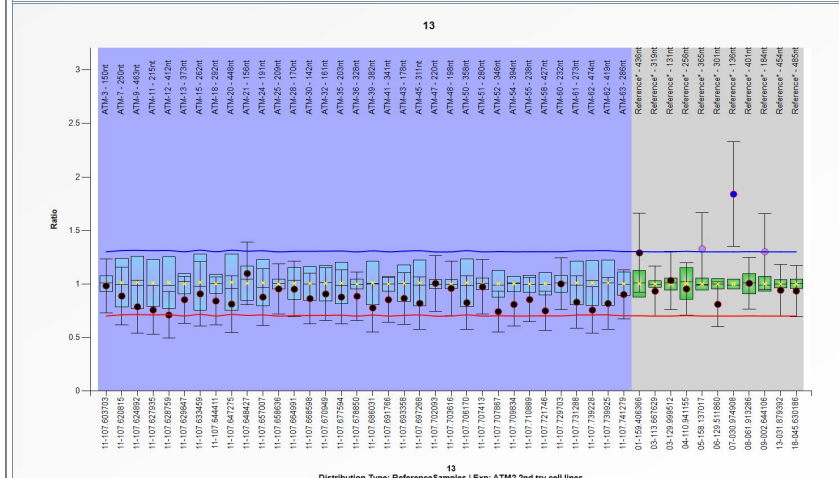
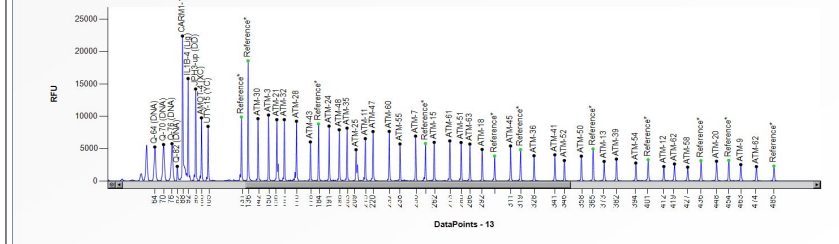
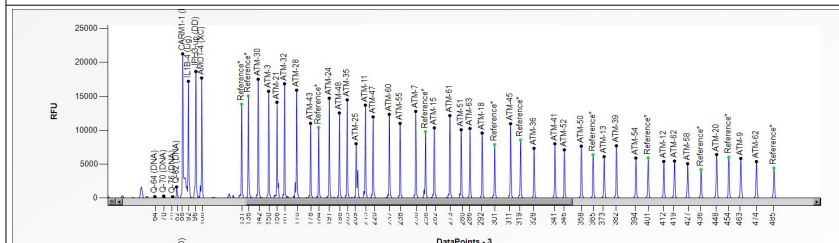
Sample report: 13

Sample type: Sample | Project: ATM analysis | Experiment: ATM2 | Dye: 6-FAM | Performed by: Admin
 Machine: ABI-3730 | Report date: 15/08/2018 | Run date: 07/10/2015 | Software Version: v.140721.1958 | Normal range: 0.7 - 1.3

Authorization	
Date	

MLPA probe mix: P042-ATM-2 Nr of test probes: 45/45 FRSS: Warning 70%
 Lot number: B1-0314 Nr of ref probes: 11/11 FRMS: Bad 40%
 Sheet date: 28/08/2015 11:01:16 DNA concentration: Warning PSLS: Warning -20%
 Control fragments: CF-003-[brown] QDX2 (A2-0 DNA denaturation OK RSQ: OK
 Analysis method: Block SSC: On Expected gender: Male RPO: Bad
 Used metric: Peak height Residual primer % OK 15% CAS: Bad 25%

Reference Samples: 7 | 6 | 13 | 15 | 14 | 112



D [nt]	Gene-Exon	Chr.band	hg18 loc.	Height	Area	Ratio ^H	Stdev	[REF]	[Sam]	Width	d[nt]
150	ATM-3	11q22.3	11-107.603703	10186	99601	0.98	0.13	=	=	60	0.0
250	ATM-7	11q22.3	11-107.620815	6928	69292	0.89	0.14	=	=	36	0.0
463	ATM-9	11q22.3	11-107.624892	2522	37052	0.79	0.12	=	=	61	-0.1
215	ATM-11	11q22.3	11-107.627935	6536	64087	0.76	0.11	=	=	31	-0.1
412	ATM-12	11q22.3	11-107.628759	2222	29736	0.71	0.11	=	=	59	0.0
373	ATM-13	11q22.3	11-107.629847	3011	39215	0.85	0.11	=	=	77	0.0
262	ATM-15	11q22.3	11-107.633459	5964	63964	0.91	0.15	=	=	69	0.0
292	ATM-18	11q22.3	11-107.644411	4866	53861	0.84	0.11	=	=	66	-0.1
448	ATM-20	11q22.3	11-107.647275	3040	43092	0.81	0.13	=	=	58	-0.1
156	ATM-21	11q22.3	11-107.648427	9473	93899	1.1	0.15	=	=	34	0.0
191	ATM-24	11q22.3	11-107.657007	8477	84528	0.88	0.13	=	=	67	0.0
209	ATM-25	11q22.3	11-107.658836	4828	50250	0.95	0.12	=	=	48	0.9
170	ATM-28	11q22.3	11-107.664991	9226	89550	0.95	0.13	=	=	33	0.0
142	ATM-30	11q22.3	11-107.668598	9626	93919	0.86	0.12	=	=	41	0.0
161	ATM-32	11q22.3	11-107.670949	9475	89528	0.91	0.12	=	=	30	0.0
203	ATM-35	11q22.3	11-107.677594	8162	80424	0.88	0.13	=	=	37	0.0
328	ATM-36	11q22.3	11-107.678850	3893	45269	0.89	0.11	=	=	66	-0.1
382	ATM-39	11q22.3	11-107.686031	3376	43848	0.78	0.11	=	=	74	0.0
341	ATM-41	11q22.3	11-107.691766	4034	47663	0.85	0.1	=	=	63	0.0
178	ATM-43	11q22.3	11-107.693358	6027	58459	0.87	0.12	=	=	35	0.1
311	ATM-45	11q22.3	11-107.697268	5403	61904	0.82	0.12	=	=	61	-0.1
220	ATM-47	11q22.3	11-107.702093	7634	83786	1.01	0.13	=	=	91	0.0
198	ATM-48	11q22.3	11-107.703616	7910	77925	0.96	0.13	=	=	34	0.0
358	ATM-50	11q22.3	11-107.706170	3829	47028	0.83	0.12	=	=	66	0.0
280	ATM-51	11q22.3	11-107.707413	5936	62144	0.97	0.13	=	=	36	0.0
346	ATM-52	11q22.3	11-107.707867	3152	36700	0.74	0.1	=	=	59	-0.1
394	ATM-54	11q22.3	11-107.709834	2763	36337	0.81	0.1	=	=	71	0.0
238	ATM-55	11q22.3	11-107.710889	5710	59232	0.85	0.1	=	=	59	0.0
427	ATM-58	11q22.3	11-107.721746	2127	28841	0.75	0.09	=	=	61	-0.1
232	ATM-60	11q22.3	11-107.729703	7654	76246	1	0.12	=	=	34	0.0
273	ATM-61	11q22.3	11-107.731288	6185	64686	0.83	0.12	=	=	33	0.0
474	ATM-62	11q22.3	11-107.739228	2213	32609	0.76	0.11	=	=	77	0.0
419	ATM-62	11q22.3	11-107.739925	2619	35535	0.82	0.12	=	=	78	-0.1
286	ATM-63	11q22.3	11-107.741279	5694	62373	0.9	0.12	=	=	63	-0.1
436	Reference*	01q23.3	01-159.406366	3131	43332	1.29	0.18	=	=	65	0.0
319	Reference*	03q13.2	03-113.667629	4838	55930	0.93	0.12	=	=	61	-0.1
131	Reference*	03q21.3	03-129.999512	9870	95126	1.03	0.14	=	=	37	0.0
256	Reference*	04q25	04-110.941155	5783	57730	0.95	0.12	=	=	28	0.0
365	Reference*	05q33.3	05-158.137017	4948	62028	1.33	0.17	v*	?	84	0.0
301	Reference*	06q22.33	06-129.511860	3845	41303	0.81	0.11	=	=	28	0.0
136	Reference*	07p14.3	07-030.974908	18574	183426	1.84	0.25	>>	v*	81	0.0
401	Reference*	08q12.2	08-061.913286	3289	44356	1.01	0.12	=	=	80	0.0
184	Reference*	09p24.2	09-002.644106	8808	87747	1.3	0.18	v*	?	73	0.0
454	Reference*	13q13.1	13-031.879392	3183	44516	0.94	0.12	=	=	59	-0.1
485	Reference*	18q21.1	18-045.630186	2301	34661	0.93	0.12	=	=	82	-0.1

Median value all probe values: 5403 58459 0.89 0.12* 61 -0.03

232

Normal range: 0.7 - 1.3 Essential information on the use of this product is present in the product description which is available on <http://www.mlpa.com>. For questions, <mailto:info@mlpa.com>.
 MRC-Holland does not and cannot warrant the performance or results you may obtain by using the software. In no event will MRC-Holland be liable for any damages, claims or costs whatsoever or any consequential, indirect, incidental, damages, or any lost profits or lost savings, even if an MRC-Holland representative has been advised of the possibility of such loss, damages, claims or costs.

Reference DNA Sample



Sample report: 6

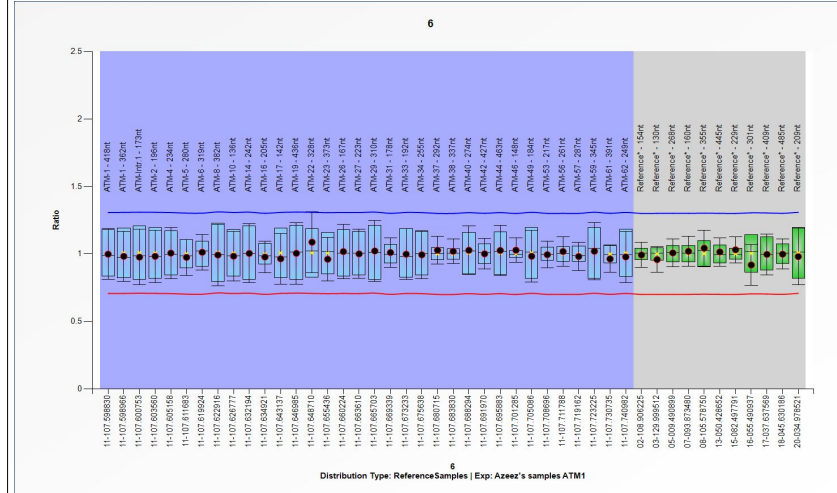
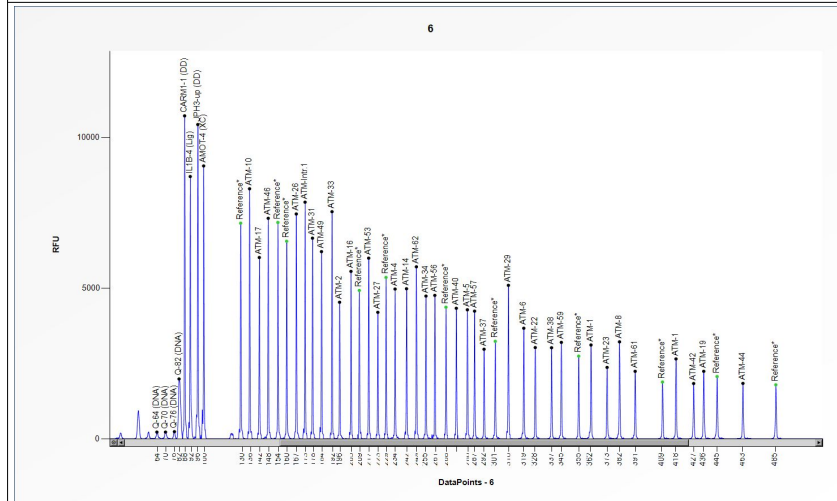
Sample type: Reference | Project: ATM analysis | Experiment:
Machine: ABI-3730 | Report date: 15/08/2018 | Run date: 29/11/2015 | Software Version: v.140721.1958 | Normal range: 0.7 - 1.3

ATM1 | Dye: 6-FAM | Performed by: Admin

Authorization	
Date	

MLPA probe mix:	P041-ATM-1	Nr of test probes:	45/45	FRSS:	Warning 70%
Lot number:	B1-0314	Nr of ref probes:	11/11	FRMS:	OK? 75%
Sheet date:	29/11/2015 14:55:14	DNA concentration:	OK	PSLP:	OK 2%
Control fragments:	CF-003-[brown] QDX2 (A2-0)	DNA denaturation:	OK	RSQ:	OK
Analysis method:	Block SSC: On	Expected gender:	Female	RPG:	OK
Used metric:	Peak height	Residual primer %	OK 10%	CAS:	OK 90%

Reference Samples: 7 16 13 1 15 1 14 1 12



D [nt]	Gene-Exon	Chr.band	hg18 loc.	Height	Area	Ratio ^H	Stdev	[REF]	[Sam]	Width	d[nt]
418	ATM-1	11q22.3	11-107.598830	2651	38336	1	0.09	=	=	66	0.0
362	ATM-1	11q22.3	11-107.598966	3113	43938	0.98	0.09	=	=	84	0.0
173	ATM-Intr.1	11q22.3	11-107.600753	7854	79413	0.98	0.1	=	=	35	0.0
196	ATM-2	11q22.3	11-107.603560	4532	49803	0.98	0.1	=	=	91	0.0
234	ATM-4	11q22.3	11-107.605158	4970	55074	1.01	0.09	=	=	53	0.0
280	ATM-5	11q22.3	11-107.611683	4281	47563	0.98	0.07	=	=	35	0.0
319	ATM-6	11q22.3	11-107.619924	3669	46244	1.01	0.07	=	=	64	0.0
382	ATM-8	11q22.3	11-107.622916	3218	44783	0.99	0.11	=	=	69	0.0
136	ATM-10	11q22.3	11-107.626777	8299	87490	0.98	0.09	=	=	48	0.0
242	ATM-14	11q22.3	11-107.632194	4980	53938	1	0.11	=	=	35	0.0
205	ATM-16	11q22.3	11-107.634921	5556	56749	0.98	0.06	=	=	33	0.0
142	ATM-17	11q22.3	11-107.643137	6017	63054	0.96	0.09	=	=	42	0.0
436	ATM-19	11q22.3	11-107.646985	2239	34688	1	0.11	=	=	84	0.0
328	ATM-22	11q22.3	11-107.648710	3028	37550	1.09	0.11	=	=	76	0.0
373	ATM-23	11q22.3	11-107.655436	2369	32326	0.96	0.08	=	=	64	0.0
167	ATM-26	11q22.3	11-107.660224	7462	80498	1.02	0.1	=	=	83	0.0
223	ATM-27	11q22.3	11-107.663610	4198	45195	1	0.09	=	=	36	0.0
310	ATM-29	11q22.3	11-107.665703	5094	60043	1.02	0.11	=	=	36	0.0
178	ATM-31	11q22.3	11-107.669339	6659	68541	1.01	0.05	=	=	45	0.0
192	ATM-33	11q22.3	11-107.673233	7538	77081	1	0.09	=	=	45	0.0
255	ATM-34	11q22.3	11-107.675638	4737	53993	0.99	0.09	=	=	70	0.0
292	ATM-37	11q22.3	11-107.680715	2972	35124	1.03	0.05	=	=	63	0.0
337	ATM-38	11q22.3	11-107.683830	3022	37610	1.02	0.05	=	=	60	0.0
274	ATM-40	11q22.3	11-107.688294	4332	47956	1.03	0.09	=	=	31	0.0
427	ATM-42	11q22.3	11-107.691970	1834	27740	1	0.06	=	=	69	0.1
463	ATM-44	11q22.3	11-107.695883	1838	28429	1.03	0.09	=	=	74	0.0
148	ATM-46	11q22.3	11-107.701285	7319	77811	1.03	0.04	=	=	70	0.0
184	ATM-49	11q22.3	11-107.705086	6212	64981	0.98	0.1	=	=	34	0.0
217	ATM-53	11q22.3	11-107.708696	5996	63516	1	0.05	=	=	36	0.0
261	ATM-56	11q22.3	11-107.711788	4760	51291	1.02	0.05	=	=	43	0.1
287	ATM-57	11q22.3	11-107.719162	4237	49833	0.98	0.05	=	=	60	0.0
345	ATM-59	11q22.3	11-107.723225	3200	41040	1.02	0.11	=	=	66	0.0
391	ATM-61	11q22.3	11-107.730735	2239	31323	0.96	0.05	=	=	64	0.0
249	ATM-62	11q22.3	11-107.740982	5709	62266	0.98	0.09	=	=	34	0.0
154	Reference*	02q12.3	02-108.906225	7181	78319	0.99	0.05	=	=	77	0.0
130	Reference*	03q21.3	03-129.999512	7156	77418	0.96	0.05	=	=	61	0.0
268	Reference*	05p15.31	05-009.490899	4368	48028	1.01	0.05	=	=	35	0.0
160	Reference*	07q21.3	07-093.873480	6557	71680	1.02	0.05	=	=	73	0.0
355	Reference*	08q22.3	08-105.578750	2743	35558	1.04	0.07	=	=	65	0.0
445	Reference*	13q14.3	13-050.428652	2066	32076	1.02	0.05	=	=	71	0.0
229	Reference*	15q25.2	15-082.497791	5356	56812	1.03	0.05	=	=	39	0.0
301	Reference*	16q13	16-055.490937	3234	38814	0.92	0.08	=	=	73	0.0
409	Reference*	17q21.2	17-037.637569	1884	27253	1	0.08	=	=	88	0.0
485	Reference*	18q21.1	18-045.630186	1792	29135	1	0.06	=	=	84	0.1
209	Reference*	20q11.23	20-034.978521	4923	53170	0.98	0.1	=	=	48	0.0
4368				49803		1	0.08			63	0.01

Median value all probe values:

233

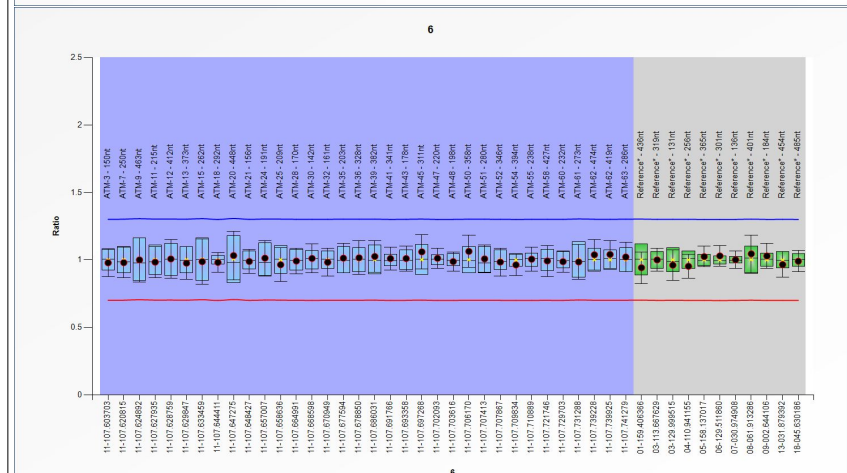
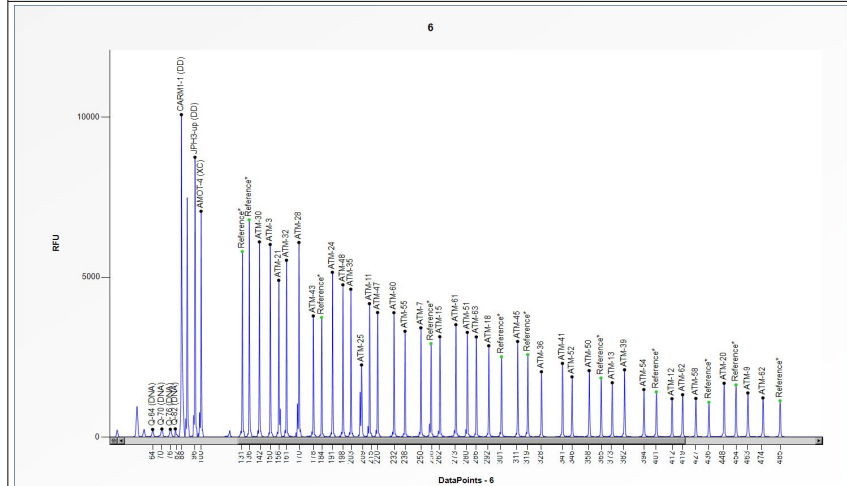
Sample report: 6

Sample type: Reference | Project: ATM analysis | Experiment: ATM2 | Dye: 6-FAM | Performed by: Admin
Machine: ABI-3730 | Report date: 15/08/2018 | Run date: 09/12/2015 | Software Version: v.140721.1958 | Normal range: 0.7 - 1.3

Authorization	
Date	

MLPA probe mix:	P042-ATM-2	Nr of test probes:	45/45	FRSS: Warning 70%
Lot number:	B1-0314	Nr of ref probes:	11/11	FRMS: OK? 85%
Sheet date:	09/12/2015 14:47:04	DNA concentration:	NA	PSL: OK 9%
Control fragments:	CF-003-[brown] QDX2 (A2-0)	DNA denaturation:	NA	RSQ: OK
Analysis method:	Block SSC: On	Expected gender:	Female	RPQ: OK
Used metric:	Peak height	Residual primer %:	OK 13%	CAS: OK 90%

Reference Samples: 7 | 6 | 3 | 1 | 5 | 1 | 1 | 4 | 1 | 2



D [nt]	Gene-Exon	Chr.band	hg18 loc.	Height	Area	Ratio ⁿ	Stdev	[REF]	[Sam]	Width	d[nt]
150	ATM-3	11q22.3	11-107.603703	6022	34512	0.98	0.05	=	=	51	0.0
250	ATM-7	11q22.3	11-107.620815	3413	22088	0.98	0.06	=	=	63	0.1
463	ATM-9	11q22.3	11-107.624892	1376	12478	1	0.08	=	=	48	0.1
215	ATM-11	11q22.3	11-107.627935	4171	24526	0.98	0.06	=	=	35	0.0
412	ATM-12	11q22.3	11-107.628759	1195	9661	1.01	0.07	=	=	43	0.0
373	ATM-13	11q22.3	11-107.629847	1696	12876	0.98	0.06	=	=	53	0.0
262	ATM-15	11q22.3	11-107.633459	3135	20608	0.99	0.08	=	=	44	0.1
292	ATM-18	11q22.3	11-107.644411	2852	18914	0.98	0.04	=	=	52	0.0
448	ATM-20	11q22.3	11-107.647275	1679	14694	1.03	0.09	=	=	62	0.0
156	ATM-21	11q22.3	11-107.648427	4900	32603	0.99	0.05	=	=	50	0.0
191	ATM-24	11q22.3	11-107.657007	5150	30738	1.01	0.07	=	=	53	0.1
209	ATM-25	11q22.3	11-107.658636	2253	15823	0.96	0.06	=	=	32	-0.1
170	ATM-28	11q22.3	11-107.664991	6084	40111	0.99	0.05	=	=	43	-0.1
142	ATM-30	11q22.3	11-107.668598	6102	35914	1.01	0.05	=	=	49	0.0
161	ATM-32	11q22.3	11-107.670949	5528	32433	0.98	0.05	=	=	38	0.0
203	ATM-35	11q22.3	11-107.677594	4621	27803	1.01	0.05	=	=	44	0.1
328	ATM-36	11q22.3	11-107.678850	2039	14022	1.02	0.06	=	=	46	0.1
382	ATM-39	11q22.3	11-107.686031	2101	16310	1.03	0.06	=	=	48	-0.1
341	ATM-41	11q22.3	11-107.691766	2301	16676	1.01	0.04	=	=	39	0.0
178	ATM-43	11q22.3	11-107.693358	3786	22481	1.01	0.05	=	=	40	0.0
311	ATM-45	11q22.3	11-107.697268	2987	20140	1.06	0.06	=	=	52	0.1
220	ATM-47	11q22.3	11-107.702093	3892	24850	1.01	0.04	=	=	51	0.0
198	ATM-48	11q22.3	11-107.703616	4759	28491	0.99	0.03	=	=	56	0.0
358	ATM-50	11q22.3	11-107.706170	2075	15530	1.06	0.06	=	=	52	0.1
280	ATM-51	11q22.3	11-107.707413	3271	21935	1.01	0.05	=	=	48	0.0
346	ATM-52	11q22.3	11-107.707867	1878	13368	0.98	0.05	=	=	35	0.1
394	ATM-54	11q22.3	11-107.709834	1482	11587	0.96	0.04	=	=	36	0.0
238	ATM-55	11q22.3	11-107.710889	3306	20349	1.01	0.04	=	=	62	0.0
427	ATM-58	11q22.3	11-107.721746	1203	10005	0.99	0.06	=	=	36	0.0
232	ATM-60	11q22.3	11-107.729703	3888	24023	0.99	0.04	=	=	75	0.0
273	ATM-61	11q22.3	11-107.731288	3513	22882	0.99	0.06	=	=	46	0.0
474	ATM-62	11q22.3	11-107.739228	1220	11254	1.04	0.06	=	=	65	0.1
419	ATM-62	11q22.3	11-107.739925	1321	10878	1.04	0.05	=	=	39	0.0
286	ATM-63	11q22.3	11-107.741279	3128	20233	1.02	0.05	=	=	38	0.0
436	Reference*	01q23.3	01-159.406366	1083	9196	0.94	0.06	=	=	42	0.0
319	Reference*	03q13.2	03-113.667629	2574	18084	1	0.04	=	=	48	0.1
131	Reference*	03q21.3	03-129.999515	5801	35032	0.96	0.06	=	=	47	0.1
256	Reference*	04q25	04-110.941155	2920	17149	0.95	0.04	=	=	22	0.0
365	Reference*	05q33.3	05-158.137017	1843	13380	1.03	0.04	=	=	43	0.1
301	Reference*	06q22.33	06-129.511860	2507	17383	1.03	0.04	=	=	49	0.0
136	Reference*	07p14.3	07-030.974908	6792	39020	1	0.03	=	=	43	0.0
401	Reference*	08q12.2	08-061.913286	1407	11272	1.05	0.07	=	=	39	0.1
184	Reference*	09p24.2	09-002.644106	3738	21511	1.03	0.05	=	=	47	0.0
454	Reference*	13q13.1	13-031.879392	1628	13754	0.97	0.05	=	=	36	0.1
485	Reference*	18q21.1	18-045.630186	1130	10370	0.99	0.04	=	=	42	0.1

Median value all probe values: **2920 18914 1 0.05 46 0.03**

Normal range: 0.7 - 1.3 Essential information on the use of this product is present in the product description which is available on <http://www.mlpa.com>. For questions, <mailto:info@mlpa.com>. MRC-Holland does not and cannot warrant the performance or results you may obtain by using the software. In no event will MRC-Holland be liable for any damages, claims or costs whatsoever or any consequential, indirect, incidental, damages, or any lost profits or lost savings, even if an MRC-Holland representative has been advised of the possibility of such loss, damages, claims or costs.

STS 13/12 W2



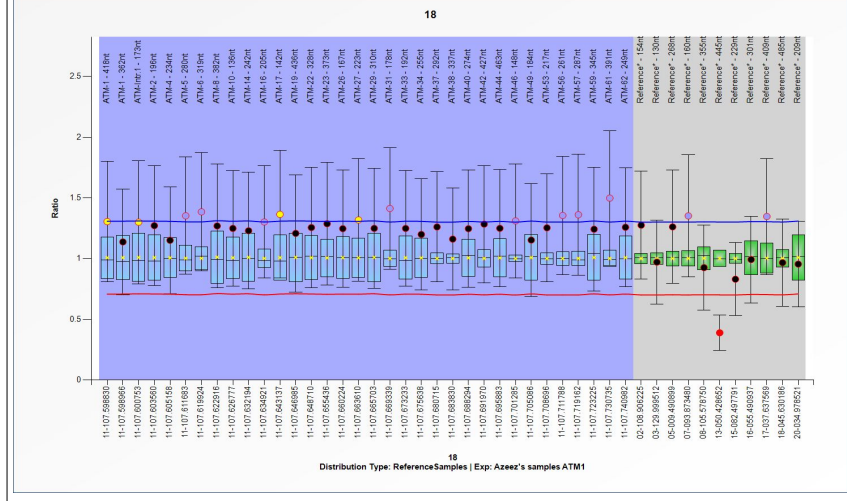
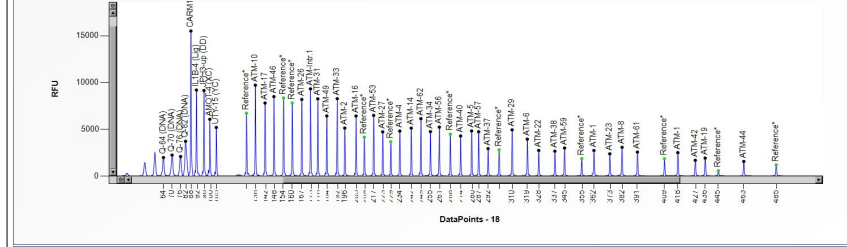
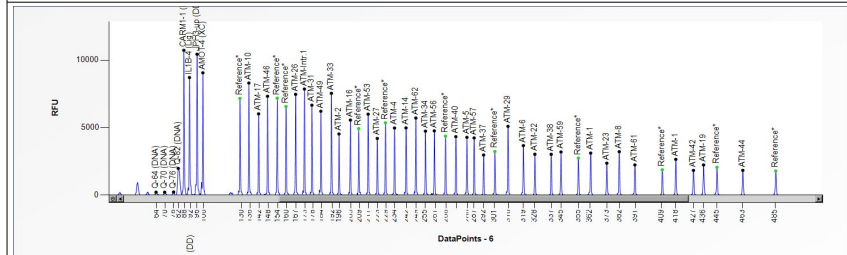
Sample report: 18

Sample type: Sample | Project: ATM analysis | Experiment: ATM1 | Dye: 6-FAM | Performed by: Admin
Machine: ABI-3730 | Report date: 15/08/2018 | Run date: 29/11/2015 | Software Version: v.140721.1958 | Normal range: 0.7 - 1.3

Authorization	
Date	

MLPA probe mix: P041-ATM-1	Nr of test probes: 45/45	FRSS: Warning 70%
Lot number: B1-0314	Nr of ref probes: 11/11	FRMS: Bad 30%
Sheet date: 29/11/2015 14:55:14	DNA concentration: OK	PSLP: Warning -19%
Control fragments: CF-003-[brown] QDX2 (A2-0)	DNA denaturation: OK	RSQ: OK
Analysis method: Block SSC: On	Expected gender: Male	RPG: Bad
Used metric: Peak height	Residual primer %: OK 11%	CAS: Bad 25%

Reference Samples: 7 | 6 | 1 | 3 | 1 | 5 | 1 | 4 | 1 | 2



D [nt]	Gene-Exon	Chr.band	hg18 loc.	Height	Area	Ratio [#]	Stdev	[REF]	[Sam]	Width	d[nt]
418	ATM-1	11q22.3	11-107.598830	2492	34034	1.31	0.25	?	?	67	0.0
362	ATM-1	11q22.3	11-107.598966	2719	37481	1.14	0.22	=	=	82	-0.1
173	ATM-Intr.1	11q22.3	11-107.600753	9322	94096	1.3	0.25	?	?	35	-0.1
196	ATM-2	11q22.3	11-107.603560	5120	54387	1.27	0.25	=	=	81	0.0
234	ATM-4	11q22.3	11-107.605158	4802	51957	1.15	0.22	=	=	69	-0.1
280	ATM-5	11q22.3	11-107.611683	4810	52768	1.35	0.24	>*	?	51	-0.1
319	ATM-6	11q22.3	11-107.619924	3936	48248	1.38	0.24	>*	?	83	0.0
382	ATM-8	11q22.3	11-107.622916	3058	40953	1.27	0.25	=	=	76	-0.1
136	ATM-10	11q22.3	11-107.626777	9711	98983	1.25	0.24	=	=	38	-0.1
242	ATM-14	11q22.3	11-107.632194	5119	52926	1.23	0.24	=	=	32	-0.1
205	ATM-16	11q22.3	11-107.634921	6414	65078	1.3	0.23	>*	?	33	0.0
142	ATM-17	11q22.3	11-107.643137	7802	81270	1.36	0.26	?	?	38	-0.1
436	ATM-19	11q22.3	11-107.646985	1906	28344	1.21	0.24	=	=	68	-0.1
328	ATM-22	11q22.3	11-107.648710	2722	32015	1.26	0.25	=	=	58	0.0
373	ATM-23	11q22.3	11-107.655436	2368	31139	1.29	0.25	=	=	81	-0.1
167	ATM-26	11q22.3	11-107.660224	8189	87047	1.25	0.24	=	=	67	-0.1
223	ATM-27	11q22.3	11-107.663610	4715	47980	1.32	0.25	?	?	37	0.0
310	ATM-29	11q22.3	11-107.665703	4928	58969	1.25	0.25	=	=	88	0.0
178	ATM-31	11q22.3	11-107.669339	8254	83460	1.41	0.25	>*	?	35	0.0
192	ATM-33	11q22.3	11-107.673233	8268	82463	1.25	0.24	=	=	35	-0.1
255	ATM-34	11q22.3	11-107.675638	4738	53413	1.2	0.23	=	=	69	-0.1
292	ATM-37	11q22.3	11-107.680715	2920	34187	1.26	0.23	=	=	62	-0.1
337	ATM-38	11q22.3	11-107.683830	2650	32667	1.16	0.21	=	=	75	0.0
274	ATM-40	11q22.3	11-107.688294	4279	46143	1.25	0.24	=	=	33	-0.1
427	ATM-42	11q22.3	11-107.691970	1670	23962	1.28	0.24	=	=	81	-0.1
463	ATM-44	11q22.3	11-107.695883	1548	22276	1.25	0.24	=	=	61	-0.1
148	ATM-46	11q22.3	11-107.701285	8488	89124	1.31	0.24	>*	?	65	-0.1
184	ATM-49	11q22.3	11-107.705086	6417	65900	1.15	0.23	=	=	33	0.0
217	ATM-53	11q22.3	11-107.708696	6475	69098	1.25	0.22	=	=	71	0.0
261	ATM-56	11q22.3	11-107.711788	5221	56944	1.36	0.24	>*	?	64	-0.1
287	ATM-57	11q22.3	11-107.719162	4729	53698	1.36	0.25	>*	?	63	-0.1
345	ATM-59	11q22.3	11-107.723225	2986	36909	1.24	0.25	=	=	67	-0.1
391	ATM-61	11q22.3	11-107.730735	2557	34906	1.5	0.28	>*	>*	83	0.0
249	ATM-62	11q22.3	11-107.740982	6126	63528	1.26	0.25	=	=	35	0.0
154	Reference*	02q12.3	02-108.906225	8346	88679	1.27	0.22	=	=	85	-0.1
130	Reference*	03q21.3	03-129.999512	6710	67555	0.97	0.17	=	=	25	0.0
268	Reference*	05p15.31	05-009.490899	4470	47707	1.26	0.23	=	=	34	-0.1
160	Reference*	07q21.3	07-093.873480	7813	84913	1.35	0.25	>*	?	89	-0.1
355	Reference*	08q22.3	08-105.578750	1845	23600	0.93	0.18	=	=	73	-0.1
445	Reference*	13q14.3	13-050.428652	555	8622	0.39	0.07	<<*	<<*	69	-0.1
229	Reference*	15q25.2	15-082.497791	3656	38009	0.83	0.15	=	=	35	0.0
301	Reference*	16q13.3	16-055.490937	2789	30387	0.99	0.18	=	=	27	-0.1
409	Reference*	17q21.2	17-037.637569	1846	25210	1.35	0.24	>*	?	63	0.0
485	Reference*	18q21.1	18-045.630186	1176	18265	0.97	0.18	=	=	70	0.0
209	Reference*	20q11.23	20-034.978521	4145	43634	0.95	0.18	=	=	36	0.0
Median value all probe values:	4715	48248	1.26	0.24*		64	-0.05				

235

Normal range: 0.7 - 1.3 Essential information on the use of this product is present in the product description which is available on <http://www.mipa.com>. For questions, <mailto:info@mipa.com>. MRC-Holland does not and cannot warrant the performance or results you may obtain by using the software. In no event will MRC-Holland be liable for any damages, claims or costs whatsoever or any consequential, indirect, incidental, damages, or any lost profits or lost savings, even if an MRC-Holland representative has been advised of the possibility of such loss, damages, claims or costs.



Sample report: 18

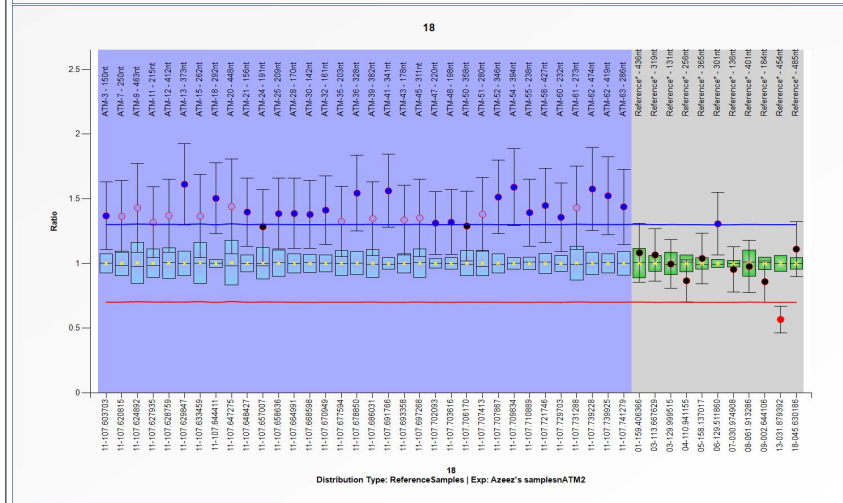
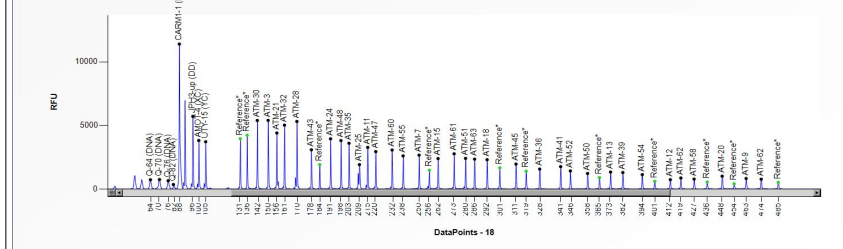
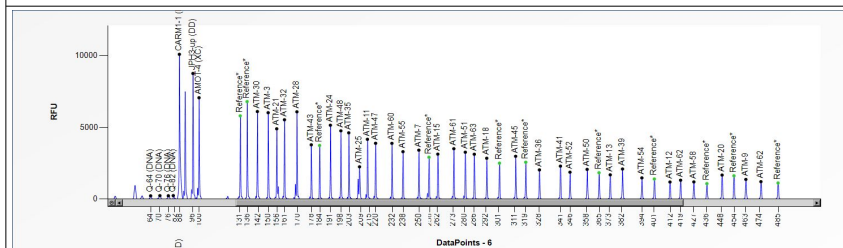
Sample type: Sample | Project: ATM analysis | Experiment: ATM2 | Dye: 6-FAM | Performed by: Admin
Machine: ABI-3730 | Report date: 15/08/2018 | Run date: 09/12/2015 | Software Version: v.140721.1958 | Normal range: 0.7 - 1.3

Table with 2 columns: Authorization, Date

MLPA probe mix: P042-ATM-2
Lot number: B1-0314
Sheet date: 09/12/2015 14:47:04
Control fragments: CF-003-[brown] QDX2 (A2-0)
Analysis method: Block SSC: On
Used metric: Peak height
Nr of test probes: 45/45
Nr of ref probes: 11/11
DNA concentration: NA
DNA denaturation: NA
Expected gender: Female
Residual primer %: OK 16%

FRSS: Warning 70%
FRMS: Warning 70%
PSL: OK -15%
RSQ: OK
RPQ: Warning
CAS: Warning 60%

Reference Samples: 7 | 6 | 1 | 3 | 1 | 5 | 1 | 4 | 1 | 2



Main data table with columns: D [nt], Gene-Exon, Chr.band, hg18 loc., Height, Area, Ratio, Stdev, [REF], [Sam], Width, d[nt]. Contains 48 rows of probe data.

Median value all probe values:

1912 12718 1.37* 0.14* 44 -0.03

Normal range: 0.7 - 1.3 Essential information on the use of this product is present in the product description which is available on http://www.mlpa.com. For questions, mailto:info@mlpa.com.
MRC-Holland does not and cannot warrant the performance or results you may obtain by using the software. In no event will MRC-Holland be liable for any damages, claims or costs whatsoever or any consequential, indirect, incidental, damages, or any lost profits or lost savings, even if an MRC-Holland representative has been advised of the possibility of such loss, damages, claims or costs.

hTERT-RPE1



Sample report: 13

Sample type: Sample | Project: ATM analysis | Experiment: ATM1 | Dye: 6-FAM | Performed by: Admin
 Machine: ABI-3730 | Report date: 15/08/2018 | Run date: 29/11/2015 | Software Version: v.140721.1958 | Normal range: 0.7 - 1.3

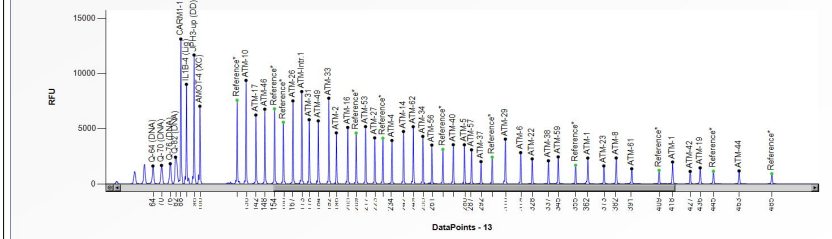
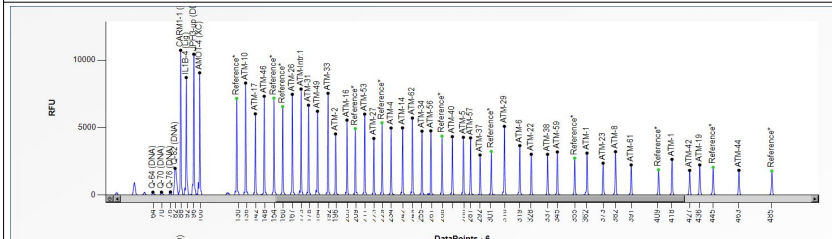
Authorization	
Date	

MLPA probe mix: P041-ATM-1
 Lot number: B1-0314
 Sheet date: 29/11/2015 14:55:14
 Control fragments: CF-003-[brown] QDX2 (A2-0)
 Analysis method: Block SSC: On
 Used metric: Peak height

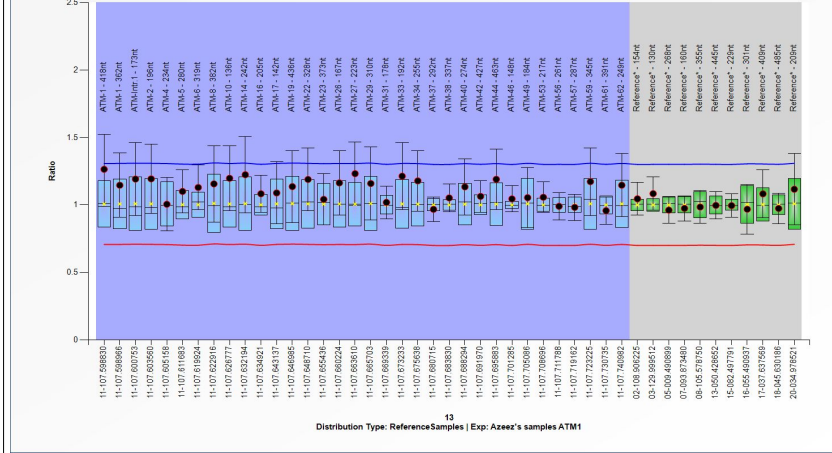
Nr of test probes: 45/45
 Nr of ref probes: 11/11
 DNA concentration: OK
 DNA denaturation: OK
 Expected gender: Female
 Residual primer %: OK 13%

FRSS: Warning
 FRMS: Bad 30%
 PSLP: Bad -33%
 RSQ: OK
 RPO: OK
 CAS: Warning 50%

Reference Samples: 7 | 6 | 1 | 3 | 1 | 5 | 1 | 14 | 1 | 12



13



D [nt]	Gene-Exon	Chr.band	hg18 loc.	Height	Area	Ratio ⁴¹	Stdev	[REF]	[Sam]	Width	d[nt]
418	ATM-1	11q22.3	11-107.598830	1983	28132	1.26	0.13	=	=	73	0.0
362	ATM-1	11q22.3	11-107.598966	2341	33818	1.15	0.12	=	=	97	0.0
173	ATM-Intr.1	11q22.3	11-107.600753	8361	84191	1.19	0.14	=	=	40	0.0
196	ATM-2	11q22.3	11-107.603560	4625	47314	1.19	0.13	=	=	39	0.0
234	ATM-4	11q22.3	11-107.605158	3932	43727	1.01	0.1	=	=	83	0.0
280	ATM-5	11q22.3	11-107.611683	3544	38538	1.1	0.08	=	=	43	0.0
319	ATM-6	11q22.3	11-107.619924	2832	32345	1.13	0.08	=	=	32	0.0
382	ATM-8	11q22.3	11-107.622916	2348	31708	1.16	0.14	=	=	78	0.0
136	ATM-10	11q22.3	11-107.626777	9375	94338	1.2	0.12	=	=	38	0.0
242	ATM-14	11q22.3	11-107.632194	4747	49906	1.22	0.14	=	=	32	-0.1
205	ATM-16	11q22.3	11-107.634921	5114	52192	1.08	0.07	=	=	36	0.0
142	ATM-17	11q22.3	11-107.643137	6237	66531	1.09	0.12	=	=	59	0.0
436	ATM-19	11q22.3	11-107.646985	1454	22398	1.14	0.13	=	=	72	0.0
328	ATM-22	11q22.3	11-107.648710	2265	27299	1.19	0.12	=	=	67	0.0
373	ATM-23	11q22.3	11-107.655436	1629	21686	1.04	0.09	=	=	57	0.0
167	ATM-26	11q22.3	11-107.660224	7520	78650	1.16	0.12	=	=	72	0.0
223	ATM-27	11q22.3	11-107.663610	4168	43762	1.23	0.12	=	=	39	0.0
310	ATM-29	11q22.3	11-107.665703	4058	46082	1.16	0.14	=	=	33	0.0
178	ATM-31	11q22.3	11-107.669339	5817	58969	1.02	0.06	=	=	36	0.0
192	ATM-33	11q22.3	11-107.673233	7761	78415	1.21	0.12	=	=	36	0.0
255	ATM-34	11q22.3	11-107.675638	4303	46031	1.18	0.11	=	=	36	0.0
292	ATM-37	11q22.3	11-107.680715	2018	23259	0.97	0.05	=	=	60	0.0
337	ATM-38	11q22.3	11-107.683830	2096	25745	1.05	0.05	=	=	64	0.0
274	ATM-40	11q22.3	11-107.688294	3549	39041	1.13	0.1	=	=	27	0.0
427	ATM-42	11q22.3	11-107.691970	1131	16369	1.06	0.06	=	=	62	-0.1
463	ATM-44	11q22.3	11-107.695883	1176	18021	1.19	0.11	=	=	67	-0.1
148	ATM-46	11q22.3	11-107.701285	6769	71992	1.05	0.05	=	=	84	0.0
184	ATM-49	11q22.3	11-107.705086	5708	58401	1.05	0.11	=	=	33	0.0
217	ATM-53	11q22.3	11-107.708696	5190	53061	1.06	0.06	=	=	35	0.0
261	ATM-56	11q22.3	11-107.711788	3516	38355	0.99	0.05	=	=	59	0.0
287	ATM-57	11q22.3	11-107.719162	3089	35604	0.98	0.05	=	=	79	0.0
345	ATM-59	11q22.3	11-107.723225	2447	31199	1.17	0.13	=	=	63	-0.1
391	ATM-61	11q22.3	11-107.730735	1373	20666	0.96	0.05	=	=	83	0.0
249	ATM-62	11q22.3	11-107.740982	5181	54409	1.15	0.12	=	=	31	0.0
154	Reference*	02q12.3	02-108.906225	6802	73513	1.05	0.06	=	=	100	0.0
130	Reference*	03q21.3	03-129.999512	7583	75582	1.08	0.06	=	=	25	0.0
268	Reference*	05p15.31	05-009.490899	3129	33415	0.96	0.05	=	=	27	0.0
160	Reference*	07q21.3	07-093.873480	5587	57537	0.98	0.05	=	=	35	0.0
355	Reference*	08q22.3	08-105.578750	1693	22098	0.99	0.06	=	=	59	-0.1
445	Reference*	13q14.3	13-050.428652	1150	17500	1	0.05	=	=	67	-0.1
229	Reference*	15q25.2	15-082.497791	4136	42058	1	0.04	=	=	24	-0.1
301	Reference*	16q13	16-055.490937	2429	26693	0.97	0.09	=	=	26	0.0
409	Reference*	17q21.2	17-037.637569	1226	17673	1.08	0.09	=	=	72	-0.1
485	Reference*	18q21.1	18-045.630186	932	15202	0.97	0.06	=	=	61	0.0
209	Reference*	20q11.23	20-034.978521	4610	47682	1.12	0.13	=	=	37	0.0
3549				39041	1.08	0.09				57	-0.03

Median value all probe values:

237



Sample report: 13

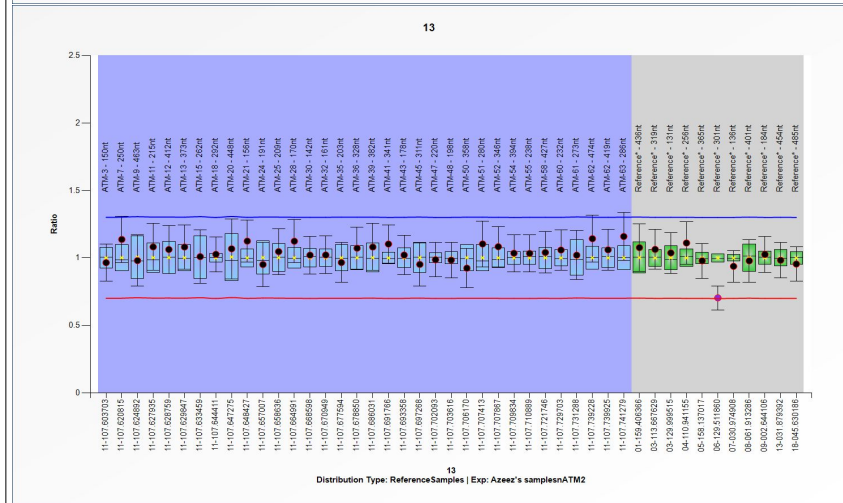
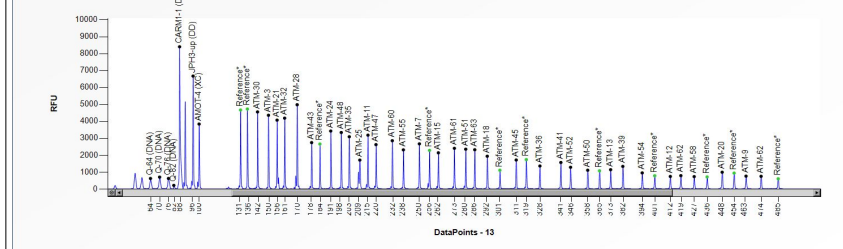
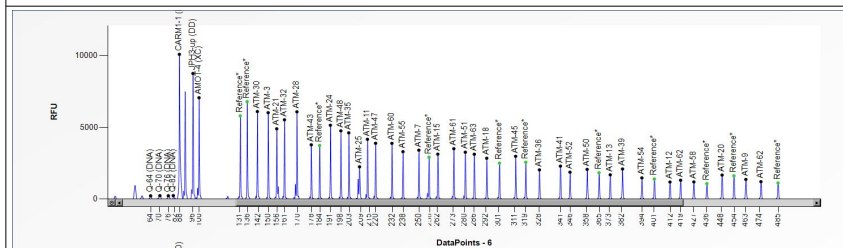
Sample type: Sample | Project: ATM analysis | Experiment: ATM2 | Dye: 6-FAM | Performed by: Admin
Machine: ABI-3730 | Report date: 15/08/2018 | Run date: 09/12/2015 | Software Version: v.140721.1958 | Normal range: 0.7 - 1.3

Table with 2 columns: Authorization, Date

MLPA probe mix: P042-ATM-2
Lot number: B1-0314
Sheet date: 09/12/2015 14:47:04
Control fragments: CF-003-[brown] QDX2 (A2-0)
Analysis method: Block SSC: On
Used metric: Peak height
Nr of test probes: 45/45
Nr of ref probes: 11/11
DNA concentration: NA
DNA denaturation: NA
Expected gender: Female
Residual primer %: OK 14%

FRSS: Warning 70%
FRMS: Warning 70%
PSL: Warning -15%
RSQ: OK
RPQ: OK
CAS: OK? 75%

Reference Samples: 7 | 6 | 1 | 3 | 15 | 14 | 1 | 2



Main data table with columns: D [nt], Gene-Exon, Chr.band, hg18 loc., Height, Area, Ratio, Stdev, [REF], [Sam], Width, d[nt]. Contains data for probes ATM-3 through ATM-63 and Reference* probes.

Median value all probe values:

1934 13573 1.04 0.08 43 -0.05

Normal range: 0.7 - 1.3 Essential information on the use of this product is present in the product description which is available on http://www.mlpa.com. For questions, mailto:info@mlpa.com.
MRC-Holland does not and cannot warrant the performance or results you may obtain by using the software. In no event will MRC-Holland be liable for any damages, claims or costs whatsoever or any consequential, indirect, incidental, damages, or any lost profits or lost savings, even if an MRC-Holland representative has been advised of the possibility of such loss, damages, claims or costs.

Appendix 4

The Targeted Panel of 55 Cancer Genes including the *ATM* used in the NGS Experiment. NGS Services Provided by the Children's Hospital, Sheffield, UK.

<i>BRCA1</i>	<i>STK11</i>	<i>EPCAM</i>	<i>GPC3</i>	<i>FANCD2</i>
<i>BRCA2</i>	<i>PPM1D</i>	<i>SMAD4</i>	<i>HNF1A</i>	<i>FANCE</i>
<i>TP53</i>	<i>NBN</i>	<i>MEN1</i>	<i>MET</i>	<i>FANCF</i>
<i>ATM</i>	<i>MLH1</i>	<i>PRKAR1A</i>	<i>MITF</i>	<i>FANCG</i>
<i>BAP1</i>	<i>MSH2</i>	<i>RET</i>	<i>TSC1</i>	<i>FANCI</i>
<i>BRIP1</i>	<i>MSH6</i>	<i>SDHB</i>	<i>TSC2</i>	<i>FANCL</i>
<i>CDH1</i>	<i>PMS1</i>	<i>SDHC</i>	<i>VHL</i>	<i>FANCM</i>
<i>CHEK2</i>	<i>PMS2</i>	<i>SDHD</i>	<i>WT1</i>	<i>PALB2</i>
<i>RAD51D</i>	<i>APC</i>	<i>SDHAF2</i>	<i>FANCA</i>	<i>RAD51C</i>
<i>RB1</i>	<i>MUTYH</i>	<i>FH</i>	<i>FANCB</i>	<i>SLX4</i>
<i>PTEN</i>	<i>BMPR1A</i>	<i>FLCN (BHD)</i>	<i>FANCC</i>	<i>ERCC4</i>